A Thesis for the Degree of Doctor of Philosophy

Molecular Analysis of the *Vibrio vulnificus* Genes Encoding *N*-acetylglucosamine Binding Protein and Phospholipase A_2 Induced by Mucin

뮤신에 의해 유도되는 패혈증비브리오균의 *N*-acetylglucosamine 부착단백질과 Phospholipase A_2를 암호화하는 유전자의 분자 수준 분석

August, 2016

Kyung Ku Jang

Department of Agricultural Biotechnology

College of Agriculture and Life Sciences

Seoul National University

Molecular Analysis of the *Vibrio vulnificus* genes encoding *N*-acetylglucosamine Binding Protein and Phospholipase A_2 Induced by Mucin

뮤신에 의해 유도되는 패혈증비브리오균의 *N*-acetyl glucosamine 부착단백질과 Phospholipase A_2를 암호화하는 유전자의 분자 수준 분석

지도교수 최 상 호

이 논문을 농학박사학위논문으로 제출함
2016 년 05 월

서울대학교 대학원
농생명공학부
장 경 구

장경구의 박사학위논문을 인준함
2016 년 06 월

위 원 장 유 상 렬 (인)
부위원장 최 상 호 (인)
위 원 성 영 재 (인)
위 원 하 남 출 (인)
위 원 김 건 수 (인)

Abstract

Molecular Analysis of the *Vibrio vulnificus* Genes Encoding *N*-acetylglucosamine Binding Protein and Phospholipase A_2 Induced by Mucin

Kyung Ku Jang

Department of Agricultural Biotechnology

The Graduate School

Seoul National University

Mucin is a glycoprotein composed of a polypeptide backbone with branched oligosaccharide side chains and a major component of mucus layer that serves as the first line of defense against many enteric pathogens. To survive and cause disease, the pathogens interact with mucin and change their transcriptomic profile to adapt to the host environment. In this study, to better understand the bacterium's interactions to the mucus layer, transcriptional response of *Vibrio vulnificus* to the mucin and the mucin-secreting HT29-methotrexate (MTX) cells was investigated. The growth and survival of *V. vulnificus* cells exposed to M9 medium supplemented with 0.6%

(*wt*/*vol*) mucin (M9M) and the HT29-MTX cells were monitored, respectively. To monitor the levels of all transcripts in the bacteria grown in the M9 medium supplemented with 0.4% (*wt*/*vol*) glucose (M9G) and M9M, RNA-seq technology was used. Also, transcriptomes of the bacteria exposed to basal medium eagle (BME) and the HT29-MTX cells was analyzed using the same technology. From the analysis, 337 genes were identified to be differentially expressed with significance between M9G and M9M. In addition, the analysis and comparison of RNA-seq data identified 650 genes with altered transcript level in the bacteria exposed to the HT29-MTX cells compared to BME. Furthermore, several virulence related genes encoding metalloprotease, *N*-acetylglucosamine binding protein, cytolysin, and phospholipase were induced by the mucin and the mucin-secreting host cells.

Among the genes whose expression was up-regulated when *V. vulnificus* cells were grown in M9M, a gene encoding an *N*-acetylglucosamine binding protein GbpA, a homologue of *Vibrio cholerae* GbpA, was selected and further studied. A mutational analysis demonstrated that GbpA contributes to the ability of adherence to the HT29-MTX cells as well as the mucin. Furthermore, compared with the wild type, the *gbpA* mutant exhibited reduced intestinal colonization and virulence in mice. The *gbpA* transcription was growth-phase dependent, reaching a maximum during the

exponential phase. The Fe-S cluster regulator (IscR) and the cyclic AMP receptor protein (CRP) coactivated whereas SmcR, a LuxR homologue, repressed *gbpA* expression at the transcriptional level. The cellular levels of IscR, CRP, and SmcR were not significantly affected by one another, indicating that the regulator proteins function cooperatively to regulate *gbpA* rather than sequentially in a regulatory cascade. Primer extension analysis revealed that the transcription of *gbpA* begins at a single site. Direct bindings of IscR, SmcR, and CRP to P_{gbpA} were demonstrated by EMSA. The binding sites for the regulator proteins were mapped based on a deletion analysis of the P_{gbpA} and confirmed by DNase I protection assays. Interestingly, *gbpA* was induced by exposure to H_2O_2, and the induction appeared to be mediated by elevated intracellular levels of IscR. The combined results proposed a model in which IscR, CRP, and SmcR cooperate for precise control of the *gbpA* expression during infection.

Among the *V. vulnificus* genes specifically induced by exposure to the mucin and the mucin-secreting host cells, a gene, annotated as *plp* encoding a putative phospholipase Plp, was identified and further characterized. The amino acid sequences of *V. vulnificus* Plp (*Vv*Plp) were 67% identical to those of *Vibrio*

anguillarum phospholipase (*Va*Plp). To examine the role of *Vv*Plp, a mutant with disruption of the *plp* gene was constructed by allelic exchanges, and its virulence was evaluated. Compared with the wild type, the *plp* mutant showed a low level of cytotoxicity toward the HT29-MTX cells and reduced virulence in mice. Genetic and biochemical analyses using the recombinant Plp protein demonstrated that Plp is a secreted phospholipase A_2 essential for pathogenesis of *V. vulnificus*. Examination of global regulatory proteins on the expression of *plp* revealed that the transcription activator HlyU and CRP upregulate the *plp* expression. The cellular levels of HlyU and CRP were not significantly affected by one another, indicating that the regulator proteins function cooperatively to activate *plp* rather than sequentially in a regulatory cascade. The regulatory proteins directly bound to the upstream of the *plp* promoter P_{plp}. DNase I protection assays, together with the deletion analyses of P_{plp}, demonstrated that HlyU binds three distinct sequences centered at -174, -139.5, and -109.5 and CRP binds specifically to the sequences centered at -69.5 relative to the transcription start site of P_{plp}. Consequently, the combined results indicated that *V. vulnificus plp* encodes a phospholipase A_2 essential for virulence and is cooperatively activated by HlyU and CRP.

Keywords: ***Vibrio vulnificus*****, Mucin, Transcriptome analysis, Pathogenesis, *N*-acetylglucosamine binding protein (GbpA), Phospholipase A_2 (Plp), Gene regulation, IscR, CRP, SmcR, HlyU**

Student Number: 2011 − 23534

Contents

Abstract ..... **I**

Contents ..... **VI**

List of Figures ..... **XI**

List of Tables ..... **XIII**

Chapter I. **1**

I-1. *Vibrio vulnificus* 2

I-1-1. Disease caused by *V. vulnificus* 3

I-1-2. Virulence factors of *V. vulnificus* 5

I-1-3. Regulation of virulence factors in *V. vulnificus* 12

I-2. Mucus layer 16

I-2-1. Mucus layer and mucin 16

I-2-2. Pathogens' strategies to penetrate and avoid the mucus layer 17

I-3. Objective of this study 20

Chapter II. **21**

II-1. Introduction 22

II-2. Materials and Methods 26

II-2-1. Strains, plasmids, and culture conditions 26

II-2-2. Growth kinetics of *V. vulnificus* 30

II-2-3. Development of the mucin-secreting cells and survival kinetics of *V. vulnificus* 31

II-2-4. RNA preparation, library construction, and sequencing 32

II-2-5. First and second strand synthesis 33

II-2-6. DNA fragmentation and preparation of libraries for Illumina sequencing platform 35

II-2-7. Sequencing and data analysis 36

II-3. Results and Discussion 37

II-3-1. Growth kinetics of *V. vulnificus* 37

II-3-2. Survival kinetics of *V. vulnificus* 39

II-3-3. Summary statistics for the RNA-seq data 42

II-3-4. Effect of mucin as a sole carbon source on the transcriptional change of *V. vulnificus* 44

II-3-5. Effect of exposure to the mucin-secreting host cell on the transcriptional change of *V. vulnificus* 45

II-3-6. Genes up-regulated by mucin and mucin-secreting HT29-MTX cells 51

II-3-7. Genes down-regulated by mucin and mucin-secreting HT29-MTX cells 83

Chapter III. 111

III-1. Introduction 112

III-2. Materials and Methods 116

III-2-1. Strains, plasmids, and culture conditions 116

III-2-2. Generation and complementation of the *gbpA* and *iscR crp* mutants 117
III-2-3. Mucin binding assay 123
III-2-4. Adhesion assay 124
III-2-5. Mouse lethality and competition assay 125
III-2-6. RNA purification and transcript analysis 127
III-2-7. Protein purification and Western blot analysis 129
III-2-8. Electrophoretic mobility shift assay (EMSA) 130
III-2-9. Construction of a set of *gbpA-luxCDABE* transcriptional fusions 131
III-2-10. DNase I protection assay 132
III-2-11. Data analysis 132
III-3. Results 133
III-3-1. Identification and sequence analysis of GbpA 133
III-3-2. GbpA is essential for mucin binding and virulence of *V. vulnificus* 134
III-3-3. Expression of *gbpA* is growth-phase dependent and regulated by IscR, CRP, and SmcR 140
III-3-4. IscR and CRP coactivate *gbpA* additively 144
III-3-5. IscR, CRP, and SmcR function cooperatively rather than sequencially to regulate *gbpA* 146

III-3-6. Mapping the regulatory region of *gbpA*..... 149

III-3-7. IscR, CRP, and SmcR regulate *gbpA* by directly binding to P_{gbpA} 155

III-3-8. Identification of binding sites for IscR, CRP, and SmcR..... 159

III-3-9. IscR activates P_{gbpA} by sensing reactive oxygen species (ROS)163

III-4. Discussion..... 167

Chapter IV. 172

IV-1. Introduction..... 173

IV-2. Materials and Methods 177

IV-2-1. Strains, plasmids, and culture conditions..... 177

IV-2-2. Complementation and generation of the *plp*, *hlyU*, and *hlyU crp* mutants..... 177

IV-2-3. Protein purification..... 179

IV-2-4. Preparation of polyclonal antibody and Western blot analysis. 181

IV-2-5. Cytotoxicity and mouse lethality..... 182

IV-2-6. Phospholipase A_2 (PLA_2) activity assay 183

IV-2-7. RNA purification and transcripts analysis..... 184

IV-2-8. Construction of a set of *plp-luxCDABE* transcriptional fusions185

IV-2-9. Electrophoretic mobility shift assay (EMSA) and DNase I protection assay..... 186

IV-2-10. Data analyses..... 187

IV-3. Results 188

IV-3-1. Identification and sequence analysis of Plp 188

IV-3-2. Plp is essential for cytotoxicity toward mucin secreting host cells *in vitro* and virulence in mice 189

IV-3-3. Plp is a phospholipase A_2 and secreted via the T2SS. 193

IV-3-4. Expression of *plp* is growth-phase dependent and regulated by HlyU and CRP 197

IV-3-5. HlyU and CRP coactivates *plp* additively 200

IV-3-6. HlyU and CRP function cooperatively rather than sequentially to regulate *plp* 203

IV-3-7. Mapping the regulatory region of *plp* 205

IV-3-8. HlyU and CRP regulate *plp* by directly binding to P_{plp} 211

IV-3-9. Identification of binding sites for HlyU and CRP 214

IV-4. Discussion 218

Chapter V. 222

References 226

국문초록 250

List of Figures

Figure II-1. Development of the mucin-secreting HT29-MTX cells……..…… 38

Figure II-2. Growth and survival kinetics of *V. vulnificus*……..……..……41

Figure II-3. Transcriptome comparisons of the RNA-seq samples……..…….47

Figure II-4. Functional categorization of genes differentially expressed by exposure to mucin-containing media and mucin-secreting host cells……..…..50

Figure III-1. Effect of GbpA on mucin binding and host cell adhesion of *V. vulnificus*….....137

Figure III-2. Mouse lethality and colonization activity of the *V. vulnificus* strains 139

Figure III-3. Effect of growth phases and global regulatory proteins on the *gbpA* expression……..142

Figure III-4. IscR and CRP coactivate *gbpA* additively.....145

Figure III-5. Cellular levels of IscR, CRP, and SmcR are unaffected by one another.....…148

Figure III-6. Transcription start site and sequences of the *gbpA* regulatory region.....152

Figure III-7. Deletion analysis of the P_{gbpA} regulatory region.....154

Figure III-8. Specific bindings of IscR, CRP, and SmcR to P_{gbpA}.....158

Figure III-9. Sequences for binding of IscR, CRP, and SmcR to P_{gbpA}.....162

Figure III-10. Effects of oxidative stress and apo-IscR on the activity of P_{gbpA}.....166

Figure IV-1. Cytotoxicity and mouse mortality of *V. vulnificus*…….……192

Figure IV-2. Enzyme activity and secretion of Plp mediated by the T2SS of *V. vulnifcus*…….……...196

Figure IV-3. Effect of growth phases and global regulatory proteins on the *plp* expression…….……..……199

Figure IV-4. HlyU and CRP coactivate *plp* additively…….……202

Figure IV-5. Cellular levels of HlyU and CRP are unaffected by one another……204

Figure IV-6. Transcription start site and sequences of the *plp* regulatory region.....208

Figure IV-7. Deletion analysis of the P_{plp} regulatory region.....210

Figure IV-8. Specific bindings of HlyU and CRP to P_{plp} 213

Figure IV-9. Sequences for binding of HlyU and CRP to P_{plp}.....217

List of Tables

Table II-1. Bacterial strains and plasmids used in this study..... 27

Table II-2. Analysis of RNA-seq data mapped to the *V. vulnificus* MO6-24/O genome.....43

Table II-3. List of genes up-regulated by mucin..... 56

Table II-4. List of genes up-regulated by HT29-MTX cells.....67

Table II-5. List of genes down-regulated by mucin..... 85

Table II-6. List of genes down-regulated by HT29-MTX cells.....94

Table III-1. Oligonucleotides used in this study.....119

Chapter I.

Background

I-1. *Vibrio vulnificus*

Vibrio vulnificus is Gram-negative, motile, and curved rod-shaped bacteria with a single polar flagellum, and belongs to *Vibrio* genus in *Vibrionaceae.* Its ability to ferment lactose is the distinctive feature from other members of the *Vibrio* genus (Baumann *et al.*, 1981; Strom and Paranjpye, 2000). The bacterium occurs naturally in estuarine and marine environments throughout the world and the food vehicle is primarily raw/undercooked oysters, which account for the 93% of ingestion cases (Horseman and Surani, 2011; Oliver, 2015). Although the number of *V. vulnificus* in estuarine waters is below 10 colony forming unit (CFU)/ml, it becomes concentrated in molluscan shellfish such as oysters (10^5 CFU/g of tissue) because of their filter-feeding unit for obtaining food (Oliver, 2015). *V. vulnificus* is usually found from waters where temperatures range from 9°C to 31°C and prefers tropical to subtropical climates. It multiplicates in areas where temperature exceed 18°C and salinities is a range of 15-25 parts per thousand (ppt) (Strom and Paranjype, 2000). Salinities at greater than 30 ppt will have an adverse effect on the survival of *V. vulnificus* regardless of the water temperature (Horseman and Surani, 2011). Interestingly, *V. vulnificus* cells enter dormancy state and fail to grow on the rich media at temperature below 13°C. This state commonly referred as the “viable but nonculturable” (VBNC) state. In the case of *V. vulnificus*, resuscitation (culturable

state) occurs at warmer temperature (Oliver, 2013).

I-1-1. Disease caused by *V. vulnificus*

V. vulnificus characteristically produces three distinct syndromes: primary septicemia, wound infection, and gastrointestinal tract-limited infections (Chiang and Chuang, 2003; Daniel, 2011).

Consumption of raw or undercooked shellfish is capable of causing a fulminant septicemia since most oysters bought at retail contained *V. vulnificus* (DePaola *et al.*, 2010). The main symptoms of the infection are fever, chills, nausea, abdominal pain, hypotension, and the development of secondary lesions (Jones and Oliver, 2009; Oliver, 2013). The vast majority of *V. vulnificus*-related illness has occurred in males over the age of 40 years with one or more chronic, underlying disease including liver damage, excess levels of iron, and immunocompromised conditions (Horseman and Surani, 2011; Oliver, 2013). Although the reason for the age risk factor is not known, estrogen, the major female hormone, appears to be a protective material after exposure to endotoxin (Oliver, 2005a). The symptoms are typically developed within 7 h post-ingestion of oysters, to 10 days (Oliver, 2005a). The mortality rate for *V. vulnificus* septicemia is over 50%, and death can occur within the first 24 h after onset of illness (Daniels, 2011; Horseman and Surani, 2011).

In addition to ingestion of *V. vulnificus*, the bacterium also can infect pre-existing wounds. Most cases are wounds acquired during cleaning shellfish, or contact of a wound into the seawater containing *V. vulnificus* (Oliver, 2005a). Like ingestions cases, most of wound cases are in males. Symptoms of the wound infection include fever, chills, edema, and cellulitis (Oliver, 2015). During rapid progression of wound infection, necrotizing fasciitis and cellulitis occur in the lesions from which *V. vulnificus* is isolated (Oliver, 2005b). Chronic disease such as liver damage does not appear to be a prerequisite to these infections and the mortality for the wound infection is ranging from 20% to 30% (Oliver 2005b; Oliver 2015).

Although least important among the three syndromes manifested by *V. vulnificus*, the bacterium is also realized to produce mild symptoms including diarrhea and abdominal cramps (Horseman and Surani, 2011). Like the case of fetal septicemia infection, this gastroenteritis appears to be associated with ingestion of raw seafood. However, no fatalities from *V. vulnificus* gastroenteritis have been reported (Oliver, 2005a).

In South Korea, total number of reported *V. vulnificus* infection is 181 for the last three years (from 2012 to 2014), among which 108 were dead (60%) (Korea Centers for Disease Control and Prevention, KCDC; http://is.cdc.go.kr/nstat/index.jsp). In

Taiwan, most reported cases occur in people of southern region (Hsueh *et al.*, 2004). In the United States, the incidence of *V. vulnificus* infection is increasing. There was an average 52 cases/year reported to the Cholera and Other *Vibrio* Illness Surveillance (COVIS) system from 2000 to 2010 while 24/year were reported between 1988 and 1999 (Oliver, 2015).

I-1-2. Virulence factors of *V. vulnificus*

There have been many studies aimed at investigating a complex phenomenon of *V. vulnificus* infections and numerous individual bacterial surface factors and extracellular proteins have been characterized (Jones and Oliver, 2009). The following sections will describe the characteristics of important virulence factors of *V. vulnificus* consisting of capsular polysaccharide (CPS), lipopolysaccharide (LPS), hemolysin (VvhA), multifunctional-autoprocessing repeats-in-toxin (MARTX, RtxA1), adhesion factors, and so forth.

Capsular polysaccharide (CPS)

Of all known virulence factors among many pathogens, the presence of a polysaccharide capsule is well described (Cress *et al.*, 2014). *V. vulnificus* also produces a firmly linked form of extracellular polysaccharide called capsular polysaccharide (CPS) (Chatzidaki-Livanis *et al.*, 2006). The change of colonies

morphology is dependent on whether the CPS is present or absent on the surface of *V. vulnificus*; encapsuled strain is opaque and nonencapsuled strain is translucent (Wright *et al*., 1999; Oliver, 2005a). The surface expression of CPS confers resistance to opsonization and evasion of phagocytosis by complement and macrophages, respectively (Kashimoto *et al*., 2003; Williams *et al*., 2014). In addition, the presence of CPS contributes to survival of *V. vulnificus* in serum by masking immunogenic structure (Strom and Paranjpye, 2000; Williams *et al*., 2014). Consequently, the encapsuled *V. vulnificus* cells are more invasive in subcutaneous tissue and are more slowly cleared from the bloodstream compared to the nonencapsuled cells (Yoshida *et al*., 1985). Indeed, injection of the opaque morphotype into mice yields lower LD_{50} values than the translucent morphotype (Simpson *et al*., 1987). Consistent with this, inactivation of genes related to CPS biosnythesis (*wbpP*) or transportation (*wza*) of *V. vulnificus* abolished capsule expression and resulted in attenuated virulence (Wright *et al*., 2001; Park *et al*., 2006).

Lipopolysaccharide (LPS)

While the CPS of *V. vulnificus* is important for invasion of host cells and survival in serum, lipopolysaccharide (LPS) of the pathogen plays a crucial role for development of severe disease. Infection by using purified LPS isolated from *V. vulnificus* resulted in dramatic decline in heart rate and blood pressure of mice,

leading to rapid death within 30-60 min (McPherson *et al*., 1991; Jones and Oliver, 2009). In addtion, LPS not only elicits small cytokine response in mice but also stimulates host immune response via nitric oxide synthesis activity (McPherson *et al.*, 1991; Elmore *et al*., 1992). Especially, low density lipoprotein (LDL) cholesterol and estrogen appear to be protective against LPS. Pretreatment of LDL prior to LPS exposure shows significantly reduced mortality compared to LPS expsoure (control) in the mouse model (Strom and Pyranjype, 2000).

Hemolysin (VvhA) and RtxA1 toxin

VvhA, secreted hemolysin encoded by *vvhA*, contributes to the pathogenesis of *V. vulnificus* through the hemolytic and cytotoxic activity (Wright and Morris, 1991; Miyoshi *et al*., 1993). A C-terminal domain of VvhA is a β-trefoil lectin and displays a preference for terminal group including *N*-acetylgalactosamine (GalNAc) and *N*-acetyllactosamine (Kaus *et al*., 2014). Secreted VvhA monomers oligomerize into a pre-pore intermediate in a cholesterol dependent manner (Kim and Kim, 2002) and undergo rearrangement of structure that forms transmembrane channels in a target cell membrane (Kaus *et al*., 2014). When the purified VvhA is intradermally administrated into mice, damaged or necrotic fat cells, capillary endothelial, and muscle cells, inflammatory infiltration, and acute cellulitis are observed (Gray and Kreger, 1987; Lee *et al*., 2005). Additionally, VvhA causes cell death by pore

formation in the cellular membrane followed by an increase of vascular permeability and hypotension (Kim *et al*., 1993). Apoptosis of endothelial cell, induction of inducible nitric oxide synthase (iNOS) activity, and nuclear factor (NF)-κB-dependent mitochondrial cell death also have been demonstrated to be caused by VvhA (Kwon *et al*., 2001; Kang *et al*., 2002; Lee *et al*., 2015a). In spite of the detrimental effect of the purified VvhA, a mutant in which the *vvhA* gene was inactivated exhibits no significant change in mouse mortality compared to the wild type (Wright and Morris, 1991; Fan *et al*., 2001). Therefore, VvhA is not solely responsible for the lethality and the tissue damage.

MARTX toxins are large single polypeptide toxins produced by various *Vibrio* genus (Satchell, 2015). In *V. vulnificus*, an *rtxA1* gene encodes a full-length MARTX toxin (Lee *et al*., 2007). RtxA1 produced by *V. vulnificus* showed high level of identity (80% ~ 90% in amino acid sequences) with that produced by *Vibrio cholerae*, and genetic organization of two *rtx* cluster (*rtxHCA* and *rtxBDE*) is also similar (Kim *et al*., 2008). However, RtxA1 domain structure among the *V. vulnificus* isolates are strikingly diverse (Kwak *et al*., 2011; Satchell, 2015). The secretion of the RtxA1 is mediated by a type I secretion system (T1SS) comprised of ATPases RtxB and RtxE, a transmembrane linker RtxD, and the outer membrane porin TolC (Boardman and Satchell, 2004; Lee *et al*., 2008; Gavin and Satchell, 2015). The most remarkable

ability of RtxA1 is to induce cytolysis of a wide range of host cell types including erythrocytes, epithelial cells, and macrophages (Lee *et al.*, 2007; Lo *et al.*, 2011; Jeong and Satchell, 2012). RtxA1 is required for necrotic and apoptotic cell death by triggering increased generation of reactive oxygen species (ROS) via activation of Rac2 and Nox (Chung *et al.*, 2010). Additionally, RtxA1 also contributes to host cellular changes such as cytoskeleton rearrangement, bleb formation, actin aggregation, and survival of *V. vulnificus* against killing effect of macrophages (Kim *et al.*, 2008; Lo *et al.*, 2011). In mouse model where the bacterial cells are delivered both intraperitonially and subcutaneously, the strain deficient in RtxA1 shows a significant higher LD_{50} than the wild type (Lee *et al.*, 2007; Liu *et al.*, 2007; Kim *et al.*, 2008). Interestingly, for intragastric infection, the RtxA1 has been shown to have a most substantial impact on infection than other two infection routes (Kwak *et al.*, 2011; Jeong and Satchell, 2012). During intestinal infection, RtxA1 and VvhA have been demonstrated to play an additive role in tissue damage and inflammation that promotes dissemination of the infecting bacteria to the bloodstream and other organs (Jeong and Satchell, 2012).

Adhesion factors

Adhesion to the mucosal and host surfaces followed by colonization on host tissue is considered to constitute the first stages of the bacterial infection process (Ofek *et*

al., 2013). Like many other pathogenic bacteria, *V. vulnificus* also expresses diverse adhesion molecules including pili, a flagellum, a lipoprotein, and OmpU that are essential for adhesion to human epithelial cells *in vitro* and virulence in mice (Kim and Rhee, 2003; Lee *et al*., 2004; Paranjpye and Strom, 2005; Goo *et al*., 2006; Lee *et al*., 2010).

Pili are adhesive hair-like organelles that stock out form the surface of bacteria. These filamentous structures constitute a scaffold-like rod protruding on the surface of bacterial outer membrane and is a bacterial adherence factor located at the top of the scaffold (Pizarro-Cerdá and Cossart, 2006). In *V. vulnificus*, an increased piliation correlates with adherence of the pathogen (Strom and Paranjpye, 2000). Consistently, the inactivation of genes required for the biosynthesis of type IV pili, *pilA* and *pilD* encoding the pilin structural protein and pre-pilin peptidase, respectively, abolishes expression of surface pili and results in reduced adherence to host cells as well as decreased virulence of *V. vulnificus* in mice (Paranjpye *et al*., 1998; Paranjpye and Strom, 2005).

A single polar flagellum also provides the bacterium with effective means of motility and plays a crucial role in adhesion and lethality to mice. Loss of two flagella structural components, encoded by *flgC* and *flgE*, resulted in a significant decrease

in motility, adhesion, and cytotoxicity compared to wild type, suggesting that the *flg* genes contribute to the pathogenesis of *V. vulnificus* (Kim and Rhee, 2003; Lee *et al*., 2004).

In addition, a membrane-bound lipoprotein (IlpA) and OmpU are also adhesion molecules as virulence factors of *V. vulnificus* (Lee *et al*., 2010). An *ilpA*-deleted *V. vulnificus* mutant exhibited decreased adherence and cytotoxicity to human intestinal epithelial cells (Lee *et al*., 2010). IlpA protein also triggers cytokine production by activating toll-like receptor 1 (TLR1)/TLR2, MyD88, and NF-κB/activator protein-1 (AP-1) (Lee *et al*., 2011). OmpU, one of the major outer proteins of *V. vulnificus*, is a fibronectin binding protein essential for cytoadherence to HEp-2 cells and mortality in mice (Goo *et al*., 2006).

Other virulence factors

Phospholipases destabilize the membrane of the host cells and induce cell lysis by cleaving phospholipids (Schmiel and Miller, 1999; Ghannoum, 2000). In *V. vulnificus*, the phospholipase A (PLA) activity is important in *V. vulnificus*-induced cytotoxicity and lethality (Koo *et al*., 2007). Since a gene encoding PLA has not been identified, the studies for elucidating the functional and regulatory mechanism of PLA must be needed.

I-1-3. Regulation of virulence factors in *V. vulnificus*

For acquiring the maximum efficiency during pathogenesis, the expressions of many virulence factors of pathogens are tightly regulated by common regulatory proteins in response to environmental changes. This coordinated regulation stimulates the cooperation of virulence factors and is essential for the overall success of the pathogens during infection (Cotter and DiRita, 2000; Maston *et al*., 2007). Although studies about regulatory proteins involved in the regulation of *V. vulnificus* virulence factors are still limited, the roles of iron-sulfur cluster regulator (IscR), cAMP receptor protein (CRP), a LuxR homologue SmcR, and transcriptional activator HlyU on the virulence gene regulation have been characterized (Choi *et al.*, 2002; Liu *et al*., 2009; Lim and Choi, 2014; Jang *et al*., 2016).

Iron-sulfur cluster regulator (IscR)

IscR, an iron-sulfur (Fe-S) cluster containing transcription factor, functions as a sensor of the cellular Fe-S cluster status and adjusts the synthesis of the Fe-S biogenesis for maintaining Fe-S homeostasis in *Escherichia coli* (Schwartz *et al.*, 2001; Giel *et al*., 2013). Under conditions favoring stabilization of the Fe-S cluster (mostly in anaerobic growth), sufficient Fe-S cluster occupies IscR to result in [2Fe-2S]-IscR (holo-IscR). When the [2Fe-2S] cluster in IscR is disrupted under conditions such as oxidative stress or iron starvation, the resulting clusterless IscR

(apo-IscR) relieves the repression of the *isc* operon, increases the cellular level of IscR, most likely in its apo-form, and accordingly, promotes Fe-S cluster biogenesis (Schwartz *et al*., 2001; Giel *et al*., 2013; Zheng *et al*., 2001; Outten *et al*., 2004; Imlay, 2006). IscR binds two distinct DNA sequences, Type 1 and Type 2, depending on the [2Fe-2S] occupancy of the protein. (Nesbit *et al*., 2009; Fleischhacker *et al*., 2012; Yeo *et al*., 2006). Furthermore, IscR regulates many genes seemingly related to the pathogenesis of pathogens including *V. vulnificus*, *Yersinia pseudotuberculosis*, *Xanthomonas campestris*, and *Pseudomonas aeruginosa* (Kim *et al*., 2009; Lim and Choi, 2014; Miller *et al*., 2014; Fuangthong *et al*., 2015). As examplified by *V. vulnificus*, IscR upregulates many genes most likely involved in motility and adhesion to host cells, hemolytic activity, and survival under oxidative stress and its expression is induced by exposure to host cells (Lim and Choi, 2014; Lim *et al*., 2014; Jang *et al*., 2016).

cAMP receptor protein (CRP)

CRP, cyclic-AMP (cAMP) receptor protein, perceives carbon and energy shortage by sensing the level of cAMP and controls transcription at more than 100 promoters in *E. coli* (Busby and Ebright, 1997; Green *et al*., 2014). Each monomer of CRP homodimer comprises three major structural features. A high-affinity cAMP-binding domain and a helix-turn-helix DNA-binding domain are located at the N-terminal and the C-terminal domain, respectively. These two domains are linked by a long

helix that forms a coiled-coil at the interface of CRP dimer (Green *et al*., 2014). In addition, CRP also regulates genes required for DNA uptake system by binding to unusual CRP-binding site called CRP-S (Cameron and Redfield, 2007). Moreover, CRP regulation has been observed in the synthesis of the virulence factors of *V. vulnificus* such as hemolysin, elastase, iron-binding protein, and mucin-binding protein (Choi *et al*., 2002; Jeong *et al*., 2003; Oh *et al*., 2009; Jang *et al*., 2016).

SmcR

Quorum sensing is a bacterial cell-to-cell communication process that involves the sensing of diffusible signaling molecules as a method to monitor their cell population (Ng and Bassler, 2009). This communication has been recognized as a global regulatory system controlling the expression of numerous virulence factors in pathogens (Autunes *et al*., 2010; Rutherford and Bassler, 2012). *Vibrio harveyi* luminescence gene regulation in response to the cell density is frequently used as a model for quorum sensing. LuxR, a quorum-sensing master regulator in *V. harveyi*, is a transcriptional activator of the luminescence operon, and its synthesis is regulated by the levels of three autoinducers: AI-1, AI-2, and CAI-1 (Ng and Bassler, 2009). SmcR, a LuxR homologue, has been proposed as a quorum sensing master regulator of *V. vulnificus* because of similarities between the components of quorum-sensing systems in *V. vulnificus* and *V. harveyi* (McDougald *et al*., 2000). Recent studies demonstrated that SmcR appears to control many genes related to the

virulence and survival of the pathogen (McDougald *et al*., 2001; Jeong *et al*., 2003; Lee *et al*., 2007; Kim *et al*., 2012; Jang *et al*., 2016).

HlyU

HlyU is a metal-regulated transcriptional regulatory protein and belongs to SmtB/ArsR family (Saha *et al*., 2006). HlyU is first identified in *V. cholerae* as an activator of *hlyA* encoding a hemolysin (Williams *et al*., 1993) and is also a positive regulator of toxin genes in *Vibrio* species (Liu *et al*., 2009; Li *et al*., 2011). Especially, *V. vulnificus* HlyU activates *rtxHCA* operon and *vvhA* by direct binding to their promoter regions, respectively (Liu *et al*., 2009; Shao *et al*., 2011). Since *rtxHCA* and *vvhA* encodes RtxA and VvhA essential for the pathogenesis of *V. vulnificus* (Kim *et al*., 2008; Jeong and Satchell, 2012), a mutant with disruption of *hlyU* had attenuated virulence in a mouse model (Liu *et al*., 2007). Althoguh exact mechanism of *rtxA* regulation by HlyU is still unknown, the mechanism to activate *rtxA* expression of HlyU is considered as derepression of bound histon-ike nucleoid-structuring protein (H-NS), a global repressor in Gram-negative bacteria, from the region around the *rtxHCA* promoter with higher DNA binding affinity (Stoebel *et al*., 2008; Liu *et al*., 2009). Therefore, HlyU might control other virulence factors as a master regulator of *V. vulnificus* pathogenesis.

I-2. Mucus layer

I-2-1. Mucus layer and mucin

The human gut is a complex ecosystem where the extensive intraction between microbiota, nutreients, and host cell have a huge impact upon health and disease (Etzold and Juge, 2014). In order to prevent the gut from pathogenic bacteria, the gastrointestinal (GI) tract, from the stomach to the rectum, is covered by mucus layer (McGuckin *et al*., 2011). Mucus of entire GI tract varies in thickness; 700 μm in the stomach and large intestine and 150-300 μm in the small intestine (McGuckin *et al*., 2011). This barrier is divided into an inner dense layer which is sterile and separates then from the epithelium surface, and an outer loose layer that is rich in secreted mucins and nonspecific and specific antimicrobials (Linden *et al*., 2008; McGuckin *et al*., 2011).

Mucin is a cell surface and secreted large and heavily *O*-linked glycoproteins and carbohydrates of the mucin acoount for up to 80% of the total mass (Johansson *et al*., 2011; Juge *et al*., 2016). There are five oligomerizing secreted mucins (MUC2, MUC5AC, MUC5B, MUC6, and MUC19) and nine cell surface mucins (MUC1, MUC3A, MUC3B, MUC4, MUC12, MUC13, MUC15, MUC16, and MUC17). The glycan core structures present in the mucins are diverse and comprise four core

oligosaccharides including galactose (Gal), *N*-acetylglucosamine (GlcNAc), and *N*-acetylgalactosamine (GalNAc) (Jensen *et al*., 2010). In addition, sialic acid and fucose are also major mucin glycan epitopes (Juge *et al*., 2016).

Furthermore, the mucus layer contains numerous types of antimicrobial molecules. These molecules are produced by Paneth cells and consist of cathecidines, lysozymes, lipopolysaccharide-binding protein, collectins, histatins, and secretory phospholipase A_2 (White *et al*., 1995; McGuckin *et al*., 2011). Although the structures of these molecules are vary, most of them lyse bacterial cells by interacting with microbial cell membranes. Mucin oligosaccharides also bind microbes and have direct antimicrobial activity. For example, an N-terminal histidine peptide domain of MUC7 inhibits the growth of *Candidia* spp. in saliva (Gururaja *et al*., 1999; Linden *et al*., 2008). The secretory immunoglobulin A (IgA) and IgG, produced by B cells, are essential components of the mucus layer (Strugnell and Wijburg, 2010). The antibodies affect the fitness and homeostasis of the commensal microbiota and limit the growth of the pathogen by stimulating entrapment of them.

I-2-2. Pathogens' strategies to penetrate and avoid the mucus layer

Aside from the secreted and the surface mucin, GI epithelial cells form an adjacent barrier by linking intracellular junctions and this barrier is highly resistant to

microbial passage (MuGuckin *et al*., 2011). However, many enteric pathogens have evolved a variety of elaborate strategies to penetrate and circumvent the secreted and cellular barriers to infection. These strategies include mechanisms to allow efficient penetration of the mucs layer, enzymes capable of degrading the mucins, and toxins that can disrupt epithelial cells.

Most mucosal pathogens are flagellated and flagellin-mediated motility allowing the pathogen to promote themselves within the viscous mucus barrier. Consistent with this, pathogens with disrupted flagellin function showed reduced mortility and virulence (Ramos *et al*., 2004). Especially, some pathogens such as *Helicobacter pylori* decrease the viscoelasticity of the mucus by increasing the pH of its local space, and thereby promote their motility (Celli *et al*., 2009).

In conjuction with the motility, many pathogens also produce degradative enzymes such as glycosulfatases, sialidases, *O*-acetylesterases, and mucinases to destabilize and remove the mucus layer (Corfiled *et al*., 1992; Homer *et al*., 1994; Silva *et al*., 2003). As examplified by *V. cholerae*, the expression of *hapA* encoding hemagglutinin protease HapA is induced after the exposure to intestinal mucus and this protease exhibits both cyototoxic and mucolytic activity and is required for translocation of *V. cholerae* thorugh mucin-conitaing-gels (Silva *et al*., 2003).

Furthermore, in the point of view of nutritional availability, the pathogens also have evolved glycosidases to acquire alternative nutrient such sialic acid. Recent studies suggested that the catabolic utilization of sialic acid is eseential for pathogenesis of the bacteria by enhancing growth and survival during infection (Almagro-Moreno and Boyd, 2009; Jeong *et al*., 2009)

After the pathogens have reached the epithelium, they secrete toxins to disrupt eptihelial cells and alter the production of mucins and antimcirobial molecules (Katz *et al*., 2000; Sakaquchi, *et al*., 2002). Cell lysis, apoptosis, and modulation of inflammatory signalling caused by these toxins facilitate invasion by the pathogens as well as alter the response of commensal microbiota to the mucus layer (Walk *et al*., 2010). In addition, some toxins can collapse the tight functions of epitehlial cells and this damage leads the pathogen to invade underlying tissues and promotes symptoms of gastroenteritis (Guttman and Finlay, 2009).

I-3. Objective of this study

Mucus layer is the first barrier that the enteropathogens encounter and prevents the pathogens from reaching and persisting on the intestinal epithelial surfaces, and being a major component of innate immunity. Among the components of the mucus layer, mucins are complex linear polymorphic glycoproteins and up to 85% of their dry weight is carbohydrate such as fucose, galactose, *N*-acetylglucosamine, and sialic acid. Therefore, many pathogens including *V. vulnificus* have evolved a range of strategies to subvert and avoid the mucus layer and thereby enhance the overall success during pathogenesis. For this reason, understanding the pathogen's strategies to interact the mucin is critically important for successful control of the pathogen. However, until now, the studies investigating transcriptomic changes of *V. vulnificus* in response to the mucus layer exposure have not been still limited. In the present study, transcriptomic profiles of *V. vulnificus* exposed to mucin-containing media and mucin-secreting host cells were determined by RNA-sequencing to identify the genes that are involved in the interaction between *V. vulnificus* and the mucin. Based on the result of transcriptome analyses, I further investigated functional and regulatory characteristics of previously unidentified genes, *gbpA* and *plp*, in the pathogenesis of *V. vulnificus*.

Chapter II.

Identification of *Vibrio vulnificus gbpA* and *plp* Genes Induced by Mucin and Mucin-secreting HT29-MTX Cell Using RNA-sequencing

II-1. Introduction

When bacteria are ingested into human intestine, they encounter the mucus layer that covers epithelium. Mucus layer, rich in mucin glycoproteins and diverse range of antimicrobial molecules including immunoglobulins, is the first barrier that the enteropathogens encounter and prevents the pathogens from reaching and persisting on the intestinal epithelial surfaces, and thereby is a major component of innate immunity (McGuckin *et al*., 2011). Mucins are complex linear polymorphic glycoproteins with molecular weights ranging from 5×10^3 to 4×10^6 Da. (Neutra and Frostner, 1987; Wiggins *et al*., 2001). Therefore, the pathogens have developed a range of strategies to subvert and avoid the mucus layer including enzymatic degradation of the mucins, secretion of toxins to mucin producing host cells, and evasion of the mucins by entering via non-mucus-covered host cells (Lindén *et al*., 2008; MuGuckin *et al*., 2011).

Vibrio vulnificus, a model enteropathogens, is a Gram-negative bacterium capable of causing diseases ranging from mild gastroenteritis to primary septicemia and wound infection (Horseamn and Surani, 2011; Oliver, 2015). The mortality of primary septicemia caused by *V. vulnificus* is approximately 50% and death can occur within one to two days after the first signs of illness (Jones and Oliver, 2009). Numerous

individual bacterial surface factors and extracellular proteins have been accounted for the fulminating and destructive nature of *V. vulnificus* infections (Jones and Oliver, 2009). The expression of these factors is coordinately regulated by global regulators such as cAMP receptor protein (CRP), Fe-S cluster protein IscR, a luxR homologue SmcR, and transcriptional activator HlyU (Choi *et al*., 2002; Jeong *et al*., 2003; Oh *et al*., 2009; Liu *et al*., 2009; Lim and Choi, 2014). Since *V. vulnificus* cells were usually ingested in the host as a contaminant of raw seafood (Oliver, 2013), they might be exposed to the mucus layer at the initiation stage of infection and alter their gene expression patterns to adapt and survive in the mucus layer. However, until now, the studies investigating global-level gene expression of *V. vulnificus* in response to the mucus layer exposure are still limited (Bisharat *et al*., 2013).

In recent year, RNA sequencing technology has emerged as conceptually novel approach for studying bacterial transcriptomes such as comparison of gene expression profiling, discovery of unannotated genes, and determination of operons (Metzker, 2010; Pinto *et al*., 2011; Creecy and Concway, 2015). Since most previous methods of transcriptome analysis were dependent on hybridization of particular oligonucleotides to target loci for their sequence specificity, RNA-seq offers several advantages including an unbiased and higher sensitivity for low abundance transcripts, greater dynamic range for measuring variability in expression levels, and

single nucleotide resolution of transcript boundaries (Croucher and Thomson, 2010; Sorek and Cossart, 2010). Furthermore, recent studies showed that dual RNA-seq allow the host and pathogen transcriptomes to be analyzed in parallel and reveal the complex interaction between a bacterial pathogen and its mammalian host during infection (Westermann *et al*., 2012; Baddal *et al*., 2015; Westernmann *et al*., 2016). Therefore, RNA-seq is capable of characterizing the entire transcription of the specific organism in the result using the sample containing host and pathogen RNA, both quantitatively and qualitatively (Sheikh *et al*., 2011; Bisharat *et al*., 2013; Jorth *et al*., 2013).

In the present study, transcriptional response of *V. vulnificus* to the mucin and mucin-secreting host cells was investigated. The growth and survival of *V. vulnificus* cells exposed to M9 medium supplemented with 0.6% (*wt*/*vol*) mucin (M9M) and HT29-metotrexate (MTX) cells were monitored, respectively. I used the method of RNA-seq to monitor the levels of all transcripts in the bacteria grown in the M9 medium supplemented with 0.4% (*wt*/*vol*) glucose (M9G) and M9M. Also, transcriptomes of the bacteria exposed to basal medium eagle (BME) and the HT29-MTX cells were analyzed using the same method. From the analysis, 337 genes were identified to be differentially expressed with significance between the M9G and the M9M. In addition, the analysis of RNA-seq data and comparison identified 650 genes with

altered transcript level in the bacteria exposed to the HT29-MTX cells compared to the BME. Furthermore, several virulence related genes encoding metalloprotease, *N*-acetylglucosamine binding protein, cytolysin, and phospholipase were induced by the mucin and the mucin-secreting host cells.

II-2. Materials and Methods

II-2-1. Strains, plasmids, and culture conditions

The strains and plasmids used in this study are listed in Table II-1. Unless otherwise noted, the *V. vulnificus* MO6-24/O were grown in Luria-Bertani (LB) medium supplemented with 2% (*wt/vol*) NaCl (LBS) at 30°C, and their growth was monitored spectrophotometrically at 600 nm (A_{600}).

Table II-1. Bacterial strains and plasmids used in this study

Strain or plasmid	Relevant characteristics[a]	Reference or source
Bacterial strains		
V. vulnificus		
MO6-24/O	Clinical isolate; virulent	Wright *et al*., 1990
MORR	MO6-24/O with spontaneous Rif^r mutation, virulent	Hwang *et al*., 2013
MORSR	MO6-24/O with spontaneous Rif^r, Sm^r mutation, virulent	Hwang *et al*., 2013
HS03	MO6-24/O with *smcR::nptI*; Km^r	Jeong *et al*., 2003
DI0201	MO6-24/O with Δ*crp*	Choi *et al*., 2002
MS023	MO6-24/O with Δ*pilD*	Lim *et al*., 2011
JK093	MO6-24/O with Δ*iscR*	Lim and Choi, 2014
JK128	MO6-24/O with $iscR_{3CA}$ encoding the apo-locked IscR, $IscR_{3CA}$	Lim *et al*., 2014
SO111	MO6-24/O with Δ*gbpA*	This study
KK131	MO6-24/O with Δ*plp*	This study
KK141	MORSR Δ*gbpA*; Rif^r, Sm^r	This study
KK142	MO6-24/O with Δ*iscR*Δ*crp*	This study
KK151	MO6-24/O with Δ*hlyU*Δ*crp*	This study
ZW141	MO6-24/O with Δ*hlyU*	This study
E. coli		
S17-1λ*pir*	λ-*pir* lysogen; *thi pro hsdR hsdM*$^+$ *recA* RP4-2 Tc::Mu-Km::Tn7;Tp^r Sm^r; host for π-requiring plasmids; conjugal donor	Simon *et al*., 1983
BL21 (DE3)	F$^-$ *ompT hsdS*$_B$ (r_B^- m_B^-) *gal dcm* (DE3)	Laboratory collection
Plasmids		
pGEM-T easy	PCR product cloning vector; Ap^r	Promega
pKK1401	pGEM-T Easy with 390-bp fragment of *gbpA* upstream region; Ap^r	This study

pKK1501	pGEM-T Easy with 461-bp fragment of *plp* upstream region; Ap^r	This study
pDM4	R6K γ *ori sacB*; suicide vector; *oriT* of RP4; Cm^r	This study
pSO1101	pDM4 with Δ*gbpA*; Cm^r	This study
pBS0907	pDM4 with Δ*crp*; Cm^r	This study
pKK1301	pDM4 with Δ*plp;* Cm^r	This study
pZW1401	pDM4 with Δ*hlyU;* Cm^r	This study
pJK1113	pKS1101 with *nptI*; Ap^r, Km^r	Lim *et al*., 2014
pKK1402	pJK1113 with *gbpA*; Ap^r, Km^r	This study
pKK1403	pJK1113 with *iscR*; Ap^r, Km^r	This study
pKK1404	pJK1113 with *crp*; Ap^r, Km^r	This study
pKK1405	pJK1113 with *smcR*; Ap^r, Km^r	This study
pJH0311	0.3-kb MCS of pUC19 cloned into pCOS5; Ap^r, Cm^r	Goo *et al*., 2006
pMS0908	pJH0311 with pilD; Ap^r, Cm^r	Lim *et al*., 2011
pKK1320	pJH0311 with *plp*; Ap^r, Cm^r	This study
pZW1510	pJH0311 with *hlyU*; Ap^r, Cm^r	This study
pKK1502	pJH0311 with *crp*; Ap^r, Cm^r	This study
pET22a(+)	His_6 tag fusion expression vector; Ap^r	Novagen
pET28a(+)	His_6 tag fusion expression vector; Km^r	Novagen
pMBP-paralell	Protein expression vector; Ap^r	Sheffield *et al*., 1999
pSO1201	pET22a(+) with *gbpA*; Ap^r	This study
pJK0928	pET28a(+) with *iscR*; Ap^r	Lim and Choi, 2014
pHK0201	pRSET A with *crp*; Ap^r	Choi *et al*., 2002
pHS104	pRSET C with *SmcR*; Ap^r	Jeong *et al*., 2003
pYU1317	pET28a(+) with *hlyU*; Km^r	This study
pKK1503	pMBP-parallel with *plp*::His_6; Ap^r	This study
pKK1504	pET28a(+) with truncated *plp*; Km^r	This study
pBBR-lux	Broad host range vector with *luxCDABE* operon; Cm^r	Lenz *et al*., 2004
pKK1407	pBBR-lux with 555-bp fragment of *gbpA* upstream region; Cm^r	This study
pKK1408	pBBR-lux with 451-bp fragment of *gbpA* upstream region; Cm^r	This study
pKK1409	pBBR-lux with 411-bp fragment of *gbpA* upstream region; Cm^r	This study

pKK1410	pBBR-lux with 341-bp fragment of *gbpA* upstream region; Cm^r	This study
pKK1514	pBBR-lux with 378-bp fragment of *plp* upstream region; Cm^r	This study
pKK1515	pBBR-lux with 308-bp fragment of *plp* upstream region; Cm^r	This study
pKK1516	pBBR-lux with 228-bp fragment of *plp* upstream region; Cm^r	This study
pKK1517	pBBR-lux with 129-bp fragment of *plp* upstream region; Cm^r	This study

[a] Rif, rifampicin resistant; Sm^r, streptomycin resistant; Km^r, kanamaycin resistant; Tp^r, trimethoprim resistant; Ap^r, ampicillin resistant; Cm^r, chloramphenicol resistant

II-2-2. Growth kinetics of *V. vulnificus*

Pig gastric mucin powder (Sigma, St. Louis, MO) was sterilized by mixing with 95% (*vol/vol*) ethanol for 1 h, dried at 70°C for 24 h (Yeung *et al.*, 2012) and then added to M9 minimal medium (Sambrook and Russell, 2001) without carbon sources, to the final concentration of 0.6% (*wt/vol*). The *V. vulnificus* MO6-24/O cells were grown M9G or M9M for 10 h, and the growth was monitored by enumerating bacterial cells as number of colony forming unit (CFU) on LBS agar plates.

II-2-3. Development of the mucin-secreting cells and survival kinetics of *V. vulnificus*

The human colonic HT29 cells (ATCC®HTB-38™) (ATCC, Manassas, VA) in McCoy's 5A media (Gibco-BRL, Gaithersburg, MD) containing 1% (*vol/vol*) fetal bovine serum (MCF) were developed into mucin-secreting cells, named HT29-MTX, as described previously (Lesuffleur *et al*., 1990). The HT29-MTX cells were fixed with para-formaldehyde and treated with DAPI (4', 6-diamidino-2-phenylindole). Mucin secretion of the HT29-MTX cells was detected with the anti-mucin5AC (MUC5AC) primary antibody (Merck Millipore, Darmsadt, Germany), labeled with the fluorescein isothiocyanate (FITC)-conjugated secondary antibody (Abcam, Cambridge, UK), and visualized using a confocal laser scanning microscope (CLSM) (LSM710, Zeiss, Jena, Germany) (Kapuscinski, 1995; Vieira *et al*., 2010).

The wild type cells (~2×10^8 CFU) were exposed to either basal medium eagle (BME) or HT29-MTX cells (approximately 1×10^7 cells per well) in the 12-well culture dishes. Non-adherent bacterial cells in the culture supernatants were recovered after 1- to 5-h exposure and then the culture dishes treated with 0.1% Triton X-100 for 20 min to recover adherent bacteria. The total bacterial cells were enumerated as CFU per well.

II-2-4. RNA preparation, library construction, and sequencing

The wild type cultures were grown in M9G for 4 h and M9M for 3 h, fixed with 2:1 volumes of RNAprotect Bacteria Reagent (Qiagen, Valencia, CA) and harvested. Similarly, the wild type cells (~2×10^8 CFU) were also exposed to BME or HT29-MTX cells (approtximately 2×10^7 cells in cell culture dish (SPL, Gyeonggi, South Korea)), fixed and harvested. Total RNA was isolated from the pellet using miRNeasy Mini Kit (Qiagen) according to manufacturer's instructions. Genomic DNA in the purified RNA was removed with digestion using TURBO^{TM} DNase (Ambion, Austin, TX) to below PCR-detectable levels. RNA quality was determined using Bioanalyser (Agilent, Palo Alto, CA) and quantified using Nano-Vue (Ge Healthcare, New Jersey, USA) after every manipulation step. 23S and 16S rRNA were depleted using MICROBExpress kit (Ambion).

II-2-5. First and second strand synthesis

First and second strand synthesis (FSS and SSS) reactions were performed following the procedures developed by Parkhomchuk *et al.*, 2009 with minor modifications. Briefly, FSS reaction was prepared by mixing 0.5 µg of the enriched mRNA and 40 ng of $(dN)_6$ primers (Invitrogen, Carlsbad, CA) in 8.5 µl of 1× reverse transcription buffer (Invitrogen), 0.5 mM dNTPs, 5 mM $MgCl_2$ and 10 mM DTT. The mixture was incubated at 98°C for 1 min to melt RNA secondary structures, then at 70°C for 5 min and was cooled to 15°C. At 15°C 60 ng of actinomycin D, 20 units of RNase OUT (Invitrogen), and 100 units of Superscript® III polymerase (Invitrogen) were added to the reaction. The reverse transcription reaction was performed at 42°C for 45 min and 50°C for 25 min and the polymerase was finally inactivated at 75°C for 15 min. Remaining dNTPs were removed using mini Quick Spin DNA Columns (Roche, Basel, Switzerland).

Since the Invtirogen kit was used for the SSS, the FSS buffer had to be restored after gel filtration. Water was added to the purified FSS reaction mixture to bring the final volume to 52.5 µl. The mixture was cooled on ice. Then, 22.5 µl of the 'second strand mixture' [1 µl of 10× reverse transcription buffer (Invitrogen); 0.5 µl of 100 mM $MgCl_2$; 1 µl of 0.1 M DTT; 2 µl of 10 mM mixture of each: dATP, dGTP, dCTP, and dUTP; 15 µl of 5× SSS buffer (Invitrogen); 5 units of *E. coli* ligase (NEB, Ipswich,

MA); 20 units of DNA polymerase I (NEB); and 1 unit of RNase H (Invitrogen)] were added. The SSS reaction were incubated at 16℃ for 2 h. double strand (ds) cDNA was purified on QIAquick columns (Qiagen) according to the manufacturer's instruction.

II-2-6. DNA fragmentation and preparation of libraries for Illumina sequencing platform

About 250 ng of ds cDNA was fragmented by 0.1 units of DNase I (NEB) treatment at room temperature (RT) for 1 min. The 5' and 3' ends of the cDNA fragment were repaired by using Quick Blunting^{TM} Kit (NEB). A single 3' adenosine moiety was added to the cDNA fragment using Klenow exo^{-} and dATP (NEB). The Illumina adapters (containing primer sites for sequencing and flowcell surface annealing) were ligated onto the repaired ends on the cDNA fragment using Quick LingationTm Kit (NEB). Uridine digestion was performed at 37°C for 15 min using 1 unit of Uracil *N*-Glycosylase (UNG; Applied Biosystems, Foster City, CA). The libraries were amplified by 18 cycles of PCR using Phusion® High-Fidelity DNA polymerase (NEB).

II-2-7. Sequencing and data analysis

Sequencing libraries were denatured with sodium hydroxide and diluted to 3.5 pM in hybridization buffer for loading onto a single lane of an Illumina GAIIx flowcell. Cluster formation, primer hybridization, and single-end, 36 cycle sequencing were performed by Chunlab (http://www.chunlab.com).

The reads obtained from RNA-sequencing were mapped to the *V. vulnificus* MO6-24/O reference genome (GenBank accession numbers CP002490 and CP002470) using CLC Genomics Workbench 5. 5. 1 (CLC Bio, Aarhus, Denmark). The relative transcript abundance was measured in reads per kilobase of transcript per million mapped sequence reads (RPKM) (Mortazavi *et al.*, 2008). The fold changes of RPKM values and their significance were assigned and the genes with 4 or greater fold change with *P*-values ≤ 0.05 were considered to be differentially expressed by the mucin and the mucin-secreting HT-29 MTX cells. To avoid outlier ratios that can result from a small number of reads, genes with fewer than 10 RPKM were sorted out. The graphs describing the results of RNA-seq, Volcano plot was created using CLC Genomics Workbench 5. 5. 1 (CLC Bio).

II-3. Results and Discussion

II-3-1. Growth kinetics of *V. vulnificus*

To assay the ability of *V. vulnificus* to use a mucin as a sole carbon source, growth was determined for the wild type in M9G or M9M as a sole carbon source (Fig. II-2*A*). When the mucin was used as a sole carbon source, the growth rate of the cells grown in the M9M was even higher than that in the M9G. However, no significant differences in the stationary-phase yield of cells were observed between the M9G and M9M, indicating that *V. vulnificus* could metabolize the mucin (Fig. II-2*A*). Interestingly, the number of wild type cells grown in the M9M for 3 h was identical to that grown in the M9G for 4 h, suggesting that this condition is suitable for identifying genes required for the mucin utilization.

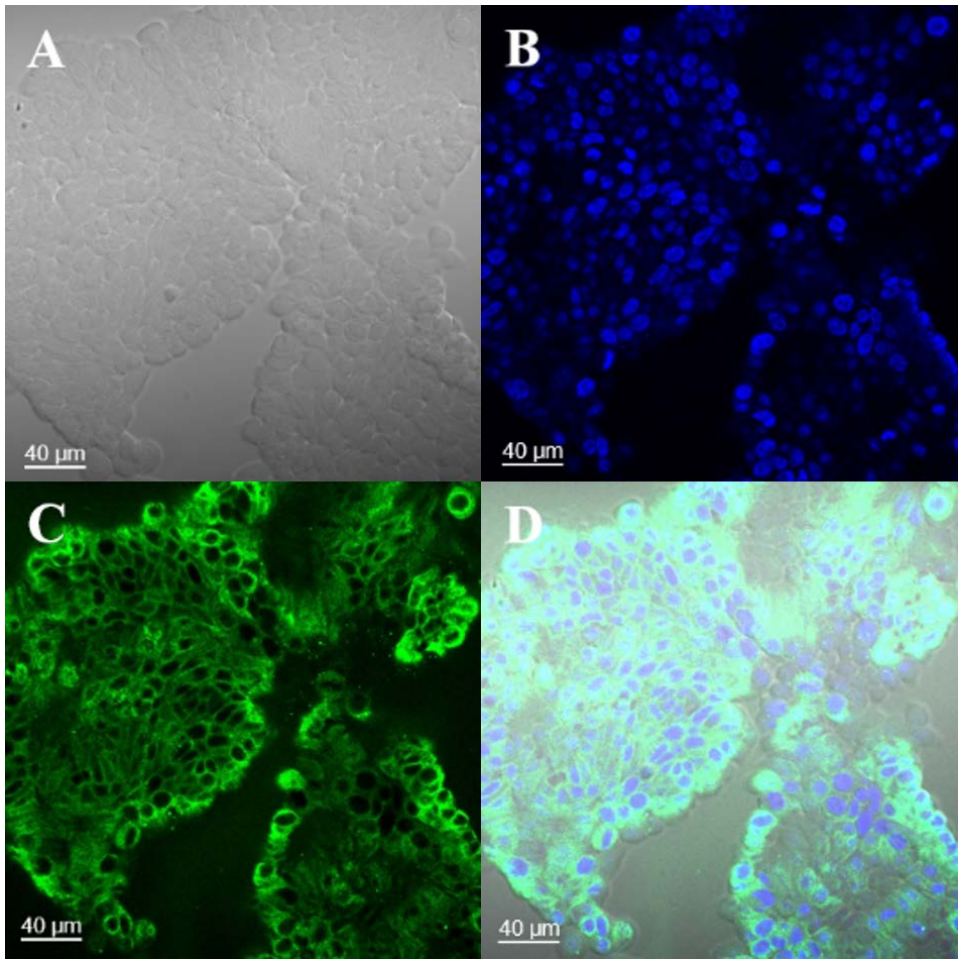

Figure II-1. Development of the mucin-secreting HT29-MTX cells. *A*, bright-field image of HT29-MTX cells. *B*, nucleus of HT29-MTX cells was stained blue with DAPI. *C*, mucin of HT29-MTX cells was stained green with the anti-MUC5AC primary antibody and then labeled with FITC-conjugated secondary antibody. *D*, the merged image of *A*, *B*, and *C*. images are visualized using a CLSM. Scale bar is 40 μm.

II-3-2. Survival kinetics of *V. vulnificus*

Previous study demonstrated that *V. vulnificus* cells is capable of using carbon sources from host cells during infection (Jeong *et al*., 2009). Therefore, it is reasonable hypothesis that the mucins secreted by host cells also could be consumed by *V. vulnificus* as a nutrition source. To examine this hypothesis, the HT-29 MTX cells, monolayers of which mimic human intestinal epithelial cells that produce and secrete mucins (Lesuffleur *et al*., 1990), were developed. Mucin secretion of the HT29-MTX cells was confirmed using a CLSM (Fig. II-1). The wild type cells were incubated with either BME or HT29-MTX cells and the total bacterial cells were enumerated (Fig. II-2*B*). The result revealed that the number of wild type cells exposed to the HT29-MTX cells was significantly higher than that exposed to the BME during the incubation, implying that *V. vulnificus* cells could utilize mucin from the host cells. It is noteworthy that the growth rate of the bacterial cells exposed to the HT29-MTX cells for 2 h is the maximum, and thus the condition is appropriate to select differentially expressed genes when *V. vulnificus* uses the mucin from the host cells.

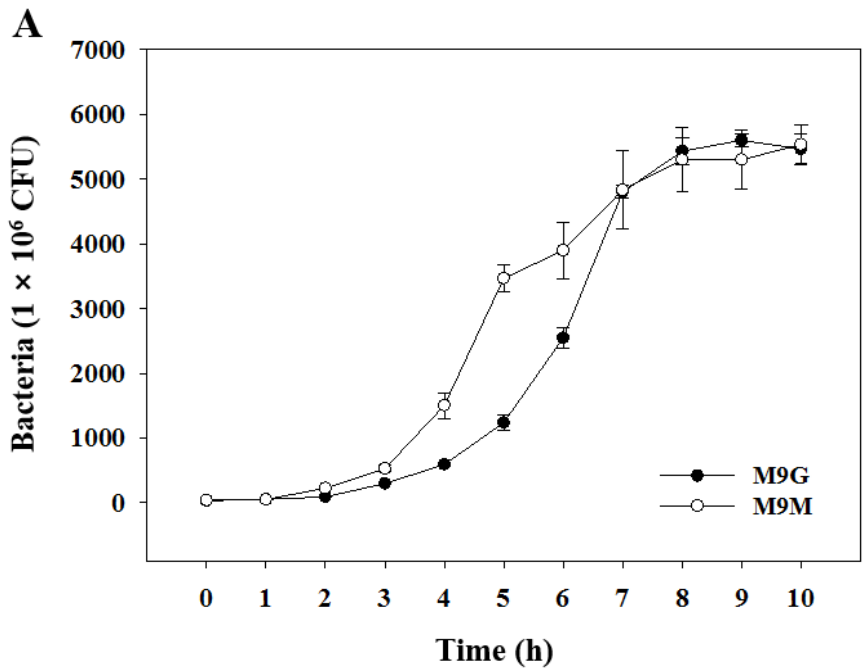
A
Bacteria (1 × 10⁶ CFU)
7000
6000
5000
4000
3000
2000
1000
0
0 1 2 3 4 5 6 7 8 9 10
Time (h)
M9G
M9M

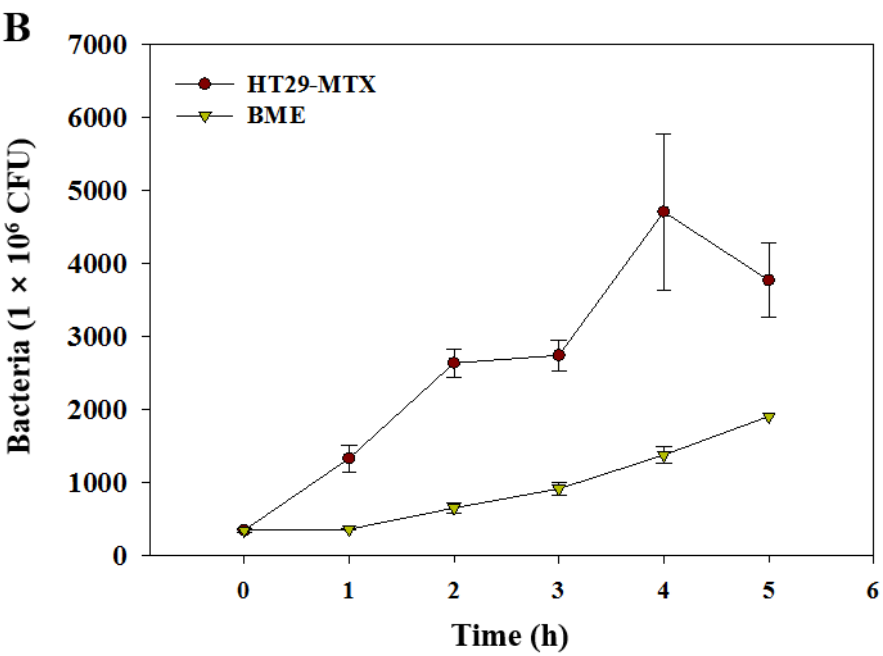
B
Bacteria (1 × 10⁶ CFU)
7000
6000
5000
4000
3000
2000
1000
0
0 1 2 3 4 5 6
Time (h)
HT29-MTX
BME

Figure II-2. Growth and survival kinetics of *V. vulnificus*. *A*, growth of the wild type culture in the M9 minimal medium supplemented with 0.4% (*wt/vol*) glucose or 0.6% (*wt/vol*) mucin was monitored by enumerating CFU on LBS agar plates. *B*, survival of the wild type cells (approximately 4×10^9 CFU) exposed to the BME or the HT29-MTX cells (approximately 2×10^8 cells) for 5 h. the bacterial cells during exposure were enumerated as described above. M9G, M9 minimal medium supplemented with 0.4% (*wt/vol*) glucose; M9M, M9 minimal medium supplemented with 0.6% (*wt/vol*) mucin; BME, basal medium eagle.

II-3-3. Summary statistics for the RNA-seq data

A mean of 38.4 million reads was obtained per each sample, of which ~99% of the reads were mapped to a single location of *V. vulnificus* MO6-24/O reference genome (Table II-2). The portion of reads derived from mRNA is relatively low (2.74%-17.8%). Since previous report demonstrated that 1 to 2 million mRNA reads per sample could identify a significant number of genes differentially expressed by 2-fold or more with high statistical significance when data from well-correlated biological replicates are included (Haas *et al.*, 2012), the number of mRNA reads from each sample was enough to examine differentially expressed genes with high accuracy (Table II-2). The similarity of the transcriptomes was analyzed by principal component analysis (PCA) (data not shown). The PCA plot of the transcriptomes derived from the bacterial cells grown in the M9G and the M9M was clearly separated. Similarly, the PCA plot of the transcriptomes derived from the bacterial cells exposed to the BME and the HT29-MTX cells was also clearly separated, proving the significant differences in their transcriptomic level.

Table II-2. Analysis of RNA-seq data mapped to the *V. vulnificus* MO6-24/O genome[a].

Number of	M9G[b,c]		M9M[b,c]		BME[b,c]		HT29-MTX[b,]	
reads	#1	#2	#1	#2	#1	#2	#1	#2
Total read	30,247,838	35,440,082	37,318,287	40,751,213	41,677,910	40,260,778	41,106,445	40,096,386
mRNA read	3,414,173	4,333,651	6,638,795	6,158,228	5,877,062	6,574,122	1,126,768	2,479,230
rRNA read	23,734,373	28,807,584	37,318,287	26,113,821	27,748,617	23,884,815	15,114,036	13,450,374
Intergenic read	2,338,096	1,561,171	3,889,176	2,583,723	7,948,793	9,673,833	1,137,144	1,361,732
Unmapped read	761,196	737,676	676,495	357,091	103,438	128,008	23,728,498	22,805,050

[a]GenBank accession numbers (CP002469 and CP002470, www.ncbi.nlm.nih.gov).

[b] #1 and 2 represent biological duplicates.

[c] M9G, M9 minimal medium supplemented with 0.4% (*wt/vol*) glucose; M9M, M9 minimal medium supplemented with 0.6% (*wt/vol*) mucin; BME, basal medium eagle.

II-3-4. Effect of mucin as a sole carbon source on the transcriptional change of *V. vulnificus*

To identify the genes involved in the growth of *V. vulnificus* in the M9M, discriminative gene expression patterns were identified from the comparison between the transcriptome of *V. vulnificus* grown in the M9G or M9M. Average RPKM value from the biological duplicate samples was used to represent the expression level of each gene. The Volcano plot exhibited that a number of genes were expressed differentially with significance (*P*-value $\leq$ 0.05, 4 fold threshold) (Fig. II-3*A*). The analysis of RNA-seq data identified 373 genes with altered transcript levels, with 202 genes showing an increase and 171 genes a decrease in mRNA concentration in the bacteria grown in the M9M compared to the M9G (Tables II-3 and II-5). The differentially expressed genes were clustered into functionally related groups using the Cluster of Orthologous Groups (COG) database for the *V. vulnificus* MO6-24/O genome (http://www.ncbi.nlm.nih.gov/COG/) (Tatusov *et al*., 1997; Tatusov *et al*., 2003). According to their COGs, the expression level of genes with various functions including amino acid metabolism and transport was significantly differed. (Fig. II-4*A*).

II-3-5. Effect of exposure to the mucin-secreting host cell on the transcriptional change of *V. vulnificus*

To identify the genes of *V. vulnificus* involved in the exposure of the HT29-MTX cells, the transcriptomes of *V. vulnificus* exposed to the BME or the HT29-MTX cells were analyzed and compared. Average RPKM values from the biological duplicate samples were also used to represent the expression level of each gene and the Volcano plot exhibited that a number of genes are discriminatively expressed with significance (*P*-value $\leq$ 0.05, 4-fold threshold) (Fig. II-3*B*). As a result, 650 genes were identified to be expressed in different level; 319 up-regulated and 331 down-regulated (Tables II-4 and II-6). To gain a broader perspective on genes differentially expressed by the HT29-MTX cells, I performed a Cluster of Orthologous Groups (COG) enrichment analysis to define distinctively regulated groups of genes (Tatusov *et al.*, 1997; Tatusov *et al.*, 2003) (Fig. II-4*B*). This analysis first clusters genes on the basis of their putative function and then examines whether a particular category is enriched for differentially expressed genes by the HT29-MTX cells (Fig. II-4*B*), indicating that *V. vulnificus* undergoes substantial changes in metabolism during the host cell exposure.

A

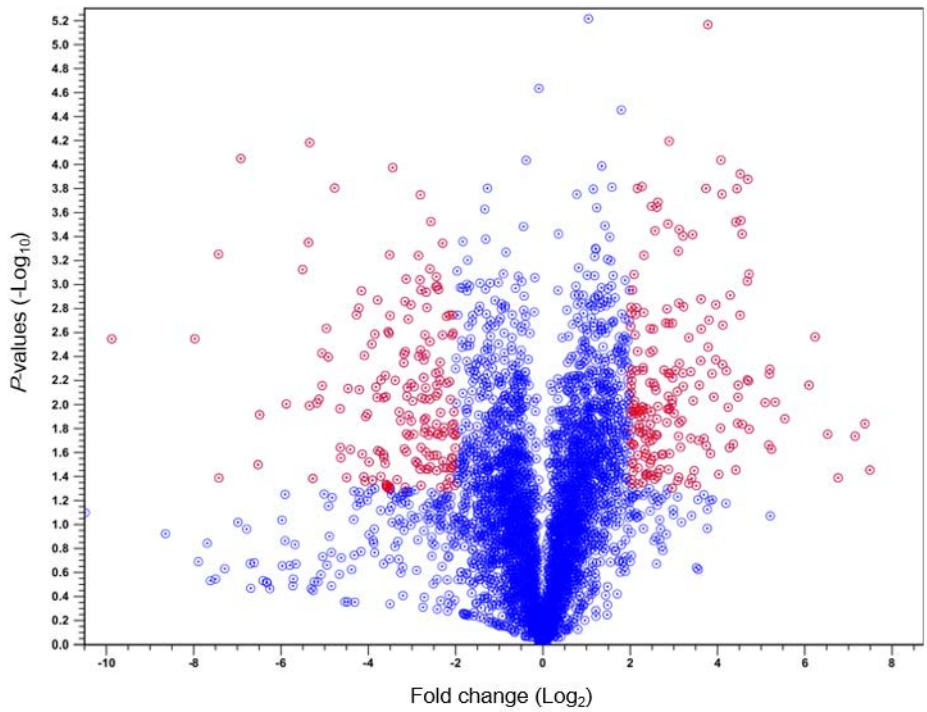
P-values (-Log10)
Fold change (Log2)

B

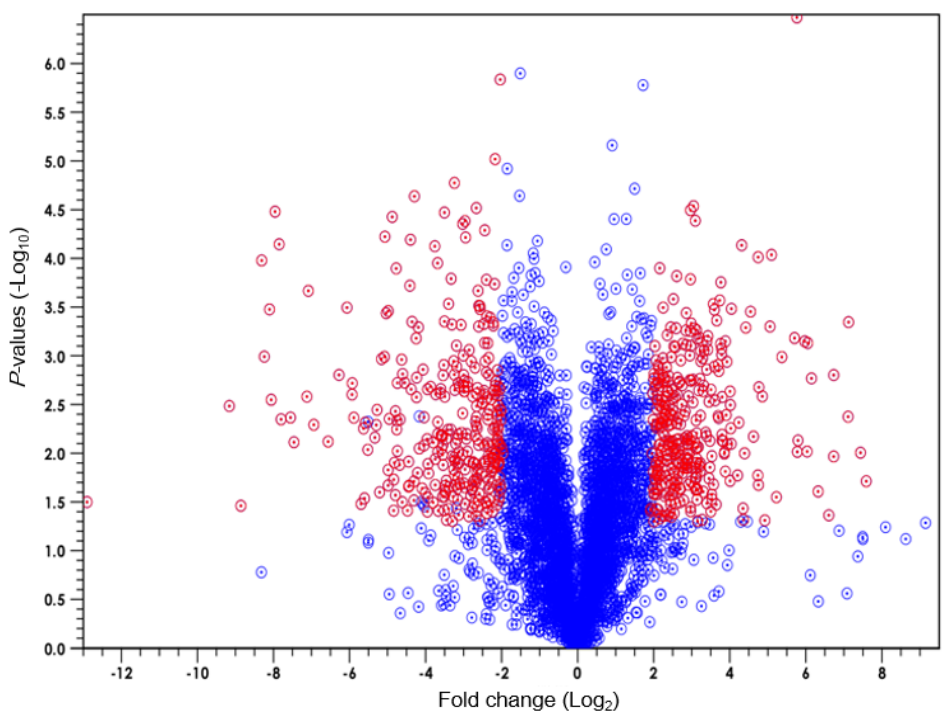
P-values (-Log10)
Fold change (Log2)

Figure II-3. Transcriptome comparisons of the RNA-seq samples. *A,* Volcano-plot of genes differentially expressed between the wild type cells grown with M9 minimal medium supplemented with 0.4% (*wt/vol*) glucose or 0.6% (*wt/vol*) mucin. *B,* Volcano-plot of genes differentially expressed between the cells exposed to the BME and the HT29-MTX cells. Number on the X- and Y-axis represent the fold change ($\log_2$) and *P*-value ($\log_{10}$). Red dots indicated that differentially expressed genes.

A

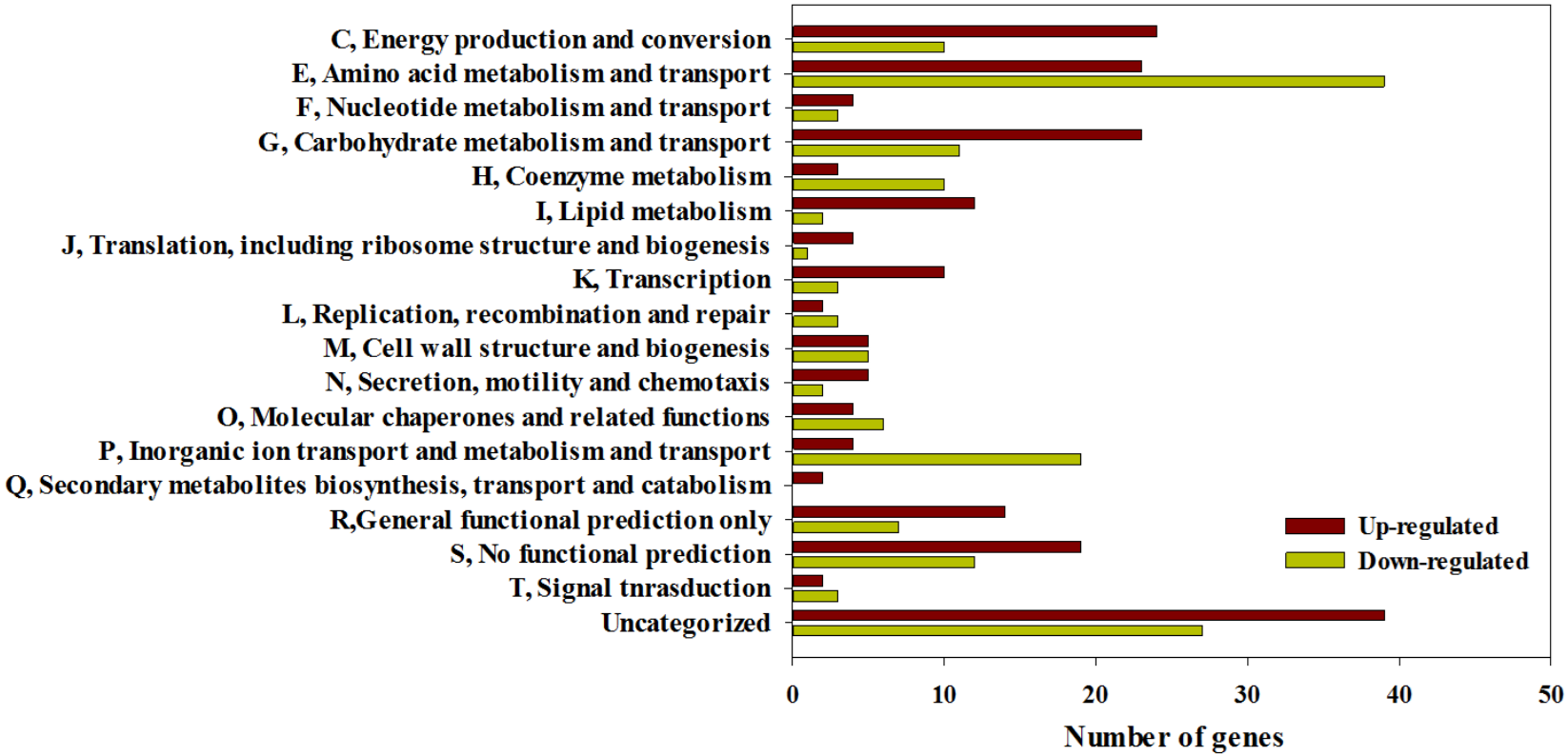
C, Energy production and conversion
E, Amino acid metabolism and transport
F, Nucleotide metabolism and transport
G, Carbohydrate metabolism and transport
H, Coenzyme metabolism
I, Lipid metabolism
J, Translation, including ribosome structure and biogenesis
K, Transcription
L, Replication, recombination and repair
M, Cell wall structure and biogenesis
N, Secretion, motility and chemotaxis
O, Molecular chaperones and related functions
P, Inorganic ion transport and metabolism and transport
Q, Secondary metabolites biosynthesis, transport and catabolism
R,General functional prediction only
S, No functional prediction
T, Signal tnrasduction
Uncategorized
Up-regulated
Down-regulated
0
10
20
30
40
50
Number of genes

B

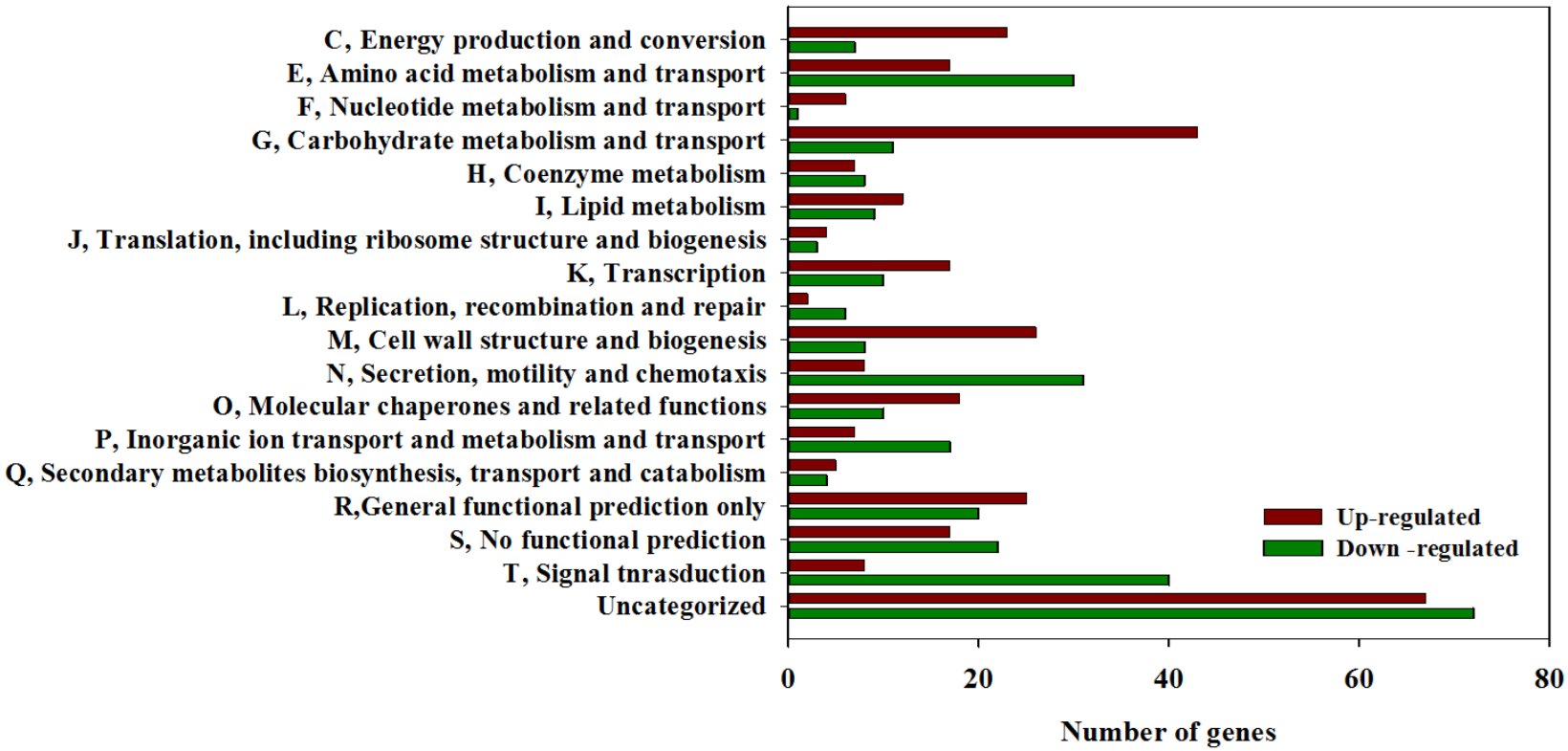
C, Energy production and conversion
E, Amino acid metabolism and transport
F, Nucleotide metabolism and transport
G, Carbohydrate metabolism and transport
H, Coenzyme metabolism
I, Lipid metabolism
J, Translation, including ribosome structure and biogenesis
K, Transcription
L, Replication, recombination and repair
M, Cell wall structure and biogenesis
N, Secretion, motility and chemotaxis
O, Molecular chaperones and related functions
P, Inorganic ion transport and metabolism and transport
Q, Secondary metabolites biosynthesis, transport and catabolism
R,General functional prediction only
S, No functional prediction
T, Signal tnrasduction
Uncategorized
Up-regulated
Down -regulated
0
20
40
60
80
Number of genes

Figure II-4. Functional categorization of genes differentially expressed by mucin. *A*, genes with expression ratios of ≥ 4.0 in the basis of RNA-seq results derived from the transcriptomes of the wild type cells grown with M9 minimal medium supplemented with 0.4% (*wt/vol*) glucose or 0.6% (*wt/vol*) mucin. *B*, genes with expression ratios of 4.0 in the basis of RNA-seq results derived from the RNA-seq results derived those of the cells exposed to the BME or the HT29-MTX cells. Functional categories (COG) are based on the database for the *V. vulnificus* MO6-24/O genome, which was retrieved from GenBank (accession numbers CP002468 and CP002470).

II-3-6. Genes up-regulated by mucin and mucin-secreting HT29-MTX cells

202 and 319 genes that were up-regulated by the mucin and the HT29-MTX cells were summarized in Table II-3 and Table II-4, respectively. Selected categories of genes were further discussed below.

Transport system of oligopeptide and peptide. Among the genes induced by the mucin, the expression of genes encoding putative oligopeptide and peptide transporter was increased (Table II-3). These genes comprise the *opp* operon (*oppA*, *oppB*, *oppC*, *oppD*, and *oppF*) and *sap* operon (*sapA*, *sapB*, *sapC*, *sapD*, and *sapE*). In *Listeria monocytogenes*, *oppA*, one gene consisting *opp* operon, encode OppA protein mediating the transport of oligopeptides. OppA protein is also required for bacterial growth at low temperature and contributes to intracellular survival in macrophages and in bacterial growth *in vivo* (Borezee *et al.*, 2000). Interestingly, the *opp* operon in *V. vulnificus* displayed the same genetic organization as that in *L. monocytogenes* and the OppA of *V. vulnificus* was 54% identical in amino acid sequences to those of *L. monocytogenes* (data not shown). A *sap* operon, firstly identified in *Salmonella enterica* Typhimurium, is required for virulence and resistance to the antimicrobial peptides melittin and protamine (Groisman *et al.*, 1992; Parra-Lopez *et al.*, 1993). In addition, a *sap* operon in *Erwinia chrysanthemi* also plays a role in the resistance to the antimicrobial peptides and the bacterial

pathogenesis (Solanilla *et al*., 1998). Especially, the open reading frames (ORFs) of *sapA* to *sapF* operon from *V. vulnificus* were closely related (55% overall amino acid identity) and were in the same order as those of the *sap* operon from *S. enterica* Typhimurium. Therefore, it is not surprising that up-regulated expression of the *opp* and the *sap* operon might contribute to *V. vulnificus* growth in the host as well as utilization of exogenous oligopeptides and peptides derived from protein backbone of mucin.

Catabolic system of sialic acid. Many enteric pathogens harbors *nan* cluster to utilize *N*-acetylneuraminic acid (Neu5Ac), which is found at the distal end of carbohydrate side chains of the mucin (Vimr *et al*., 2004; Almagro-Moreno and Boyd, 2009). In this study, seven genes (*nanA*, $nanT_L$, $nanT_S$, $nanT_P$, *nanE*, *nanK*, and *nagA*) of *nan* cluster were highly induced when *V. vulnificus* cells were grown in the M9M and exposed to the HT29-MTX cells (Table II-3 and II-5), implying that *V. vulnificus* could metabolize the Neu5Ac as a sole carbon source. Among the genes of the *nan* cluster, it has been well known that NanA contributes to *V. vulnificus* virulence by ensuring growth, adhesion, and survival during infection (Jeong *et al*., 2009) and the expression of the *nan* cluster is cooperatively regulated by NanR, CRP, and *N*-acetylmannosamine 6-phosphate (Kim *et al*., 2011). Therefore, *V. vulnificus* cells could activate the *nan* cluster genes to support the survival and growth in the

host when *V. vulnificus* cells are starved during infection.

Virulence factors. Several genes encoding putative virulence factors in *V. vulnificus* were up-regulated by the mucin and the HT29-MTX cells (Tables II-3 and II-4). The expression of *gbpA* (VVMO6_03494) encoding a homolog of *V. cholerae* GbpA (*Vc*GbpA) was up-regulated when *V. vulnificus* cells were grown in M9M. *Vc*GbpA has an elongated four domains and the mucin-binding ability of *Vc*GbpA contributes to bacterial colonization in mice (Kirn *et al*., 2005; Wong *et al*., 2012).

vvpE (VVMO6_04367) expression was highly up-regulated during the growth of *V. vulnificus* in the M9M. VvpE is a 45kDa metalloprotease that has elastase activity (Jeong *et al*., 2003). Although the role of VvpE on the virulence of *V. vulnificus* was highly controversal (Jeong *et al*., 2000; Ha *et al*., 2014), recent studies showed that the purified VvpE inhibits mucin 2 expression and stimulates IL-1β production, implying that VvpE might play an important role in intestinal colonization during infection. (Lee *et al*., 2015a; 2015b; 2016). Interestingly, the expression of *iscR* was also up-regulated under the condition that *V. vulnificus* cells were grown in the M9M. IscR, a global regulator, activates the virulence regulated genes such as *prx3*, *gbpA*, and *vvhA* and is essential for the pathogenesis of *V. vulnificus* (Lim and Choi, 2014; Lim *et al*., 2014; Jang *et al*., 2016).

The expression of *vvhBA* (VVMO6_03880 and 03881) and *toxRS* (VVMO6_02227 and 2228) operon was highly induced by exposure of *V. vulnificus* to HT29-MTX cells. VvhA, encoded by *vvhA*, is cytolytic pore-forming hemolysin and is one of essential virulence factors of *V. vulnificus* by promoting rapid growth and epithelial tissue necrosis during intestinal infection (Jeong and Satchell, 2012). The *V. cholerae toxR* and *toxS* (*VctoxR* and *VctoxS*) genes are clustered in an operon and encode transmembrane proteins *Vc*ToxR and *Vc*ToxS, respectively. *Vc*ToxR regulates expression of multiple *V. cholerae* virulence factors such as cholera toxin (*ctx*) and toxin-coregulated pilus (*tcp*) (Goss *et al*., 2013; Almargo-Moreno *et al*., 2015). Similarly, *V. vulnificus* ToxR and ToxS (*Vv*ToxR and *Vv*ToxS) activate the *vvhBA* expression (Lee *et al*., 2000). Consequently, it is perhaps not surprising that the up-regulated expression of *vvhA* might be attributed to the increased *toxRS* expression.

It is noteworthy that *plp* (VVMO6_03257) encoding putative phospholipase was highly up-regulated by the mucin and the HT29-MTX cells. The deduced *V. vulnificus* Plp (*Vv*Plp) amino acid sequence showed homology with *Vibrio angullarum* Plp (*Va*Plp) (identity, 69%; similarity, 82%). *Va*Plp, a secreted phospholipase, exhibits phospholipase A_2 activity against phosphatidylcholine and has a significant effect on hemolytic activity toward fish red blood cells (Li *et al*., 2013). Consistent with this, the study about phospholipase A (PLA) of *V. vulnificus*

indicated that PLA activity is important in *V. vulnificus*-induced cytotoxicity and lethality (Koo *et al*., 2007). Therefore, *Vv*Plp might be essential for the pathogenesis of *V. vulnificus*.

Table II-3. List of genes up-regulated by mucin

Locus tag[a]	Gene product	RPKM		Fold change	*P*-value
		M9G	M9M		
Energy production and conversion					
VVMO6_00260	Succinylglutamic semialdehyde dehydrogenase	134.83	772.31	5.73	1.E-02
VVMO6_00678	Glycerol kinase	36.23	358.91	9.91	1.E-02
VVMO6_01688	2-methylcitrate dehydratase FeS dependent	14.39	136.18	9.46	1.E-02
VVMO6_01689	2-methylcitrate synthase	17.69	421.79	23.84	1.E-03
VVMO6_01711	Glycerophosphoryl diester phosphodiesterase	33.23	179.81	5.41	2.E-03
VVMO6_01965	NrfC protein	11.25	195.6	17.39	2.E-03
VVMO6_02002	Proton/glutamate symport protein	79.45	428.17	5.39	3.E-03
VVMO6_02075	22C4-dienoyl-CoA reductase	15.67	100.23	6.40	1.E-02
VVMO6_02452	Isocitrate lyase	62.04	2079.02	33.51	6.E-03
VVMO6_02453	Malate synthase	23.14	1102.54	47.65	2.E-02
VVMO6_02595	Ubiquinol-cytochrome C reductase iron-sulfur subunit	560.79	2578.74	4.60	2.E-02
VVMO6_02875	Phosphoenolpyruvate carboxykinase	176.86	2730.86	15.44	4.E-03
VVMO6_03142	4Fe-4S ferredoxin2C iron-sulfur binding	4.86	37.34	7.68	1.E-02
VVMO6_03181	Proton/glutamate symport protein	43.26	342.52	7.92	2.E-04
VVMO6_03414	Malate synthase-related protein	18.01	301.65	16.75	2.E-04
VVMO6_03711	Iron-containing alcohol dehydrogenase	63.77	560.25	8.79	5.E-03
VVMO6_03883	Glycerophosphoryl diester phosphodiesterase	3.30	71.32	21.61	5.E-03
VVMO6_03939	Branched-chain alpha-keto acid dehydrogenase2C E1 component2C beta subunit	0.88	7.35	8.35	4.E-02
VVMO6_03940	Dihydrolipoamide acyltransferase	1.42	7.91	5.57	5.E-03

	component of branched-chain alpha-keto acid dehydrogenase complex				
VVMO6_04097	Nitrate reductase cytochrome c550-type subunit	38.94	357.4	9.18	5.E-02
VVMO6_04098	Cytochrome c-type protein NapC	60.7	612.91	10.10	9.E-03
VVMO6_04237	Aldehyde dehydrogenase	3.94	108.71	27.59	4.E-04
VVMO6_04508	Delta 1-pyrroline-5-carboxylate dehydrogenase domain protein	25.57	729.37	28.52	7.E-03
VVMO6_04509	Proline dehydrogenase / Delta-1-pyrroline-5-carboxylate dehydrogenase	31.41	780.75	24.86	2.E-02
Cell division and chromosome partitioning					
VVMO6_00299	Cell division protein	21.08	163.01	7.73	8.E-03
VVMO6_01351	Prevent host death protein2C Phd antitoxin	3.96	19.91	5.03	1.E-02
Amino acid metabolism and transport					
VVMO6_00258	Acetylornithine aminotransferase / Succinylornithine transaminase	567.36	3106.55	5.48	1.E-02
VVMO6_00355	Serine--pyruvate aminotransferase / L-alanine:glyoxylate aminotransferase	184.11	1017.85	5.53	2.E-04
VVMO6_00394	Arginine deiminase	13.98	1192.13	85.27	7.E-03
VVMO6_00658	Putative oxidoreductase	1.57	67.42	42.94	1.E-02
VVMO6_01133	L-serine dehydratase	32.23	192.57	5.97	2.E-02
VVMO6_01134	Serine transporter	10.90	334.66	30.70	6.E-03
VVMO6_01505	ABC transporter2C periplasmic spermidine putrescine-binding protein PotD	39.85	231.37	5.81	5.E-03
VVMO6_01759	Cysteine desulfurase	11.71	656.69	56.08	1.E-02
VVMO6_01893	Alanine dehydrogenase	191.16	4853.63	25.39	1.E-04
VVMO6_02014	Oligopeptide ABC transporter2C	714.14	4680.36	6.55	2.E-04

	periplasmic oligopeptide-binding protein OppA				
VVMO6_02096	Cysteine synthase B	10.53	455.05	43.21	5.E-03
VVMO6_02415	Sodium/alanine symporter	139.37	705.68	5.06	3.E-02
VVMO6_03045	Sodium/dicarboxylate symporter	41.98	297.27	7.08	7.E-03
VVMO6_03441	Di-/tripeptide transporter	10.71	458.92	42.85	2.E-02
VVMO6_03443	L-serine dehydratase	18.16	99.31	5.47	1.E-02
VVMO6_03858	Arginase/agmatinase/formimionoglutamate hydrolase2C arginase family	112.02	564.92	5.04	4.E-02
VVMO6_03925	Phenylalanine-4-hydroxylase	4.04	51.65	12.78	2.E-02
VVMO6_04030	L-lysine permease	1.76	12.82	7.28	2.E-02
VVMO6_04367	Vibriolysin2C extracellular zinc protease	14.58	308.6	21.17	2.E-04
VVMO6_00257	Para-aminobenzoate synthase2C amidotransferase component	21.29	125.38	5.89	4.E-03
VVMO6_04103	*N*-acetylneuraminate lyase	24.33	259.83	10.68	5.E-03
VVMO6_02013	Oligopeptide transport system permease protein OppB	93.48	603.98	6.46	2.E-02
VVMO6_04507	Proline/sodium symporter PutP	39.61	788.93	19.92	1.E-03
Nucleotide metabolism and transport					
VVMO6_02224	Adenylate kinase	106.46	1800.41	16.91	7.E-06
VVMO6_02366	Xanthine-guanine phosphoribosyltransferase	110.85	813.04	7.33	7.E-03
VVMO6_04085	GMP reductase	58.43	669.04	11.45	2.E-02
VVMO6_04324	MutT/nudix family protein	7.59	42.39	5.58	1.E-02
Carbohydrate metabolism and transport					
VVMO6_00656	Putative isomerase	6.44	38.13	5.92	5.E-03
VVMO6_00659	Evolved beta-D-galactosidase2C beta subunit	3.71	38.85	10.47	2.E-02
VVMO6_00660	Evolved beta-D-galactosidase2C alpha subunit	4.03	38.87	9.65	1.E-02

VVMO6_00679	Glycerol uptake facilitator protein	10.14	317.6	31.32	8.E-04
VVMO6_01231	Multidrug resistance protein D	3.95	22.32	5.65	2.E-02
VVMO6_01690	Methylisocitrate lyase	36.02	401.4	11.14	1.E-02
VVMO6_02068	Putative sugar isomerase involved in processing of exogenous sialic acid	13.43	78.78	5.87	1.E-02
VVMO6_02131	TRAP-type C4-dicarboxylate transport system2C periplasmic component	3.56	86.92	24.42	2.E-02
VVMO6_02633	PTS system2C mannitol-specific IIC component / PTS system2C mannitol-specific IIB component	9.23	60.32	6.54	4.E-02
VVMO6_02702	Fructose-12C6-bisphosphatase2C type I	149.55	869.36	5.81	2.E-04
VVMO6_02934	Multidrug resistance transporter2C Bcr/CflA family	19.28	361.23	18.74	9.E-03
VVMO6_03135	Galactose/methyl galactoside ABC transport system2C D-galactose-binding periplasmic protein MglB	571.16	7816.72	13.69	2.E-03
VVMO6_03513	Ribose ABC transport system2C periplasmic ribose-binding protein RbsB	7.62	98.89	12.98	5.E-03
VVMO6_03619	Methylglyoxal synthase	111.06	1799.97	16.21	2.E-02
VVMO6_03829	Permease of the major facilitator superfamily	27.17	148.97	5.48	4.E-02
VVMO6_03877	Glycosidase	2.76	24.71	8.95	6.E-03
VVMO6_03882	Glycerol-3-phosphate transporter	4.60	76.00	16.52	3.E-03
VVMO6_04011	Chitinase	5.55	29.23	5.27	2.E-03
VVMO6_04104	TRAP-type transport system2C large permease component2C predicted *N*-acetylneuraminate transporter	8.34	93.97	11.27	7.E-03
VVMO6_04105	TRAP-type transport system2C small permease component2C	3.00	83.07	27.69	1.E-02

	predicted *N*-acetylneuraminate transporter				
VVMO6_04106	TRAP-type transport system2C periplasmic component2C predicted *N*-acetylneuraminate-binding protein	14.16	400.27	28.27	2.E-03
VVMO6_04135	NADPH-dependent glyceraldehyde-3-phosphate dehydrogenase	99.87	1465.2	14.67	7.E-03
VVMO6_04458	TRAP-type C4-dicarboxylate transport system2C periplasmic component	3.97	27.92	7.03	1.E-02
Coenzyme metabolism					
VVMO6_02380	Aminobenzoyl-glutamate transport protein	56.9	381.65	6.71	4.E-02
VVMO6_03219	32C4-dihydroxy-2-butanone 4-phosphate synthase	22.61	170.59	7.54	3.E-02
VVMO6_03924	Pterin-4-alpha-carbinolamine dehydratase	13.55	94.19	6.95	3.E-02
Lipid metabolism					
VVMO6_00152	CDP-diacylglycerol-serine O-phosphatidyltransferase	59.46	335.07	5.64	2.E-03
VVMO6_00187	Acetyl-coenzyme A synthetase	562.25	4397.58	7.82	1.E-02
VVMO6_00855	Long-chain fatty acid transport	103.95	1568.69	15.09	1.E-03
VVMO6_01659	1-acyl-*sn*-glycerol-3-phosphate acyltransferase	4.48	30.66	6.84	2.E-04
VVMO6_01686	Propionate--CoA ligase	13.36	98.34	7.36	7.E-03
VVMO6_02005	Acyl-CoA thioesterase YciA2C involved in membrane biogenesis	8.53	59.48	6.97	1.E-02
VVMO6_03024	Predicted hydrolase or acyltransferase	33.45	372.81	11.15	5.E-03
VVMO6_03498	Membrane-associated	2.18	19.17	8.79	6.E-03

	phospholipid phosphatase				
VVMO6_03518	Delta-9 fatty acid desaturase	16.86	158.69	9.41	2.E-03
VVMO6_03787	Hypothetical protein	205.4	1085.6	5.29	9.E-03
VVMO6_01923	Putative oxidoreductase	150.47	873.15	5.80	2.E-02
VVMO6_01166	Hypothetical protein	6.94	49.59	7.15	4.E-03
Translation, including ribosome structure and biognenesis					
VVMO6_02298	Peptidyl-tRNA hydrolase	53.40	321.78	6.03	1.E-02
VVMO6_02395	Outer membrane lipoprotein SmpA2C a component of the essential YaeT outer-membrane protein assembly complex	25.11	140.33	5.59	2.E-02
VVMO6_02626	SSU ribosomal protein S21p	285.51	1726.9	6.05	3.E-02
VVMO6_04246	Tyrosyl-tRNA synthetase	4.48	393.76	87.89	3.E-03
Transcription					
VVMO6_00179	HTH-type transcriptional regulator ZntR	16.80	88.31	5.26	5.E-02
VVMO6_00607	Transcriptional regulator2C MarR family	7.97	54.29	6.81	2.E-02
VVMO6_01504	NAD-dependent protein deacetylase of SIR2 family	54.8	711.21	12.98	3.E-03
VVMO6_01691	Propionate catabolism operon transcriptional regulator of GntR family	19.78	146.96	7.43	2.E-03
VVMO6_02561	Transcriptional regulator2C LysR family	7.33	148.8	20.30	9.E-05
VVMO6_02852	Transcription elongation factor GreB	10.59	62.18	5.87	3.E-02
VVMO6_03132	Galactose operon repressor2C GalR-LacI family of transcriptional regulators	17.78	95.65	5.38	1.E-02
VVMO6_03984	Cold shock protein CspE	1032.8	10099.6	9.78	4.E-02
VVMO6_04075	Regulator of nucleoside	127.20	1120.85	8.81	1.E-02

	diphosphate kinase				
VVMO6_04418	Transcriptional repressor of *aga* operon	0.26	2.43	9.35	3.E-02
Replication, recombination, and repair					
VVMO6_02351	Exodeoxyribonuclease VII small subunit	18.49	377.99	20.44	4.E-02
Cell wall structure and biogenesis					
VVMO6_00583	Outer membrane protein OmpU	2769.6	24170.5	8.73	6.E-05
VVMO6_00768	Membrane-bound lytic murein transglycosylase D precursor	21.82	145.57	6.67	1.E-02
VVMO6_02279	membrane protein	7.50	1240.73	165.4	2.E-02
VVMO6_04037	Outer membrane protein N2C non-specific porin	5.72	64.8	11.33	5.E-03
VVMO6_04180	Small-conductance mechanosensitive channel	8.70	78.38	9.01	3.E-04
Secretion, motility, and chemotaxis					
VVMO6_00180	Methyl-accepting chemotaxis protein	47.67	344.87	7.23	3.E-02
VVMO6_01025	Methyl-accepting chemotaxis protein	4.97	24.63	4.96	1.E-03
VVMO6_01129	Methyl-accepting chemotaxis protein I	11.18	238.51	21.33	5.E-03
VVMO6_03834	Methyl-accepting chemotaxis protein	63.03	745.08	11.82	4.E-04
VVMO6_03878	Methyl-accepting chemotaxis protein2C hemolysin secretion protein HylB	27.29	211.23	7.74	4.E-04
Molecular chaperones and related functions					
VVMO6_01963	Cytochrome c-type heme lyase subunit NrfE2C nitrite reductase	4.13	45.89	11.11	1.E-02

	complex assembly				
VVMO6_02039	Glutaredoxin-related protein	294.00	1978.72	6.73	2.E-02
VVMO6_03989	Thiol-disulfide isomerase	36.71	196.23	5.35	2.E-03
VVMO6_01962	Putative thiol disulfide oxidoreductase2C nitrite reductase complex assembly	9.92	50.12	5.05	2.E-03
Inorganic ion transport and metabolism					
VVMO6_01964	NrfD protein	5.30	147.00	27.74	3.E-04
VVMO6_01966	Cytochrome c-type protein NrfB precursor	6.73	205.41	30.52	1.E-04
VVMO6_01967	Cytochrome c552 precursor	17.50	239.25	13.67	4.E-04
VVMO6_04095	Periplasmic nitrate reductase component NapD	98.08	590.36	6.02	1.E-02
Secondary metabolites biosynthesis, transport, and catabolism					
VVMO6_01272	Imidazolonepropionase	10.21	179.76	17.61	3.E-02
VVMO6_04034	2-keto-4-pentenoate hydratase	24.68	175.35	7.10	4.E-03
General function prediction only					
VVMO6_00149	RNA-binding protein	62.51	329.46	5.27	2.E-02
VVMO6_00193	Acetate permease ActP	30.96	1598.78	51.64	1.E-02
VVMO6_00451	Lysine efflux permease	7.59	80.23	10.57	8.E-03
VVMO6_00894	Proteinase inhibitor2C putative	2.65	22.65	8.55	6.E-03
VVMO6_01226	Lipase precursor	1.23	35.55	28.90	2.E-04
VVMO6_02562	Putative membrane protein YfcA	4.24	443.38	104.6	2.E-02
VVMO6_02710	YtfJ precursor	71.36	372.02	5.21	8.E-03
VVMO6_03049	Cytochrome oxidase biogenesis protein Sco1/SenC/PrrC2C putative copper metallochaperone	28.58	186.17	6.51	1.E-02
VVMO6_03519	Histone acetyltransferase HPA2	16.49	522.52	31.69	9.E-04
VVMO6_03604	MazG-related protein	19.93	107.21	5.38	6.E-03
VVMO6_03752	Isopenicillin N synthase	21.40	589.52	27.55	9.E-03
VVMO6_03876	Acetyltransferase	12.15	116.57	9.59	1.E-02

VVMO6_04355	Predicted thioesterase	0.46	66.49	144.5	4.E-02
VVMO6_04378	TRAP transporter solute receptor2C TAXI family precursor	27.85	425.28	15.27	2.E-02
No functional prediction					
VVMO6_00123	Putative inner membrane protein	6.69	1467.82	8.93	4.E-02
VVMO6_00194	Hypothetical protein	18.31	133.98	219.4	3.E-02
VVMO6_00408	Predicted transmembrane protein	435.19	2951.7	7.32	4.E-02
VVMO6_00682	DNA damage-inducible gene in SOS regulon2C dependent on cyclic AMP and H-NS	3.58	23.54	6.78	4.E-02
VVMO6_00866	Hypothetical protein	8.74	1744.74	6.58	1.E-02
VVMO6_01760	Hypothetical protein	21.65	199.01	199.6	2.E-03
VVMO6_02277	Hypothetical protein	28.94	160.78	9.19	8.E-04
VVMO6_02316	Proposed lipoate regulatory protein YbeD	24.1	129.00	5.56	1.E-02
VVMO6_02560	Putative inner membrane protein	1.02	7.10	5.35	2.E-03
VVMO6_02932	Integral membrane protein	9.52	198.15	6.96	2.E-02
VVMO6_03017	Membrane protein	32.58	386.21	20.81	2.E-03
VVMO6_03048	Copper metallochaperone2C bacterial analog of Cox17 protein	18.54	120.52	11.85	2.E-02
VVMO6_03395	Predicted arginine uptake transporter	7.16	45.95	6.50	2.E-02
VVMO6_03791	Hypothetical protein	32.8	212.9	6.42	2.E-03
VVMO6_03985	YaeQ protein	7.52	133.48	6.49	6.E-03
VVMO6_04100	Sialic acid-induced transmembrane protein YjhT(NanM)2C possible mutarotase	5.50	238.24	17.75	6.E-03
VVMO6_04101	Sialic acid-induced transmembrane protein YjhT(NanM)2C possible mutarotase	4.89	49.92	43.32	4.E-02
VVMO6_04311	Hypothetical protein	17.19	341.74	10.21	4.E-03

Signal transduction, intracellular trafficking, and defense mechanism					
VVMO6_00189	Predicted signal-transduction protein	35.61	785.36	22.05	2.E-03
VVMO6_01229	Two-component system sensor protein	4.08	41.29	10.12	5.E-04
VVMO6_00592	Preprotein translocase subunit SecG	1388.1	6277.2	4.52	5.E-02
Uncategorized					
VVMO6_00261	Hypothetical protein	56.71	1540.41	27.16	3.E-04
VVMO6_00482	Hypothetical protein	1.60	9.15	5.72	5.E-02
VVMO6_00681	Hypothetical protein	7.71	72.29	9.38	3.E-02
VVMO6_00743	YaeH	162.58	807.47	4.97	6.E-03
VVMO6_00927	Hypothetical protein	16.68	128.45	7.70	2.E-02
VVMO6_01124	Hypothetical protein	66.11	418.22	6.33	4.E-02
VVMO6_01141	Hypothetical protein	69.60	462.16	6.64	4.E-02
VVMO6_01156	Hypothetical protein	12.21	284.84	23.33	1.E-02
VVMO6_01260	Hypothetical protein	10.00	108.78	10.88	3.E-04
VVMO6_01411	Hypothetical protein	6.74	89.13	13.22	5.E-02
VVMO6_01467	Hypothetical protein	9.70	104.63	10.79	1.E-03
VVMO6_01694	Hypothetical protein	5.52	145.02	26.27	1.E-02
VVMO6_01773	Hypothetical protein	291.19	2507.57	8.61	9.E-03
VVMO6_01837	Membrane protein	1148.0	16824.9	14.66	2.E-02
VVMO6_01882	Hypothetical protein	556.35	17615.8	31.66	2.E-02
VVMO6_01960	Hypothetical protein	11.18	57.91	5.18	7.E-03
VVMO6_01968	NrfF	52.68	318.31	6.04	1.E-02
VVMO6_02364	Curlin genes transcriptional activator	181.62	1023.56	5.64	5.E-02
VVMO6_02372	Pressure-regulated ORF-like protein	4.80	64.68	13.48	4.E-02
VVMO6_02530	Hypothetical protein	1.64	10.86	6.62	4.E-02
VVMO6_02535	Hypothetical protein	244.88	1314.01	5.37	3.E-02
VVMO6_02549	Hypothetical protein	1.10	6.74	6.13	5.E-02
VVMO6_02780	Predicted protein	1.01	13.35	13.22	5.E-02

VVMO6_02884	Hypothetical protein	5.59	53.01	9.48	2.E-03
VVMO6_03021	Hypothetical protein	15.12	396.3	26.21	4.E-02
VVMO6_03050	Hypothetical protein	42.69	231.43	5.42	5.E-03
VVMO6_03239	Hypothetical protein	3.81	25.59	6.72	1.E-02
VVMO6_03368	Hypothetical protein	30.96	167.92	5.42	1.E-02
VVMO6_03547	Hypothetical protein	4.49	42.19	9.40	5.E-02
VVMO6_03548	Pyruvate/2-oxoglutarate Dehydrogenase complex2C	4.38	27.44	6.26	3.E-02
VVMO6_03754	Hypothetical protein	2.13	16.17	7.59	3.E-02
VVMO6_03811	Hypothetical protein	85.04	446.95	5.26	3.E-02
VVMO6_03833	Hypothetical protein	9.23	79.68	8.63	3.E-02
VVMO6_03875	Hypothetical protein	8.86	45.20	5.10	2.E-02
VVMO6_04076	Hypothetical protein	4.49	35.56	7.92	3.E-02
VVMO6_04091	Hypothetical protein	139.69	1857.79	13.30	9.E-03
VVMO6_04099	Hypothetical protein	34.2	481.67	14.08	4.E-02
VVMO6_04478	Hypothetical protein	4.37	26.27	6.01	6.E-04
VVMO6_04506	Hypothetical protein	16.92	121.94	7.21	2.E-02

[a] Locus tags are based on the database for the *V. vulnificus* MO6-24/O genome, which was retrieved from GenBank (accession number CP002469 and CP002470).

Table II-4. List of genes up-regulated by HT29-MTX cells

Locus tag[a]	Gene product	RPKM		Fold change	*P*-value
		BME	HT29-MTX		
Energy production and conversion					
VVMO6_00029	Type cbb3 cytochrome oxidase biogenesis protein CcoG2C involved in Cu oxidation	24.74	125.00	5.05	2.E-03
VVMO6_00219	Succinate dehydrogenase flavoprotein subunit	45.21	285.80	6.32	4.E-03
VVMO6_00676	Aerobic glycerol-3-phosphate dehydrogenase	9.75	3,096.79	317.6	1.E-04
VVMO6_00678	Glycerol kinase	31.27	3,834.05	122.6	5.E-03
VVMO6_01492	Iron-sulfur cluster-binding protein	12.07	262.67	21.76	1.E-02
VVMO6_01495	Formate dehydrogenase-O2C major subunit	9.37	252.20	26.92	5.E-03
VVMO6_01496	Formate dehydrogenase-O2C iron-sulfur subunit	11.68	213.05	18.24	5.E-04
VVMO6_01497	Formate dehydrogenase -O2C gamma subunit	31.02	210.13	6.77	3.E-03
VVMO6_02075	22C4-dienoyl-CoA reductase	9.83	262.54	26.71	9.E-03
VVMO6_02192	Succinyl-CoA ligase alpha chain	822.05	3,441.46	4.19	1.E-02
VVMO6_02193	Succinyl-CoA ligase beta chain	577.45	3,263.72	5.65	3.E-03
VVMO6_02195	2-oxoglutarate dehydrogenase E1 component	449.57	2,274.85	5.06	1.E-03
VVMO6_02197	Succinate dehydrogenase flavoprotein subunit	212.38	1,288.67	6.07	5.E-04
VVMO6_02198	Succinate dehydrogenase hydrophobic membrane anchor protein	150.83	1,588.33	10.53	3.E-04
VVMO6_02198	Succinate dehydrogenase hydrophobic membrane anchor protein	53.14	434.17	8.17	1.E-02

VVMO6_02452	Isocitrate lyase	66.66	592.76	8.89	3.E-02
VVMO6_02453	Malate synthase	55.53	557.74	10.04	2.E-04
VVMO6_02875	Phosphoenolpyruvate carboxykinase	94.69	1,272.19	13.44	1.E-02
VVMO6_03181	Proton/glutamate symport protein	14.76	102.02	6.91	2.E-02
VVMO6_03464	Anaerobic glycerol-3-phosphate dehydrogenase subunit A	2.28	1,305.39	572.5	3.E-03
VVMO6_03466	Anaerobic glycerol-3-phosphate dehydrogenase subunit C	3.81	879.58	230.9	7.E-05
VVMO6_03883	Glycerophosphoryl diester phosphodiesterase	6.03	1,130.74	187.5	4.E-03
VVMO6_04168	Predicted L-lactate dehydrogenase2C Iron-sulfur cluster-binding subunit YkgF	24.32	103.95	4.27	2.E-03
Amino acid metabolism and transport					
VVMO6_00199	Aspartate ammonia-lyase	132.84	2,137.02	16.09	3.E-02
VVMO6_00657	Putative oxidoreductase	2.09	31.42	15.03	2.E-02
VVMO6_00658	Putative oxidoreductase	1.20	34.43	28.69	2.E-02
VVMO6_01133	L-serine dehydratase	30.91	129.17	4.18	8.E-03
VVMO6_01134	Serine transporter	37.2	337.55	9.07	1.E-03
VVMO6_01269	Histidine ammonia-lyase	9.78	51.45	5.26	1.E-03
VVMO6_01270	Urocanate hydratase	5.59	44.88	8.03	1.E-03
VVMO6_01271	Formiminoglutamase	3.00	13.07	4.36	3.E-02
VVMO6_01724	Peptidase2C M20A family	8.99	74.54	8.29	6.E-03
VVMO6_02432	Peptidase B	123.38	493.47	4.00	1.E-03
VVMO6_03317	Protease II	233.4	1,069.77	4.58	1.E-02
VVMO6_03441	Di-/tripeptide transporter	14.26	385.73	27.05	6.E-03
VVMO6_03465	Anaerobic glycerol-3-phosphate dehydrogenase subunit	4.36	1,083.76	248.6	3.E-05
VVMO6_03685	Glycine dehydrogenase	34.32	325.02	9.47	1.E-02
VVMO6_03686	Glycine cleavage system H protein	95.65	487.78	5.10	1.E-02
VVMO6_03687	Serine hydroxymethyltransferas	16.44	185.56	11.29	3.E-03
VVMO6_04222	Tryptophanase	27.47	190.85	6.95	1.E-03

Nucleotide metabolism and transport					
VVMO6_00938	Uridine phosphorylase	287.28	1,480.09	5.15	7.E-04
VVMO6_01259	Cytidine deaminase	46.56	913.05	19.61	2.E-05
VVMO6_01725	Putative UDP-sugar hydrolase	20.55	233.42	11.36	3.E-05
VVMO6_02340	DNA/RNA endonuclease G	4.30	22.73	5.29	3.E-02
VVMO6_02722	2'2C3'-cyclic-nucleotide 2'-phosphodiesterase	76.32	513.08	6.72	1.E-02
VVMO6_03172	*N*-Ribosylnicotinamide phosphorylase	43.88	317.02	7.22	1.E-02
Carbohydrate metabolism and transport					
VVMO6_00656	Putative isomerase	2.84	26.78	9.43	2.E-02
VVMO6_00659	Evolved beta-D-galactosidase2C beta subunit	0.75	19.08	25.44	5.E-03
VVMO6_00660	Evolved beta-D-galactosidase2C alpha subunit	2.85	25.94	9.10	2.E-02
VVMO6_00679	Glycerol uptake facilitator protein	12.88	2,872.87	223.1	4.E-03
VVMO6_01101	Maltodextrin glucosidase	18.96	80.71	4.26	1.E-02
VVMO6_02633	PTS system2C mannitol-specific IIABC component	11.6	68.64	5.92	3.E-04
VVMO6_02634	Mannitol-1-phosphate 5-dehydrogenase	23.08	93.23	4.04	4.E-03
VVMO6_03033	Maltoporin	128.92	17,934.9	139.1	3.E-03
VVMO6_03036	Maltose/maltodextrin ABC transporter2C substrate binding periplasmic protein MalE	25.94	143.32	5.53	2.E-03
VVMO6_03039	Type II secretory pathway2C pullulanase	4.32	214.42	49.63	6.E-03
VVMO6_03056	Glycogen phosphorylase	344.02	1,822.96	5.30	5.E-02
VVMO6_03057	4-alpha-glucanotransferase	173.34	1,517.94	8.76	4.E-02
VVMO6_03058	12C4-alpha-glucan branching enzyme2C GH-13-type	189.65	851.58	4.49	2.E-03
VVMO6_03133	Galactose/methyl galactoside ABC	282.39	1,818.04	6.44	5.E-03

	transport system2C permease protein MglC				
VVMO6_03134	Galactose/methyl galactoside ABC transport system2C ATP-binding protein MglA	172.04	1,517.22	8.82	6.E-03
VVMO6_03135	Galactose/methyl galactoside ABC transport system2C D-galactose-binding periplasmic protein MglB	751.23	8,737.53	11.63	1.E-02
VVMO6_03138	Alpha-galactosidase	4.94	30.41	6.16	5.E-02
VVMO6_03139	Melibiose carrier protein2C Na^+/melibiose symporter	6.08	100.27	16.49	8.E-03
VVMO6_03149	Mannose-6-phosphate isomerase	8.59	666.49	77.59	2.E-03
VVMO6_03150	PTS system2C fructose-specific IIABC component	6.56	1,155.56	176.2	8.E-03
VVMO6_03154	PTS system2C fructose-specific IIABC component	18.17	74.61	4.11	2.E-02
VVMO6_03157	PTS system2C fructose-specific IIBC component	10.21	468.64	45.90	9.E-03
VVMO6_03162	Beta-mannosidase	5.66	117.72	20.80	2.E-03
VVMO6_03203	Glycosidase	34.14	374.08	10.96	7.E-03
VVMO6_03354	Maltose/maltodextrin ABC transporter2C substrate binding periplasmic protein MalE	332.74	12,893.0	38.75	4.E-03
VVMO6_03355	Maltose/maltodextrin ABC transporter2C permease protein MalF	87.55	998.93	11.41	4.E-02
VVMO6_03356	Maltose/maltodextrin ABC transporter2C permease protein MalG	183.86	1,210.08	6.58	3.E-02
VVMO6_03389	Glycosidase	14.80	69.35	4.69	5.E-02
VVMO6_03510	Ribose ABC transport system2C high affinity permease RbsD	1.82	171.66	94.32	8.E-03
VVMO6_03511	Ribose ABC transport system2C ATP-binding protein RbsA	3.11	122.12	39.27	5.E-03

VVMO6_03512	Ribose ABC transport system2C permease protein RbsC	3.72	137.56	36.98	3.E-02
VVMO6_03514	Ribokinase	8.98	147.71	16.45	4.E-03
VVMO6_03877	Glycosidase	8.05	59.52	7.39	2.E-03
VVMO6_03882	Glycerol-3-phosphate transporter	5.74	1,580.87	275.4	3.E-04
VVMO6_03975	Hexose phosphate transport protein UhpT	3.35	1,012.94	302.4	1.E-03
VVMO6_03978	Hexose phosphate uptake regulatory protein UhpC	3.91	70.18	17.95	9.E-03
VVMO6_03979	Mannose-6-phosphate isomerase	0.80	38.40	48.00	5.E-03
VVMO6_04028	Phosphosugar mutase of unknown sugar	297.91	2,577.56	8.65	2.E-03
VVMO6_04288	Periplasmic alpha-amylase	20.83	227.67	10.93	5.E-02
VVMO6_04458	TRAP-type C4-dicarboxylate transport system2C periplasmic component	2.03	10.47	5.16	4.E-03
VVMO6_04474	L-ribulose-5-phosphate 4-epimerase	0.62	2.58	4.16	5.E-02
VVMO6_04531	PTS system2C *N*-acetylmuramic acid-specific IIBC component	2.02	22.69	11.23	2.E-02
VVMO6_04473	Ascorbate-specific PTS system2C EIIA component	0.36	4.25	11.81	9.E-03
Coenzyme metabolism					
VVMO6_01478	Molybdopterin-guanine dinucleotide biosynthesis protein MobB	45.18	352.47	7.80	4.E-05
VVMO6_01479	Molybdopterin-guanine dinucleotide biosynthesis protein MobA	40.94	387.22	9.46	2.E-05
VVMO6_01481	ABC-type tungstate transport system2C permease protein	35.56	457.57	12.87	1.E-04
VVMO6_01482	ABC-type tungstate transport system2C periplasmic binding	131.12	2,040.16	15.56	7.E-03

	protein				
VVMO6_03171	Ribosyl nicotinamide transporter2C PnuC-like	66.68	356.71	5.35	3.E-02
VVMO6_03332	BatA	16.13	145.22	9.00	1.E-02
VVMO6_02405	D-alanine-D-alanine ligase	1.33	10.34	7.77	2.E-02
Lipid metabolism					
VVMO6_00735	3-oxoacyl-(acyl carrier protein) synthase	9.11	83.78	9.20	2.E-02
VVMO6_00780	Butryl-CoA dehydrogenase	12.46	422.13	33.88	1.E-03
VVMO6_00858	3-ketoacyl-CoA	10.70	717.67	67.07	3.E-04
VVMO6_00859	Enoyl-CoA hydratase / 3-hydroxybutyryl-CoA epimerase	21.61	634.63	29.37	4.E-05
VVMO6_01781	Butryl-CoA dehydrogenase	44.77	691.4	15.44	2.E-03
VVMO6_02674	1-acyl-sn-glycerol-3-phosphate acyltransferase	78.37	379.03	4.84	3.E-03
VVMO6_02953	Enoyl-CoA hydratase / Delta(3)-cis-delta(2)-trans-enoyl-CoA isomerase	38.66	956.11	24.73	1.E-03
VVMO6_02954	3-ketoacyl-CoA thiolase	24.63	518.25	21.04	6.E-05
VVMO6_03224	Membrane-associated phospholipid phosphatase	21.32	206.81	9.70	3.E-02
VVMO6_03370	hypothetical protein	37.14	338.14	9.10	8.E-04
VVMO6_02173	Long-chain-fatty-acid--CoA ligase	89.98	387.9	4.31	4.E-03
VVMO6_03257	Putative phospholipase	4.59	94.04	20.49	4.E-04
Translation, including ribosome structure and biogenesis					
VVMO6_02395	Outer membrane lipoprotein SmpA2C a component of the essential YaeT outer-membrane protein assembly complex	48.65	363.4	7.47	2.E-03
VVMO6_02626	SSU ribosomal protein S21p	425.58	1,852.84	4.35	7.E-03
VVMO6_04052	Putative translation initiation inhibitor2C YjgF family protein	3.09	13.04	4.22	1.E-02

VVMO6_04337	Translation elongation factor G-related protein	19.30	170.52	8.84	2.E-03
Transcription					
VVMO6_00300	Transcriptional regulator CytR	100.95	654.97	6.49	7.E-03
VVMO6_00468	RNA polymerase sigma factor RpoE	473.25	2,428.92	5.13	4.E-03
VVMO6_01770	Regulator of competence-specific genes	60.53	259.46	4.29	5.E-03
VVMO6_01782	Predicted transcriptional regulator for fatty acid degradation FadQ2C TetR family	14.78	379.3	25.66	1.E-02
VVMO6_02227	Transcriptional activator ToxR	160.54	838.74	5.22	4.E-04
VVMO6_02561	Transcriptional regulator2C LysR family	8.28	38.49	4.65	5.E-04
VVMO6_02645	Probable transcriptional activator for *leuABCD* operon	53.19	1,501.09	28.22	1.E-02
VVMO6_02676	YrbA protein	278.39	1,374.19	4.94	4.E-04
VVMO6_02853	Transcription accessory protein	13.30	194.49	14.62	2.E-03
VVMO6_03055	Transcriptional activator of maltose regulon2C MalT	22.10	107.13	4.85	2.E-02
VVMO6_03132	Galactose operon repressor2C GalR-LacI family of transcriptional regulators	16.96	107.35	6.33	5.E-03
VVMO6_03374	Transcriptional regulator LuxT	221.13	1,217.20	5.50	2.E-03
VVMO6_03657	Probable transcriptional activator for *leuABCD* operon	18.73	79.44	4.24	2.E-03
VVMO6_04137	Transcriptional regulator2C LysR family	33.01	562.6	17.04	2.E-02
VVMO6_04249	Transcriptional regulator	3.13	40.11	12.81	1.E-02
VVMO6_01067	L-fucose operon activator	0.19	1.94	10.21	2.E-02
VVMO6_04108	*N*-acetylmannosamine kinase	6.72	42.26	6.29	2.E-02
Replication, recombination, and repair					

VVMO6_00548	ATP-dependent helicase HrpB	15.14	71.55	4.73	1.E-02
VVMO6_02603	Topoisomerase IV subunit B	50.03	205.21	4.10	2.E-03
Cell wall structure and biogenesis					
VVMO6_00255	Hypothetical protein	3.24	197.79	61.05	2.E-03
VVMO6_00333	Membrane protein	36.64	157.73	4.30	1.E-03
VVMO6_00549	Multimodular transpeptidase-transglycosylase	31.62	191.90	6.07	8.E-03
VVMO6_00583	Outer membrane protein OmpU	1,130	15,735.1	13.92	8.E-03
VVMO6_00699	Outer membrane protein OmpK	120.83	659.3	5.46	1.E-02
VVMO6_00995	Outer membrane lipoprotein	124.94	591.48	4.73	1.E-02
VVMO6_01035	TolA protein	56.71	357.59	6.31	2.E-03
VVMO6_01177	Capsular polysaccharide synthesis enzyme CpsA2C sugar transferase	18.20	213.53	11.73	1.E-02
VVMO6_01180	Capsular polysaccharide synthesis enzyme CpsD2C exopolysaccharide synthesis	13.42	80.96	6.03	8.E-03
VVMO6_01184	Putative glycosyltransferase protein	20.81	205.00	9.85	1.E-02
VVMO6_01185	Alpha-*D*-GlcNAc alpha-12C2-L-rhamnosyltransferase	15.07	82.15	5.45	8.E-03
VVMO6_01262	Outer membrane protein	33.04	612.34	18.53	2.E-02
VVMO6_02279	Membrane protein	14.57	193.73	13.30	2.E-03
VVMO6_02675	UDP-N-acetylglucosamine 1-carboxyvinyltransferase	249.63	1,086.20	4.35	4.E-03
VVMO6_02996	ABC-type transport system2C involved in lipoprotein release2C permease component	0.58	3.97	6.84	2.E-02
VVMO6_03205	Phosphoglycerol transferase I	34.48	144.93	4.20	3.E-02
VVMO6_03207	Diacylglycerol kinase	17.71	271.18	15.31	1.E-02
VVMO6_03300	Protease-related protein	114.06	585.03	5.13	8.E-03
VVMO6_03331	TPR domain protein in aerotolerance operon	14.03	109.23	7.79	3.E-02
VVMO6_03696	Membrane protein	8.19	218.82	26.72	2.E-03

VVMO6_04175	Membrane protein	118.34	1,194.47	10.09	6.E-03
VVMO6_04180	Small-conductance mechanosensitive channel	23.24	223.1	9.60	1.E-03
VVMO6_04320	Membrane fusion protein of RND family multidrug efflux pump	57.11	242.9	4.25	3.E-03
VVMO6_04401	Membrane-fusion protein	5.24	35.46	6.77	2.E-02
VVMO6_04183	Lipoprotein	74.58	19,906.7	266.9	3.E-03
VVMO6_04400	Type I secretion outer membrane protein2C TolC precursor	4.36	34.53	7.92	2.E-03
Secretion, motility, and chemotaxis					
VVMO6_02822	Methyl-accepting chemotaxis protein	34.00	201.82	5.94	3.E-04
VVMO6_03721	Methyl-accepting chemotaxis protein	88.30	362.53	4.11	3.E-02
VVMO6_03834	Methyl-accepting chemotaxis protein	14.55	59.97	4.12	2.E-03
VVMO6_03878	Methyl-accepting chemotaxis protein2C hemolysin secretion protein HylB	22.47	423.33	18.84	2.E-03
VVMO6_02866	General secretion pathway protein I	53.71	242.23	4.51	1.E-02
VVMO6_02870	General secretion pathway protein E	82.53	356.84	4.32	1.E-02
VVMO6_02871	General secretion pathway protein D	63.82	402.72	6.31	3.E-03
VVMO6_03886	MSHA pilin protein MshA BUT NOT	10.13	128.52	12.69	4.E-02
Molecular chaperones and related functions					
VVMO6_00209	Heat shock protein 60 family co-chaperone GroES	23.02	497.96	21.63	2.E-02
VVMO6_00210	Heat shock protein 60 family	156.87	1,000.73	6.38	2.E-02

	chaperone GroEL				
VVMO6_00276	FKBP-type peptidyl-prolyl *cis*-trans isomerase FkpA precursor	418.83	1,877.76	4.48	2.E-03
VVMO6_00298	ATP-dependent protease HslV	16.68	139.8	8.38	5.E-04
VVMO6_01019	Hypothetical protein	82.20	501.53	6.10	1.E-02
VVMO6_01157	Radical activating enzyme	419.85	2,387.82	5.69	3.E-03
VVMO6_01195	DnaK-related protein	17.29	75.35	4.36	2.E-02
VVMO6_01804	Heat shock protein HslJ	220.69	2,986.19	13.53	8.E-05
VVMO6_02226	Chaperone protein HtpG	40.15	210.05	5.23	4.E-02
VVMO6_02525	Thiol:disulfide interchange protein DsbC	94.13	466.51	4.96	2.E-02
VVMO6_02600	Outer membrane stress sensor protease DegQ2C serine protease	252.91	1,568.31	6.20	2.E-02
VVMO6_02966	Heat shock protein A	37.36	424.46	11.36	3.E-02
VVMO6_03217	Periplasmic thiol:disulfide interchange protein DsbA	19.12	85.17	4.45	2.E-03
VVMO6_03256	Regulatory P domain of the Subtilisin-like proprotein convertase	6.57	61.8	9.41	2.E-03
VVMO6_03319	Hypothetical with regulatory P domain of a subtilisin-like proprotein convertase	135.75	740.48	5.45	1.E-02
VVMO6_03462	Hypothetical protein	6.86	3,179.16	463.4	3.E-02
VVMO6_04522	Heat shock protein 60 family chaperone GroEL	195.56	811.85	4.15	2.E-02
VVMO6_04523	Heat shock protein 60 family co-chaperone GroES	16.09	305.75	19.00	7.E-04
Inorganic ion transport and metabolism					
VVMO6_00232	Transporter2C putative	16.46	70.44	4.28	7.E-03
VVMO6_00937	Lead2C cadmium2C zinc and mercury transporting ATPase	15.28	187.16	12.25	2.E-03
VVMO6_01480	ABC-type tungstate transport system2C ATP-binding protein	74.73	671.15	8.98	7.E-03

VVMO6_01756	Di-and tricarboxylate transporter	18.61	198.32	10.66	6.E-03
VVMO6_03318	TonB-dependent heme receptor HutR	142.34	886.31	6.23	6.E-03
VVMO6_04064	Putative transporter	2.72	57.83	21.26	2.E-04
VVMO6_04488	Sulfate permease	0.81	3.56	4.40	1.E-02
Secondary metabolites biosynthesis, transport, and catabolism					
VVMO6_01110	TRAP transporter solute receptor2C unknown substrate 6	12.59	294.34	23.38	2.E-03
VVMO6_01111	TRAP dicarboxylate transporter2C DctQ subunit2C unknown substrate 6	6.18	207.41	33.56	6.E-05
VVMO6_01112	TRAP dicarboxylate transporter2C DctM subunit2C unknown substrate 6	11.54	94.00	8.15	4.E-03
VVMO6_02678	Uncharacterized ABC transporter2C auxiliary component YrbC	164.19	1,235.87	7.53	6.E-03
VVMO6_02679	Uncharacterized ABC transporter2C periplasmic component YrbD	101.73	1,168.70	11.49	1.E-03
General function prediction only					
VVMO6_00198	C4-dicarboxylate transporter DcuA	30.15	161.05	5.34	2.E-02
VVMO6_00256	Extracellular deoxyribonuclease Xds	28.42	116.67	4.11	1.E-06
VVMO6_00265	Hydrolase2C alpha/beta fold family functionally coupled to Phosphoribulokinase	48.05	615.71	12.81	5.E-03
VVMO6_00275	WD40 repeat	3.36	119.91	35.69	1.E-03
VVMO6_01493	Putative formate dehydrogenase-specific chaperone	88.40	359.85	4.07	4.E-03
VVMO6_01535	ABC transporter ATP-binding	25.39	140.11	5.52	5.E-04

	protein Uup				
VVMO6_02229	Predicted permease	4.37	51.71	11.83	7.E-03
VVMO6_02562	Putative membrane protein YfcA	329.8	1,525.29	4.62	2.E-03
VVMO6_02677	Uncharacterized protein YrbB	17.65	143.71	8.14	4.E-05
VVMO6_03049	Cytochrome oxidase biogenesis protein Sco1/SenC/PrrC2C putative copper metallochaperone	0.28	2.61	9.32	4.E-02
VVMO6_03107	ABC-type oligopeptide transport system2C ATPase component	23.73	176.83	7.45	1.E-02
VVMO6_03206	Predicted membrane-associated metal-dependent hydrolase	17.39	191.19	10.99	2.E-02
VVMO6_03334	Hypothetical protein	12.02	380.48	31.65	1.E-02
VVMO6_03335	MoxR-like ATPase in aerotolerance operon	4.64	24.08	5.19	3.E-03
VVMO6_03440	Hypothetical protein	28.45	121.20	4.26	6.E-03
VVMO6_03720	Putative phosphatase YieH	12.78	144.39	11.30	2.E-02
VVMO6_03752	Isopenicillin N synthase	14.69	74.71	5.09	2.E-02
VVMO6_03824	CoA-disulfide reductase	72.59	450.12	6.20	4.E-02
VVMO6_03835	C4-dicarboxylate like transporter	34.52	223.85	6.48	1.E-03
VVMO6_04029	Histone acetyltransferase HPA2	14.78	128.65	8.70	1.E-02
VVMO6_04244	Phenazine biosynthesis protein PhzF like	3.27	64.60	19.76	3.E-02
VVMO6_04355	Predicted thioesterase	26.29	206.23	7.84	2.E-03
VVMO6_04383	Hypothetical protein	0.74	3.10	4.19	2.E-02
VVMO6_04520	Multimeric flavodoxin WrbA	2.16	32.70	15.14	2.E-02
VVMO6_04530	*N*-acetylmuramic acid 6-phosphate etherase	30.15	161.05	5.34	2.E-02
No functional prediction					
VVMO6_00109	Predicted membrane protein	10.89	66.41	6.10	3.E-02
VVMO6_00119	Inner membrane protein	16.85	191.36	11.36	4.E-04
VVMO6_00264	Hypothetical protein	15.33	80.83	5.27	2.E-04
VVMO6_00401	Inner membrane protein YjgN	41.32	214.59	5.19	8.E-03
VVMO6_00453	Protein of unknown function	184.58	2,239.55	12.13	2.E-03

VVMO6_00725	Hypothetical protein	36.02	2,321.11	64.44	5.E-02
VVMO6_01143	Membrane protein YcjF	57.38	339.39	5.91	5.E-02
VVMO6_01256	Hypothetical protein	52.66	1,287.15	24.44	3.E-02
VVMO6_01498	Hypothetical protein	47.94	294.49	6.14	2.E-04
VVMO6_01794	Membrane protein	35.55	1,017.08	28.61	4.E-02
VVMO6_02092	Lipoprotein-related protein	101.04	2,797.86	27.69	4.E-03
VVMO6_02410	Membrane protein	13.40	68.16	5.09	2.E-02
VVMO6_02960	Probable transmembrane protein	10.79	83.21	7.71	6.E-05
VVMO6_03048	Copper metallochaperone2C bacterial analog of Cox17 protein	44.23	419.01	9.47	2.E-03
VVMO6_03204	Inner membrane protein YccF	74.54	597.43	8.01	2.E-02
VVMO6_03251	Iron-uptake factor PiuB	12.35	122.44	9.91	5.E-04
VVMO6_04351	Putative secreted protein	47.64	440.30	9.24	8.E-03
Signal transduction, intracellular trafficking, and defense mechanism					
VVMO6_01796	Signal transduction histidine kinase	56.82	599.66	10.55	4.E-02
VVMO6_02617	Arylsulfatase	98.42	458.68	4.66	6.E-03
VVMO6_03977	Sensor histidine protein kinase UhpB2C glucose-6-phosphate specific	4.24	102.93	24.28	2.E-03
VVMO6_04385	Heavy metal sensor histidine kinase	3.79	50.99	13.45	2.E-02
VVMO6_01795	Two-component system response regulator QseB	87.63	1,030.65	11.76	3.E-02
VVMO6_03281	Putative two-component response regulator	10.53	82.04	7.79	1.E-02
VVMO6_03976	Transcriptional regulatory protein UhpA	7.48	204.30	27.31	1.E-04
VVMO6_04384	DNA-binding heavy metal response regulator	2.13	69.88	32.81	4.E-04
Intracellular trafficking, and defense mechanism					
VVMO6_00195	Multiple antibiotic resistance	8.32	60.39	7.26	4.E-02

	protein MarC				
VVMO6_00847	Cytochrome c-type biogenesis protein CcmD2C interacts with CcmCE	25.15	103.28	4.11	8.E-03
VVMO6_01033	MotA/TolQ/ExbB proton channel family protein	79.42	525.21	6.61	1.E-02
VVMO6_01034	Tol biopolymer transport system2C TolR protein	88.48	482.05	5.45	7.E-04
VVMO6_02872	General secretion pathway protein C	69.73	325.08	4.66	5.E-04
VVMO6_03849	WD40 repeat	19.04	127.33	6.69	2.E-02
VVMO6_00539	ABC-type multidrug transport system2C ATPase component	6.03	24.43	4.05	5.E-03
Uncategorized					
VVMO6_00120	Hypothetical protein	24.90	216.82	8.71	1.E-02
VVMO6_00211	Uncharacterized low-complexity protein	951.31	7,528.41	7.91	2.E-03
VVMO6_00342	Putative inner membrane protein	12.13	65.96	5.44	5.E-05
VVMO6_00440	Hypothetical protein	34.31	171.79	5.01	3.E-02
VVMO6_00489	Hypothetical protein	4.54	18.29	4.03	5.E-02
VVMO6_00720	Methyl-accepting chemotaxis protein	35.27	313.53	8.89	2.E-02
VVMO6_00723	Hypothetical protein	365.21	2,300.34	6.30	1.E-02
VVMO6_00978	Hypothetical protein	9.46	49.03	5.18	4.E-02
VVMO6_01018	Hypothetical protein	150.36	693.00	4.61	1.E-02
VVMO6_01141	Hypothetical protein	53.67	422.62	7.87	2.E-03
VVMO6_01156	Hypothetical protein	85.87	520.49	6.06	3.E-04
VVMO6_01159	Hypothetical protein	4.99	35.03	7.02	3.E-02
VVMO6_01178	Capsular polysaccharide synthesis enzyme Cpsb	16.02	127.84	7.98	2.E-03
VVMO6_01196	Hypothetical protein	10.16	77.38	7.62	7.E-03
VVMO6_01260	Hypothetical protein	36.79	175.56	4.77	1.E-02
VVMO6_01398	Hypothetical protein	18.55	93.34	5.03	1.E-02

VVMO6_01399	Hypothetical protein	46.67	189.26	4.06	2.E-02
VVMO6_01490	Hypothetical protein	55.90	251.37	4.50	5.E-03
VVMO6_01494	Formate dehydrogenase subunit or accessory protein	2.00	118.30	59.15	4.E-03
VVMO6_01534	Hypothetical protein	203.36	1,328.93	6.53	2.E-02
VVMO6_01639	Putative lipoprotein	118.97	1,525.48	12.82	6.E-03
VVMO6_01837	Membrane protein	38.32	445.81	11.63	2.E-03
VVMO6_01933	Hypothetical protein	7.60	1,030.21	135.6	2.E-04
VVMO6_02015	Hypothetical protein	3.87	23.22	6.00	3.E-02
VVMO6_02101	Hypothetical protein	0.72	6.19	8.60	2.E-02
VVMO6_02228	Transmembrane regulatory protein Toxs	174.18	792.11	4.55	2.E-04
VVMO6_02278	Hypothetical protein	1.18	25.79	21.86	2.E-02
VVMO6_02347	Hypothetical protein	0.70	9.76	13.94	3.E-02
VVMO6_02535	Hypothetical protein	152.00	649.51	4.27	8.E-03
VVMO6_03021	Hypothetical protein	17.60	212.67	12.08	7.E-03
VVMO6_03034	Maltose operon periplasmic protein Malm	46.19	511.9	11.08	3.E-02
VVMO6_03050	Hypothetical protein	22.25	95.95	4.31	7.E-03
VVMO6_03063	Hypothetical protein	9.55	264.34	27.68	3.E-02
VVMO6_03117	Hypothetical protein	33.08	135.54	4.10	4.E-03
VVMO6_03160	Hypothetical protein	10.63	44.30	4.17	3.E-02
VVMO6_03239	Hypothetical protein	23.58	950.82	40.32	7.E-03
VVMO6_03250	Hypothetical protein	24.18	115.17	4.76	1.E-02
VVMO6_03255	ATPase of the AAA^{+} class	23.90	229.00	9.58	1.E-02
VVMO6_03295	Hypothetical protein	32.98	209.92	6.37	4.E-02
VVMO6_03330	Batd	22.91	107.83	4.71	4.E-02
VVMO6_03353	Hypothetical protein	34.95	342.39	9.80	5.E-02
VVMO6_03409	Hypothetical protein	42.81	1,327.34	31.01	4.E-03
VVMO6_03463	Hypothetical protein	0.21	1,593.57	7588	3.E-02
VVMO6_03547	Hypothetical protein	21.20	669.82	31.60	3.E-04
VVMO6_03548	Pyruvate/2-oxoglutarate dehydrogenase complex2c dihydrolipoamide dehydrogenase	11.54	706.29	61.20	3.E-03

	component				
VVMO6_03573	Head-to-tail joining protein	0.20	2.38	11.90	7.E-03
VVMO6_03616	Hypothetical protein	56.53	1,067.20	18.88	3.E-03
VVMO6_03650	Hypothetical protein	0.37	7.29	19.70	2.E-02
VVMO6_03664	NADH:ubiquinone oxidoreductase subunit 2	71.16	441.79	6.21	2.E-03
VVMO6_03731	Hypothetical protein	179.58	966.89	5.38	1.E-03
VVMO6_03880	Cytolysin secretion protein	30.95	479.59	15.50	4.E-02
VVMO6_03881	Cytolysin precursor	34.43	528.9	15.36	3.E-02
VVMO6_03890	Succinyl-CoA synthetase2c alpha subunit	16.81	121.42	7.22	9.E-04
VVMO6_03974	Hypothetical protein	50.77	214.11	4.22	1.E-02
VVMO6_04069	Ribosome recycling factor	26.03	117.31	4.51	1.E-05
VVMO6_04070	Hypothetical protein	34.06	216.02	6.34	3.E-05
VVMO6_04136	Hypothetical protein	94.56	2,989.60	31.62	2.E-02
VVMO6_04181	Phenylalanyl-tRNA synthetase beta subunit	54.17	907.40	16.75	1.E-03
VVMO6_04182	Hypothetical protein	183.94	1,729.31	9.40	1.E-02
VVMO6_04225	Hypothetical protein	91.85	1,072.57	11.68	8.E-03
VVMO6_04350	ATPase involved in DNA repair	20.34	138.74	6.82	4.E-02
VVMO6_04362	TPR repeat protein	0.45	4.02	8.93	2.E-02
VVMO6_04485	Hypothetical protein	0.04	0.75	18.75	4.E-03
VVMO6_04505	Hypothetical protein	4.13	91.69	22.20	4.E-02
VVMO6_04506	Hypothetical protein	11.44	557.56	48.74	3.E-02
VVMO6_04511	Hypothetical protein	5.20	25.93	4.99	4.E-03
VVMO6_04535	Microbial collagenase2c secreted	0.47	24.17	51.43	3.E-02

[a] Locus tags are based on the database for the *V. vulnificus* MO6-24/O genome, which was retrieved from GenBank (accession number CP002469 and CP002470).

II-3-7. Genes down-regulated by mucin and mucin-secreting HT29-MTX cells

202 and 319 genes that were down-regulated by the mucin and the mucin-secreting HT29-MTX cells were summarized in Table II-5 and Table II-6, respectively. Selected categories of genes were further discussed below.

Biosynthesis of amino acids. Among the genes repressed during growth in the M9M, 27 genes related to biosynthesis of amino acids were down-regulated (Table II-5). For instance, the protein products of 5 (VVMO6_00312 to 00315) out of 27 genes were predicted to participate arginine biosynthesis. 8 genes (VVMO6_01857 to 01864) encoding putative enzymes for histidine biosynthesis were also highly repressed. In addition, the decreased expression of genes related to anabolic pathways of leucine, arginine, and tryptophan was also identified. These results implied that amino acids from the mucin protein backbone might be enough to synthesize proteins essential for growth of *V. vulnificus*. In contrast, the expressions of *opp* operon and *sap* operon encoding transporter for oligopeptide and peptide were highly increased by mucin (Table II-3). It is noteworthy that *vvpE* is also induced during mucin utilization and VvpE was 69% identical in amino acid sequences to those of HapA, mucinase produced by *V. cholerae* (data not shown) (Silva *et al.*, 2003). Therefore, the uptake of the oligopeptide and peptide derived from the hydrolysis of the mucin by VvpE might lead the decreased expression of amino acid

biosynthesis at the transcriptional level.

Synthesis of flagellin and pilus. From the RNA-seq analysis, the entire group of genes encoding protein involved in the flagellin (*flaF*, *flaD*, *flaA*, *flaE*, *flaD*, and *flaC*) and pilus (*tadA*, *tadB*, and *tadC*) assembly was highly repressed in the *V. vulnificus* cells exposed to the HT-29 MTX cells (Table II-6). Especially, genes encoding self-assembling building blocks of flagellar filament are required for motility and adhesion of *V. vulnificus* (Kim *et al*., 2014). In other words, the flagellum and pilus prime *V. vnlificus* for initial colonization of host intestinal tissue, which is an important step required for the onset of its infectious cycle. However, upon establishing preferred colonization niches with the increase in population density, the motility might be superfluous, even detrimental, for a successful infection of host by the bacteria. In this context, the decreased mRNA level of genes related to flagellin and pilus synthesis could result in saving the nutrients from being used up for the flagellin and the pilus synthesis and the remaining nutrient could provide the bacteria with better chance of survival in the host.

In conclusion, I showed that *V. vulnificus* discriminatively expressed 337 and 650 genes involved in various functional factors by the exposure to mucin and the mucin-secreting host cells. This work provides a wealth of information about a bacterial response to host component and leads us to a better understanding of host-microbe interaction.

Table II-4. List of genes down-regulated by mucin

Locus tag[a]	Gene product	RPKM		Fold change	*P*-value
		M9G	M9M		
Energy production and conversion					
VVMO6_00310	Phosphoenolpyruvate carboxylase	924.11	83.77	-11.03	1.E-03
VVMO6_01906	Probable thiol oxidoreductase with 2 cytochrome c heme-binding sites	264.22	50.87	-5.19	3.E-02
VVMO6_02043	Alcohol dehydrogenase	5485.3	817.25	-6.71	3.E-02
VVMO6_03472	Alcohol dehydrogenase	1732.6	174.27	-9.94	3.E-02
VVMO6_03502	Cytochrome c553	203.98	48.18	-4.23	1.E-03
VVMO6_03645	Acetate kinase	629.94	31.52	-19.99	1.E-02
VVMO6_03796	NAD(P) transhydrogenase subunit beta	1793.4	360.00	-4.98	3.E-02
VVMO6_03797	NAD(P) transhydrogenase alpha subunit	1596.0	348.05	-4.59	5.E-03
VVMO6_03887	Anaerobic C4-dicarboxylate transporter DcuC	176.8	34.31	-5.15	4.E-03
VVMO6_02651	3-isopropylmalate dehydrogenase	575.45	98.46	-5.84	4.E-03
Amino acid metabolism and transport					
VVMO6_00307	52C10-methylenetetrahydrofolate reductase	1473.0	132.08	-11.15	2.E-02
VVMO6_00312	*N*-acetyl-gamma-glutamyl-phosphate reductase	574.62	47.33	-12.14	4.E-02
VVMO6_00313	Acetylglutamate kinase	1802.2	49.74	-36.23	8.E-04
VVMO6_00314	Argininosuccinate synthase	2957.5	87.77	-33.70	7.E-05
VVMO6_00315	*N*-acetylglutamate synthase	554.81	27.75	-19.99	3.E-02
VVMO6_00393	Ornithine carbamoyltransferase	404.89	58.14	-6.96	2.E-03
VVMO6_01094	5-methyltetrahydro-Pteroyltriglutamate-homocysteine methyltransferase	4243.9	4.88	-869.7	3.E-03
VVMO6_01857	Phosphoribosyl-AMP cyclohydrolase	524.16	81.59	-6.42	1.E-02

VVMO6_01858	Imidazole glycerol phosphate synthase cyclase subunit	509.96	74.03	-6.89	9.E-04
VVMO6_01859	Phosphoribosylformimino-5-aminoimidazole carboxamide ribotide isomerase	580.77	84.59	-6.87	7.E-03
VVMO6_01860	Imidazole glycerol phosphate synthase amidotransferase subunit	540.77	74.39	-7.27	4.E-03
VVMO6_01861	Histidinol-phosphatase	596.06	65.97	-9.04	6.E-04
VVMO6_01862	Histidinol-phosphate aminotransferase	461.44	45.22	-10.20	9.E-03
VVMO6_01863	Histidinol dehydrogenase	553.98	56.60	-9.79	6.E-03
VVMO6_01864	ATP phosphoribosyltransferase	702.18	75.10	-9.35	2.E-03
VVMO6_02000	Tryptophan synthase beta chain	637.47	104.06	-6.13	7.E-03
VVMO6_02001	Tryptophan synthase alpha chain	653.54	134.27	-4.87	9.E-03
VVMO6_02247	Cysteine synthase	1551.3	197.95	-7.84	1.E-02
VVMO6_02320	Serine hydroxymethyltransferase	3255.4	691.94	-4.70	8.E-03
VVMO6_02490	Cyclohexadienyl dehydrogenase	852.67	150.46	-5.67	4.E-03
VVMO6_02491	2-keto-3-deoxy-D-arabino-heptulosonate-7-phosphate synthase I alpha	1081.4	94.18	-11.48	3.E-03
VVMO6_02540	Threonine synthase	1277.0	287.07	-4.45	1.E-03
VVMO6_02541	Homoserine kinase	504.42	95.44	-5.29	3.E-03
VVMO6_02542	Aspartokinase / Homoserine dehydrogenase	1567.2	147.04	-10.66	4.E-02
VVMO6_02552	Glutamate synthase large chain	2311.3	10.50	-220.1	3.E-03
VVMO6_02650	2-isopropylmalate synthase	505.38	85.22	-5.93	3.E-02
VVMO6_02652	3-isopropylmalate dehydratase large subunit	520.53	97.29	-5.35	2.E-02
VVMO6_02883	Glutamine synthetase type I	4538.4	1128.96	-4.02	2.E-02
VVMO6_03179	Argininosuccinate synthase	220.53	16.06	-13.73	4.E-03
VVMO6_03996	Tripeptide aminopeptidase	159.94	14.34	-11.15	9.E-03
VVMO6_04187	Arginine ABC transporter2C permease protein ArtM	128.62	9.78	-13.15	1.E-02
VVMO6_02564	Carbamoyl-phosphate synthase	1584.6	298.22	-5.31	1.E-03

	large chain				
VVMO6_00054	Ketol-acid reductoisomerase	5718.9	347.37	-16.46	3.E-02
VVMO6_00347	Phosphoadenylyl-sulfate reductase	978.46	45.33	-21.59	2.E-04
VVMO6_01996	Anthranilate synthase2C aminase component	289.12	47.89	-6.04	3.E-02
VVMO6_02720	Sulfate adenylyltransferase subunit 2	689.3	19.69	-35.01	4.E-04
VVMO6_03104	ABC-type dipeptide/oligopeptide/nickel transport system2C permease component	4.61	1.00	-4.61	2.E-03
VVMO6_02553	Glutamate synthase small chain	2329.8	16.27	-143.2	6.E-04
VVMO6_03201	ABC-type amino acid transport2C signal transduction systems2C periplasmic component/domain	160.5	38.22	-4.20	2.E-03
Nucleotide metabolism and transport					
VVMO6_00177	Phosphoribosylamine--glycine ligase	769.94	146.84	-5.24	2.E-03
VVMO6_02374	Phosphoribosylformylglycinamidine synthase2C synthetase subunit t	744.8	130.27	-5.72	9.E-04
VVMO6_03995	dCMP deaminase	275.01	65.95	-4.17	2.E-02
Carbohydrate metabolism and transport					
VVMO6_00207	6-phosphofructokinase	2686.9	375.40	-7.16	9.E-03
VVMO6_00230	22C3-bisphosphoglycerate-independent phosphoglycerate mutase	1459.6	195.85	-7.45	4.E-03
VVMO6_00338	Glucose-6-phosphate isomerase	1632.6	398.19	-4.10	1.E-02
VVMO6_00413	6-phospho-beta-glucosidase	91.40	21.66	-4.22	3.E-03
VVMO6_00488	Enolase	3824.5	910.60	-4.20	3.E-02
VVMO6_01934	PTS system2C glucose-specific IIBC component	4118.6	440.04	-9.36	1.E-02
VVMO6_02082	Aldose 1-epimerase family protein	342.93	53.69	-6.39	9.E-03

	YeaD				
VVMO6_02249	Phosphoenolpyruvate-protein phosphotransferase of PTS system	1350.6	297.56	-4.54	2.E-02
VVMO6_03056	Glycogen phosphorylase	391.0	81.80	-4.78	2.E-02
VVMO6_03254	Permease of the major facilitator superfamily	257.2	37.24	-6.91	2.E-02
VVMO6_03699	Fructose-specific phosphocarrier protein HPr / PTS system2C fructose-specific IIA component	90.01	18.35	-4.91	3.E-02
Coenzyme metabolism					
VVMO6_01883	Dethiobiotin synthetase	363.34	83.72	-4.34	9.E-03
VVMO6_02544	Ribonuclease E inhibitor RraA	437.9	91.72	-4.77	7.E-04
VVMO6_02721	Uroporphyrinogen-III methyltransferase	294.77	9.88	-29.84	9.E-03
VVMO6_02938	Thiazole biosynthesis protein ThiG	870.79	166.73	-5.22	7.E-03
VVMO6_02940	Sulfur carrier protein adenylyltransferase ThiF	1009.9	204.71	-4.93	3.E-02
VVMO6_02941	Thiamin-phosphate pyrophosphorylase	928.49	174.79	-5.31	2.E-02
VVMO6_02942	Thiamin biosynthesis protein ThiC	1997.4	454.98	-4.39	4.E-02
VVMO6_03382	Radical SAM family protein HutW2C	541.81	6.74	-80.39	3.E-02
VVMO6_00454	D-3-phosphoglycerate dehydrogenase	1964.4	383.51	-5.12	2.E-02
VVMO6_02937	Thiazole biosynthesis protein ThiH	662.29	124.96	-5.30	1.E-02
Lipid metabolism					
VVMO6_00612	Putative lipid carrier protein	148.04	30.09	-4.92	3.E-03
VVMO6_03851	Acyl dehydratase	232.49	55.83	-4.16	1.E-02
Translation, including ribosome structure and biogenesis					
VVMO6_00728	LSU ribosomal protein L31p	38.00	7.48	-5.08	1.E-02

Transcription					
VVMO6_00637	Transcriptional regulator2C AraC family	114.51	21.72	-5.27	5.E-02
VVMO6_01093	Transcriptional activator MetR	351.30	85.06	-4.13	1.E-02
VVMO6_03312	Transcriptional regulator2C MerR family2C associated with photolyase	77.94	12.84	-6.07	5.E-02
VVMO6_03527	Response regulator	102.89	21.17	-4.86	3.E-02
Replication, recombination and repair					
VVMO6_01585	Phage exonuclease2C putative	2.65	0.34	-7.81	2.E-02
VVMO6_01591	DNA polymerase	1.75	0.38	-4.61	3.E-02
VVMO6_03555	DNA polymerase	3.28	0.66	-4.97	2.E-02
Cell wall structure and biogenesis					
VVMO6_01618	Outer membrane protein SypB	1.32	0.22	-6.00	9.E-03
VVMO6_02636	Glucosamine--fructose-6-phosphate aminotransferase	489.9	117.47	-4.17	3.E-03
VVMO6_03300	Protease-related protein	76.66	16.68	-4.60	3.E-04
VVMO6_03380	Ferric siderophore transport system2C periplasmic binding protein TonB	51.11	0.70	-73.01	4.E-02
VVMO6_03837	Ferric siderophore transport system2C periplasmic binding protein TonB	300.43	37.53	-8.01	4.E-02
Secretion, motility and chemotaxis					
VVMO6_03492	Methyl-accepting chemotaxis protein	170.3	37.60	-4.53	5.E-02
VVMO6_03521	Aerotaxis sensor receptor protein	68.80	17.02	-4.04	5.E-02
Molecular chaperones and related functions					
VVMO6_00610	Putative protease	57.30	10.46	-5.48	2.E-04
VVMO6_01266	Putative protein-S-isoprenyl-	76.42	17.65	-4.33	3.E-02

	cysteine methyltransferase				
VVMO6_02966	Heat shock protein A	242.59	59.17	-4.10	3.E-02
VVMO6_03217	Periplasmic thiol:disulfide interchange protein DsbA	161.48	29.87	-5.41	2.E-02
VVMO6_03967	Alkyl hydroperoxide reductase protein F	19.81	4.94	-4.01	2.E-02
VVMO6_04020	Heme A synthase2C cytochrome oxidase biogenesis protein Cox15-CtaA	106.24	15.49	-6.86	2.E-02
Inorganic ion transport and metabolism					
VVMO6_00285	Bacterioferritin-associated ferredoxin	2185.7	252.08	-8.67	6.E-03
VVMO6_00345	Sulfite reductase flavoprotein alpha-component	905.99	30.38	-29.82	1.E-02
VVMO6_00346	Sulfite reductase hemoprotein beta-component	1437.5	56.21	-25.57	2.E-03
VVMO6_00558	Ferric iron ABC transporter2C iron-binding protein	2813.8	703.46	-4.00	5.E-03
VVMO6_01148	Transporter2C putative	55.69	10.34	-5.39	1.E-03
VVMO6_01189	Hypothetical protein	61.75	14.89	-4.15	1.E-03
VVMO6_01907	Iron-regulated protein A precursor	1730.9	186.51	-9.28	2.E-03
VVMO6_02185	Ferrous iron transport protein B	651.73	50.41	-12.93	3.E-02
VVMO6_02186	Ferrous iron transport protein A	404.12	25.44	-15.89	2.E-03
VVMO6_02717	Adenylylsulfate kinase	319.01	30.26	-10.54	6.E-03
VVMO6_02718	Sulfate permease2C Trk-type	376.12	14.88	-25.28	4.E-03
VVMO6_02719	Sulfate adenylyltransferase subunit	1189.3	23.94	-49.68	1.E-02
VVMO6_03607	Ferric vibriobactin2C enterobactin transport system2C permease protein VctD	58.00	6.51	-8.91	1.E-04
VVMO6_03608	Ferric vibriobactin2C enterobactin transport system2C permease protein VctG	126.39	8.44	-14.98	1.E-03
VVMO6_03609	Ferric vibriobactin2C enterobactin	236.04	12.88	-18.33	7.E-03

	transport system2C ATP-binding protein				
VVMO6_03867	Nitrate ABC transporter2C ATP-binding protein	3.71	0.28	-13.26	2.E-02
VVMO6_03869	Nitrate ABC transporter2C nitrate-binding protein	2.19	0.33	-6.64	6.E-03
VVMO6_04221	Hypothetical protein	510.77	31.60	-16.16	5.E-02
VVMO6_04406	Ferric aerobactin ABC transporter2C permease component	82.33	16.38	-5.03	4.E-03
General function prediction only					
VVMO6_01815	Putative sodium-dependent transporter	433.00	104.02	-4.16	5.E-03
VVMO6_01905	Iron-regulated protein A precursor	381.98	71.63	-5.33	1.E-02
VVMO6_01932	Sodium-dependent transporter	221.11	16.13	-13.71	1.E-02
VVMO6_02539	Pyruvate formate lyase	1840.7	189.18	-9.73	3.E-02
VVMO6_02551	Predicted Fe-S oxidoreductase	48.51	4.04	-12.01	3.E-03
VVMO6_03242	Permease of the drug/metabolite transporter superfamily	28.3	6.31	-4.48	8.E-03
No functional prediction					
VVMO6_00350	Uncharacterized conserved protein	234.21	55.24	-4.24	1.E-02
VVMO6_00416	PhnB protein; putative DNA binding 3-demethylubiquinone-9 3-methyltransferase domain protein	327.49	66.70	-4.91	5.E-04
VVMO6_00802	Hypothetical protein	286.48	71.30	-4.02	5.E-02
VVMO6_00902	Uncharacterized iron-regulated protein	174.06	26.56	-6.55	7.E-03
VVMO6_00966	Hypothetical protein	1580.2	106.26	-14.87	2.E-03
VVMO6_01903	L2CD-transpeptidase YcbB	45.21	10.53	-4.29	9.E-04
VVMO6_01904	Putative exported protein	229.07	41.46	-5.53	9.E-03
VVMO6_02416	Hypothetical protein	68.23	12.24	-5.57	6.E-04
VVMO6_03240	Uncharacterized conserved protein	148.18	36.88	-4.02	3.E-02

VVMO6_03311	Uncharacterized conserved protein	439.73	29.23	-15.04	8.E-03
VVMO6_03906	Uncharacterized protein ImpC	66.723	15.13	-4.41	6.E-03
VVMO6_04322	Hypothetical protein	75.99	10.91	-6.97	2.E-02
Signal prediction					
VVMO6_01169	Hypothetical protein	115.9	18.09	-6.41	1.E-03
VVMO6_02989	Signal transduction histidine kinase	68.20	16.87	-4.04	2.E-02
VVMO6_03073	HDIG domain protein	112.64	26.63	-4.23	3.E-02
VVMO6_03192	DNA-binding HTH domain-containing protein	60.86	13.80	-4.41	2.E-03
Intracellular trafficking, secretion					
VVMO6_00652	TPR repeat protein	65.65	15.58	-4.21	4.E-02
VVMO6_01212	Flp pilus assembly protein TadC	6.58	0.78	-8.43	1.E-02
VVMO6_03378	Biopolymer transport protein ExbD1	95.52	5.29	-18.06	2.E-02
VVMO6_03379	Ferric siderophore transport system2C biopolymer transport protein ExbB	96.56	3.41	-28.32	4.E-03
VVMO6_03840	MotA/TolQ/ExbB proton channel family protein	310.79	42.08	-7.39	5.E-03
VVMO6_04116	Protein-export membrane protein SecF	284.36	55.54	-5.12	6.E-03
Uncategorized					
VVMO6_00089	Hypothetical protein	782.40	156.75	-4.99	3.E-03
VVMO6_00972	Hypothetical protein	831.24	83.13	-10.00	3.E-02
VVMO6_01047	Hypothetical protein	235.83	11.87	-19.87	2.E-02
VVMO6_01230	Hypothetical protein	4.60	1.08	-4.26	9.E-03
VVMO6_01243	MoxR-like ATPase	24.95	5.22	-4.78	5.E-02
VVMO6_01602	WD40 repeat	49.14	7.22	-6.81	2.E-02
VVMO6_01716	Hypothetical protein	116.11	24.14	-4.81	2.E-02
VVMO6_01995	Trp operon leader peptide	108.32	6.07	-17.85	4.E-02

VVMO6_02373	Hypothetical protein	34.13	8.47	-4.03	2.E-02
VVMO6_02545	Hypothetical protein	141.56	20.17	-7.02	1.E-03
VVMO6_02640	Hypothetical protein	11.93	1.38	-8.64	3.E-03
VVMO6_03029	Hypothetical protein	258.42	63.88	-4.05	4.E-03
VVMO6_03278	Hypothetical protein	6.53	1.44	-4.53	7.E-03
VVMO6_03381	Hypothetical protein	69.09	1.15	-60.08	1.E-02
VVMO6_03397	Gfa-like protein	34.29	6.91	-4.96	2.E-02
VVMO6_03574	Hypothetical protein	4.12	0.90	-4.58	5.E-02
VVMO6_03580	Hypothetical protein	4.18	0.91	-4.60	7.E-03
VVMO6_03587	Hypothetical protein	3.27	0.77	-4.25	3.E-02
VVMO6_03605	Conserved hypothetical protein	441.47	15.92	-27.73	7.E-03
VVMO6_03606	Hypothetical protein	127.64	11.29	-11.31	7.E-03
VVMO6_03612	Hypothetical protein	483.17	116.99	-4.13	3.E-02
VVMO6_03843	Hypothetical protein	44.44	9.38	-4.74	5.E-02
VVMO6_03931	Hypothetical protein	126.92	26.84	-4.73	3.E-02
VVMO6_04163	Hypothetical protein	115.33	3.20	-36.04	1.E-02
VVMO6_04345	Hypothetical protein	23.45	4.49	-5.22	2.E-02
VVMO6_04388	Permease of the major facilitator superfamily	6.34	0.36	-17.61	4.E-02
VVMO6_04390	Hypothetical protein	201.22	1.68	-119.8	9.E-05

[a] Locus tags are based on the database for the *V. vulnificus* MO6-24/O genome, which was retrieved from GenBank (accession number CP002469 and CP002470).

Table II-4. List of genes down-regulated by HT29-MTX cells

Locus tag[a]	Gene product	RPKM		Fold change	*P*-value
		BME	HT29-MTX		
Energy production and conversion					
VVMO6_00310	Phosphoenolpyruvate carboxylase	593.11	105.75	-5.61	7.E-03
VVMO6_00418	Uncharacterized flavoprotein	279.44	27.88	-10.02	9.E-04
VVMO6_00947	NADH dehydrogenase	298.17	69.87	-4.27	3.E-02
VVMO6_03628	Cytochrome c553	19.96	4.57	-4.37	1.E-02
VVMO6_03874	Assimilatory nitrate reductase large subunit	687.66	3.57	-192.6	2.E-02
VVMO6_04024	Cytochrome c oxidase polypeptide III	60.83	6.96	-8.74	2.E-02
VVMO6_04237	Aldehyde dehydrogenase	47.48	4.29	-11.07	5.E-02
Amino acid metabolism and transport					
VVMO6_00063	Dipeptide-binding ABC transporter2c periplasmic substrate-binding component	2,603	219.36	-11.87	3.E-04
VVMO6_00307	52C10-methylenetetrahydrofolate reductase	654.17	44.21	-14.80	7.E-04
VVMO6_00556	Nitrogen regulatory protein P-II	4,348	83.48	-52.09	7.E-04
VVMO6_01094	Methyltetrahydropteroyltriglutamate-homocysteine methyltransferase	1,630	9.41	-173.3	1.E-02
VVMO6_01664	Amino acid ABC transporter2c permease protein	558.43	38.39	-14.55	1.E-02
VVMO6_01665	Amino acid ABC transporter2c permease protein	322.88	33.43	-9.66	5.E-02
VVMO6_01666	ABC-type polar amino acid transport system2c ATPase component	623.96	70.23	-8.88	5.E-02
VVMO6_02552	Glutamate synthase large chain	266.57	30.62	-8.71	2.E-02
VVMO6_02883	Glutamine synthetase type I	10,541	914.69	-11.52	3.E-02

VVMO6_03179	Argininosuccinate synthase	21.88	4.97	-4.40	8.E-03
VVMO6_03218	Hypothetical protein	133.23	20.48	-6.51	5.E-03
VVMO6_03401	Spermidine synthase-like protein	58.42	9.75	-5.99	2.E-02
VVMO6_03493	Glutamate decarboxylase	302.74	21.72	-13.94	3.E-03
VVMO6_03872	Anthranilate phospho ribosyltransferase like	600.13	30.74	-19.52	5.E-02
VVMO6_04334	ABC-type branched-chain amino acid transport system2c periplasmic component	63.21	13.60	-4.65	4.E-03
VVMO6_04367	Vibriolysin2C extracellular zinc protease	539.74	127.60	-4.23	3.E-03
VVMO6_04389	Methyltetrahydropteroyltriglutama te-homocysteine methyltransferase	825.86	5.93	-139.3	5.E-04
VVMO6_00064	Peptide ABC transporter2c permease component	313.53	57.72	-5.43	3.E-02
VVMO6_00065	Dipeptide transport system permease protein Dppc	380.77	62.25	-6.12	5.E-03
VVMO6_02833	Oligopeptide transport ATP-binding protein Oppd	415.17	95.47	-4.35	2.E-03
VVMO6_01723	4-hydroxyphenylpyruvate dioxygenase	2,764	589.37	-4.69	5.E-02
VVMO6_02553	Glutamate synthase small chain	290.17	34.58	-8.39	2.E-02
VVMO6_01165	ABC transporter2c periplasmic substrate-binding protein-related protein	68.31	13.34	-5.12	6.E-04
VVMO6_01663	Glutamate aspartate periplasmic binding protein precursor	3,036	137.87	-22.03	5.E-02
VVMO6_02988	ABC-type amino acid transport/signal transduction system	273.71	30.19	-9.07	2.E-03
VVMO6_03082	ABC-type amino acid transport/signal transduction system	21.26	2.61	-8.15	3.E-03
VVMO6_03201	ABC-type amino acid transport2c	522.81	37.90	-13.79	8.E-04

	signal transduction systems2c periplasmic component/domain				
VVMO6_03703	Hypothetical protein	232.02	16.80	-13.81	1.E-03
VVMO6_04192	ABC-type amino acid transport/signal transduction systems	93.34	19.32	-4.83	2.E-03
Nucleotide and Carbohydrate metabolism and transport					
VVMO6_00099	Adenylate cyclase	631.83	154.44	-4.09	8.E-04
VVMO6_00230	22C3-bisphosphoglycerate-independent phosphoglycerate mutase	2,053	240.15	-8.55	2.E-02
VVMO6_00288	Triosephosphate isomerase	2,259	539.45	-4.19	5.E-03
VVMO6_01934	PTS system2c glucose-specific IIBC component	2,965	688.74	-4.31	5.E-02
VVMO6_01987	EAL domain	138.63	25.23	-5.49	1.E-03
VVMO6_02081	NAD-dependent glyceraldehyde-3-phosphate dehydrogenase	12,054	2,062.41	-5.84	5.E-02
VVMO6_02082	Aldose 1-epimerase family protein Yead	331.97	78.75	-4.22	2.E-02
VVMO6_02248	Phosphocarrier protein of PTS system	2,305	423.09	-5.45	5.E-04
VVMO6_02249	Phosphoenolpyruvate-protein phosphotransferase of PTS system	2,005	359.80	-5.58	2.E-02
VVMO6_03706	Pyruvate kinase	7.50	1.68	-4.46	5.E-02
VVMO6_03714	Glucose-1-phosphate adenylyltransferase	1,220	58.29	-20.95	1.E-02
VVMO6_04045	Multidrug resistance protein D	186.30	35.82	-5.20	1.E-02
Coenzyme metabolism					
VVMO6_00146	Outer membrane vitamin B12 receptor Btub	40.91	8.80	-4.65	3.E-03
VVMO6_00730	Multidrug efflux pump component Mtrf	814.01	19.71	-41.30	1.E-03

VVMO6_01108	GTP cyclohydrolase II	3,138	271.85	-11.55	1.E-02
VVMO6_02987	GTP cyclohydrolase II	144.27	7.64	-18.88	5.E-03
VVMO6_03366	NAD synthetase	1,465	243.87	-6.01	5.E-04
VVMO6_03844	Uroporphyrinogen-III methyltransferase	56.43	7.53	-7.49	2.E-02
VVMO6_03873	Uroporphyrinogen-III methyltransferase	378.54	3.89	-97.31	4.E-02
VVMO6_00454	D-3-phosphoglycerate dehydrogenase	1,793	299.36	-5.99	3.E-02
Lipid metabolism					
VVMO6_01217	FMN-dependent NADH-azoreductase	178.96	42.33	-4.23	3.E-03
VVMO6_01532	3-hydroxydecanoyl-[acyl-carrier-protein] dehydratase	1,162	138.71	-8.38	5.E-04
VVMO6_03518	Delta-9 fatty acid desaturase	175.65	10.69	-16.43	8.E-03
VVMO6_03962	Methylcrotonyl-CoA carboxylase carboxyl transferase subunit	26.72	5.48	-4.88	4.E-02
VVMO6_03963	Methylglutaconyl- CoA hydratase	48.48	6.85	-7.08	4.E-03
VVMO6_04112	Polyhydroxyalkanoic acid synthase	745.51	84.01	-8.87	2.E-02
VVMO6_04114	Acetyl- CoA acetyltransferase	956.11	107.52	-8.89	5.E-02
VVMO6_00870	3-oxoacyl-[acyl-carrier-protein] synthase2c KASI	946.81	145.69	-6.50	2.E-02
VVMO6_04115	Acetoacetyl- CoA reductase	678.84	64.39	-10.54	7.E-04
Translation, including ribosome structure and biogenesis					
VVMO6_00728	LSU ribosomal protein L31p	22,391	279.42	-80.13	2.E-02
VVMO6_00729	LSU ribosomal protein L36p	18,991	178.64	-106.3	1.E-02
VVMO6_01191	Acetyltransferase	233.53	45.72	-5.11	2.E-03
Transcription					
VVMO6_00497	RNA polymerase sigma factor RpoS	1,694	414.35	-4.09	2.E-02

VVMO6_00637	Transcriptional regulator2C AraC family	213.02	21.46	-9.93	2.E-03
VVMO6_03023	Transcriptional regulator2C TetR family	85.59	18.76	-4.56	2.E-02
VVMO6_03241	Transcriptional regulator2C LysR family	56.25	13.19	-4.26	5.E-03
VVMO6_03312	Transcriptional regulator2C MerR family2C associated with photolyase	271.11	44.07	-6.15	2.E-03
VVMO6_02637	Transcriptional regulator of glmS gene2C DeoR family	801.6	61.33	-13.07	4.E-03
VVMO6_03527	Response regulator	286.65	26.74	-10.72	9.E-04
VVMO6_04089	Hypothetical protein	224.21	47.21	-4.75	3.E-04
VVMO6_04374	Response regulator	101.82	14.64	-6.95	4.E-03
VVMO6_04548	Serine phosphatase RsbU	208.36	27.71	-7.52	3.E-03
Replication, recombination and repair					
VVMO6_00073	Chromosome segregation ATPase	44.02	5.99	-7.35	1.E-02
VVMO6_02537	Uracil-DNA glycosylase2C family	2,494	66.73	-37.38	3.E-02
VVMO6_02538	Endonuclease IV	161.73	30.67	-5.27	2.E-02
VVMO6_02908	Transposase and inactivated derivatives	6.80	0.77	-8.83	3.E-02
VVMO6_03313	Deoxyribodipyrimidine photolyase	148.10	36.89	-4.01	2.E-03
VVMO6_01135	Hypothetical hydrolase YeaB	201.21	37.89	-5.31	8.E-03
Cell wall structure and biogenesis					
VVMO6_00985	Outer membrane protein OmpT	15,735	3,142.19	-5.01	1.E-02
VVMO6_01624	Glycosyltransferase SypH	137.46	27.07	-5.08	2.E-02
VVMO6_01752	Outer membrane phospholipase A	186.82	37.02	-5.05	1.E-03
VVMO6_01876	S-adenosyl-L-methionine dependent methyltransferase2C	336.90	69.21	-4.87	7.E-03
VVMO6_02636	Glucosamine--fructose-6-phosphate aminotransferase	1,286	130.62	-9.85	2.E-03
VVMO6_02842	Ferric siderophore transport	374.13	13.96	-26.80	1.E-04

	system2C periplasmic binding protein TonB				
VVMO6_03946	Alanine racemase	251.37	34.30	-7.33	7.E-03
VVMO6_03988	Protein F-related protein	186.98	30.77	-6.08	2.E-04
Secretion, motility and chemotaxis					
VVMO6_00135	Flagellar biosynthesis protein FliL	633.3	161.04	-3.93	2.E-03
VVMO6_00807	Flagellin protein FlaF	237.4	35.33	-6.72	2.E-03
VVMO6_00808	Flagellin protein FlaD	760.85	140.73	-5.41	4.E-02
VVMO6_00809	Flagellin protein FlaA	1,566	332.47	-4.71	3.E-03
VVMO6_02251	Flagellin protein FlaE	434.46	95.38	-4.56	1.E-02
VVMO6_02252	Flagellin protein FlaD	655.70	116.14	-5.65	3.E-02
VVMO6_02255	Flagellin protein FlaC	1,534	368.47	-4.16	1.E-02
VVMO6_02256	Flagellar hook-associated protein FlgL	237.84	56.99	-4.17	1.E-03
VVMO6_02257	Flagellar hook-associated protein FlgK	251.27	57.17	-4.40	1.E-03
VVMO6_02259	Flagellar P-ring protein FlgI	444.02	98.37	-4.51	8.E-03
VVMO6_02263	Flagellar hook protein FlgE	2,881	692.38	-4.16	5.E-03
VVMO6_01488	Methyl-accepting chemotaxis protein I	109.63	20.92	-5.24	5.E-03
VVMO6_01814	Methyl-accepting chemotaxis protein	148.84	14.22	-10.47	7.E-03
VVMO6_02139	Methyl-accepting chemotaxis protein I	87.65	17.70	-4.95	4.E-03
VVMO6_02222	Methyl-accepting chemotaxis protein I	160.91	12.75	-12.62	4.E-04
VVMO6_03059	Methyl-accepting chemotaxis protein I	277.51	22.95	-12.09	1.E-03
VVMO6_03390	Methyl-accepting chemotaxis protein	117.33	20.76	-5.65	3.E-03
VVMO6_03392	Methyl-accepting chemotaxis protein	371.92	67.00	-5.55	2.E-03
VVMO6_03492	Methyl-accepting chemotaxis	1,070	45.85	-23.36	4.E-04

	protein				
VVMO6_03521	Aerotaxis sensor receptor protein	122.38	8.81	-13.89	6.E-03
VVMO6_03814	Methyl-accepting chemotaxis protein	21.43	4.34	-4.94	2.E-02
VVMO6_03945	Methyl-accepting chemotaxis protein I	128.95	22.40	-5.76	9.E-03
VVMO6_04090	Chemotaxis protein CheC inhibitor of MCP methylation	341.19	76.49	-4.46	1.E-04
VVMO6_04372	Methyl-accepting chemotaxis protein I	323.40	39.17	-8.26	3.E-05
VVMO6_04550	Methyl-accepting chemotaxis protein	273.16	28.02	-9.75	1.E-03
VVMO6_04551	Chemotaxis response regulator protein-glutamate methylesterase CheB	69.83	12.34	-5.66	4.E-03
VVMO6_04552	Chemotaxis protein CheD	94.97	18.50	-5.13	1.E-02
VVMO6_04553	Chemotaxis protein methyltransferase CheR	109.61	18.94	-5.79	2.E-02
VVMO6_04554	Methyl-accepting chemotaxis protein I	133.30	30.74	-4.34	3.E-03
VVMO6_00651	Type II/IV secretion system protein TadC2C associated with Flp pilus assembly	55.87	7.34	-7.61	1.E-02
VVMO6_02258	Flagellar protein FlgJ	453.73	113.7	-3.99	2.E-02
Molecular chaperones and related functions					
VVMO6_00641	Predicted ATPase with chaperone activity2C associated with Flp pilus assembly	43.73	4.43	-9.87	2.E-02
VVMO6_01702	Secreted trypsin-like serine protease	235.07	17.38	-13.53	8.E-04
VVMO6_03691	Secreted trypsin-like serine protease	116.80	22.26	-5.25	2.E-03
VVMO6_04019	Heme O synthase2C protoheme IX	190.38	18.44	-10.32	6.E-03

	farnesyltransferase				
VVMO6_04020	Heme A synthase2C cytochrome oxidase biogenesis protein Cox15	366.6	28.32	-12.94	4.E-03
VVMO6_04025	Cytochrome oxidase biogenesis protein Cox11-CtaG2C copper delivery to Cox1	40.36	6.42	-6.29	7.E-03
VVMO6_04141	Antioxidant2C putative	1,703	301.02	-5.66	1.E-02
VVMO6_04438	Glutaredoxin 3	3.63	0.76	-4.78	5.E-03
VVMO6_00640	ABC-type uncharacterized transport system2C permease component	232.30	3.50	-66.37	7.E-04
VVMO6_01205	Hypothetical protein	401.09	46.58	-8.61	2.E-02
Inorganic ion transport and metabolism					
VVMO6_00133	Thiosulfate sulfurtransferase GlpE	727.79	140.56	-5.18	8.E-03
VVMO6_00557	Ammonium transporter	5,110	153.59	-33.28	5.E-04
VVMO6_01189	Hypothetical protein	415.19	25.17	-16.50	3.E-04
VVMO6_01621	Phosphonate ABC transporter phosphate-binding periplasmic component	48.43	9.50	-5.10	1.E-02
VVMO6_02185	Ferrous iron transport protein B	2,200	292.16	-7.53	1.E-02
VVMO6_02186	Ferrous iron transport protein A	1,186	167.16	-7.10	5.E-02
VVMO6_02189	Zinc ABC transporter2C periplasmic-binding protein ZnuA	1,486	164.78	-9.02	9.E-03
VVMO6_02190	Zinc ABC transporter2C ATP-binding protein ZnuC	862.04	110.97	-7.77	6.E-04
VVMO6_02191	Zinc ABC transporter2C inner membrane permease protein ZnuB	598.44	109.66	-5.46	4.E-03
VVMO6_02386	Zinc ABC transporter2C inner membrane permease protein ZnuB	1,453	20.46	-71.04	2.E-03
VVMO6_02387	Zinc ABC transporter2C periplasmic-binding protein ZnuA	3,013	54.3	-55.49	7.E-03
VVMO6_02712	Predicted zinc-binding protein	2,565	435.23	-5.90	3.E-03
VVMO6_02837	TonB-dependent receptor; outer	523.04	24.42	-21.42	5.E-04

	membrane receptor for ferrienterochelin and colicins				
VVMO6_03074	Na/Pi cotransporter II-related protein	9.22	2.22	-4.15	2.E-03
VVMO6_03236	Outer membrane receptor for ferrienterochelin and colicins	10.09	2.06	-4.90	3.E-03
VVMO6_03869	Nitrate ABC transporter2C nitrate-binding protein	1,255	2.21	-568.0	5.E-02
VVMO6_03929	Cobalt-zinc-cadmium resistance protein	2,925	712.24	-4.11	1.E-02
Secondary metabolites biosynthesis, transport, and catabolism					
VVMO6_02632	TRAP transporter solute receptor2C unknown substrate 6	23.54	5.58	-4.22	2.E-02
VVMO6_03220	Isochorismatase	86.14	19.16	-4.50	3.E-03
VVMO6_04197	Phosphopantetheinyl transferase component of siderophore synthetase	1,096	231.68	-4.73	1.E-03
VVMO6_04451	Isochorismatase	69.23	14.96	-4.63	5.E-03
General function only					
VVMO6_00247	Sodium-type polar flagellar protein motX	432.4	76.76	-5.63	4.E-03
VVMO6_01098	ABC transporter substrate-binding protein	204.03	36.97	-5.52	5.E-02
VVMO6_01099	ABC-type uncharacterized transport system2C permease component	126.74	31.60	-4.01	5.E-02
VVMO6_01636	Hypothetical protein	29.98	7.24	-4.14	2.E-02
VVMO6_01803	Predicted Fe-S protein	222.41	36.21	-6.14	3.E-03
VVMO6_01878	Amine oxidase2C flavin-containing	317.23	73.67	-4.31	2.E-03
VVMO6_01879	Oxidoreductase2C short-chain dehydrogenase/reductase family	402.72	96.07	-4.19	5.E-03

VVMO6_02539	Pyruvate formate-lyase	3,351	773.61	-4.33	4.E-02
VVMO6_02551	Predicted Fe-S oxidoreductase	74.55	10.60	-7.03	7.E-03
VVMO6_02832	Oligopeptide transport ATP-binding protein OppF	438.3	92.79	-4.72	6.E-03
VVMO6_03242	Permease of the drug/metabolite transporter superfamily	2,713	25.51	-106.4	2.E-03
VVMO6_03402	Glycosyltransferase involved in cell wall biogenesis	73.19	12.02	-6.09	1.E-02
VVMO6_03506	Hypothetical protein	279.72	65.75	-4.25	2.E-02
VVMO6_03864	Hypothetical protein	165.78	23.08	-7.18	1.E-02
VVMO6_03933	ABC-type sugar transport system2C ATPase component	80.07	9.98	-8.02	7.E-03
VVMO6_04094	Ferredoxin-type protein NapF	154.10	35.24	-4.37	2.E-02
VVMO6_04177	Zn-dependent hydrolase	272.99	31.19	-8.75	6.E-03
VVMO6_04195	Putative phosphatase	34.76	7.11	-4.89	4.E-03
VVMO6_04325	Phospholipid-binding protein	158.15	25.87	-6.11	2.E-02
VVMO6_04336	Histone acetyltransferase HPA2	644.56	39.56	-16.29	6.E-03
No functional prediction					
VVMO6_00350	Uncharacterized conserved protein	625.00	98.66	-6.33	2.E-03
VVMO6_00416	Putative DNA binding 3-demethylubiquinone-9 3-methyltransferase domain protein	450.58	89.98	-5.01	3.E-03
VVMO6_00443	Putative cytochrome c oxidase2C subunit I	308.44	25.51	-12.09	3.E-04
VVMO6_00581	Hypothetical protein	129.15	28.34	-4.56	1.E-02
VVMO6_00645	Von Willebrand factor type A Domain protein2C associated with Flp pilus assembly	89.60	6.31	-14.20	8.E-03
VVMO6_00962	SpoVR-like protein	754.45	131.9	-5.72	3.E-04
VVMO6_00963	Hypothetical protein	990.24	126.74	-7.81	3.E-05
VVMO6_01693	Tricarboxylate transport protein TctC	311.19	60.02	-5.18	4.E-02
VVMO6_01696	Tricarboxylate transport	232.89	29.75	-7.83	4.E-02

	membrane protein TctA				
VVMO6_01877	Hypothetical protein	239.85	51.20	-4.68	2.E-03
VVMO6_01903	L2CD-transpeptidase YcbB	177.54	33.46	-5.31	3.E-03
VVMO6_02272	Flagellar protein FlgP	583.20	142.69	-4.09	2.E-03
VVMO6_02273	Flagellar protein FlgO	770.63	190.32	-4.05	3.E-02
VVMO6_02412	Kef-type K^+ transport system2C Predicted NAD-binding component	85.85	11.77	-7.29	1.E-02
VVMO6_02536	Hypothetical protein	408.11	75.41	-5.41	3.E-02
VVMO6_03311	Uncharacterized conserved protein	734.59	53.99	-13.61	2.E-04
VVMO6_03471	Membrane protein	387.32	26.22	-14.77	2.E-02
VVMO6_03507	Uncharacterized protein	102.25	8.84	-11.57	3.E-02
VVMO6_03508	Putative PRS2 protein	198.45	27.06	-7.33	7.E-03
VVMO6_03825	Hypothetical protein	18.09	3.35	-5.40	4.E-03
VVMO6_04022	Cytochrome oxidase biogenesis protein Surf12C facilitates heme A insertion	58.84	10.66	-5.52	1.E-02
VVMO6_04322	Hypothetical protein	179.98	22.95	-7.84	8.E-04
Signal transduction					
VVMO6_00074	Response regulator	51.70	7.97	-6.49	1.E-02
VVMO6_00351	GGDEF domain	277.92	55.66	-4.99	4.E-03
VVMO6_00481	GGDEF domain protein	63.57	15.23	-4.17	1.E-02
VVMO6_00616	C-di-GMP phosphodiesterase A	169.75	25.45	-6.67	3.E-03
VVMO6_00881	Response regulator	899.85	124.21	-7.24	1.E-02
VVMO6_00936	Inosine monophosphate dehydrogenase-related protein	715.39	35.12	-20.37	4.E-02
VVMO6_00961	GGDEF family protein	119.41	19.64	-6.08	2.E-02
VVMO6_00964	Serine protein kinase	1,306	153.16	-8.53	4.E-05
VVMO6_01132	Sensory box/GGDEF family protein	154	26.89	-5.73	2.E-02
VVMO6_01137	Probable sensor/response regulator	345.68	43.72	-7.91	2.E-03
VVMO6_01169	Hypothetical protein	122.43	14.17	-8.64	5.E-03
VVMO6_01190	GGDEF family protein	324.26	24.73	-13.11	1.E-03

VVMO6_01239	Hypothetical protein	34.55	8.09	-4.27	2.E-02
VVMO6_01622	Signal transduction histidine kinase SypF	33.03	5.53	-5.97	9.E-03
VVMO6_01623	Sigma-54 dependent transcriptional regulator SypG	139.09	35.11	-3.96	5.E-03
VVMO6_02885	Nitrogen regulation protein NR(II)	353.72	43.29	-8.17	2.E-03
VVMO6_02886	Nitrogen regulation protein NR(I)	303.48	27.69	-10.96	3.E-03
VVMO6_02887	GGDEF family protein	217.8	24.84	-8.77	1.E-02
VVMO6_02907	Hypothetical protein	305.95	48.02	-6.37	1.E-02
VVMO6_02989	Signal transduction histidine kinase	202.84	15.65	-12.96	1.E-03
VVMO6_03030	GGDEF family protein	501.46	46.71	-10.74	6.E-04
VVMO6_03070	EAL domain protein	149.00	25.22	-5.91	1.E-02
VVMO6_03073	HDIG domain protein	214.80	29.06	-7.39	1.E-02
VVMO6_03199	Putative diguanylate cyclase / phosphodiesterase with PAS domain	26.26	5.96	-4.41	2.E-03
VVMO6_03243	Chemotactic transducer-related protein	543.35	15.90	-34.17	9.E-05
VVMO6_03522	RsbR2C positive regulator of sigma-B	69.44	9.18	-7.56	7.E-03
VVMO6_03524	Anti-sigma B factor RsbT	85.64	21.54	-3.98	2.E-02
VVMO6_03526	Two-component system sensor protein	60.58	9.67	-6.26	2.E-02
VVMO6_03638	GGDEF family protein	344.35	39.43	-8.73	1.E-02
VVMO6_03757	GGDEF family protein	237.42	41.04	-5.79	8.E-04
VVMO6_03870	Putative two-component response regulatory protein	81.49	5.06	-16.10	2.E-02
VVMO6_03934	Signal transduction histidine kinase	110.53	15.37	-7.19	6.E-04
VVMO6_04047	GGDEF family protein	1,011	75.84	-13.34	3.E-04
VVMO6_04132	CheY-like receiver	517.43	59.38	-8.71	5.E-04
VVMO6_04323	Signal transduction histidine kinase	109.65	11.65	-9.41	9.E-04

VVMO6_04335	GGDEF domain	175.15	14.28	-12.27	3.E-03
VVMO6_04373	CheY-like receiver	160.63	20.30	-7.91	5.E-04
VVMO6_04549	Anti-anti-sigma regulatory factor	321.16	41.68	-7.71	2.E-03
VVMO6_04559	Anti-anti-sigma regulatory factor	400.07	33.60	-11.91	2.E-02
VVMO6_04558	Chemotaxis regulator - transmits chemoreceptor signals to flagelllar motor components CheY	238.56	30.91	-7.72	1.E-03
Intracellular trafficking, secretion, and defense mechanism					
VVMO6_00642	Flp pilus assembly protein RcpC/CpaB	35.16	2.43	-14.47	1.E-02
VVMO6_00643	Type II/IV secretion system secretin RcpA/CpaC2C associated with Flp pilus assembly	31.59	1.71	-18.47	2.E-02
VVMO6_00646	Hypothetical protein	129.04	8.02	-16.09	2.E-03
VVMO6_00648	Type II/IV secretion system ATPase TadZ/CpaE2C associated with Flp pilus assembly	116.86	15.51	-7.53	8.E-03
VVMO6_00649	Type II/IV secretion system ATP hydrolase TadA/VirB11/CpaF2C TadA subfamily	71.86	7.81	-9.20	7.E-04
VVMO6_00650	Flp pilus assembly protein TadB	57.34	6.83	-8.40	8.E-03
VVMO6_00652	TPR repeat protein	160.91	14.43	-11.15	1.E-02
VVMO6_01207	Flp pilus assembly protein2C secretin CpaC	95.11	16.96	-5.61	8.E-03
VVMO6_01209	Pilus assembly protein CpaE-like protein	184.08	29.82	-6.17	4.E-03
VVMO6_01210	Flp pilus assembly protein TadA	133.50	21.03	-6.35	9.E-03
VVMO6_01211	Flp pilus assembly protein TadB	127.76	13.55	-9.43	1.E-03
VVMO6_01212	Flp pilus assembly protein TadC	117.19	12.62	-9.29	2.E-03
VVMO6_01213	Flp pilus assembly protein TadD2C contains TPR repeat	177.05	20.18	-8.77	9.E-03
VVMO6_01214	Hypothetical protein	96.23	6.95	-13.85	7.E-03
VVMO6_01215	Hypothetical protein	127.39	8.49	-15.00	4.E-03

VVMO6_02839	MotA/TolQ/ExbB proton channel family protein	447.07	22.47	-19.90	7.E-05
VVMO6_02840	Ferric siderophore transport system2C biopolymer transport protein ExbB	276.41	18.19	-15.20	1.E-03
VVMO6_02841	Biopolymer transport protein ExbD/TolR	212.10	20.11	-10.55	3.E-02
VVMO6_03667	Multidrug resistance protein A	46.30	10.16	-4.56	2.E-02
VVMO6_03952	RTX toxin transporter	30.50	7.03	-4.34	1.E-03
VVMO6_04056	Predicted membrane fusion protein component of efflux pump2C membrane anchor protein YbhG	151.26	21.95	-6.89	3.E-02
VVMO6_04057	ABC-type multidrug transport system2C ATPase component	63.09	8.59	-7.34	8.E-03
VVMO6_04058	ABC-type multidrug transport system2C permease component	98.89	9.61	-10.29	5.E-02
Uncategorized					
VVMO6_00419	Methyl-accepting chemotaxis protein	310.17	52.39	-5.92	8.E-04
VVMO6_00479	Hypothetical protein	115.14	24.85	-4.63	4.E-02
VVMO6_00480	Hypothetical protein	40.70	10.05	-4.05	3.E-02
VVMO6_00638	Flp pilus assembly protein	403.05	13.93	-28.93	3.E-03
VVMO6_00639	Flp pilus assembly protein	703.64	11.21	-62.77	7.E-04
VVMO6_00644	Hypothetical protein	103.33	5.04	-20.50	5.E-02
VVMO6_00647	Similar to TadZ/CpaE2C associated with Flp pilus assembly	96.92	10.32	-9.39	4.E-03
VVMO6_00882	Hypothetical protein	90.64	16.45	-5.51	4.E-02
VVMO6_00900	Hypothetical protein	1,256	207.65	-6.05	7.E-03
VVMO6_00901	Hypothetical protein	361.29	75.89	-4.76	8.E-03
VVMO6_00919	Hypothetical protein	99.64	22.77	-4.38	1.E-02
VVMO6_01047	Hypothetical protein	407.35	26.48	-15.38	8.E-03
VVMO6_01125	Hypothetical protein	407.25	43.51	-9.36	1.E-02
VVMO6_01136	Guanylate cyclase-related protein	550.59	76.04	-7.24	4.E-04

VVMO6_01200	Hypothetical protein	116.80	27.80	-4.20	4.E-02
VVMO6_01202	Hypothetical protein	366.40	46.68	-7.85	2.E-02
VVMO6_01208	Hypothetical protein	194.20	33.5	-5.80	2.E-02
VVMO6_01216	Hypothetical protein	199.38	22.56	-8.84	7.E-04
VVMO6_01223	Hypothetical protein	7.66	1.32	-5.80	4.E-02
VVMO6_01268	Hypothetical protein	303.85	48.96	-6.21	1.E-02
VVMO6_01527	Hypothetical protein	224.21	34.27	-6.54	1.E-03
VVMO6_01602	WD40 repeat	300.02	38.43	-7.81	4.E-02
VVMO6_01697	Hypothetical protein	6.84	1.72	-3.98	2.E-02
VVMO6_01716	Hypothetical protein	222.83	45.45	-4.90	2.E-03
VVMO6_01873	Putative lipoprotein precursor	305.57	58.51	-5.22	2.E-03
VVMO6_01874	Hypothetical periplasmic protein	416.55	80.53	-5.17	5.E-03
VVMO6_01875	Hypothetical protein	379.90	43.86	-8.66	9.E-03
VVMO6_01959	Hypothetical protein	5,236	192.72	-27.17	2.E-03
VVMO6_02184	Ferrous iron transport protein C	1,423	197.01	-7.23	8.E-04
VVMO6_02188	Hypothetical protein	836.25	51.66	-16.19	3.E-03
VVMO6_02388	Zinc-regulated TonB-dependent outer membrane receptor	3,658	67.31	-54.35	3.E-07
VVMO6_02389	Hypothetical protein	7,123	108.64	-65.57	1.E-02
VVMO6_02390	Hypothetical protein	7,123	130.00	-54.80	1.E-02
VVMO6_02460	Hypothetical protein	28.11	7.09	-3.96	2.E-03
VVMO6_02711	Hypothetical protein	2,033	448.9	-4.53	5.E-03
VVMO6_02761	Hypothetical protein	0.90	0.03	-30.00	5.E-02
VVMO6_02838	TonB system biopolymer transport component; Chromosome segregation ATPase	265.67	9.96	-26.67	2.E-02
VVMO6_02843	TPR domain protein2C putative component of TonB system	521.42	21.17	-24.63	7.E-03
VVMO6_02854	Putative ATP-dependent Lon protease	1,224	191.12	-6.41	2.E-03
VVMO6_03002	Hypothetical protein	73.72	17.22	-4.28	2.E-02
VVMO6_03008	Hypothetical protein	221.39	42.80	-5.17	2.E-03
VVMO6_03029	Hypothetical protein	597.64	65.57	-9.11	1.E-02
VVMO6_03069	Hypothetical protein	204.13	30.30	-6.74	1.E-02

VVMO6_03079	Hypothetical protein	12.21	0.45	-27.13	2.E-02
VVMO6_03194	Hypothetical protein	58.09	6.21	-9.35	2.E-02
VVMO6_03215	12C4-alpha-glucan branching enzyme	3,850	571.51	-6.74	2.E-02
VVMO6_03231	ABC-type amino acid transport/signal transduction system	65.67	9.68	-6.78	8.E-04
VVMO6_03340	Cell Exterior; surface polysaccharides/antigens	101.71	20.25	-5.02	3.E-02
VVMO6_03391	Hypothetical protein	33.69	6.23	-5.41	8.E-03
VVMO6_03397	Gfa-like protein	94.61	7.57	-12.50	3.E-02
VVMO6_03433	Hypothetical protein	2.14	0.19	-11.26	4.E-02
VVMO6_03485	Protein chain release factor A	142.90	22.17	-6.45	3.E-02
VVMO6_03525	Serine phosphatase RsbU2C regulator of sigma subunit	83.46	20.74	-4.02	2.E-03
VVMO6_03529	Hypothetical protein	56.77	11.29	-5.03	2.E-02
VVMO6_03599	Hypothetical protein	4.52	0.52	-8.69	2.E-02
VVMO6_03612	Hypothetical protein	714.48	146.05	-4.89	3.E-02
VVMO6_03613	Hypothetical protein	2,780	432.54	-6.43	2.E-02
VVMO6_03843	Hypothetical protein	135.97	17.43	-7.80	2.E-04
VVMO6_03875	Hypothetical protein	861.74	77.32	-11.15	7.E-03
VVMO6_04021	Hypothetical protein in Cytochrome oxidase biogenesis cluster	75.64	6.90	-10.96	2.E-02
VVMO6_04023	Hypothetical protein	90.39	9.79	-9.23	1.E-02
VVMO6_04087	Outer membrane receptor protein	458.04	97.21	-4.71	2.E-03
VVMO6_04099	Hypothetical protein	97.82	17.82	-5.49	5.E-03
VVMO6_04113	Hypothetical protein	1,768	168.22	-10.51	1.E-03
VVMO6_04133	Hypothetical protein	165.63	14.58	-11.36	2.E-03
VVMO6_04134	ABC-type sulfate transport system2C permease component	184.74	23.39	-7.90	1.E-02
VVMO6_04176	Hypothetical protein	172.54	24.71	-6.98	1.E-02
VVMO6_04213	Hypothetical protein	17.67	3.02	-5.85	2.E-02
VVMO6_04277	ABC-type amino acid	36.31	7.90	-4.60	9.E-03

	transport/signal transduction system				
VVMO6_04341	Hypothetical protein	2,280	473.43	-4.82	4.E-03
VVMO6_04391	Hypothetical protein	916.78	6.63	-138.3	4.E-03
VVMO6_04394	Hypothetical protein	24.23	3.27	-7.41	1.E-02

[a] Locus tags are based on the database for the *V. vulnificus* MO6-24/O genome, which was retrieved from GenBank (accession number CP002469 and CP002470).

Chapter III.

Functional Analysis and Regulatory Characteristics of *Vibrio vulnificus gbpA* Encoding a Mucin-binding Protein

III-1. Introduction

Epithelial surfaces of the intestine are the most common portals by which enteropathogenic bacteria enter the deeper tissues of a mammalian host. The epithelial surfaces are covered by a mucus layer, which is produced by specialized cells found throughout the entire intestinal tract (MuGuckin *et al.*, 2011). The mucus layer is the first barrier that the enteropathogens encounter and it prevents the pathogens from reaching and persisting on the intestinal epithelial surfaces, and thereby is a major component of innate immunity (MuGuckin *et al.*, 2011). The mucus layer is composed of a variety of factors, but its characteristic physico-chemical properties are attributable to the presence of mucins, which are complex linear polymorphic glycoproteins (Neutra and Forstner, 1987; MuGuckin *et al.*, 2011). Mucins are highly glycosylated large glycoproteins (with molecular weights ranging from 5×10^3 to 4×10^6 Da), and up to 85% of their dry weight is carbohydrates (Wiggins *et al.*, 2001). Although mucin contains extensively different types of carbohydrates, the residue, *N*-acetyl-D-glucosamine (GlcNAc), is one of the most abundant sugars in the carbohydrate side chains (Thornton and Sheehan, 2004).

Adhesion to the mucosal surfaces followed by colonization on the mucosal tissue is considered to constitute the first stages of the infectious process (Ofek *et al.*, 2013). Accordingly, mutants of enteropathogenic bacteria that have difficulty in adhesion

to the mucus layer were substantially defective in intestinal colonization, leading to attenuated virulence (Kirn *et al*., 2005; Weening *et al*., 2005). Although numerous factors (known as adhesins) are involved in the adhesion of enteropathogens, information on the adhesins with specificity towards mucin carbohydrates is still limited (Juge, 2012). The GlcNAc-binding protein A of *V. cholerae* (*Vc*GbpA) is a lectin-like mucus adhesin and is characterized at the molecular level (Kirn *et al*., 2005; Bhowmick *et al*., 2008; Jude *et al*., 2009; Wong *et al*., 2012). *Vc*GbpA is a common adhesin required for *V. cholera*e to adhere to chitinous and intestinal surfaces (Kirn *et al*., 2005). *Vc*GbpA plays an important role in the survival of *V. cholerae* by attachment to the surface of chitinous zooplankton in the aquatic ecosystem (Kirn *et al*., 2005; Wong *et al*., 2012). *Vc*GbpA is a mucin-binding protein that binds to GlcNAc residues of mucin and contributes to intestinal colonization and virulence in a mouse model (Kirn *et al*., 2005; Wong *et al*., 2012). Structural analysis demonstrated that *Vc*GbpA possesses a four-domain structure of which domains 1 and 4 interact with chitin and domain 1 is also crucial for mucin binding and intestinal colonization. On the other hand, domains 2 and 3 anchor to the *V. cholerae* surfaces (Wong *et al*., 2012). It has been reported that *Vc*GbpA expression was induced by mucin and negatively regulated by cyclic di-guanosine monophosphate (c-di-GMP) at the post-transcription level and by quorum sensing at the post-translation level (Bhowmick *et al*., 2008; Sudarsan *et al*., 2008; Jude *et al*.,

2009). However, neither the promoter(s) of the *gbpA* gene nor any *trans*-acting regulatory protein(s) required for the transcription of *gbpA* has been identified previously.

V. vulnificus is a Gram-negative bacterium commonly associated with human disease caused by ingestion of undercooked oysters or contact of the organism with an open wound (Froelich and Oliver, 2013). Like many other enteropathogenic bacteria, *V. vulnificus* also expresses diverse adhesin molecules. The *V. vulnificus* adhesins include a flagellum, a type IV pilus, a lipoprotein, and OmpU that are crucial for adhesion to human epithelial cells *in vitro* and virulence in mice (Kim and Rhee 2003; Lee *et al*., 2004; Paranjpye and Strom, 2005; Goo *et al*., 2006; Lee *et al*., 2010). However, there is still no information about the factors responsible for the initial adhesion of the pathogen to mucin. In the present study, a *V. vulnificus* open reading frame (ORF) encoding a homologue of *Vc*GbpA was identified. Construction of the *gbpA* mutant and evaluation of its phenotypes provided evidences that *V. vulnificus* GbpA (*Vv*GbpA) is also a mucin-binding protein and plays a crucial role in the pathogenesis of the organism. Efforts to understand the regulatory mechanisms of the *gbpA* expression were initiated by determining the *gbpA* mRNA levels in cells of different growth phases. Since IscR (iron-sulfur (Fe-S) cluster regulator) (Schwartz *et al*., 2001), CRP (cyclic AMP receptor protein) (Green *et al*., 2014), and SmcR (LuxR homologue) (Shao and Hor, 2001) were previously reported to affect the

pathogenesis of *V. vulnificus* (Jeong *et al*, 2003; Oh *et al*., 2009; Shao *et al*., 2011; Kim *et al*., 2013; Lim *et al*., 2014), influences of the global regulatory proteins on the expression of *gbpA* were also examined. Genetic and biochemical studies demonstrated that IscR and CRP coactivated and SmcR repressed *gbpA* in a growth-phase dependent manner. Furthermore, the three regulatory proteins regulate *gbpA* cooperatively rather than sequentially and exert their effects by directly binding to the *gbpA* promoter P_{gbpA}. Deletion analyses of the upstream region of P_{gbpA} and DNase I protection assays were performed to identify the binding sequences of IscR, CRP, and SmcR. Finally, the influence of hydrogen peroxide (H_2O_2) on the intracellular levels of IscR was examined to explain how IscR can mediate the induction of *gbpA* by oxidative stress.

III-2. Materials and Methods

III-2-1. Strains, plasmids, and culture conditions

The strains and plasmids used in this study are listed in Table II-1. Unless otherwise noted, the *V. vulnificus* strains, wild type MO6-24/O and its mutants, were grown in Luria-Bertani (LB) medium supplemented with 2% (*wt/vol*) NaCl (LBS) at 30°C, and their growth was monitored spectrophotometrically at 600 nm (A_{600}). Anaerobic conditions were obtained by using an anaerobic chamber with an atmosphere of 90% N_2, 5% CO_2 and 5% H_2 (Coy laboratory products, Grass Lake, MI). For anaerobic culture, the media were pre-incubated to remove dissolved O_2 in the anaerobic chamber, which was verified by adding 0.00001% (*wt/vol*) resazurin salt (Sigma) to the media (Kim *et al*., 2014).

III-2-2. Generation and complementation of the *gbpA* and *iscR crp* mutants

The *gbpA* gene was inactivated *in vitro* by deletion of the ORF of *gbpA* (318-bp of 1458-bp) using the PCR-mediated linker-scanning mutation method as described previously (Kim *et al*., 2014). Briefly, pairs of primers GBPA01-F and -R (for amplification of the 5' amplicon) or GBPA02-F and -R (for amplification of the 3' amplicon) were designed and used (Table III-1). The *gbpA* gene with 318-bp deletion was amplified by PCR using the mixture of both amplicons as the template and GBPA01-F and GBPA02-R as primers. The resulting Δ*gbpA* was ligated into SpeI-SphI-digested pDM4 (Milton *et al*., 1996) to generate pSO1101 (Table II-1). *E. coli* S17-1 *λ pir, tra* strain (Simon *et al*., 1983) containing pSO1101 was used as a conjugal donor to *V. vulnificus* MO6-24/O and MORSR (MO6-24/O with rifampicin and streptomycin resistance, Hwang *et al*., 2013) to generate the *gbpA* mutant SO111 and KK141, respectively (Table II-1). Similarly, pBS0907, which was constructed previously to carry a mutant allele of *V. vulnificus crp* on pDM4 (Table II-1) (Kim *et al*., 2011), was used to generate the *iscR crp* double mutant of *V. vulnificus*. *E. coli* S17-1 *λ pir, tra* containing pBS0907 was used as a conjugal donor in conjugation with the *iscR* mutant JK093 as a recipient (Lim and Choi, 2014). The resulting *iscR crp* double mutant was named KK142 (Table II-1). The conjugation and isolation of the transconjugants were conducted using the method described previously (Kim *et*

al., 2011).

To complement the *gbpA, iscR, crp,* and *smcR* (constructed previously, Jeong *et al*., 2003) mutations, each ORF of *gbpA, iscR, crp,* and *smcR* was amplified by PCR using a pair of specific primers as listed in Table III-1. The amplified *gbpA, iscR, crp,* and *smcR* ORF were cloned into pJK1113 under an arabinose-inducible promoter P_{BAD} (Lim *et al*., 2014) to create pKK1402, pKK1403, pKK1404, and pKK1405, respectively (Table II-1). The plasmids were transferred into the appropriate mutants by conjugation as described above. For complementation tests, when the cultures reached an A_{600} of 0.3, arabinose was added to a final concentration of 0.1 mM to induce the expression of the recombinant genes on the plasmids.

Table III-1. Oligonucleotides used in this study

Name	Oligonucleotide Sequence (5' → 3')[a, b]	Use
For mutant construction		
GBPA01-F	GAGATGCACATCAGCAACGCG	Deletion of the *gbpA* ORF
GBPA01-R	AAAGGATCCAGCGAACTTACACAGTGT	
GBPA02-F	GCTGGATCCTTTGTCTTCCCAGATG	Deletion of the *gbpA* ORF
GBPA02-R	CGCAACAACGGAATCAAACGC	
PLP01-F	ATGAAGAAGATAACTATTCTGTTGGGTGC	Deletion of the *plp* ORF
PLP01-R	GTAGAATTCACAACGTTGCTTAATCACG	
PLP02-F	GTGAATTCTACATCATTCAGGGTTACAACATC	Deletion of the *plp* ORF
PLP02-R	TGAGCTGTGAGTGGCACAATCG	
HLYU01-F	CTATTCTGTTGGGTGCTCTGTTGC	Deletion of the *hlyU* ORF
HLYU01-R	TGGATCCGCAGCAAAATAGGTGATG	
HLYU02-F	CGGATCCAACCAATACGTGGCG	Deletion of the *hlyU* ORF
HLYU02-R	GTAGTCCGCAGAAGAGGCACGA	
For mutant complementation		
GBPA03-F	GGATCCGCCAAATAAAGTCAG	Amplification of the *gbpA* ORF
GBPA03-R	GGATCCTTACAGTTTGTCCCAC	
ISCR01-F	ATCCATGGCTATGAAACTGACATCTAAAGG	Amplification of the *iscR* ORF
ISCR01-R	ATTCTAGATTAAGAGCGGAAATTTACACCG	
CRP01-F	GAGATACCATGGTTCTAGGTAAACCTCA	Amplification of the *crp* ORF
CRP01-R	GTTAATTCTAGATTAACGAGTACCGTAAACAAC	

SMCR01-F	ATCCATGGACTCAATCGCAAAGAGAC	Amplification of the *smcR* ORF
SMCR02-R	ATTCTAGATTATTCGTGCTCGCGTTTATA	
PLP03-F	GGTACCAATAATCAAAACATAAGAAGATAG	Amplification of the *plp* ORF
PLP03-R	GGTACCCTAAAAATTAAAGCG	
HLYU03-F	GGTACCTCTCAAAGAAGAGTATTACGTG	Amplification of the *hlyU* ORF
HLYU03-R	GAGCTCTTACACCGATCCTAGACC	
CRP02-F	GGTACCACACCCTTGTGGTGCC	Amplification of the *crp* ORF
CRP02-R	GAGCTCTTAACGAGTACCGTAAACAACG	
For protein overexpression		
GBPA04-F	CCATGGCTAAAAAACAACCGCAAAAAACC	Amplification of the *gbpA* ORF
GBPA04-R	CTCGAGCAGTTTGTCCCACGCCATT	
PLP04-F	CATATGGAGCCAGCTCTCTCTCCTGAAGC	Amplification of the *plp* ORF
PLP04-R	ACTAGTCTAGTGATGGTGATGGTGATGAAAATTAAAGCGTTG	
PLP05-F	CCATGGAGCCAGCTCTCTCTCC	Amplification of the truncated *plp*
PLP05-R	GTCGACGTTGCCGGTATCAGAG	ORF
HLYU04-F	GGATCCATGAACTTAAAAGATATGGAGC	Amplification of the *hlyU* ORF
HLYU04-R	CTCGAGTTATTCTTCGCAATAAAGA	
For promoter deletion analysis		
GBPA003	GAGCTCTAAGTGCTCAATGACATAGTAAAG	Deletion of the *gbpA* regulatory region
GBPA004	GAGCTCTCACACTTTTTCGAGAAATTA	
GBPA005	GAGCTC ACATCTATAAATAACGCTTCTAAAT	
GBPA006	GAGCTCTTATGCCTGACATCACAC	
GBPA007	ACTAGTCACCATTTTCCACTGCAG	

PLP001	GAGCTCTAAAATGCCAAAAAAATCGC	Deletion of the *plp* regulatory region
PLP002	GAGCTCGAGAAAGTGAATGTTAAATTATTG	
PLP003	GAGCTCTTTTTGACTTTGGTACCAGTTTT	
PLP004	GAGCTCCAACTGGTGATTAATAATCAAAAC	
PLP005	ACTAGTGTGATCGCTTCAGGAGAGAGA	
For primer extension analysis, EMSA, and DNase I protection assay		
GBPA05-F	ATTGCCATAGCTGGTGGTTTTCA	Amplification of the *gbpA* upstream region
GBPA05-R	CCCCGCTATCTTGGGTATGGTAAAAA	Amplification of the *gbpA* upstream region, Extension of the *gbpA* transcript
PLP06-F	GCGTAAATGCGCAATGAAAAG	Amplification of the *plp* upstream region
PLP06-R	CTGCAGATGTGAAGGGCAACAGA	Amplification of the *plp* upstream region, Extension of the *plp* transcript
For qRT-PCR		
GBPA_qRT-F	TGAAAGCCTGGGGTGAAGCA	Quantification of the *gbpA* expression
GBPA_qRT-R	ATCGCGTAGCGTTGAGAGCG	
PLP_qRT-F	TTGTTGGTATCGAACGGGCA	Quantification of the *plp* expression
PLP_qRT-R	CGAGCTCCACCAATAACCGT	

[a] The oligonucleotides were designed using the *V. vulnificus* MO6-24/O genomic sequence (GenBank™ accession number CP002469 and CP002470, www.ncbi.nlm.nih.gov).

[b] Regions of oligonucleotides not complementary to the corresponding genes are underlined.

III-2-3. Mucin binding assay

Pig gastric mucin powder (Sigma) was sterilized by mixing with 95% (*vol/vol*) ethanol for 1 h, dried at 70°C for 24 h (Yeung *et al*., 2012) and then added to the 1.5% agar (*wt/vol*) solution, which was autoclaved and cooled down to 60°C, to the final concentration of 3% (*wt/vol*). The mucin-agar solution (2 ml) was solidified in each well of 12-well culture dishes (Nunc, Roskilde, Denmark). On the mucin-agar, *V. vulnificus* cultures (100 μl, approximately 10^7 colony forming units (CFU)) were added to each well and various amounts of purified GbpA were exogenously provided to the well when required. After incubation for 1 h at 30°C, the nonadherent bacteria were removed by washing with 1 ml of phosphate-buffered saline (PBS) twice and the adherent bacterial cells were recovered by treating with 200 μl of 0.1% Triton X-100 (Sigma) solution for 20 min and enumerated as CFU per well.

III-2-4. Adhesion assay

The 12-well culture dishes (Nunc) were seeded with the HT29-MTX cells (approximately 1×10^7 cells per well), infected with the *V. vulnificus* strains at a multiplicity of infection (MOI) of 10 for 30 min. The culture dishes were washed two times with PBS to remove nonadherent bacteria, and treated with 0.1% Triton X-100 for 20 min to recover adherent bacteria. The recovered bacterial cells were enumerated as CFU per well.

III-2-5. Mouse lethality and competition assay

Mouse lethality of the wild type and *gbpA* mutant was compared as described previously (Lim and Choi, 2014). Groups of (n = 10) 7-week-old ICR female mice (specific pathogen-free; Seoul National University) were starved without food and water for 12 h until infection. Then the mice, without iron-dextran pretreatment, were intragastrically administered with 100 μl of the inoculum, representing approximately 10^9 cells of either the wild type or the *gbpA* mutant. Mouse survivals were recorded for 24 h.

Previous mouse colonization assays demonstrated that *V. vulnificus* initially and mostly colonizes in small intestine and disseminates to other organs (Jeong and Satchell 2012; Lee *et al.*, 2015c). Therefore, colonization of each strain in mice small intestine was determined by competition assays as previously described (Hwang *et al.*, 2013). Briefly, four ICR female mice (7-weeks-old) were infected as described above for the mouse mortality, except that 100 μl of the inoculum, prepared by mixing MORR (MO6-24/O with rifampicin resistance, Hwang *et al.*, 2013) and KK141 at a 1:1 ratio, representing approximately 10^6 CFU of each strain, was given intragastrically to the mice. The mice were sacrificed at 1 to 24 h postinfection, and their intestines were collected, washed, and homogenized. Equal amounts of the homogenates were spread on LBS agar containing either rifampicin (100 μg/ml)

alone to enumerate the sum of the wild type and *gbpA* mutant cells or rifampicin and streptomycin (100 μg/ml) to specifically count the *gbpA* mutant cells. The ratio of CFU recovered from the intestines to the number of CFU inoculated is defined as a colonization index (Jeong *et al*., 2009). All manipulations of mice were approved by the Animal Care and Use Committee of Seoul National University and mice were humanely euthanized at the end point analysis.

III-2-6. RNA purification and transcript analysis

Total RNA from the *V. vulnificus* strains grown aerobically to various levels of A_{600} were isolated using an RNeasy® mini kit (Qiagen). When necessary, the strains grown anaerobically to an A_{600} of 0.5 were exposed to various concentrations of H_2O_2 for 10 min and harvested to isolate total RNA. For the primer extension analysis, a 26-base primer GBPA05-R (Table III-1) complementary to the regulatory region of *gbpA* was end labeled with [γ-^{32}P]ATP and added to the RNA. The primer was then extended with SuperScript II RNase H^- reverse transcriptase (Invitrogen). The cDNA product was purified and resolved on a sequencing gel alongside ladders generated from pKK1401 with the same primer. The plasmid pKK1401 was constructed by cloning the 390-bp *gbpA* upstream region extending from -301 to + 88, amplified by PCR using a pair of primers GBPA05-F and -R (Table III-1), into pGEM-T Easy (Promega, Madison, WI). The primer extension product was visualized using a phosphorimage analyser (BAS1500; Fuji Photo Film Co., Ltd., Tokyo, Japan).

For quantitative real-time PCR (qRT-PCR), the concentrations of total RNA from the strains were measured by using NanoVue Plus Spectrophotometer (GE Healthcare). cDNA was synthesized from 1 μg of the total RNA by using the iScript™ cDNA synthesis kit (Bio-Rad) and real-time PCR amplification of the cDNA was performed by using the Chromo 4 real-time PCR detection system (Bio-Rad) with a pair of

specific primers (Table III-1), as described previously (Kim *et al*., 2012). Relative expression levels of the *gbpA* mRNA in the same amounts of total RNA were calculated by using the 16S rRNA expression level as the internal reference for normalization.

III-2-7. Protein purification and Western blot analysis

The ORF of *gbpA* was amplified by PCR using a pair of primer GBPA04-F and –R. (Table III-1) and cloned into a His_6 tag expression vector, pET-22a(+) (Novagen, Madison, WI) to result in pSO1201 (Table II-1). The His-tagged GbpA protein was expressed in *E. coli* BL21 (DE3) and purified by affinity chromatography according to the manufacturer's procedure (Qiagen). In a similar way, pJK0928, pHK0201, and pHS104, which were constructed previously (Choi *et al*., 2002; Jeong *et al*., 2003; Lim and Choi, 2014) (Table II-1), were used to overexpress and purify the His-tagged IscR, CRP, and SmcR, respectively. The purified His-tagged proteins were used to raise rabbit polyclonal antibodies against GbpA, IscR, CRP, and SmcR of *V. vulnificus*, respectively (AB Frontier, Seoul, South Korea). For Western blot analyses, total proteins were isolated from the strains grown aerobically to an A_{600} of 0.5, or anaerobically to an A_{600} of 0.5 and then exposed to various concentrations of H_2O_2 for 10 min. The concentrations of the total proteins were determined by using Bradford method (Bradford, 1976). The same amounts of the total proteins (10 μg) were resolved on SDS-PAGE and immunoblotted as described previously (Kim *et al*., 2014).

III-2-8. Electrophoretic mobility shift assay (EMSA)

The 390-bp *gbpA* upstream region extending from -301 to + 88 was amplified by PCR using [γ-^{32}P]ATP labeled GBPA05-F and unlabeled GBPA05-R as primers (Table III-1). The labeled 390-bp DNA (5 nM) probe was incubated with various concentrations of purified IscR for 30 min at 30°C in a 20-μl reaction mixture containing 1× binding buffer (Giel *et al*., 2006) and 0.1 μg of poly (dI-dC) (Sigma). The protein-DNA binding reactions with purified CRP or SmcR were the same as those with IscR, except that the CRP or SmcR-binding buffer was used as a 1× binding buffer (Choi *et al*., 2002; Jeong *et al*., 2003). Electrophoretic analyses of the DNA-protein complexes were performed as described previously (Lim and Choi, 2014), and visualized as described above for the transcript analysis.

III-2-9. Construction of a set of *gbpA-luxCDABE* transcriptional fusions

The primer GBPA007 (Table III-1) including a SpeI restriction site followed by bases corresponding to the 5' end of the *gbpA* coding region, was used in conjunction with one of the following primers to amplify the DNA upstream of *gbpA*: GBPA003 (for pKK1407), GBPA004 (for pKK1408), GBPA005 (for pKK1409), or GBPA006 (for pKK1410) (Table III-1). The primers were designed to amplify the *gbpA* regulatory region extending up to -220, -106, -76, and -6 bp, respectively. A SacI restriction site was added to these primers to facilitate cloning of the PCR products. The DNA fragments were inserted into the SpeI-SacI-digested pBBR-lux (Lenz *et al*., 2004) carrying promoterless *luxCDABE* genes, thereby creating four *gbpA-lux* reporter constructs. All constructions were confirmed by DNA sequencing. The *gbpA-lux* reporters were then transferred into the *V. vulnficus* strains by conjugation. The cellular luminescences of the cultures grown to an A_{600} of 0.5 were measured with a luminometer (Tecan Infinite M200 reader, Männedorf, Switzerland) and expressed in arbitrary relative light units (RLU) as previously described (Jeong *et al*., 2003).

III-2-10. DNase I protection assay

The same labeled 390-bp DNA probe developed for EMSA was used for DNase I protection assays. The binding of IscR, CRP, or SmcR to the labeled DNA (25 nM) was performed as described above for EMSA, and DNase I digestion of the DNA-protein complexes followed the procedures described previously (Lim *et al*., 2014). After precipitation with ethanol, the digested DNA products were resolved on a sequencing gel alongside sequencing ladders of pKK1401 generated using GBPA05-F (Table III-1) as the primer. The gels were visualized as described above for the transcript analysis.

III-2-11. Data analysis

Averages and standard deviations (SD) were calculated from at least three independent experiments. Mouse mortality was evaluated using the log rank test program (http://bioinf.wehi.edu.au/software/russell/logrank/). All other data were analyzed by Student's *t* tests with the SAS program (SAS software; SAS Institute Inc.). Significance of differences between experimental groups was accepted at a *P* value of < 0.05.

III-3. Results

III-3-1. Identification and sequence analysis of GbpA

A search of the *V. vulnificus* MO6-24/O genome sequence database (GenBank™ CP002469 and CP002470) (Park *et al*., 2011) for homology to the amino acid sequences deduced from *Vc*GbpA singled out a protein, hereafter named *Vv*GbpA. The amino acid sequence analysis predicted that pre-*Vv*GbpA protein contains an N-terminal signal peptide for the type II secretion system, suggesting that *Vv*GPA is a secreted protein (data not shown; http://www.ebi.ac.uk/clustalw) (Korotkov *et al*., 2012). The deduced mature *Vv*GbpA is comprised of 485 amino acids with a theoretical mass of 52.83 kDa and a pI of 4.75. The amino acid sequence of *Vv*GbpA was 80% identical to that of *Vc*GbpA (data not shown) and exhibited a four domain modular structure consisting of two chitin binding domains and two bacterial surface binding domains as observed in *Vc*GbpA (Wong *et al*., 2012). The predicted profile of the hydrophobicity (http://web.expasy.org) was significantly similar to that of *Vc*GbpA, indicating that *Vv*GbpA is a soluble protein (data not shown) (Wong *et al*., 2012). All of this information suggested that *Vv*GbpA is a secreted but cell surface-associated protein as is *Vc*GbpA.

III-3-2. GbpA is essential for mucin binding and virulence of *V. vulnificus*

To examine the function of *Vv*GbpA, mucin binding ability of wild type and the *gbpA* mutant was examined. The number of the *gbpA* mutant that adhered to the mucin-agar in a well of 12-well culture dishes was significantly lower than that of the parental wild type (Fig. III-1*A*). This indicated that the *gbpA* mutant was defective in mucin binding. In addition, the extracellular provision of purified *Vv*GbpA was able to rescue the defect of the *gbpA* mutant in mucin binding ability in a dose-dependent manner. The mucin binding ability of the *gbpA* mutant incubated in the presence of 5 μM *Vv*GbpA was comparable to that of the parental wild type, in terms of the bacterial numbers adherent to the mucin-agar (Fig. III-1*A*).

To further understand the role of *Vv*GbpA in binding to mucin, the wild type and *gbpA* mutant were incubated with the mcuin-secreting HT29-MTX cells and the bacteria adherent to the cells were enumerated (Fig. III-1*B*). The results revealed that adhesion of the *gbpA* mutant to the HT29-MTX cells was about 2-fold lower than that of the wild type. The impaired adhesion of the *gbpA* mutant was restored to the wild type level by complementation with a functional *gbpA* gene (pKK1402). These results indicated that *Vv*GbpA is a mucin-binding protein and plays an important role in the adhesion to the mucin-secreting human epithelial cells.

To experimentally examine the role of *Vv*GbpA in pathogenesis, mouse mortality

and colonization activity of the *gbpA* mutant were evaluated. As shown in Fig. III-2*A*, the survival of mice inoculated intragastrically with the *gbpA* mutant was consistently and significantly prolonged ($P = 0.0174$, log rank test) compared to that of mice inoculated with the parental wild type. Therefore, for the mouse model infected intragastrically, the *gbpA* mutant appeared to be significantly less virulent than its parental wild type. Mice were also coinoculated intragastrically with MORR (wild type) and KK141 (*gbpA* mutant), and both strains colonized on the small intestine were recovered and enumerated (Fig. III-2*B*). The colonization index of the KK141 ranged from 10^{-3} to 10^{-2} and was consistently and significantly (about 100-fold) lower than that of MORR, demonstrating that the MORR clearly outcompeted the KK141 in the small intestine. These results indicated that *Vv*GbpA is a virulence factor essential for the intestinal colonization of *V. vulnificus*. Taken together, it is apparent that *Vv*GbpA is a mucin-binding protein contributing to the pathogenesis of *V. vulnificus*.

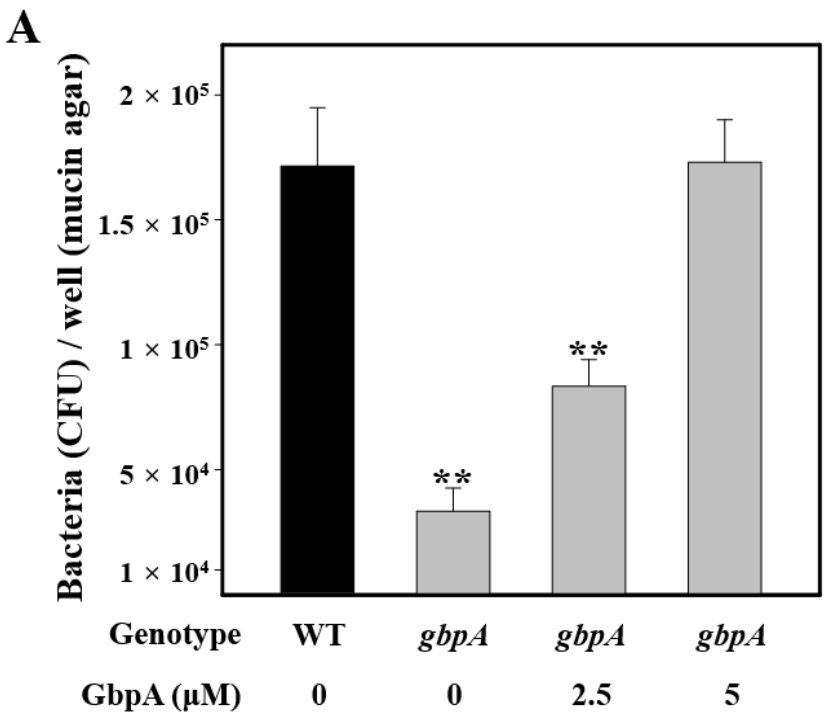
A
Bacteria (CFU) / well (mucin agar)
2 × 10^5
1.5 × 10^5
1 × 10^5
5 × 10^4
1 × 10^4
**
**
Genotype
WT
gbpA
gbpA
gbpA
GbpA (μM)
0
0
2.5
5

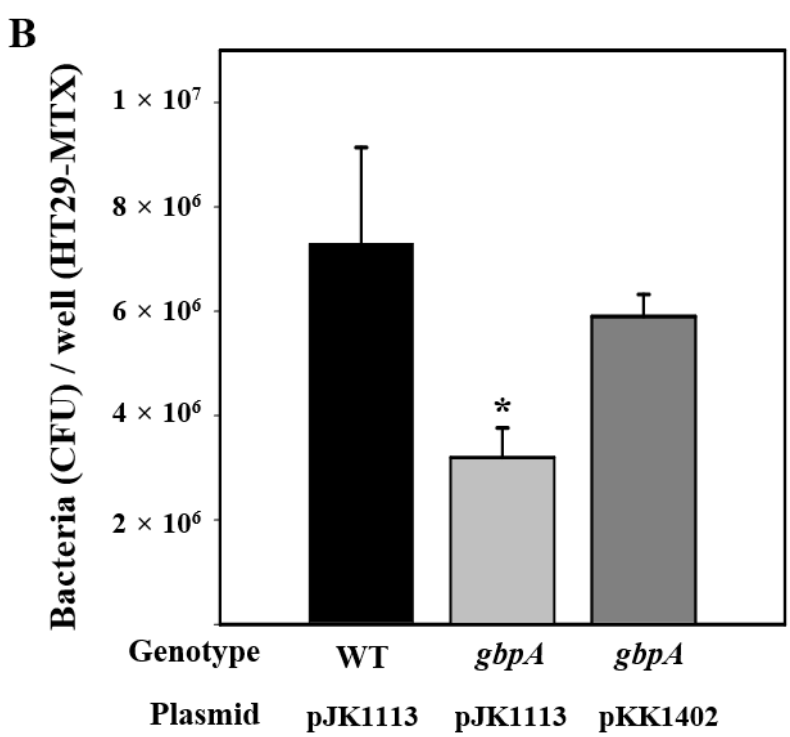
B
Bacteria (CFU) / well (HT29-MTX)
1 × 10^7
8 × 10^6
6 × 10^6
4 × 10^6
2 × 10^6
*
Genotype
WT
gbpA
gbpA
Plasmid
pJK1113
pJK1113
pKK1402

Figure III-1. Effect of GbpA on mucin binding and host cell adhesion of *V. vulnificus*. *A*, the strains (approximately 10^7 CFU) were added to each well of 12-well culture dishes containing the mucin-agar and various amounts of GbpA provided exogenously as indicated. After 1 h incubation, the adherent bacterial cells were enumerated as CFU per well. WT, wild type; *gbpA*, *gbpA* mutant. *B*, the mucin-secreting HT29-MTX cells (approximately 10^7 cells) seeded in each well of 12-well culture dishes were infected at an MOI of 10 with the strains as indicated. After 30 min incubation, the adherent bacterial cells were enumerated as CFU per well. Error bars represent the SD. *, $P < 0.05$, and **, $P < 0.005$ relative to the wild type. WT (pJK1113, empty vector), wild type; *gbpA* (pJK1113), *gbpA* mutant; *gbpA* (pKK1402), complemented strain.

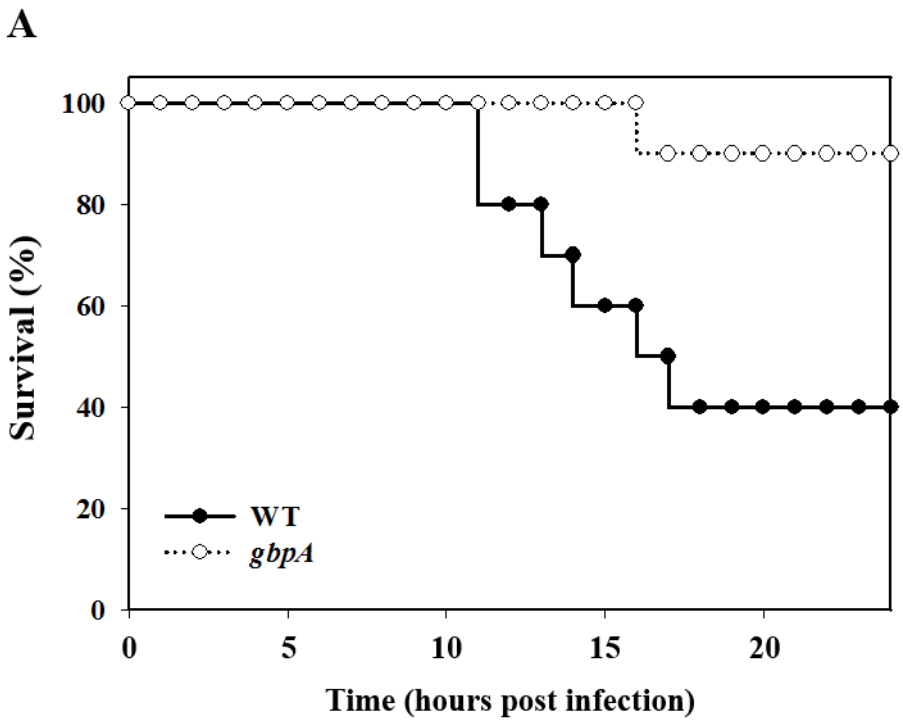
A
100
80
60
40
20
0
Survival (%)
WT
gbpA
0
5
10
15
20
Time (hours post infection)

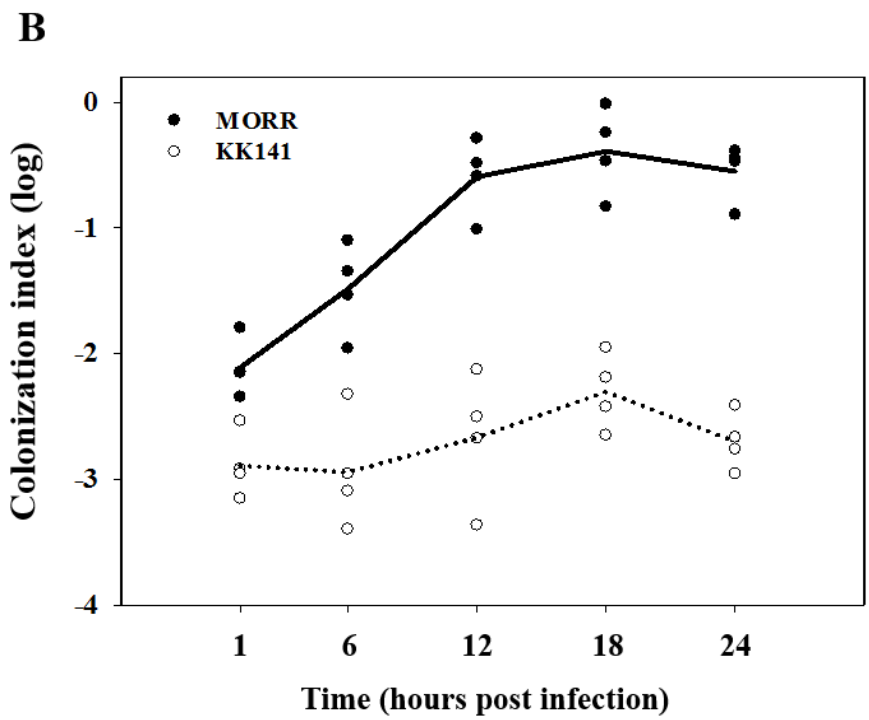
B
0
-1
-2
-3
-4
Colonization index (log)
MORR
KK141
1
6
12
18
24
Time (hours post infection)

Figure III-2. Mouse lethality and colonization activity of the *V. vulnificus* strains. *A*, seven-week-old specific pathogen-free female ICR mice were intragastrically infected with the wild type (WT) or the *gbpA* mutant (*gbpA*) (Table II-1) at doses of approximately 10^9 CFU as indicated. Mouse survival was monitored for 24 hr. *B*, four mice were intragastrically infected with an inoculum prepared by mixing equal numbers of MORR and KK141 (Table II-1), and then the bacterial cells colonized on the small intestine were enumerated as CFU at the indicated time intervals. Each circle corresponds to the ratio of CFU recovered from the intestines to the CFU inoculated (the colonization index) for an individual mouse. The median values are displayed as a solid line (MORR) or dashed line (KK141) on the graph. WT, wild type; *gbpA*, *gbpA* mutant; MORR, wild type with rifampicin resistance; KK141, *gbpA* mutant with rifampicin and streptomycin resistance.

III-3-3. Expression of *gbpA* is growth-phase dependent and regulated by IscR, CRP, and SmcR

To examine whether the production of *Vv*GbpA is influenced by growth phase, levels of the *gbpA* mRNA of the wild type culture were analyzed at various growth stages (Fig. III-3*A* and *B*). The *gbpA* transcript reached maximum levels in the exponential phase and then decreased in the stationary phase, indicating that expression of *gbpA* is growth-phase dependent. To extend our understanding on the regulation of *gbpA*, the levels of the *gbpA* transcript in the wild type and mutants which lack transcription factors IscR, CRP, and SmcR (Table II-1) were compared. The level of the *gbpA* transcript decreased in the *iscR* mutant and *crp* mutant (Fig. III-3*C*). The result indicated that both IscR and CRP act as positive regulators for the *gbpA* expression. In contrast, the *gbpA* expression of the *smcR* mutant was greater than that of the wild type, indicating that SmcR negatively regulates *gbpA* (Fig. III-3*C*). The cellular levels of *Vv*GbpA determined by Western blot analyses also varied in the mutants (Fig. III-3*D*). The magnitude of variation in the *Vv*GbpA proteins did not significantly differ from that observed in the *gbpA* transcripts, indicating that the regulation of the *gbpA* expression occurs mostly at the transcription level. The levels of the *gbpA* transcript and *Vv*GbpA protein that varied in the *iscR*, *crp*, and *smcR* mutant were restored to the levels comparable to those in the wild type by introducing pKK1403, pKK1404, and pKK1405 carrying recombinant *iscR*, *crp*, and

smcR, respectively (Fig. III-3*E* and *F*). Taken together, these results suggested that IscR and CRP activate whereas SmcR represses the *gbpA* transcription.

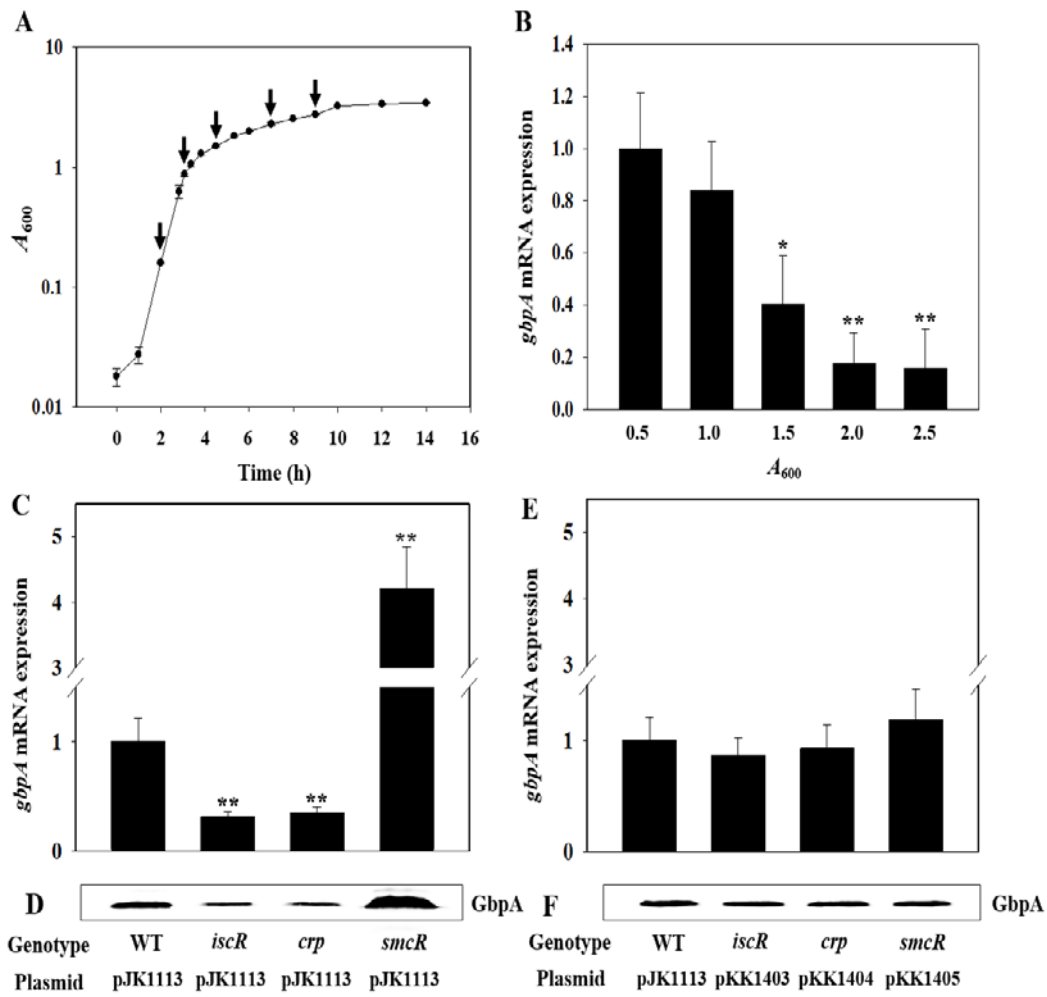
A
10
1
0.1
0.01
A_{600}
0
2
4
6
8
10
12
14
16
Time (h)
B
1.4
1.2
1.0
0.8
0.6
0.4
0.2
0.0
gbpA mRNA expression
*
**
**
0.5
1.0
1.5
2.0
2.5
A_{600}
C
5
4
3
1
0
gbpA mRNA expression
**
**
**
E
5
4
3
1
0
gbpA mRNA expression
D
GbpA
F
GbpA
Genotype WT iscR crp smcR
Plasmid pJK1113 pJK1113 pJK1113 pJK1113
Genotype WT iscR crp smcR
Plasmid pJK1113 pKK1403 pKK1404 pKK1405

Figure III-3. Effects of growth phases and global regulatory proteins on the *gbpA* expression. Upper panel, growth kinetics of *V. vulnificus* and growth-phase dependent expression of *gbpA*. *A*, growth of the wild type culture in LBS was monitored spectrophotometrically at 600 nm (A_{600}) and total RNAs were isolated from the cells harvested at different growth phases (from left, at A_{600} of 0.5, 1.0, 1.5, 2.0 and 2.5) as indicated by arrows. *B*, the *gbpA* mRNA levels were determined by qRT-PCR analyses, and the *gbpA* mRNA level in the cells grown to an A_{600} of 0.5 was set as 1. Error bars represent the SD. *, $P < 0.05$, and **, $P < 0.005$ relative to the cells grown to an A_{600} of 0.5. Lower panel, expression of *gbpA* in *V. vulnificus* with different genetic backgrounds. Samples were harvested from the cultures of the wild type (WT) and isogenic mutants grown aerobically to an A_{600} of 0.5 and analyzed to determine the *gbpA* mRNA and GbpA protein levels. (*C* and *E*) The *gbpA* mRNA levels were determined by qRT-PCR analyses, and the *gbpA* mRNA level in the wild type was set as 1. **, $P < 0.005$ relative to the wild type. (*D* and *F*) Protein samples were resolved by SDS-PAGE, and GbpA was detected by Western blotting using the rabbit anti-*V. vulnificus* GbpA serum. WT (pJK1113), wild type; *iscR* (pJK1113), *iscR* mutant; *smcR* (pJK1113), *smcR* mutant; *crp* (pJK1113), *crp* mutant; *iscR* (pKK1403), *crp* (pKK1404), and *smcR* (pKK1405), complemented strains.

III-3-4. IscR and CRP coactivate *gbpA* additively

To further examine the roles of IscR and CRP in the *gbpA* expression, the *iscR crp* double mutant KK142 was constructed and *gbpA* expression was determined. Inactivation of both *crp* and *iscR* resulted in significant reduction of the *gbpA* expression, and the residual *gbpA* mRNA level in the *iscR crp* double mutant corresponded to only one-tenth of that in the wild type (Fig. III-4). The presence of either IscR (*crp* mutant) or CRP (*iscR* mutant) alone increased the *gbpA* expression, but their *gbpA* transcript levels were much lower than that obtained by IscR and CRP together (wild type), indicating that IscR and CRP coactivate the *gbpA* expression additively (Fig. III-4). To determine whether an increased amount of IscR would compensate for a lack of CRP in the activation of *gbpA*, the *iscR* expression plasmid pKK1403 was introduced into the *iscR crp* double mutant KK142. When *iscR* was induced by arabinose, the cellular level of IscR in KK142 (pKK1403) was higher than that in the *crp* single mutant (Fig. III-4). However, the level of *gbpA* transcript in KK142 (pKK1403) was only about 80% of that in the wild type (Fig. III-4), indicating that IscR, even when overproduced, is unable to activate *gbpA* to the wild-type level in the absence of CRP. Similarly, overproduced CRP was unable to completely compensate for the lack of IscR in the activation of *gbpA* (Fig. III-4). The results indicated that both IscR and CRP are required simultaneously to activate *gbpA* to the wild-type level.

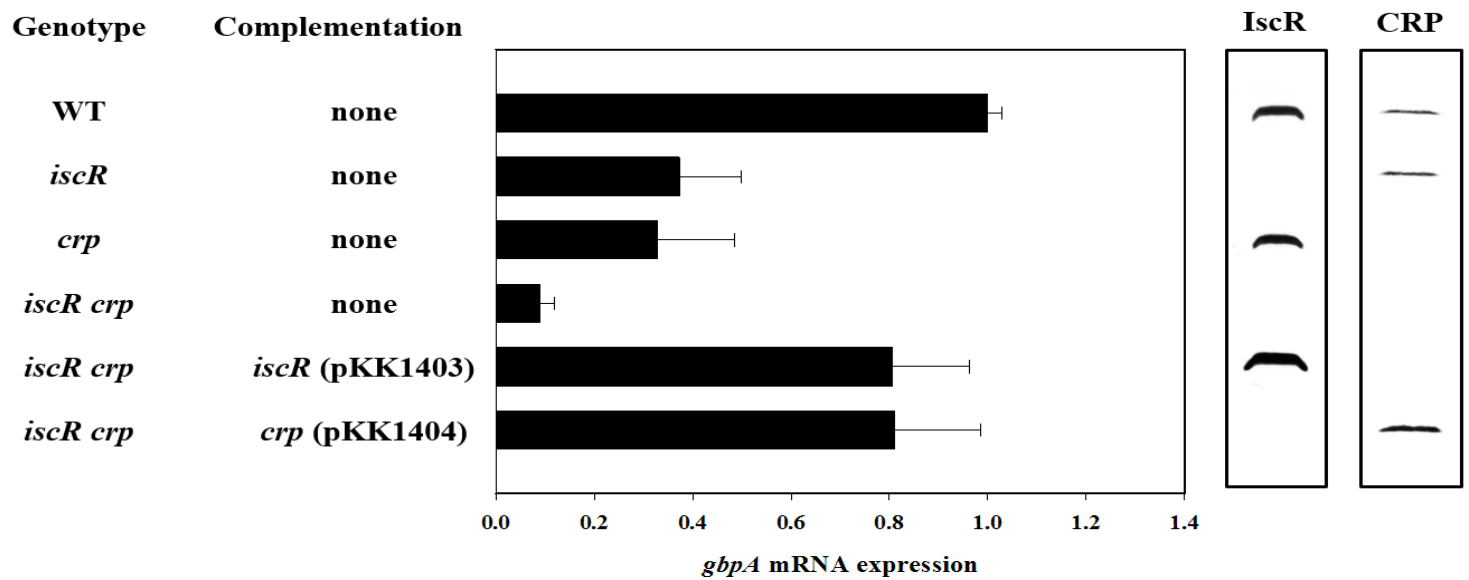

Figure III-4. IscR and CRP coactivate *gbpA* additively. Samples were harvested from the cultures of the wild type (WT) and isogenic mutants grown aerobically to an A_{600} of 0.5 and analyzed to determine the *gbpA* mRNA levels and IscR and CRP protein levels. The *gbpA* mRNA levels were determined by qRT-PCR analyses, and the *gbpA* mRNA level in the wild type was set as 1. Error bars represent the SD. The cellular levels of IscR and CRP were determined by Western blot analyses using the rabbit anti-*V. vulnificus* IscR and anti-*V. vulnificus* CRP sera, respectively. WT, wild type; *iscR*, *iscR* mutant; *crp*, *crp* mutant; *iscR crp*, *iscR crp* double mutant.

III-3-5. IscR, CRP, and SmcR function cooperatively rather than sequencially to regulate *gbpA*

Different mechanisms are possible for this coactivation of *gbpA* by IscR and CRP. For example, multiple activators function sequentially in a regulatory cascade, where one activator influences the accumulation of another regulator(s), which in turn is directly responsible for the activation of *gbpA*. To test this possibility, the cellular levels of IscR, CRP, SmcR, and *Vv*GbpA were determined from the same amount of total protein isolated from the wild type and its isogenic mutants (Fig. III-5).

Western blot analysis revealed that neither activator affected the cellular level of the other, *i.e.* compared with the wild type, the *iscR* mutant strain did not exhibit any significant changes in the cellular level of CRP and *vice versa* (Fig. III-5). From these results, it is unlikely that IscR (or CRP) indirectly activates *gbpA* by increasing the cellular level of CRP (or IscR), which directly activates *gbpA*. Similarly, neither IscR nor CRP influences the cellular levels of SmcR, indicating that the activation of *gbpA* by IscR and CRP is not the result of decreasing cellular levels of SmcR, which directly represses *gbpA*. Consequently, it appears that IscR, CRP, and SmcR function cooperatively to regulate *gbpA* rather than sequentially in a regulatory cascade. It is noteworthy that the level of IscR which activates *gbpA* was higher in the log-phase cells than in the stationary-phase cells. Although levels of CRP did not vary significantly in cells of different growth phases, SmcR which represses *gbpA*

accumulated more in cells of stationary phase (Fig. III-5). In consistent with this, the level of *Vv*GbpA was higher in the log-phase cells than the stationary-phase cells of the wild type (Fig. III-5). Therefore, it was postulated that the growth-phase dependent expression of *gbpA* (Fig.III- 3*A* and *B*) is attributed to this variation in the levels of IscR and SmcR in cells of different growth phase.

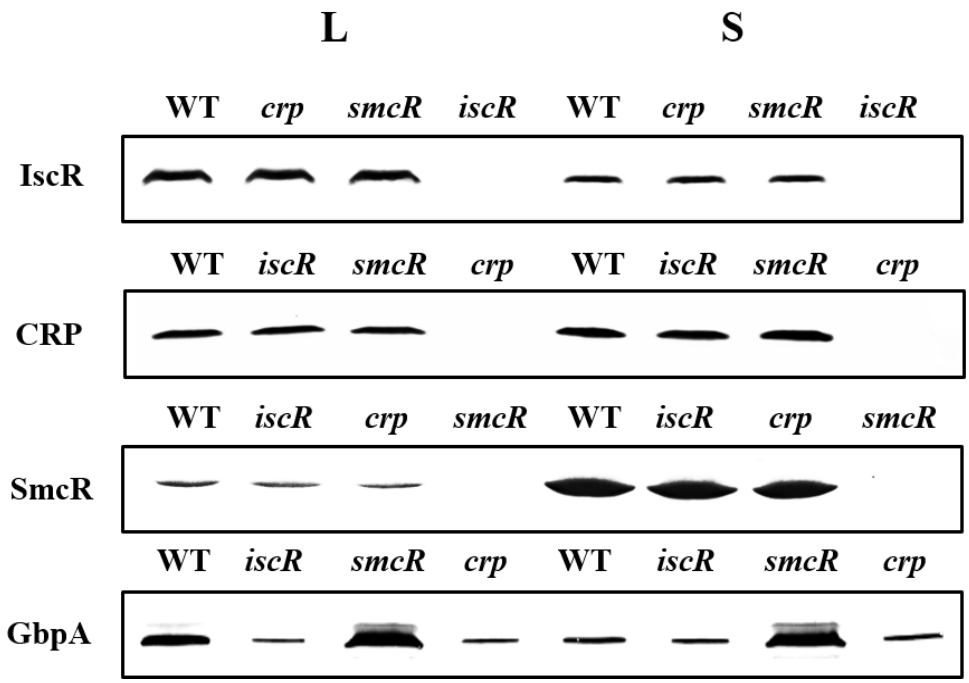

Figure III-5. Cellular levels of IscR, CRP, and SmcR are unaffected by one another. The wild type and isogenic mutants were grown aerobically to an A_{600} of 0.5 (log phase, L) and 2.0 (stationary phase, S). The cells were then examined for the presence of IscR, CRP, SmcR, and GbpA proteins by Western blot analyses using the rabbit anti-*V. vulnificus* IscR, anti-*V. vulnificus* CRP, and anti-*V. vulnificus* SmcR, anti-*V. vulnificus* GbpA sera, respectively. WT, wild type; *iscR*, *iscR* mutant; *crp*, *crp* mutant; *smcR*, *smcR* mutant.

III-3-6. Mapping the regulatory region of *gbpA*

In order to map the promoter of *gbpA*, a transcription start site of *gbpA* was determined by a primer extension analysis. A single reverse transcript was produced from primer extension of RNA isolated from the wild type grown aerobically to an A_{600} of 0.5 (Fig. III-6*A*). Several attempts to identify other transcription start sites using different sets of primers were not successful (data not shown). The 5' end of the *gbpA* transcript was located 235-bp upstream of the translational initiation codon of *gbpA* and subsequently designated +1 (Fig. III-6*B*). The putative promoter constituting this transcription start site was named P_{gbpA} and the sequences for -10 and -35 regions of P_{gbpA} were assigned on the basis of similarity to consensus sequences of the *E. coli* σ^{70} promoter (Fig. III-6*B*).

The pKK reporters carrying the upstream regulatory region of P_{gbpA} which was deleted up to different 5'-ends and fused transcriptionally to *luxCDABE* were constructed (Fig. III-7*A*). The reporters were transferred into the wild type and isogenic mutants and culture luminescence was used to quantify the P_{gbpA} activity (Fig. III-7*B*). The luminescence produced by pKK1407 carrying P_{gbpA} deleted up to -220 was ~ 6.0×10^3 RLU in the wild type but significantly reduced in the *iscR* and *crp* mutants, supporting our previous observation that IscR and CRP activate P_{gbpA}. The RLU of the *smcR* mutant containing pKK1407 increased, confirming the SmcR repression of P_{gbpA} (Fig. III-7*B*). Deletion up to -106 significantly decreased the P_{gbpA}

activity as determined based on the reduced luminescence of the strains containing pKK1408. Interestingly, the RLU of pKK1408 in the *iscR* mutant was indistinguishable from that in the wild type, indicating the absence of the region(s) necessary for IscR to activate P_{gbpA} in pKK1408. Similarly, the comparable RLU produced by pKK1409 in the *crp* mutant and wild type indicated that the region upstream from -76 is probably required for CRP activation of P_{gbpA}. In contrast, the *smcR* mutant containing pKK1409 (and pKK1408) produced still greater luminescence compared to the wild type, indicating that the region downstream from -76 is essential for SmcR repression of P_{gbpA}. The undetectable luminescence produced by pKK1410 indicates that deletion up to -6 completely impaired the P_{gbpA} activity. Taken together, the results suggested that the regulatory region extending from -220 to -6 consecutively harbors the *cis*-elements necessary for IscR, CRP, and SmcR regulation of P_{gbpA}.

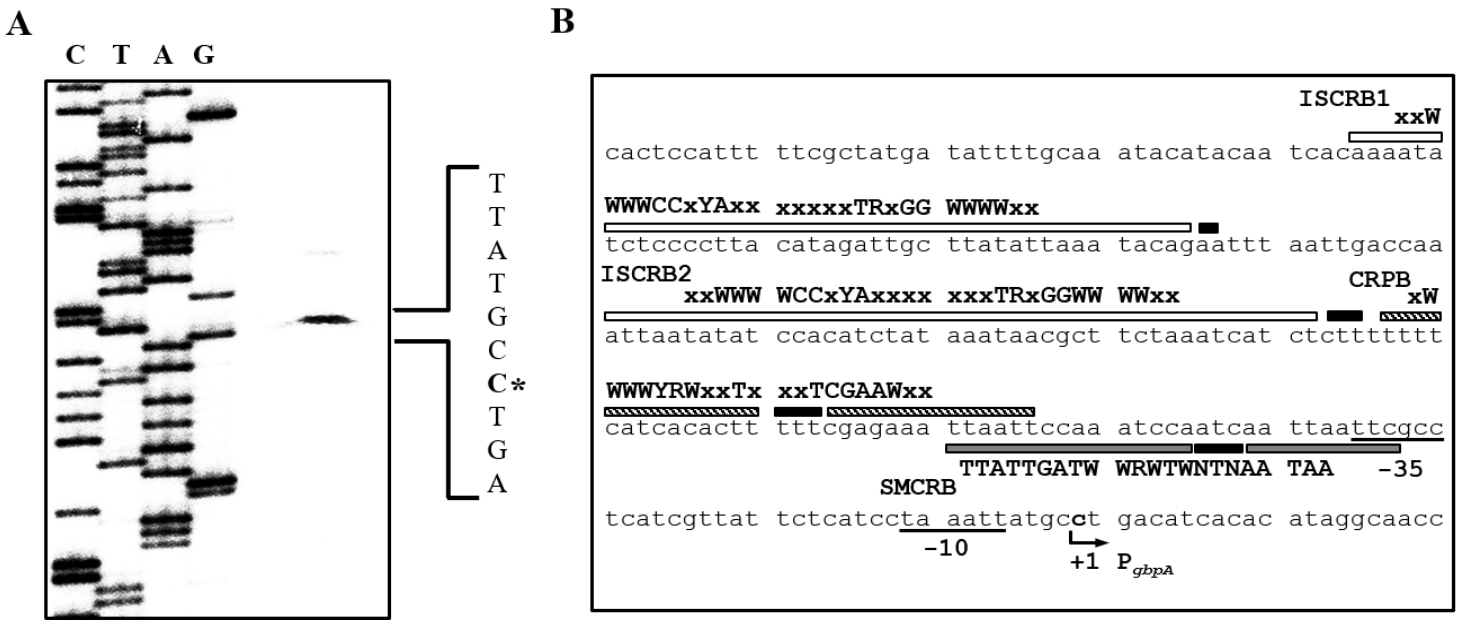
A
C T A G
T
T
A
T
G
C
C*
T
G
A
B
ISCRB1
xxW
cactccattt ttcgctatga tattttgcaa atacatacaa tcacaaaata
WWWCCxYAxx xxxxxTRxGG WWWWxx
tctcccctta catagattgc ttatattaaa tacagaattt aattgaccaa
ISCRB2
xxWWW WCCxYAxxxx xxxTRxGGWW WWxx
CRPB
xW
attaatatat ccacatctat aaataacgct tctaaatcat ctctttttt
WWWYRWxxTx xxTCGAAWxx
catcacactt tttcgagaaa ttaattccaa atccaatcaa ttaattcgcc
TTATTGATW WRWTWNTNAA TAA
-35
SMCRB
tcatcgttat tctcatccta aattatgcct gacatcacac ataggcaacc
-10
+1
P gbpA

Figure III-6. Transcription start site and sequences of the *gbpA* regulatory region. *A*, a transcription start site of *gbpA* was determined by primer extension of the RNA isolated from the wild type grown aerobically to an A_{600} of 0.5. *Lanes C, T, A,* and *G* represent the nucleotide sequencing ladders of pKK1401. The *asterisk* indicates the transcription start site of *gbpA*. *B*, the transcription start site of *gbpA* is indicated by a *bent arrow*, and the positions of the putative -10 and -35 regions are *underlined*. The sequences for binding of IscR (ISCRB1 and ISCRB2, *white boxes*), CRP (CRPB, *shaded boxes*), and SmcR (SMCRB, *gray boxes*) were determined later in this study (Fig. III-10). The nucleotides showing enhanced cleavage are indicated by *black boxes*. The consensus sequences for binding of IscR (Type 2), CRP, and SmcR are respectively indicated *above* the *V. vulnificus* DNA sequence. *R*, A or G; *Y*, C or T; *W*, A or T; *x*, any nucleotides.

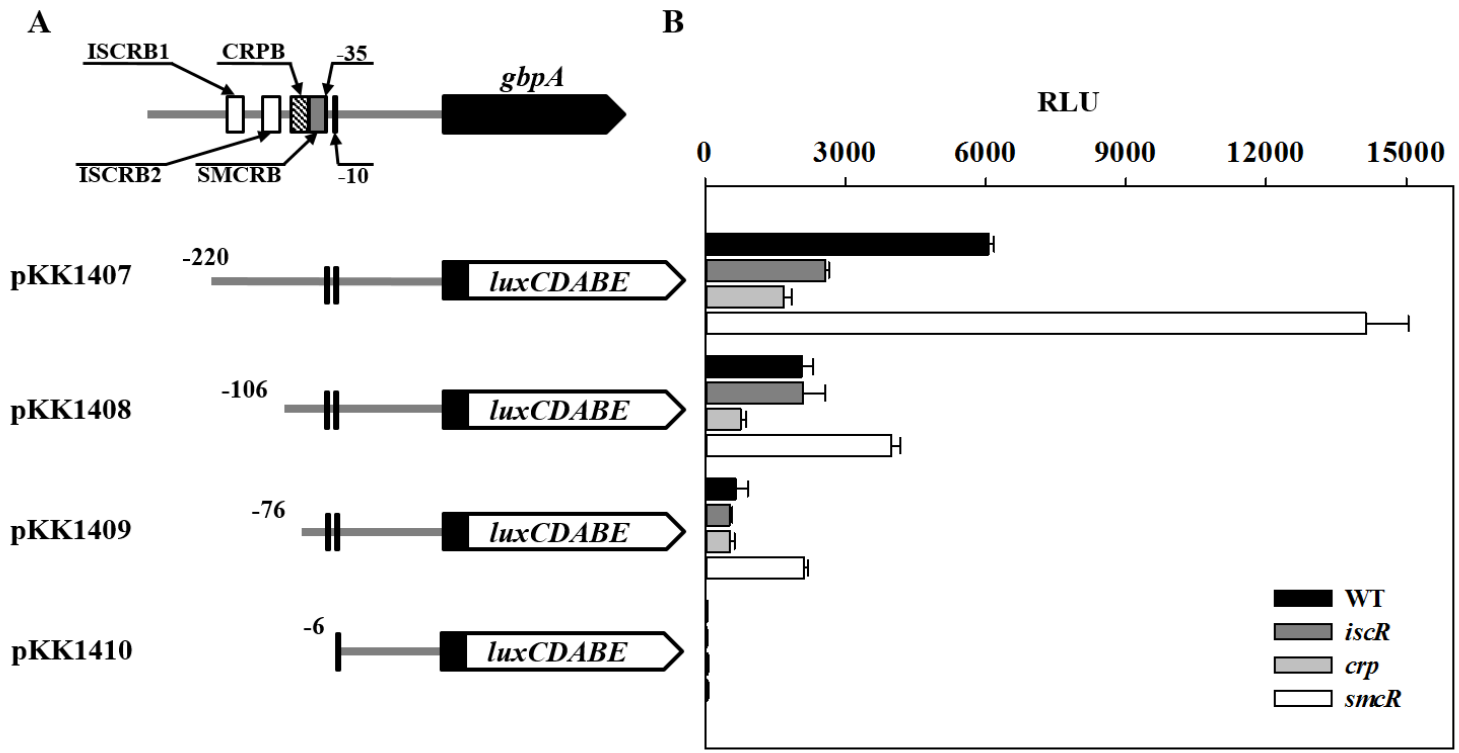
A
ISCRB1
CRPB
-35
gbpA
ISCRB2
SMCRB
-10
pKK1407
-220
luxCDABE
pKK1408
-106
luxCDABE
pKK1409
-76
luxCDABE
pKK1410
-6
luxCDABE
B
RLU
0
3000
6000
9000
12000
15000
WT
iscR
crp
smcR

Figure III-7. Deletion analysis of the P_{gbpA} regulatory region. *A*, construction of *gbpA-lux* fusion pKK reporters. PCR fragments carrying the *gbpA* regulatory region with 5'-end deletions were subcloned into pBBR-lux (Lenz *et al*., 2004) to create each pKK reporter. *Solid lines*, the upstream region of *gbpA*; *black blocks*, the *gbpA* coding region; *open blocks*, *luxCDABE*. The wild type *gbpA* regulatory region is shown on top with the proposed -10 and -35 regions, and the binding sites for IscR (ISCRB1 and ISCRB2, *white boxes*), CRP (CRPB, *the shaded box*), and SmcR (SMCRB, *the gray box*) were determined later in this study (Fig. III-10). *B*, cellular luminescence determined from the wild type (*black bars*), *iscR* mutant (*dark gray bars*), *crp* mutant (*gray bars*), and *smcR* mutant (*open bars*) containing each pKK reporter as indicated. Cultures grown aerobically to an A_{600} of 0.5 were used to measure the cellular luminescence. Error bars represent the SD. RLU, Relative luminescence units. WT, wild type; *iscR*, *iscR* mutant; *crp*, *crp* mutant; *smcR*, *smcR* mutant.

III-3-7. IscR, CRP, and SmcR regulate *gbpA* by directly binding to P_{gbpA}

There are still several possible ways for IscR, CRP, and SmcR to affect P_{gbpA} activity. One is by binding directly to the P_{gbpA} regulatory region to regulate the promoter, whereas another is by modulating the cellular level of unidentified *trans*-acting factor(s), which in turn binds directly to the P_{gbpA} regulatory region. To distinguish these two possibilities, the 390-bp labeled DNA probe encompassing the P_{gbpA} regulatory region (from -301 to +88) was incubated with increasing amounts of IscR and then subjected to electrophoresis. Since IscR was isolated, purified, and used under aerobic conditions, most of the purified IscR would be in the Fe-S clusterless apo-form (Lim and Choi, 2014; Yeo *et al*., 2006). The addition of IscR resulted in two retarded bands in a concentration-dependent manner, indicating that at least two binding sites for IscR are present in the P_{gbpA} regulatory region (Fig. III-8*A*). The binding of IscR was also specific, because assays were performed in the presence of 0.1 μg of poly (dI-dC) as a nonspecific competitor. In a second EMSA, the same but unlabeled 390-bp DNA fragment was used as a self-competitor to confirm the specific binding of IscR. The unlabeled 390-bp DNA competed for the binding of IscR in a dose-dependent manner (Fig. III-8*A*), confirming that IscR binds specifically to the P_{gbpA} regulatory region. In similar DNA-binding assays, CRP and SmcR each displayed specific binding to the P_{gbpA} regulatory region (Fig. III-8*B* and *C*). These results suggested that IscR, CRP, and SmcR regulate *gbpA* by specifically

binding to P_{gbpA}.

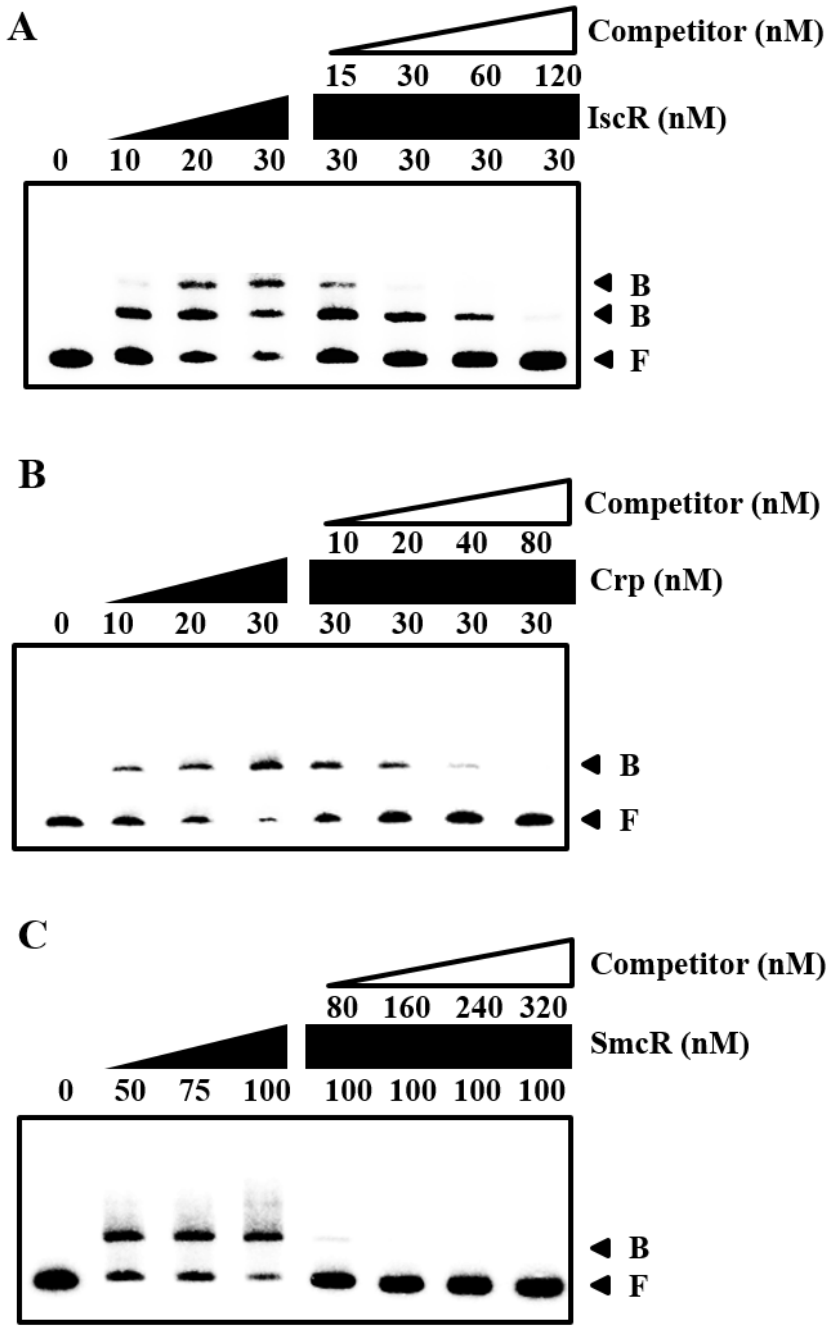
A
Competitor (nM)
15 30 60 120
IscR (nM)
0 10 20 30 30 30 30 30
B
B
F
B
Competitor (nM)
10 20 40 80
Crp (nM)
0 10 20 30 30 30 30 30
B
F
C
Competitor (nM)
80 160 240 320
SmcR (nM)
0 50 75 100 100 100 100 100
B
F

Figure III-8. Specific bindings of IscR, CRP, and SmcR to P_{gbpA}. A 390-bp DNA fragment of the *gbpA* regulatory region was radioactively labeled and then used as a probe DNA. The radiolabeled probe DNA (5 nM) was mixed with increasing amounts IscR (*A*), CRP (*B*), and SmcR (*C*) as indicated. For competition analysis, the same but unlabeled 390-bp DNA fragment was used as a self-competitor DNA. Various amounts of the self-competitor DNA were added to a reaction mixture containing the 5 nM labeled DNA prior to the addition of 30 nM IscR (*A*), 30 nM CRP (*B*), and 100 nM SmcR (*C*). *B*, bound DNA; *F*, free DNA.

III-3-8. Identification of binding sites for IscR, CRP, and SmcR

To determine the precise location of the IscR, CRP, and SmcR binding sites in the P_{gbpA} regulatory region, DNase I protection assays were performed using the same 390-bp DNA probe used for DNA-binding assays. As shown in Fig. III-9*A*, two regions extending from -184 to -145 (ISCRB1, centered at -164.5) and -124 to -88 (ISCRB2, centered at -106) were clearly protected by IscR (Fig. III-9*A*). Both sequences were equally protected by the same level of IscR, indicating that IscR bound to the two sites with a comparable affinity. The sequences of ISCRB1 and ISCRB2 revealed a 29-bp imperfect palindrome and scored about 83% and 79% identity to a consensus sequence of the Type 2 IscR-binding site, respectively, to which the apo-form of IscR most likely binds in *E. coli* (Fig. III-6*B*) (Nesbit *et al*., 2009). The CRP footprint extended from -82 to -54 (CRPB, centered at -68) (Fig. III-9*B*) and the sequences of CRPB scored 86% identity to a consensus sequence for CRP binding (Fig. III-6*B*) (Cameron and Redfiled, 2007). These positioning of ISCRB and CRPB suggested that both IscR and CRP may act as class I activators interacting with the C-terminal domains of RNA polymerase α subunits (αCTD) (Browning and Busby, 2004). The sequences protected by SmcR extended from -58 to -32 (SMCRB, centered at -45) and revealed 73% identity to a consensus sequence for SmcR binding (Lee *et al*., 2008). In contrast to ICRB and CRPB, SMCRB overlaps with the sequences of -35 region of P_{gbpA} (Fig. III-6*B*) and thus bound SmcR

could prevent RNA polymerase binding, supporting the SmcR repression of P_{gbpA}. Several nucleotides also showed enhanced cleavages, indicating that binding of the regulators altered the configuration of the DNA of P_{gbpA} (Fig. III-9*A*, *B*, and *C*). These results confirmed that IscR, CRP, and SmcR regulate *gbpA* by binding to specific sequences of P_{gbpA}.

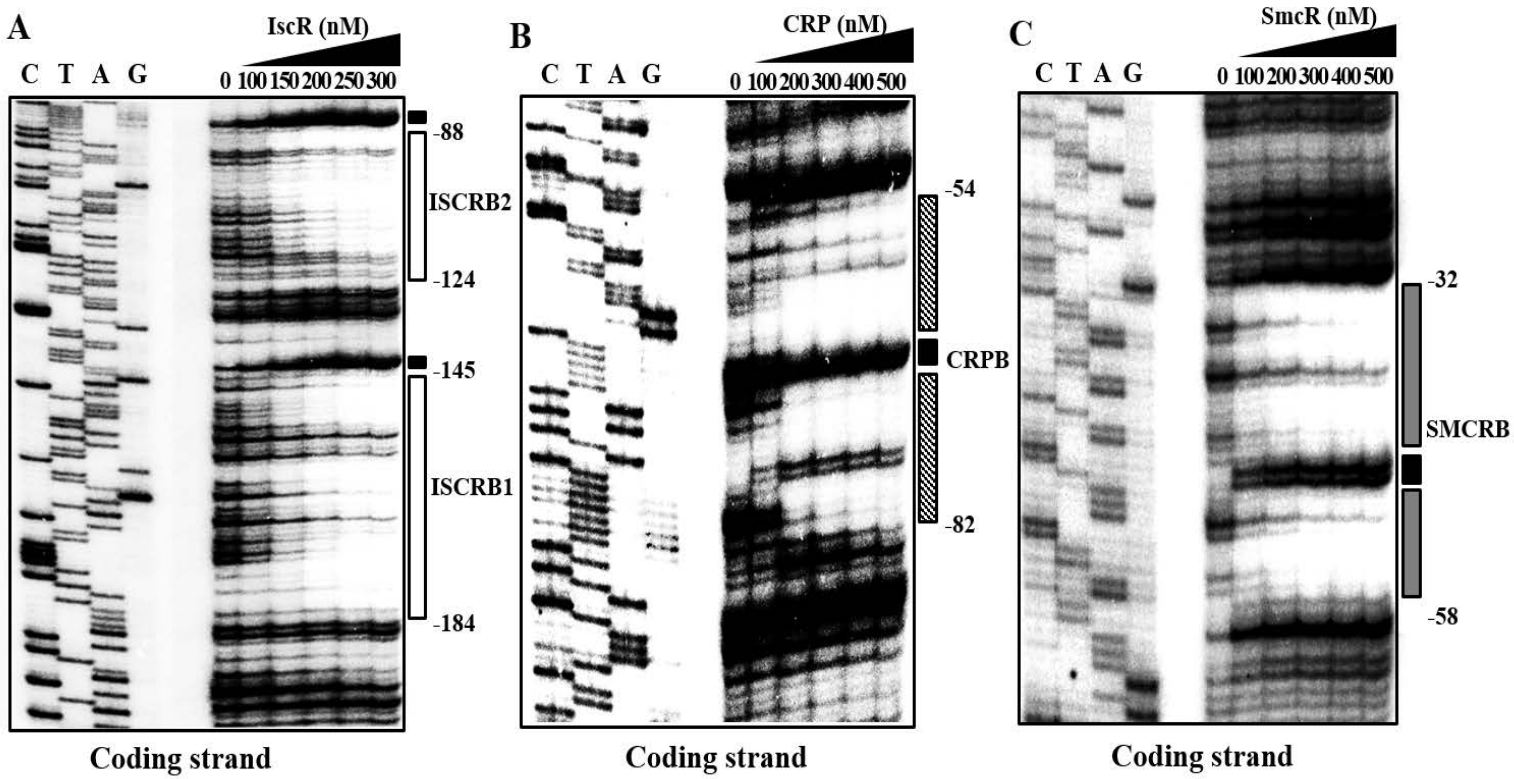
A
IscR (nM)
C T A G
0 100 150 200 250 300
-88
ISCRB2
-124
-145
ISCRB1
-184
Coding strand
B
CRP (nM)
C T A G
0 100 200 300 400 500
-54
CRPB
-82
Coding strand
C
SmcR (nM)
C T A G
0 100 200 300 400 500
-32
SMCRB
-58
Coding strand

Figure III-9. Sequences for binding of IscR, CRP, and SmcR to P_{gbpA}. A 390-bp DNA fragment of the *gbpA* regulatory region was radioactively labeled and then used as a probe DNA. The radiolabeled probe DNA (25 nM) was incubated with increasing amounts of IscR (*A*), CRP (*B*), and SmcR (*C*) as indicated. The regions protected by IscR, CRP, and SmcR are indicated by *white boxes*, *shaded boxes*, and *gray boxes*, respectively. The nucleotides showing enhanced cleavage are indicated by *black boxes*. *Lanes C*, *T*, *A*, and *G* represent the nucleotide sequencing ladders of pKK1401.

III-3-9. IscR activates P_{gbpA} by sensing reactive oxygen species (ROS)

Recently, it has been discovered that IscR senses ROS and activates the expression of numerous virulence genes (Lim and Choi, 2014; Lim *et al.*, 2014). This prompted us to examine the effect of oxidative stress on the *gbpA* expression by measuring the levels of *gbpA* transcript and *Vv*GbpA protein in the strains grown anaerobically and exposed to a range of H_2O_2. The levels of the *gbpA* transcript and *Vv*GbpA protein in the wild type were gradually elevated along with increasing concentrations of H_2O_2 (Fig. III-10*A* and *B*). In contrast, the H_2O_2-depedent increase of the *gbpA* expression was not evident in the *iscR* mutant (Fig. III-10*A* and *B*), indicating that the activation of P_{gbpA} in response to oxidative stress is mediated by IscR. Since the cellular level of IscR also increased by exposure to H_2O_2 (Fig. III-10*B)*, the increased activity of P_{gbpA} by oxidative stress was possibly attributed to the increased level of IscR. The levels of CRP and SmcR were not significantly changed in the wild type and *iscR* mutant exposed to H_2O_2 (Fig. III-10*B*).

Previous reports that the [2Fe-2S] cluster in IscR is disrupted by oxidative stress to result in the clusterless apo-form (Schwartz *et al*., 2001; Lim *et al.*, 2014; Nesbit *et al*., 2009; Giel *et al*., 2013) led us to examine whether apo-IscR indeed activates P_{gbpA} *in vivo*. The level of *gbpA* transcript in the $iscR_{3CA}$ mutant, of which the *iscR* coding region on the chromosome was replaced with $iscR_{3CA}$ encoding an apo-locked

IscR$_{3CA}$ (Lim *et* al., 2014) (Table II-1), was compared with those of the wild type and *iscR* mutant. When determined by qRT-PCR (Fig. III-10*C*) and Western blot analyses (Fig. III-10*D*), the P$_{gbpA}$ activity of the *iscR*$_{3CA}$ mutant was almost 3-and 13-fold greater than that of the wild type and *iscR* mutant, respectively, indicating that apo-IscR is able to activate P$_{gbpA}$ *in vivo*. Further, it was noted that the IscR$_{3CA}$ level of the *iscR*$_{3CA}$ mutant was significantly greater than the IscR level of the wild type, in which both holo- and apo-IscR coexist (Fig. III-10*D*) (Giel *et al*., 2013). In contrast, the levels of CRP and SmcR did not significantly differ among the strains (Fig. III-10*D*). These results indicated that the increased activity of P$_{gbpA}$ in the *iscR*$_{3CA}$ mutant was possibly attributed to the elevated cellular level of IscR$_{3CA}$. This elevated IscR$_{3CA}$ level in the *iscR*$_{3CA}$ mutant was perhaps not surprising since apo-IscR de-represses its own expression (Schwartz *et al*., 2001; Giel *et al*., 2013). Taken together, the results led us to propose a model in which IscR senses ROS and shifts to the apo-form, leading to the de-repression of the *isc* operon, elevating apo-IscR protein levels, and, accordingly, activating P$_{gbpA}$.

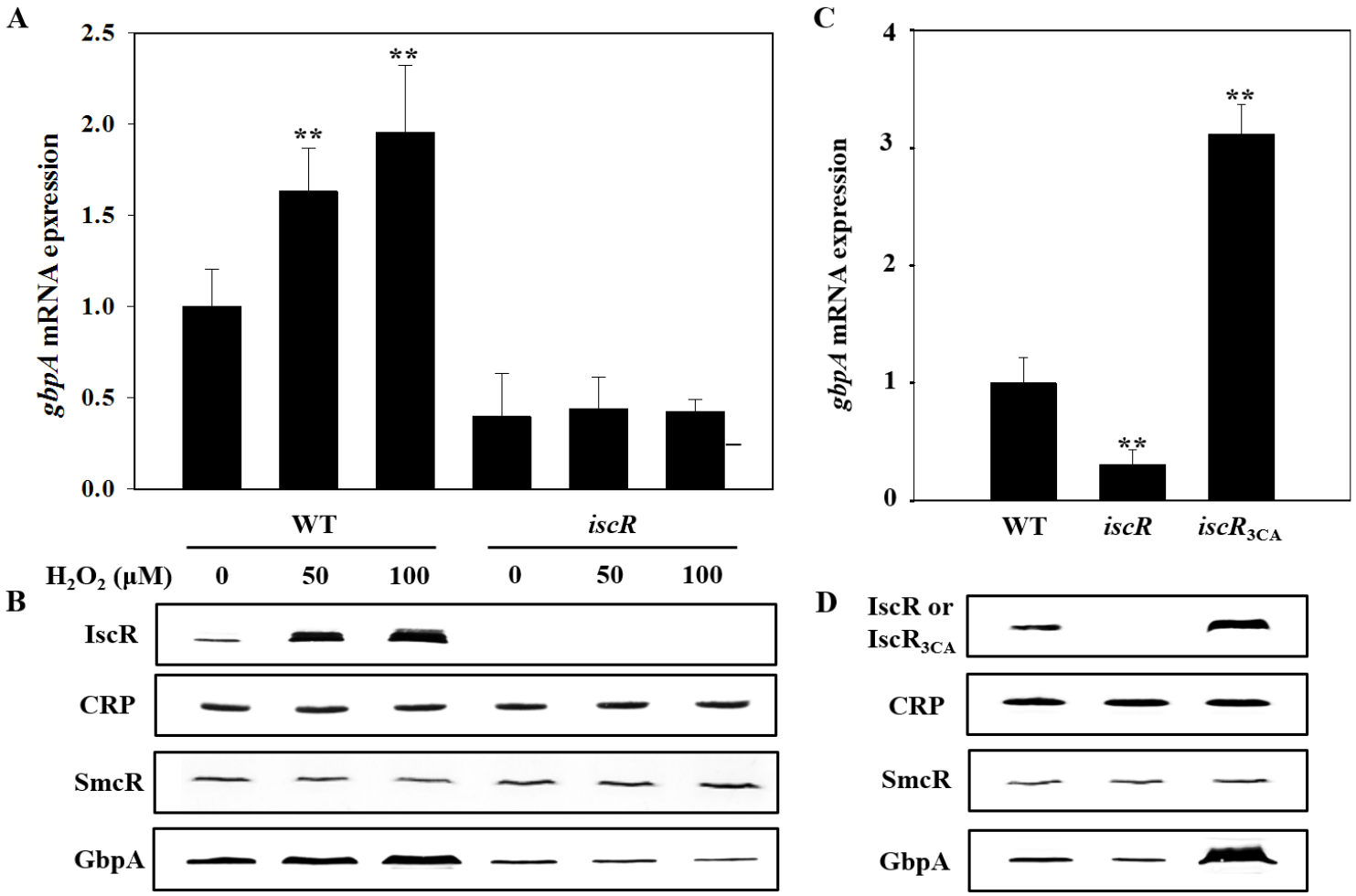
A
gbpA mRNA epxression
2.5
2.0
1.5
1.0
0.5
0.0
**
**
WT
iscR
H2O2 (μM)
0
50
100
0
50
100
B
IscR
CRP
SmcR
GbpA
C
gbpA mRNA expression
4
3
2
1
0
**
WT
iscR
iscR3CA
D
IscR or
IscR3CA
CRP
SmcR
GbpA

Figure III-10. Effects of oxidative stress and apo-IscR on the activity of P_{gbpA}. Total RNAs and proteins were isolated either from the cultures grown anaerobically to an A_{600} of 0.5 and then exposed to various concentrations of H_2O_2 for 10 min as indicated (*A* and *B*) or from the cultures grown aerobically to an A_{600} of 0.5 (*C* and *D*). *A* and *C*, the *gbpA* mRNA levels were determined by qRT-PCR analyses, and the *gbpA* mRNA level in the wild type unexposed to H_2O_2 (*A*) or the wild type (*C*) was set to 1. Error bars represent the SD. **, $P < 0.005$ relative to the wild type unexposed to H_2O_2 (*A*) or to the wild type (*C*). *B* and *D*, protein samples were resolved by SDS-PAGE, and IscR (or $IscR_{3CA}$), CRP, SmcR, and GbpA were detected by Western blotting using the rabbit anti-*V. vulnificus* IscR, anti-*V. vulnificus* CRP, anti-*V. vulnificus* SmcR, and anti-*V. vulnificus* GbpA sera, respectively. WT, wild type; *iscR*, *iscR* mutant; $iscR_{3CA}$, a strain expressing apo-locked $IscR_{3CA}$.

III-4. Discussion

There are several lines of evidence that *V. vulnificus* embed themselves in oyster tissues and form biofilms to persist in oyster as the primary route of infection (Froelich and Oliver, 2013; Paranjpye *et al*., 2007). Furthermore, biofilms are likely a form of pathogenic *V. vulnifius* and an important source for new outbreaks as they provide a means to reach a concentrated infective dose consumed by humans (Kim *et al*., 2013). Therefore, it is a reasonable hypothesis that cells of the *V. vulnificus* biofilms entering the host intestine might be detached at first and become free-living planktonic cells that disperse to epithelial surfaces for adhesion (Kim *et al*., 2013) Adhesion to the intestinal epithelia is a prerequisite step for the establishment of a successful infection and thus interference with the adhesion is an efficient way to prevent or treat infections of *V. vulnificus*. Efforts to develop the anti-adhesion therapies were initiated by identification and characterization of the adhesins of *V. vulnificus*. Previous studies demonstrated that *V. vulnificus* expresses different types of adhesin molecules essential for adhesion to human cell lines (Kim and Rhee 2003; Lee *et al*., 2004; Paranjpye and Strom, 2005; Goo *et al*., 2006; Lee *et al*., 2010). Additionally, the present study identified GbpA required for adhesion to mucin and the mucin-secreting HT29-MTX cells (Fig. III-1*A* and *B*). These observations suggested that *V. vulnificus* adheres to epithelial surfaces through multiple adhesive

interactions as observed in other pathogens (Ofek *et al*., 2013).

Nevertheless, little is known about the regulatory mechanisms adopted by *V. vulnificus* to module the expression of the adhesins. No information on the expression pattern or level of the adhesins during infection of the pathogen has been reported in previous studies. As a result of this study, the expression of *gbpA* is growth-phase dependent and decreases in the stationary-phase cells (Fig. III-3). SmcR, a master regulator of the *V. vulnificus* quorum sensing (Shao and Hor, 2001; Jeong *et al*., 2003; Lee *et al*., 2008; Jeong *et al*., 2010), represses *gbpA* at the transcription level (Fig. III-3). This result, along with elevated levels of SmcR in the stationary-phase cells (Fig. III-5), indicated that the decrease of *gbpA* expression in the stationary-phase cells attributes most likely to SmcR repression. It is noteworthy that most individual cells in biofilms are close to stationary-phase physiology with reduced growth rates and increased resistance to stress (Hall-Stoodley *et al*., 2004; Fux *et al*., 2005; Høiby *et al*., 2010). Considering the *V. vulnificus* infection in the form of biofilms, the repression of *gbpA* by the elevated SmcR in the biofilm (stationary-phase) cells could save the limited nutrients that can alternatively be used for expression of the genes responsible for the detachment of the biofilms. Consistent with this, SmcR appears to enhance the detachment of *V. vulnificus* biofilms entering the host intestine and thereby promote the dispersal of the pathogen to establish a

new infectious cycle on the intestinal surfaces (Kim *et al*., 2013). Furthermore, GbpA probably surplus upon establishing colonization and may be even detrimental to the detachment of individual cells from the established colony. SmcR, a cell-density dependent regulator, is believed to sense cell densities higher than critical levels in the colony, and then render *V. vulnificus* to leave the congested colony onto new colonization loci by repressing *gbpA*, which is crucial for pathogenesis.

Upon arrival onto new loci, CRP and IscR activate the *gbpA* expression to facilitate adhesion that is generally accompanied by the onset of accelerated (perhaps exponential) growth to colonize (Fig. III-3). CRP, which is a central regulator of energy (catabolic) metabolism (Green *et al*., 2014), may recognize host environments by sensing the starvation of specific nutrients imposed by the host cells and endogenous bacterial flora. IscR increases at the exponential phase (Fig. III-5), indicating that the maximum expression of *gbpA* at the exponential phase attributes possibly to increased IscR (Fig. III-3). The [2Fe-2S] cluster in IscR is disrupted by oxidative stress, and the resulting clusterless IscR (apo-IscR) increases the cellular level of IscR, most likely in its apo-form (Schwartz *et al*., 2001; Giel *et al*., 2013; Zheng *et al*., 2001). There are two IscR-binding sequences, Type 1 and Type 2, and the Type 2 sequence are recognized by apo-IscR, whereas the Type 1 sequence are recognized exclusively by holo-IscR (Yeo *et al*., 2006; Wu *et al*., 2009; Rajagopalan

et al., 2013). The IscR binding sequences on P_{gbpA} scored an 80% homology to the Type 2 sequences of *E. coli* (Fig. III-6*B*) (Nesbit *et al*., 2009; Rajagopalan *et al*., 2013). Furthermore, the H_2O_2-induction of *gbpA* was mediated by apo-IscR (Fig. III-10). The combined results suggested that IscR senses the oxidative stress imposed by the host defense system, turns into the apo-form, and activates the *gbpA* expression, leading to improved adhesion to the host intestinal surfaces.

In summary, *gbpA* encoding a mucin-binding protein essential for pathogenesis of *V. vulnificus* was identified in this study. The *gbpA* expression was in a growth-phase dependent manner and regulated positively by IscR and CRP, but negatively by SmcR. The regulatory proteins regulate the *gbpA* expression cooperatively rather than sequentially, and exerted their effects by directly binding to the regulatory region of P_{gbpA}. Two distinct IscR binding sequences centered at -164.5 and -106, a CRP binding sequence centered at -68, and a SmcR binding sequence centered at -45 were identified. The *gbpA* expression was induced by exposure to oxidative stress, and the induction was mediated by the elevated intracellular levels of, most probably, apo-IscR. It is still difficult to define the implications of the collaboration between IscR, CRP, and SmcR in terms of pathogenesis of *V. vulnificus*. However, it is likely that the collaboration allows more precise tuning of the *gbpA* expression by integrating the signals presumably encountered in the host intestine, such as

oxidative stress, starvation of specific nutrients, and increased cell-density, and thereby enhances the overall success of *V. vulnificus* during pathogenesis.

Chapter IV.

Functional Analysis and Regulatory Characteristics of *Vibrio vulnificus plp* Encoding a Phospholipase A_2

IV-1. Introduction

Many pathogenic bacteria secrete a wide range of substrates, including small molecules, proteins, and DNA. The secretion of these substrates requires secretion systems that are devised for the transport of the substrates across the bacterial cell envelope (Chang *et al.*, 2014; Costa *et al*., 2015). These molecules are essential for the response of the pathogen to its environment as well as for several physiological processes such as adhesion, adaptation, and pathogenesis (Backert and Meyer, 2006; Tseng *et al.*, 2009). Among them, many secreted toxins and effector proteins are considered to be necessary in the colonization and invasion of the pathogen to host cells and thereby are crucial for the pathogen to survive and multiply in the host (Cianociotto, 2005; Desvaux and Hê braud, 2006). Especially, the studies for identifying the importance of secreted phospholipases in bacterial virulence have been steadily increasing as the phospholipases could destroy or derange the host cell envelope that is mainly composed of phospholipids and proteins (Ghannoum, 2000; Sitkiewicz *et al.*, 2006; Istivan and Coloe, 2006).

Phospholipases are widespread in prokaryotic organisms and constitute a heterogeneous group of lipolytic enzymes that have the ability to hydrolyze one or more ester linkages in phospholipids, with phosphodiesterase as well as acyl

hydrolase activity (Ghannoum, 2000; Kuhle and Flieger, 2013). Phospholipases are classified into four major groups (A to D) based on their site of attack on the phospholipid. For example, phospholipase A (PLA) hydrolyzes a fatty acid from the glycerol backbone and is further differentiated by its positional specificity, preference for the acyl group attached to position 1 or 2 of the molecule, PLA_1 and PLA_2, respectively (Schmiel and Miller, 1999). Phospholipase B (PLB) has both PLA_1 and PLA_2 activity. The other types of phospholipases cleave on either side of the head group phosphate. Cleavage by phospholipase C (PLC) releases the phospho-head group and diacylglycerol, whereas phospholipase D (PLD) cleaves on the other side of head group (Schmiel and Miller, 1999). Phospholipases destabilize the membrane of the host cells and induce cell lysis by cleaving phospholipids (Schmiel and Miller, 1999; Ghannoum, 2000). In addition, the resulting cleavage products may act as secondary messengers and therefore support pathogen-driven manipulation of host signaling events and modulate inflammatory response (Huang *et al*., 2005; Zhao and Natarajan, 2013; Monturiol-Gross *et al*., 2014). Accordingly, many pathogens with disruption of genes encoding phospholipases were substantially defective in cytolysis and tissue destruction, leading to attenuated virulence (Awad *et al*., 1995; Schmiel *et al*., 1998; Flieger *et al*., 2002; Bakala N'Goma *et al*., 2015).

Like many other pathogenic bacteria, *V. vulnificus*, a foodborne pathogen and a causative agent of gastroenteritis and fatal septicemia (Oliver, 2015), also secretes diverse toxins and effectors (Testa *et al*., 1984; Jeong *et al*., 2000; Koo *et al*., 2007; Jeong and Satchell, 2012). However, the information about the genes encoding phospholipases and its importance in pathogenesis of *V. vulnificus* is still limited (Koo *et al*., 2007). Furthermore, neither the promoter(s) of the gene encoding phospholipases nor any *trans*-acting regulatory protein(s) required for the transcription of the gene has been identified previously. In chapter II, the expression gene encoding a putative phospholipase was induced by mucin and mucin-secreting host cells (Tables II-3 and II-4). The amino acid sequence of this gene was 67% identical to that of *V. anguillarum* phospholipase (*Va*Plp). In the present study, an open reading frame (ORF) encoding a *V. vulnificus* phospholipase (*Vv*Plp) was identified. Construction of the *plp* mutant and evaluation of its phenotypes provided evidences that Plp is secreted via type II secretion sytem (T2SS) and is a phospholipase A_2 crucial for the pathogenesis of the organism. Efforts to understand the regulatory mechanisms of the *plp* expression were initiated by determining the *plp* mRNA levels in cells of different growth phases. Since transcriptional activator HlyU (Liu *et al*., 2007) and CRP (Green *et al*., 2014) were previously reported to affect the pathogenesis of *V. vulnificus* (Choi *et al*., 2002; Oh *et al*., 2009; Jang *et al*., 2016), influences of global regulatory proteins as well as growth phases on the

expression of *plp* were examined. Genetic and biochemical studies demonstrated that the two regulatory proteins regulate *plp* cooperatively rather than sequentially and exerted their effects by directly binding to the *plp* promoter P_{plp}. Deletion analyses of the upstream region of P_{plp} and DNase I protection assays were performed to identify the binding sequences of HlyU and CRP.

IV-2. Materials and Methods

IV-2-1. Strains, plasmids, and culture conditions

The strains and plasmids used in this study are listed in Table II-1. Unless otherwise noted, the *V. vulnificus* strains were grown in Luria-Bertani (LB) medium supplemented with 2% (*wt/vol*) NaCl (LBS) at 30°C, and their growth was monitored spectrophotometrically at 600 nm (A_{600}).

IV-2-2. Complementation and generation of the *plp*, *hlyU*, and *hlyU crp* mutants

The *plp* gene was inactivated *in vitro* by deletion of the open reading frame (ORF) of *plp* (288-bp of 1254-bp) using the PCR-mediated linker-scanning mutation method as described previously (Kim *et al*., 2014). Briefly, pairs of primers PLP01-F and -R (for amplification of the 5' amplicon) or PLP02-F and -R (for amplification of the 3' amplicon) were designed and used (Table III-1). The *plp* gene with 645-bp deletion was amplified by PCR using the mixture of both amplicons as the template and PLP01-F and PLP02-R as primers. Similar experimental procedures were adopted for amplification of the Δ*hlyU in vitro*, except that primers HLYUF01, HLYU01R, HLYU02F, and HLYU02R (for 249-bp deleted *hlyU*) were used as indicated in Table III-1. The resulting Δ*plp* and Δ*hlyU* were ligated into SpeI-SphI-digested pDM4 (Milton *et al*., 1996) to generate pKK1301 and pZW1401,

respectively (Table II-1). *E. coli* S17-1 *λ pir, tra* strain (Simon *et al*., 1983) containing pKK1301 and pZW1401 was used as a conjugal donor to either *V. vulnificus* MO6-24/O to generate the *plp* mutant KK131 and *hlyU* mutant ZW141, respectively (Table II-1).

pBS0907, which was constructed previously to carry a mutant allele of *V. vulnificus crp* on pDM4 (Table II-1) (Kim *et al*., 2011), was used to generate the *hlyU crp* double mutant of *V. vulnificus*. *E. coli* S17-1 *λ pir, tra* containing pBS0907 was used as conjugal donor in conjugation with the *hlyU* mutant ZW141 as a recipient. The resulting *hlyU crp* double mutant was named KK151 (Table II-1). The conjugation and isolation of the transconjugants were conducted using the method described previously (Kim *et al*., 2011). To complement the *plp, hlyU,* and *crp* mutations, each ORF of *plp, hlyU,* and *crp* was amplified by PCR using a pair of specific primers as listed in Table III-1. The amplified *plp, hlyU,* and *crp* ORF were cloned into pJH0311 (Goo *et al*., 2006) to create pKK1320, pZW1510, and pKK1502, respectively (Table II-1). The plasmids were transferred into the appropriate mutants by conjugation as described above.

IV-2-3. Protein purification

The ORF of *plp* was amplified by PCR using a pair of primer PLP04–F and –R (Table III-1). To attach His_6 taq to C-terminal amino acid of Plp, sequences 'GTGATGGTGATGGTGATG' were added at 5' end of PLP04–R primer. Since overexpressed Plp proteins were insoluble (data not shown), the PCR product was used to make an in-frame gene fusion with the 3'end of the *malE* gene encoding maltose-binding protein (MBP) in pMBP parallel1 (Sheffield *et al*., 1999) and resulted in pKK1503 (Table II-1). The *malE-plp-his*$_6$ junctions of the plasmid was sequenced to confirm that the two coding region were in identical reading frames. The resulting MBP-Plp-His_6 were expressed and purified by affinity chromatography according to the manufacturer's procedures (Amylose resin; NEB). To remove MBP protein, 500 μg of MBP-Plp-His_6 was incubated with recombinant 100 μg tabacco etch virus (TEV) protease overnight at room temperature (RT). The reaction mixture were loaded onto Ni-NTA agarose resin and purified by affinity chromatography according to manufacturer's procedures (Qiagen). Finally, the collected fractions containing the His-tagged Plp protein were pooled, concentrated and separated on a HiLoad Superdex 200 gel filtration column (GE Healthcare) pre-equilibrated with 20 mM Tris-Cl (pH8.0) and 150 mM NaCl. During purification, the presence of the protein was confirmed by SDS-PAGE. The purified His-tagged Plp was concentrated to 1 mg ml^{-1} and stored frozen at -80°C. Similarly, the ORF of *hlyU* was also

amplified by PCR using a pair of primer HLYU04-F and –R. (Table III-1) and cloned into a His_6 tag expression vector, pET-28a(+) (Novagen) to result in pYU1317 (Table II-1). His-tagged HlyU proteins were expressed in *E.coli* BL21 (DE3) and purified by affinity chromatography according to the manufacturer's procedure (Qiagen). In a similar way, pHK0201 which was constructed previously (Choi *et al*., 2002) (Table II-1), were used to overexpress and purify the His-tagged CRP.

IV-2-4. Preparation of polyclonal antibody and Western blot analysis

Truncated Plp protein was overexpressed and purified to serve as the antigen to raise polyclonal antibody against Plp. Briefly, primer PLP05-F and PLP05-R (Table III-1) were used to amplify 5' end protein of *plp* gene, which encodes the truncated Plp protein (amino acid 1 to 150). PCR product was ligated into pET-28a(+) (Novagen) to result in pKK1505 (Table II-1). His tagged truncated Plp was expressed in *E. coli* BL21 (DE3). The purification of His-tagged truncated Plp by affinity chromatography was performed under denaturing condition according to the instruction of the manufacturer (Qiagen) and protein purity was determined by SDS-PAGE and Coomassie blue staining. Subsequently, the purified His-tagged truncated Plp, HlyU and CRP were used to raise rabbit polyclonal antibodies against Plp, HlyU, and CRP of *V. vulnificus*, respectively (AB Frontier). *E. coli* DnaK monoclonal antibody (Enzo lifescience, Farmingdale, NY) was used to detect Dnak as a loading control. For Western blot analyses, the bacterial cells grown in LBS was harvested, washed and broken by cOmplete Lysis-M kit (Roche), and clarified by centrifugation to generate cell lysate. Proteins (10, 20, 50, and 100 μg for detecting CRP, DnaK, Plp, and HlyU, respectively) from the cell lysates or culture supernatant (2 μg for detecting Plp) were resolved by SDS-PAGE and immunoblotted as described previsously (Kim *et al*., 2014).

IV-2-5. Cytotoxicity and mouse lethality

Cytotoxicity was evaluated by measuring cytoplasmic lactate dehydrogenase (LDH) activity that is released from the mucin-secreting HT29-MTX cells (Jang *et al*., 2016) by damage of plasma membranes (Sepp *et al*., 1996). The HT29-MTX cells were grown in McCoy's 5A media containing 1% (*vol*/*vol*) fetal bovine serum (MCF) (Gibco-BRL) in 96-well culture dishes (Nunc) as described previously (Lim and Choi, 2014). Each well with 1×10^6 HT29-MTX cells was infected with the *V. vulnificus* strains at a various multiplicity of infection (MOI) for various incubation times. The LDH activity released from the supernatant was determined using a cytotoxicity detection kit (Roche).

Mouse mortalities of the wild type and *plp* mutant were compared as described previously (Baek *et al*., 2009; Lim and Choi, 2014). Groups of (n = 15) 7-week-old ICR female mice (specific pathogen-free; Seoul National University) were starved without food and water for 12 h until infection. Then the mice were injected intraperitoneally with 30 μg of iron-dextran for each gram of body weight immediately before intragastrical administration with 100 μl of the inoculum, representing approximately 10^8 cells of either the wild type or the *plp* mutant. Mouse mortalities were recorded for 24 h. All manipulations of mice were approved by the Animal Care and Use Committee at Seoul National University.

IV-2-6. Phospholipase A_2 (PLA_2) activity assay

PLA_2 activity of recombinant Plp (rPlp) was measured using the EnzChek® Phospholipase A_2 assay kit (Invitrogen). Briefly, the cleavage of the *sn*-2 1-*O*-(6-BODIPY [dipyrromethene boron difluoride] 558/568-aminohexyl)-2-BODIPY FL C_5-*sn*-glycero-3-phosphocholine (red/green BODIPY PC-A2) by the PLA_2 enzyme results in an increase of fluorescence emission. The red/green BODIPY PC-A2 substrate was suspended to a final concentration of 1 mM in dimethyl sulfoxide. The substrate-liposome mix was prepared by mixing 25 μl of red/green BODIPY PC-A2 substrate, 25 μl of 10 mM 1,2-dioleoyl-*sn*-glycero-3-phosphocholine (DOPC), and 25 μl of 1,2-dioleoyl-*sn*-glycero-3-phospho-(1′-rac-glycerol) (sodium salt) (DOPG) in 5 ml of PLA_2 assay buffer. 50 μl of phospholipase A_2 samples containing various amount of PLA_2 from honey bee venom or rPlp was added to 50 μl of the substrate-liposome mix. The reaction mixtures were incubated room temperature for 30 min. The fluorescence emission was measured with a microplate reader (Tecan Infinite M200 reader) equipped for excitation in the 480 nm and fluorescence emission at 515 nm.

IV-2-7. RNA purification and transcripts analysis

Total RNAs from the *V. vulnificus* strains grown aerobically to various levels of A_{600} were isolated using an RNeasy® mini kit (Qiagen). For the primer extension analysis, a 23-base primer PLP06-R (Table III-1) complementary to the regulatory region of *plp* was end labeled with [γ-^{32}P]ATP and added to the RNA. The primer was then extended with SuperScript II RNase H$^-$ reverse transcriptase (Invitrogen). The cDNA products were purified and resolved on a sequencing gel alongside ladders generated from pKK1501 with the same primer. The plasmid pKK1501 was constructed by cloning the 461-bp *plp* upstream region extending from -345 to +116, amplified by PCR using a pair of primers PLP05-F and -R (Table III-1), into pGEM-T Easy (Promega). The primer extension product was visualized using a phosphorimage analyser (BAS1500).

For quantitative real-time PCR (qRT-PCR), cDNA was synthesized by using the iScript™ cDNA synthesis kit (Bio-Rad) and real-time PCR amplification of the cDNA was performed by using the Chromo 4 real-time PCR detection system (Bio-Rad) with pairs of specific primers (Table III-1), as described previously (Kim *et al*., 2012). Relative expression levels of the specific transcripts were calculated by using the 16S rRNA expression level as the internal reference for normalization.

IV-2-8. Construction of a set of *plp-luxCDABE* transcriptional fusions

The primer PLP005 (Table III-1) including a SpeI restriction site followed by bases corresponding to the 5' end of the *plp* coding region, was used in conjunction with one of the following primers to amplify the DNA upstream of *plp*: PLP001 (for pKK1514), PLP002 (for pKK1515), PLP003 (for pKK1516), or PLP004 (for pKK1517) (Table III-1). The primers were designed to amplify the *plp* regulatory region extending up to -227, -157, -77, and +26 bp, respectively. A SacI restriction site was added to these primers to facilitate cloning of the PCR products. The DNA fragments were inserted into the SpeI-SacI-digested pBBR-lux (Lenz *et al.*, 2004) carrying promoterless *luxCDABE* genes, thereby creating five *plp-lux* reporter constructs. All constructions were confirmed by DNA sequencing. The *plp-lux* reporters were then transferred into the *V. vulnficus* strains by conjugation. The cellular luminescences of the cultures grown to A_{600} of 1.0 were measured with a luminometer (Tecan Infinite M200 reader) and expressed in arbitrary relative light units (RLU) as previously described (Jeong *et al*., 2003).

IV-2-9. Electrophoretic mobility shift assay (EMSA) and DNase I protection assay

The 461-bp *plp* upstream region extending from -345 to +116 was amplified by PCR using [γ-^{32}P]ATP labeled PLP06-F and unlabeled PLP06-R as the primers (Table III-1). The labeled 461-bp DNA (5 nM) probe was incubated with various concentrations of purified HlyU for 30 min at 30℃ in a 20-μl reaction mixture containing 1× binding buffer (Liu *et al*., 2009) and 0.1 μg of poly (dI-dC) (Sigma). The protein-DNA binding reactions with purified CRP were the same as those with HlyU, except that the CRP-binding buffer was used as a 1× binding buffer (Choi *et al.*, 2002). Electrophoretic analyses of the DNA-protein complexes were performed as described previously (Lim *et al*., 2014).

The same labeled 461-bp *plp* upstream region was used for DNase I protection assays. The binding of HlyU or CRP to the labeled DNA was performed as described above, and DNase I digestion of the DNA-protein complexes followed the procedures previously described (Kim *et al*., 2011). After precipitation with ethanol, the digested DNA products were resolved on a sequencing gel alongside of sequencing ladders of pKK1501 generated using PLP06-R (Table III-1) as the primer. The gels were visualized as described above for the transcript analysis.

IV-2-10. Data analyses

Averages and standard deviations (S.D.) were calculated from at least three independent experiments. Mouse mortality was evaluated using the log rank test program (http://bioinf.wehi.edu.au/software/russell/logrank/). All other data were analyzed by Student's t tests with the SAS program (SAS software; SAS Institute Inc.). Significance of differences between experimental groups was accepted at a *P*-value of < 0.05.

IV-3. Results

IV-3-1. Identification and sequence analysis of Plp

In the previous transcriptome analysis, the expression of a gene encoding a *V. anguillarum* Plp (*Va*Plp) homologue was highly induced by mucin and mucin-secreting host cells (Tables II-3 and II-4). The amino acid sequence deduced from the putative *V. vulnificus plp* nucleotide sequence revealed a protein the putative Plp (*Vv*Plp), composed of 417 amino acids with a theoretical mass of 47.19 kDa and pI of 5.59. *Vv*Plp exhibited a high level of identity (67% in amino acid sequences) with *Va*Plp (data not shown). The amino acid sequence analysis predicted that pre-*Vv*Plp protein contains an N-terminal signal peptide, suggesting that *Vv*Plp is a secreted protein (data not shown; http://www.ebi.ac.uk/clustalw) (Petersen *et al.*, 2011). All of this information indicated that *Vv*Plp is a secreted protein as does *Va*Plp (Li *et al.*, 2013).

IV-3-2. Plp is essential for cytotoxicity toward mucin secreting host cells *in vitro* and virulence in mice

In an effort to understand the role of Plp in *V. vulnificus* pathogenesis, an isogenic mutant KK131 (Table II-1) which lacked functional *plp* gene was constructed by allelic exchanges, and its virulence in tissue culture and in mice was evaluated. For this purpose, mucin-secreting HT29-MTX cells were infected with the wild type and *plp* mutant at different MOIs were incubated for 2 h, after which the LDH-releasing activities were determined (Fig. IV-1*A*). The *plp* mutant exhibited significantly less LDH-releasing activity when the MOIs were 1, 5, and 20. The level of LDH activity released from the HT-29 MTX cells infected with the *plp* mutant was almost fourfold less than that from the cells infected with the wild type at an MOI 5. Also, the LDH activities displayed from HT-29 MTX cells infected at an MOI of 10 were compared at different incubation times as shown in Fig. IV-1*B*. When incubated for 1 h, 2 h, and 3 h, the cells infected with the *plp* mutant exhibited lower LDH activities than those of the cells infected with the wild type, indicating that Plp is important for *V. vulnificus* to infect and injure host cells (Fig IV-1*A* and *B*). Complementation of the *plp* gene in KK131 with a functional *plp* gene (pKK1320) restored the LDH-releasing activity to levels comparable to the wild-type level (Fig. IV-1*A* and *B*). Therefore, the decreased cytotoxicity of KK131 resulted from inactivation of *plp* rather than reduced expression of any genes downstream of *plp*.

To examine the role of Plp in mouse mortality, mice were infected intragastrically with the wild-type and *plp* mutant strains, ant the numbers of dead mice were counted. As shown in Fig. IV-1*C*, the deaths of mice injected with the *plp* mutant were consistently and significantly delayed (P = 0.00633, log rank test) compared to those of mice injected with the parental wild type. The combined results suggested that Plp is essential for the virulence of *V. vulnificus* in mice and in tissue culture.

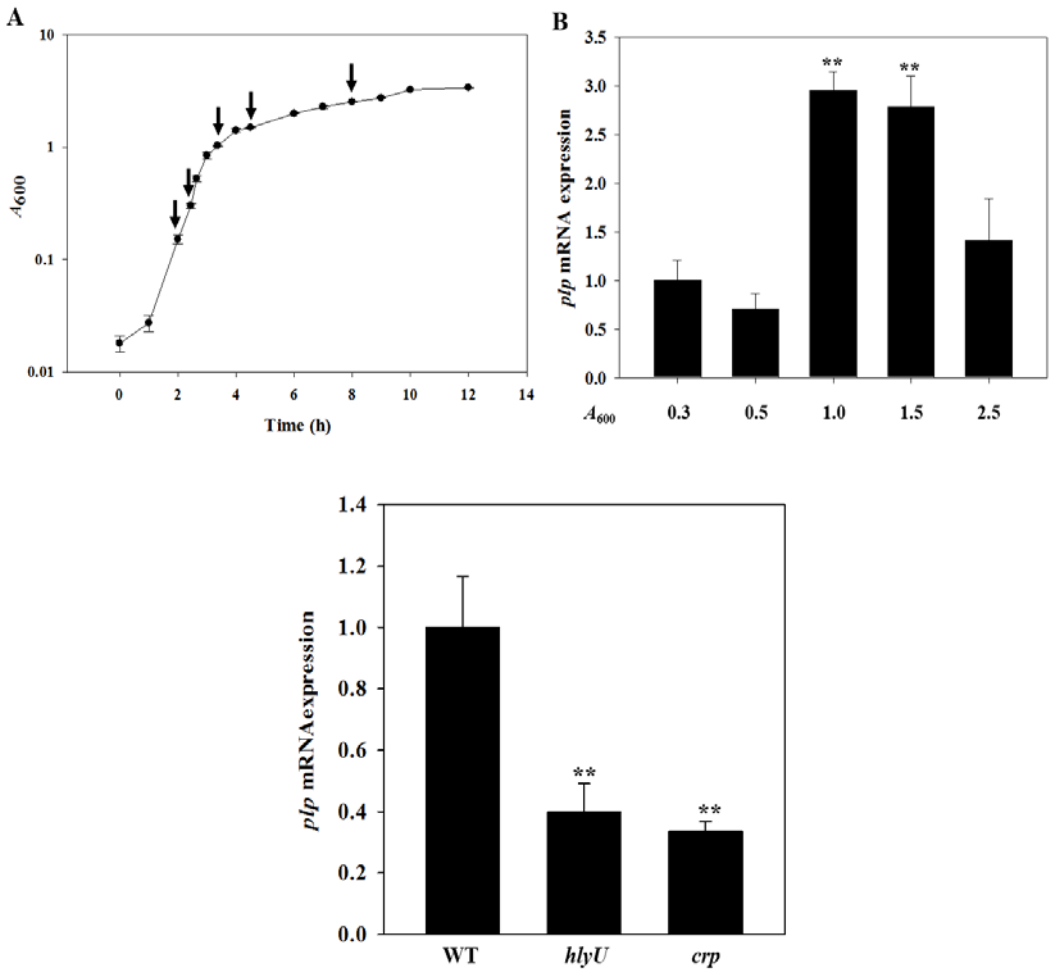
A
10
1
0.1
0.01
A_{600}
0
2
4
6
8
10
12
14
Time (h)
B
3.5
3.0
2.5
2.0
1.5
1.0
0.5
0.0
plp mRNA expression
**
**
A_{600}
0.3
0.5
1.0
1.5
2.5
1.4
1.2
1.0
0.8
0.6
0.4
0.2
0.0
plp mRNAexpression
**
**
WT
hlyU
crp

Figure IV-1. Cytotoxicity and mouse mortality of *V. vulnificus*. *A* and *B*, HT29-MTX cells were infected with wild-type, the *plp* mutant, or the complemented strain at various MOIs for 2 h (*A*) or at an MOI of 10 for various incubation times (*B*). The cytotoxicity was determined by an LDH release assay and expressed using the total LDH released from the cells completely lysed by 2% Triton X-100 as 100%. Error bars represent the S.D. ******, $P < 0.005$ relative to groups infected with the *V. vulnificus* wild type at each MOI or incubation time. *C*, seven-week-old specific pathogen-free female ICR mice, injected intraperitoneally with 30 μg of iron-dextran for each gram of body weight, were intragastrically infected with the wild type (WT) or the *plp* mutant (*plp*) (Table II-1) at doses of 10^8 CFU as indicated. WT (pJH0311), wild type; *plp* (pJH0311), *plp* mutant; *plp* (pKK1320), complemented strain.

IV-3-3. Plp is a phospholipase A_2 and secreted via the T2SS.

Recent study demonstrated that *Va*Plp has PLA_2 activity against phosphatidylcholine (Li *et al*., 2013). Therefore, we hypothesized that *Vv*Plp also have PLA_2 activity. To examine this hypothesis, the enzyme activity of rPlp was determined by a colorimetric phospholipase A_2 assay (Fig. IV-2*A*). To determine the specific activity of the rPlp, a standard curve was prepared from various units of honey bee venom PLA_2 (1 unit = 1 μg of protein that cleaves 1 μmole of BODIPY-PC per minute) by measuring the fluorescence intensities. The standard curve was linear between 0.01 U/ml and 0.5 U/ml of honey bee venom PLA_2 and correlation coefficient was 0.9997 (data not shown). Similarly, the enzymatic activity of rPlp also positively correlated to its concentration from 0.02 μg/ml to 5 μg/ml (Fig. IV-2*A*). A dilution curve for the fluorescence intensities of rPlp was linear and correlation coefficient were 0.9981 (data not shown). Therefore, the specific activity of rPlp was measured as approximately 247 U/mg. In addition, rPlp did not show PLA_1, PLC, and PLD activity (data not shown). Taken together, these result indicated that Plp is PLA_2 essential for the pathogenesis of *V. vulnificus*.

V. vulnificus has been shown to possess T2SS responsible for the extracellular secretion of at least three degradative enzymes (Paranjpye *et al*., 1998). In order to determine whether the T2SS is involved in the secretion of *plp*, a mutant that lacks

PilD, a compnent of T2SS, was constructed and the Plp secretion of the mutant was compared with that of the parental wild type (Fig. IV-2*B*). A western blot analysis revealed that the Plp protein was not detected in the culture supernatant of the *pilD* mutant, indicating that Plp of *V. vulnificus* is also secreted via T2SS. The lack of Plp secretion in the *pilD* mutant was restored by the introduction of pMS0908 (Table II-1, Lim *et al*., 2011) carrying a recombinant *pilD* (Fig. IV-2*B*). Taken toghter, these results indicated that Plp of *V. vulnificus* is secreted a phospholipase A_2 via T2SS.

A

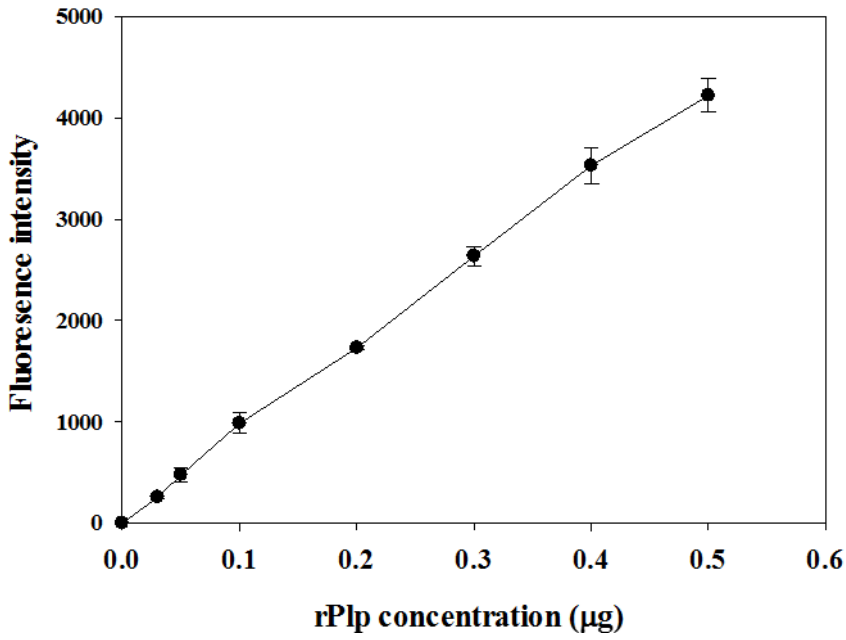
5000
4000
3000
2000
1000
0
Fluoresence intensity
0.0
0.1
0.2
0.3
0.4
0.5
0.6
rPlp concentration (μg)

B

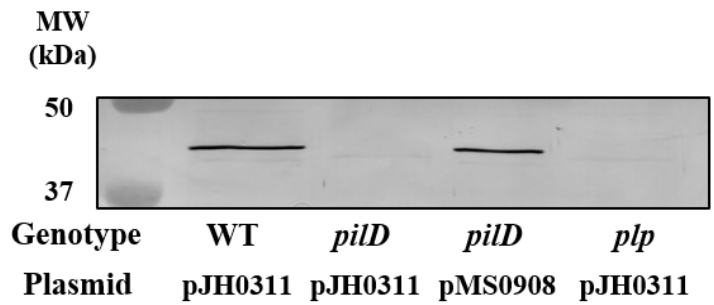
MW
(kDa)
50
37
Genotype
WT
pilD
pilD
plp
Plasmid
pJH0311
pJH0311
pMS0908
pJH0311

Figure IV-2. Enzyme activity and secretion of Plp mediated by the T2SS of *V. vulnifcus*. *A,* BIODIPY-labeled phosphatidylcholine (BIODIPY-PC) was incubated with various amount of rPlp for 30 min and the fluorescence emission was measured for excitation in the 480 nm and fluorescence emission at 515 nm. *B,* The Plp proteins in the supernatants of the *V. vulnificus* strains grown to A_{600} of 1.0 were examined by Western blot analyses using the rabbit anti-*V. vulnificus* Plp. The positions of protein size markers (Bio-Rad) are shown on the left of the gel. WT (pJH0311), wild type; *pilD* (pJH0311), *pilD* mutant; *pilD* (pMS0908), complement strain; *plp* (pJH0311), *plp* mutant.

IV-3-4. Expression of *plp* is growth-phase dependent and regulated by HlyU and CRP

To examine whether the production of *Vv*Plp is influenced by growth phase, levels of the *plp* mRNA of the wild type culture were analyzed at various growth stages (Fig. IV-3*A* and *B*). The *plp* transcript reached a maximum in the late exponential-phase and then decreased in the stationary-phase, indicating that expression of *plp* is growth-phase dependent. To extend our understanding on the regulation of *plp*, the levels of the *plp* transcript in the wild type and mutants which lack transcription factors HlyU and CRP (cAMP receptor protein) (Table II-1) were compared. The level of the *plp* transcript decreased in the *hlyU* mutant and *crp* mutant (Fig. IV-3*C*). The result indicated that both HlyU and CRP act as positive regulators for the *plp* expression.

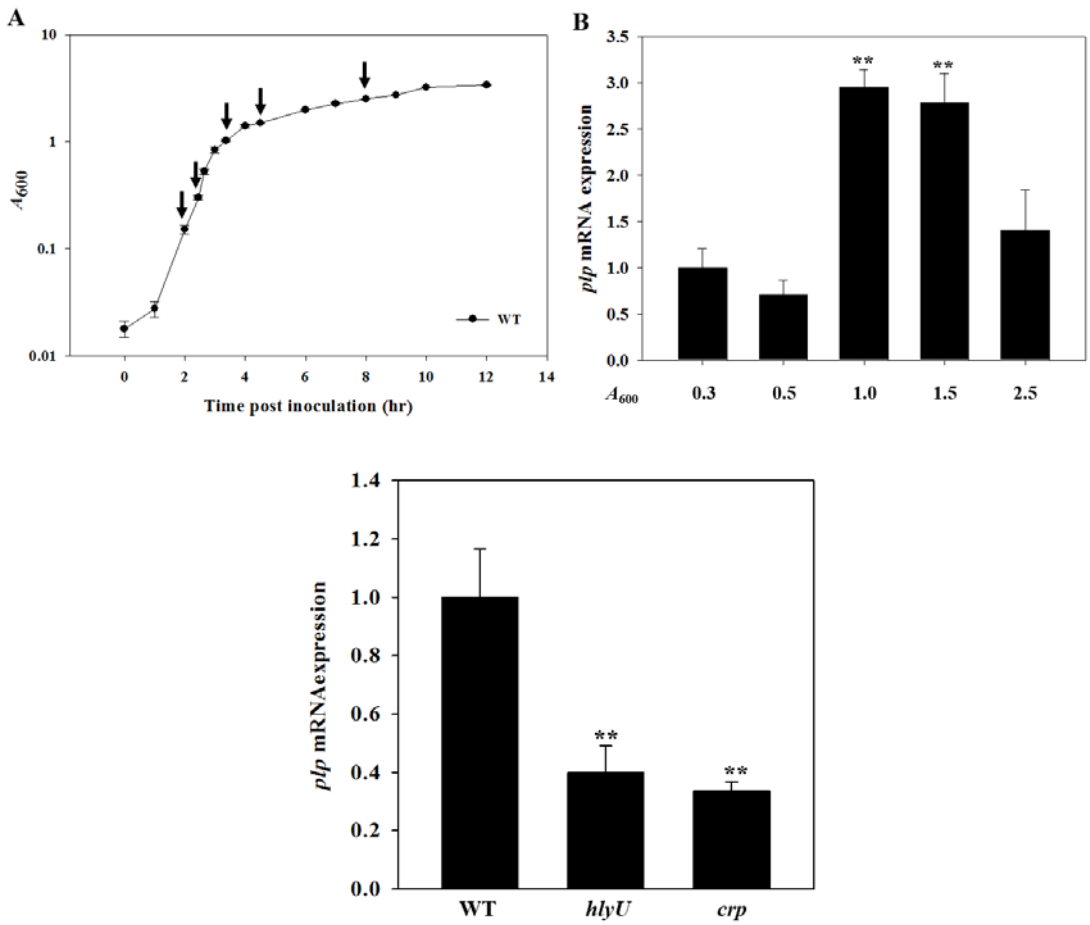
A
10
1
0.1
0.01
A_{600}
WT
0
2
4
6
8
10
12
14
Time post inoculation (hr)
B
3.5
3.0
2.5
2.0
1.5
1.0
0.5
0.0
plp mRNA expression
**
**
A_{600}
0.3
0.5
1.0
1.5
2.5
1.4
1.2
1.0
0.8
0.6
0.4
0.2
0.0
plp mRNAexpression
**
**
WT
hlyU
crp

Figure IV-3 Effect of growth phases and global regulatory proteins on the *plp* expression. *A*, growth of the wild type culture in LBS was monitored spectrophotometrically at 600 nm (A_{600}) and total RNAs were isolated from the cells harvested at different growth phases (from left, at A_{600} of 0.3, 0.5, 1.0, 1.5, and 2.5) as indicated by arrows. *B*, the *plp* mRNA levels were determined by qRT-PCR analyses, and the *plp* mRNA level in the cells grown to an A_{600} of 0.3 was set as 1. Error bars represent the SD. **, $P < 0.005$ relative to the cells grown to A_{600} of 0.3. C, Samples were harvested from the cultures of the wild type and isogenic mutants grown aerobically to an A_{600} of 1.0 and analyzed to determine the *plp* mRNA levels. The *plp* mRNA levels were determined by qRT-PCR analyses, and the *plp* mRNA level in the wild type was set as 1. Error bars represent the S.D. **, $P < 0.005$ relative to the wild type. WT, wild type; *hlyU*, *hlyU* mutant; *crp*, *crp* mutant.

IV-3-5. HlyU and CRP coactivates *plp* additively

To further examine their roles of HlyU and CRP in the *plp* expression, the *hlyU crp* double mutant KK151 was constructed, and *plp* expression was determined. Inactivation of both *hlyU* and *crp* resulted in significant reduction of the *plp* expression, and the residual *plp* mRNA level in the *hlyU crp* double mutant corresponded to only one quarter of that in the wild type (Fig. IV-4). The presence of either HlyU (*crp* mutant) or CRP (*hlyU* mutant) alone increased the *plp* expression, but their *plp* transcript levels were lower than those obtained by HlyU and CRP together (wild type), indicating that HlyU and CRP coactivate the *plp* expression additively (Fig. IV-4). To determine whether an increased amount of HlyU would compensate for a lack of CRP in the activation of *plp*, the *hlyU* expression plasmid pZW1510 was introduced into the *hlyU crp* double mutant KK151. When *hlyU* was induced, the cellular level of HlyU in KK151 (pZW1510) was higher than that in the *crp* single mutant (Fig. IV-4). However, the levels of *plp* transcript in KK151 (pZW1510) were only about 65% of those in the wild type (Fig. IV-4), indicating that HlyU, even when overproduced, is unable to activate *plp* to the wild-type level in the absence of CRP. Similarly, overproduced CRP was unable to compensate completely the lack of HlyU in the activation of *plp* (Fig. IV-4). The results confirmed that both HlyU and CRP are required simultaneously to coactivate *plp* to the wild-type level.

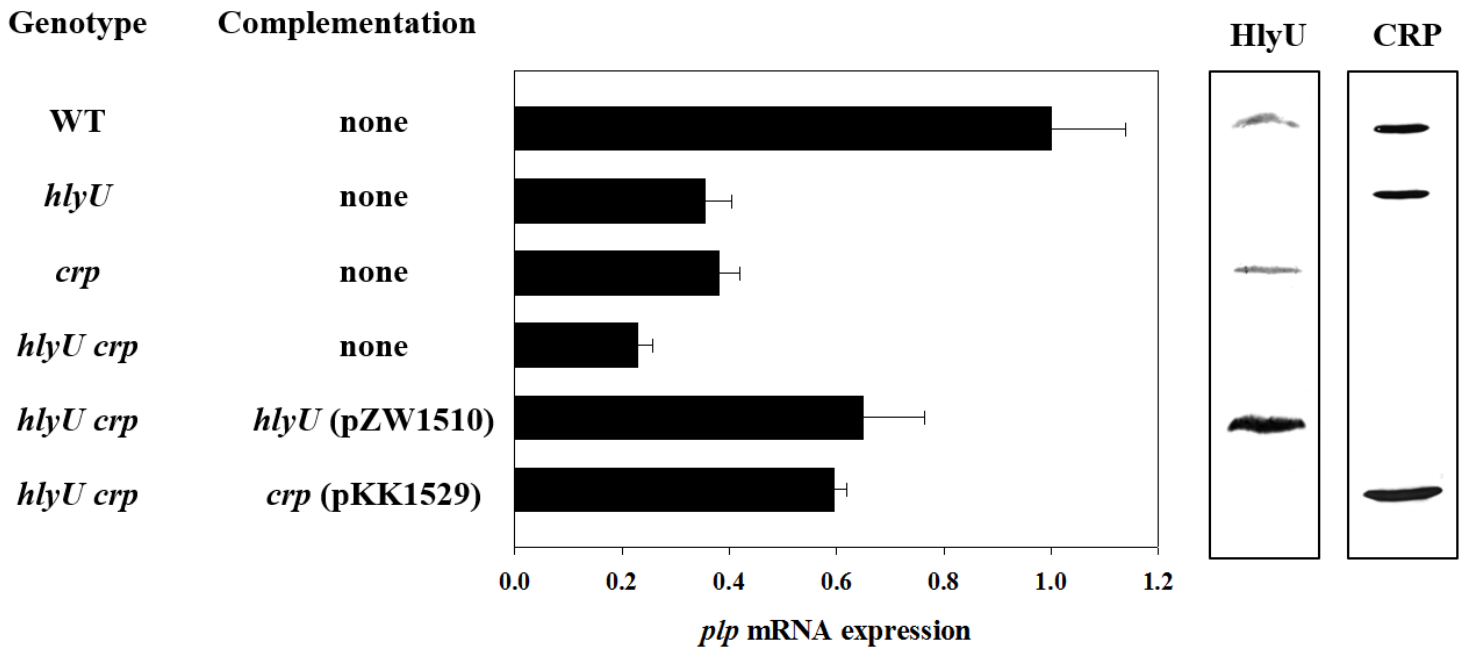
Genotype
Complementation
WT
none
hlyU
none
crp
none
hlyU crp
none
hlyU crp
hlyU (pZW1510)
hlyU crp
crp (pKK1529)
0.0
0.2
0.4
0.6
0.8
1.0
1.2
plp mRNA expression
HlyU
CRP

Figure IV-4. HlyU and CRP coactivate *plp* additively. Samples were harvested from the cultures of the *V. vulnificus* strains grown aerobically to an A_{600} of 1.0 and analyzed to determine the *plp* mRNA levels and HlyU and CRP protein levels. The *plp* mRNA levels were determined by qRT-PCR analyses, and the *plp* mRNA level in the wild type was set as 1. Error bars represent the S.D. The cellular levels of HlyU and CRP were determined by Western blot analyses using the rabbit anti-*V. vulnificus* HlyU and anti-*V. vulnificus* CRP sera, respectively. WT, wild type; *hlyU*, *hlyU* mutant; *crp*, *crp* mutant; *hlyU crp*, *hlyU crp* double mutant.

IV-3-6. HlyU and CRP function cooperatively rather than sequentially to regulate *plp*

Different mechanisms are possible for this coactivation of *plp* by HlyU and CRP. For example, multiple activators function sequentially in a regulatory cascade, where one activator influences the accumulation of another regulator(s), which in turn is directly responsible for the activation of *plp*. To test this possibility, the cellular levels of HlyU and CRP were determined in the same amount of total protein isolated from the wild type and its isogenic mutants (Fig. IV-5).

Western blot analysis revealed that neither activator affected the cellular level of the other, *i.e.* compared with the wild type, the *hlyU* mutant strain did not exhibit any significant changes in the cellular level of CRP and *vice versa* (Fig. IV-5). From this results, it is unlikely that HlyU (or CRP) indirectly activates *plp* by increasing the cellular level of CRP (or HlyU), which activates directly *plp*. Consequently, it appears that HlyU and CRP function cooperatively to regulate *plp* rather than sequentially in a regulatory cascade.

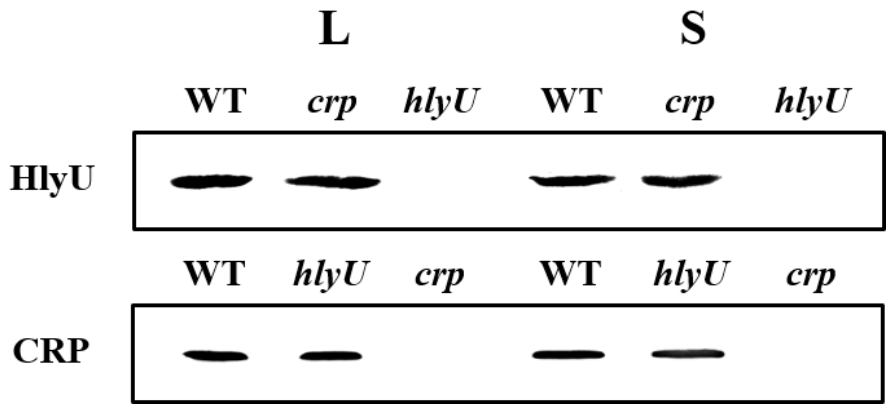

Figure IV-5. Cellular levels of HlyU and CRP are unaffected by one another. The wild type and isogenic mutants were grown aerobically to A_{600} of 0.5 (log phase, L) and 2.5 (stationary phase, S). The cells were then examined for the presence of HlyU and CRP proteins by Western blot analyses using the rabbit anti-*V. vulniicus* HlyU and anti-*V. vulnificus* CRP, respectively. WT, wild type; *hlyU*, *hlyU* mutant; *crp*, *crp* mutant.

IV-3-7. Mapping the regulatory region of *plp*

In order to map the promoter of *plp*, a transcription start site of *plp* was determined by a primer extension analysis. A single reverse transcript was produced from primer extension of RNA isolated from the wild type grown aerobically to an A_{600} of 1.0 (Fig. IV-6*A*). Several attempts to identify any other transcription start sites using different sets of primers were not successful (data not shown). The 5' end of the *plp* transcript was located 65-bp upstream of the translational initiation codon of *plp* and subsequently designated +1 (Fig. IV-6*B*). The putative promoter constituting this transcription start site was named P_{plp} and the sequences for -10 and -35 regions of P_{plp} were assigned on the basis of similarity to consensus sequences of the *E. coli* σ^{70} promoter (Fig. IV-6*B*).

The pKK reporters carrying the upstream regulatory region of P_{plp} which was deleted up to different 5'-ends and fused transcriptionally to *luxCDABE* were constructed (Fig. IV-7*A*). The reporters were transferred into the wild type and isogenic mutants and culture luminescence was used to quantify the P_{plp} activity (Fig. IV-7*B*). The luminescence produced by pKK1514 carrying P_{plp} deleted up to -227 was ~ 1.1×10^4 RLU in the wild type but significantly reduced in the *hlyU* and *crp* mutants, supporting our previous observation that HlyU and CRP activate P_{plp}. Deletion up to -157 significantly decreased the P_{plp} activity as determined based on the reduced

luminescence of the strains containing pKK1515. Interestingly, the RLU of pKK1515 in the *hlyU* mutant was indistinguishable from that in the wild type, indicating the absence of the region(s) necessary for HlyU to activate P_{plp} in pKK1515. Similarly, the comparable RLU produced by pKK1516 in the *crp* mutant and wild type indicated that the region upstream from -77 is probably required for CRP activation of P_{plp}. The undetectable luminescence produced by pKK1517 indicates that deletion up to +22 completely impaired the P_{plp} activity. Taken together, the results suggested that the regulatory region extending from -227 to -77 harbors consecutively the *cis*-elements necessary for HlyU and CRP regulation of P_{plp}.

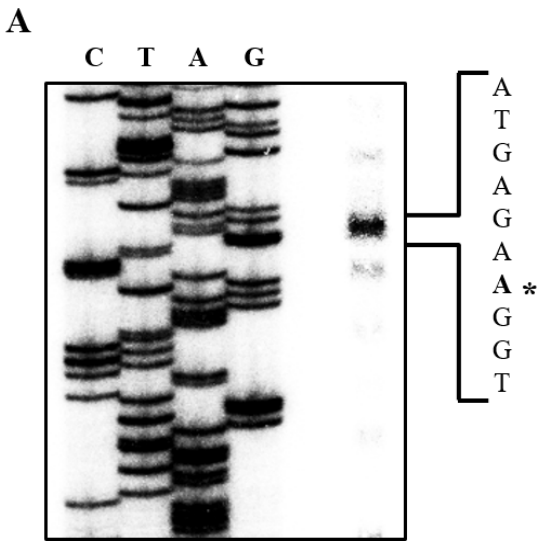
A
C T A G
A
T
G
A
G
A
A *
G
G
T

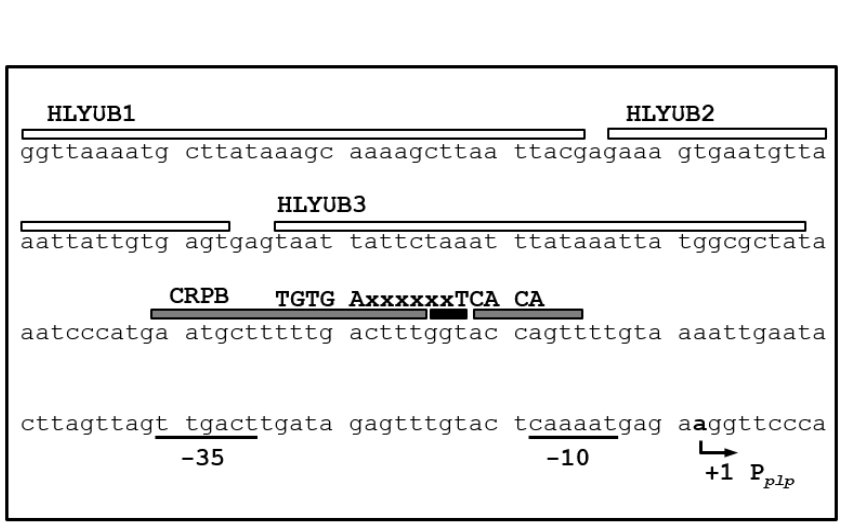
B
HLYUB1
HLYUB2
ggttaaaatg cttataaagc aaaagcttaa ttacgagaaa gtgaatgtta
HLYUB3
aattattgtg agtgagtaat tattctaaat ttataaatta tggcgctata
CRPB
TGTG AxxxxxxTCA CA
aatcccatga atgctttttg actttggtac cagttttgta aaattgaata
cttagttagt tgacttgata gagtttgtac tcaaaatgag aaggttccca
-35
-10
+1 P plp

Figure IV-6. Transcription start site and sequences of the *plp* regulatory region.

A, Transcription start site of *plp* was determined by primer extension of the RNA isolated from the wild type grown aerobically to an A_{600} of 1.0. *Lanes C, T, A,* and *G* represent the nucleotide sequencing ladders of pKK1501. The *asterisk* indicates the transcription start site of *plp*. *B*, The transcription start site of *plp* is indicated by a *bent arrow*, and the positions of the putative -10 and -35 regions are *underlined*. The sequences for binding of HlyU (HLYUB1, HLYUB2, and HLYUB3, *white boxes*) and CRP (CRPB, *shaded boxes*) determined later in this study (Fig. IV-9). The nucleotides showing enhanced cleavage are indicated by *black boxes.* The consensus sequences for binding of CRP are respectively indicated *above* the *V. vulnificus* DNA sequence. *x*, any nucleotides.

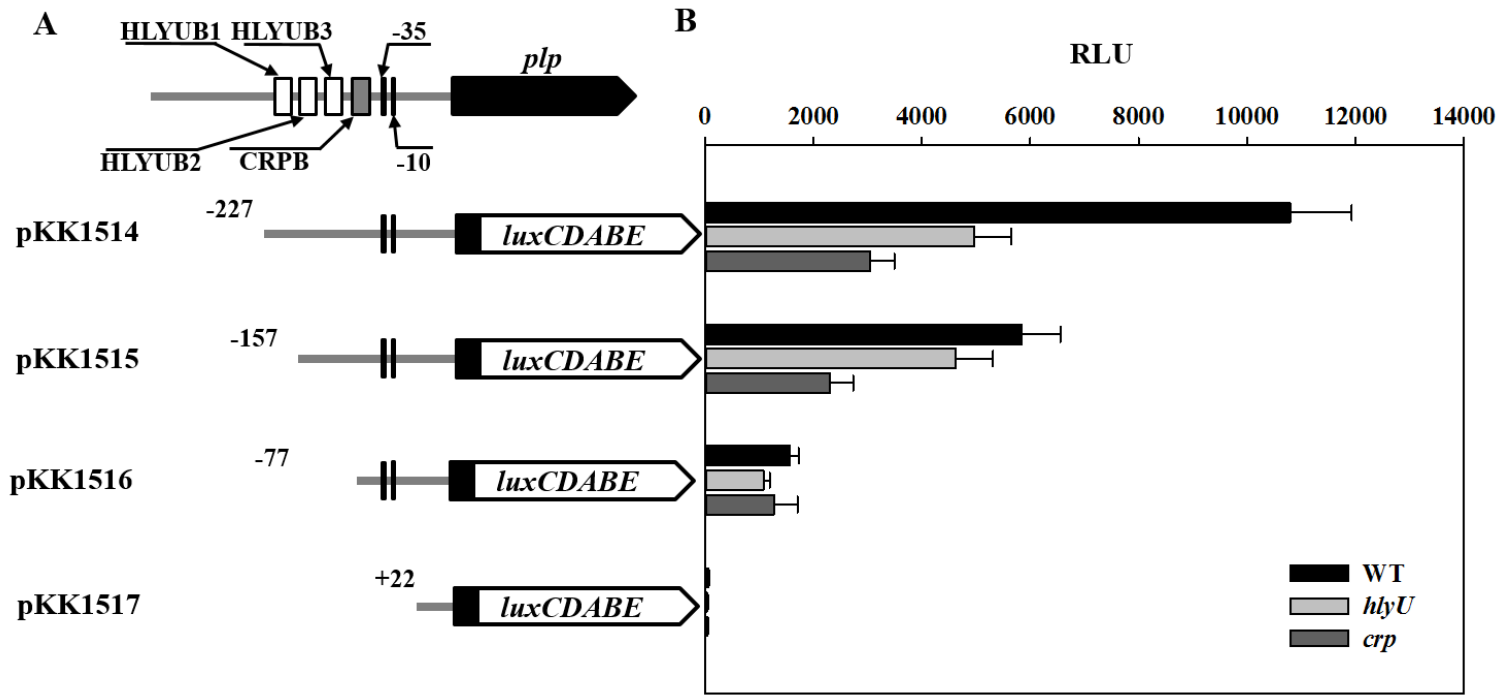
A
HLYUB1
HLYUB3
-35
plp
HLYUB2
CRPB
-10
B
RLU
0
2000
4000
6000
8000
10000
12000
14000
pKK1514
-227
luxCDABE
pKK1515
-157
luxCDABE
pKK1516
-77
luxCDABE
pKK1517
+22
luxCDABE
WT
hlyU
crp

Figure IV-7. Deletion analysis of the P_{plp} regulatory region. *A*, Construction of *plp-lux* fusion pKK reporters. PCR fragments carrying the *plp* regulatory region with 5'-end deletions were subcloned into pBBR-lux (Lenz *et al.*, 2004) to create each pKK reporter. *Solid lines*, the upstream region of *plp*; *black blocks*, the *plp* coding region; *open blocks*, the *luxCDABE*. The wild type *plp* regulatory region is shown on top with the proposed -10 and -35 regions, and the binding sites for HlyU (HLYUB1, HLYUB2, and HLYUB3, *white boxes*) and CRP (CRPB, *a shaded box*), respectively. *B*, Cellular luminescence determined from the wild type (*black bars*), *hlyU* mutant (*gray bars*), and *crp* mutant (*dark gray bars*) containing each pKK reporter as indicated. Cultures grown aerobically to an A_{600} of 1.0 were used to measure the cellular luminescence. Error bars represent the S.D. *RLU*, Relative luminescence units; WT, wild type; *hlyU*, *hlyU* mutant; *crp*, *crp* mutant

IV-3-8. HlyU and CRP regulate *plp* by directly binding to P_{plp}

There are still several possible ways for HlyU and CRP to affect the P_{plp} activity. One is by binding directly to the P_{plp} regulatory region to regulate the promoter, whereas another is by modulating the cellular level of unidentified *trans*-acting factor(s), which in turn binds directly to the P_{plp} regulatory region. To distinguish these two possibilities, the 461-bp labeled DNA probe encompassing the P_{plp} regulatory region (from -345 to +116) was incubated with increasing amount of HlyU and then subjected to electrophoresis. The addition of HlyU resulted in two retarded bands in a concentration-dependent manner, indicating that at least two binding sites for HlyU are present in the P_{plp} regulatory region (Fig. IV-8*A*). The binding of HlyU was also specific, because assays were performed in the presence of 0.1 μg of poly (dI-dC) as a nonspecific competitor. In a second EMSA, the same but unlabeled 461-bp DNA fragment was used as a self-competitor to confirm the specific binding of HlyU. The unlabeled 461-bp DNA competed for the binding of HlyU in a dose-dependent manner (Fig. IV-8*A*), confirming that HlyU binds specifically to the P_{plp} regulatory region. In similar DNA-binding assays, CRP also displayed a specific binding to the P_{plp} regulatory region (Fig. IV-8*B*). These results suggested that HlyU and CRP regulate *plp* by specifically binding to P_{plp}.

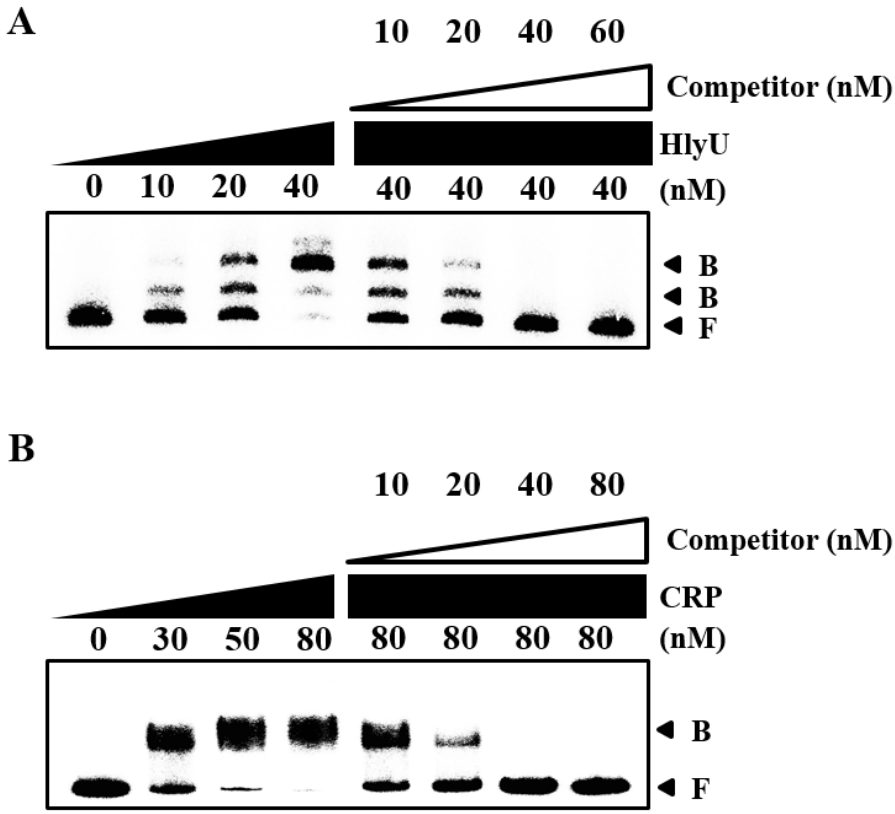
A
10 20 40 60
Competitor (nM)
HlyU
0 10 20 40 40 40 40 40
(nM)
B
B
F
B
10 20 40 80
Competitor (nM)
CRP
0 30 50 80 80 80 80 80
(nM)
B
F

Figure IV-8. Specific bindings of HlyU and CRP to P_{plp}. A 461-bp DNA fragment of the *plp* regulatory region was radioactively labeled and then used as a probe DNA. The radiolabeled probe DNA (5 nM) was mixed with increasing amounts HlyU (*A*) and CRP (*B*) as indicated. For competition analysis, the same but unlabeled 461-bp DNA fragment was used as a self-competitor DNA. Various amounts of the self-competitor DNA were added to a reaction mixture containing the 5 nM labeled DNA prior to the addition of 40 nM HlyU (*A*) and 80 nM CRP (*B*). *B*, bound DNA; *F*, free DNA.

IV-3-9. Identification of binding sites for HlyU and CRP

To determine the precise location of the HlyU and CRP binding sites in the P_{plp} regulatory region, DNase I protection assays were performed using the same 461-bp DNA probe used for DNA-binding assays. When the sequences for the binding of HlyU to the DNA probe were mapped with HlyU up to 50 nM, the HlyU footprint extended from -191 to -157 (HLYUB1) relative to the transcription start site of P_{plp} (Fig. IV-9*A*). When increasing the HlyU, another two regions extending from -151 to -128 (HLYUB2) and -126 to -93 (HLYUB3) were clearly protected from DNase I digestion (Fig. IV-9*A*). This sequential protection with increasing HlyU was consistent with the previous observation that at least two binding sites with different affinities for HlyU are present in the P_{plp} (Fig IV-8*A*). The AT-rich sequences of HLYUBs have an imperfect palindromic patterns (Fig. IV-6*B*), suggesting that HlyU could bind to these regions as a dimer (Liu *et al*., 2009; Mukherjee *et al*., 2015). The CRP footprint extended from -82 to -57 (CRPB), centered at -69.5 (Fig. IV-9*B*) and the sequences of CRPB scored 81% identity to a consensus sequence for CRP binding (Fig. IV-6*B*) (Cameron and Redfield, 2007). These positioning of HLYUB and CRPB suggested that both HlyU and CRP act as class III activators interacting with C-terminal domain of RNA polymerase α subunits (αCTD) (Browning and Busby, 2004). Several nucleotides also showed enhanced cleavages, indicating that binding of the regulators altered the configuration of the DNA of P_{plp} (Fig. IV-9).

These results confirmed that HlyU and CRP regulate *plp* by binding to the specific sequences of P_{plp}, respectively.

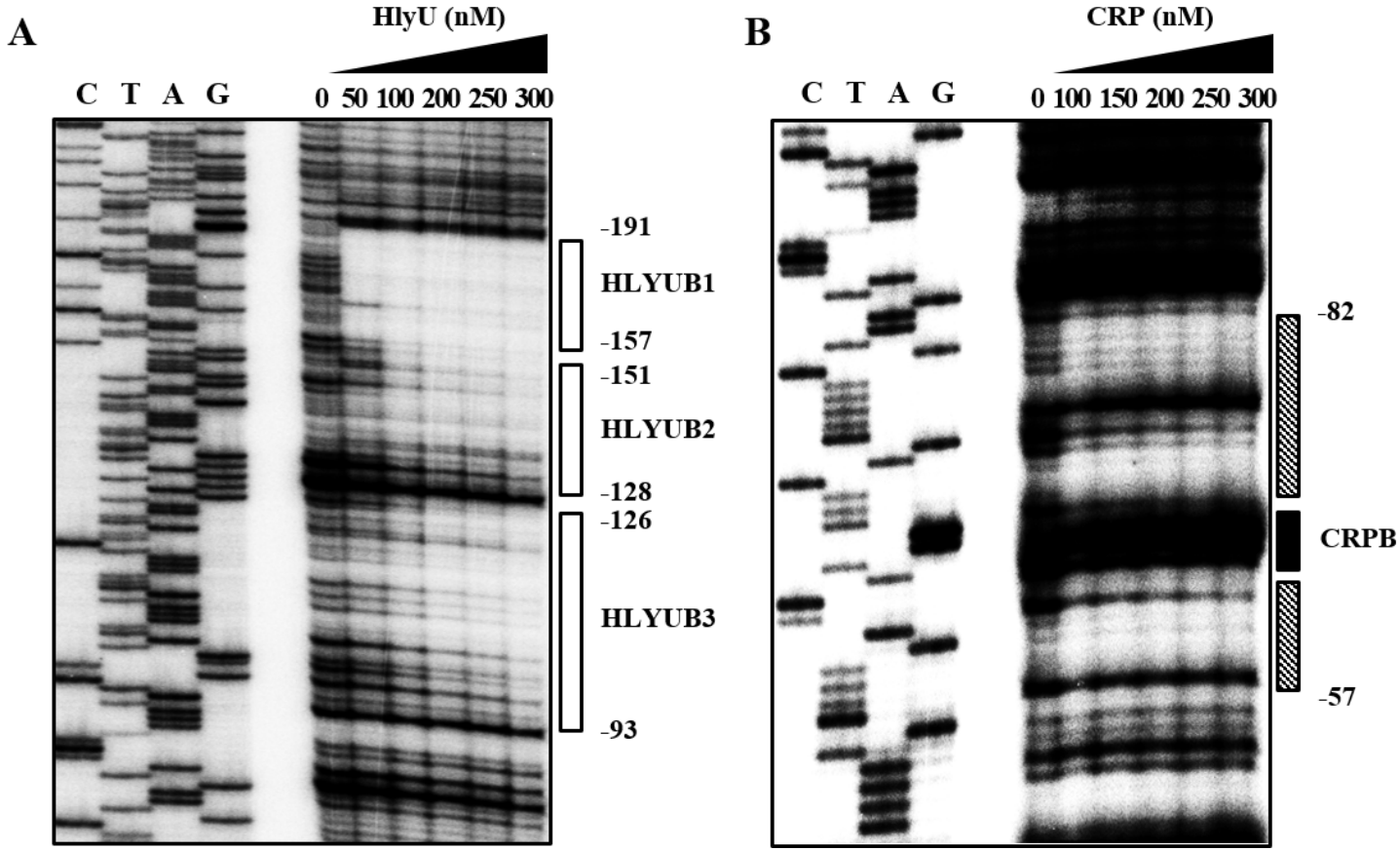
A
HlyU (nM)
C T A G
0 50 100 200 250 300
-191
HLYUB1
-157
-151
HLYUB2
-128
-126
HLYUB3
-93
B
CRP (nM)
C T A G
0 100 150 200 250 300
-82
CRPB
-57

Figure IV-9. Sequences for binding of HlyU and CRP to P_{plp}. A 461-bp DNA fragment of the *plp* regulatory region was radioactively labeled and then used as a probe DNA. The radiolabeled probe DNA (25 nM) was incubated with increasing amount of HlyU (*A*) and CRP (*B*) as indicated. The regions protected by HlyU and CRP are indicated by *white boxes* and *shaded boxes*, respectively. The nucleotides showing enhanced cleavage are indicated by *black boxes*. *Lanes C, T, A,* and *G* represent the nucleotide sequencing ladders of pKK1501.

IV-4. Discussion

There are several lines of evidence that many secreted proteins contribute to the pathogenesis of *V. vulnificus* (Lee *et al*., 2010; Jeong and Satchell, 2012; Kim *et al*., 2015; Jang *et al*., 2016). Consistent with this, the present study identified that Plp is secreted PLA_2 through T2SS and required for virulence in mice (Figs. IV-1 and IV-2). These observations suggested that *V. vulnificus* secretes multiple proteins to facilitate infection as observed in other pathogens (Chang *et al*., 2014). Additionally, recent studies showed that these proteins also play an essential role in the regulation of host gene expressions and immune reactions (Lee *et al*., 2011; Lee *et al*., 2015a; Lee *et al*., 2015b). Thus, it is reasonable hypothesis that Plp and its cleavage products might participate in multiple signaling pathways and precursor to potent mediator of the host-inflammatory response. It is noteworthy that lysophosphatidylcholine, the product from phosphatidylcholine hydrolysis by PLA_2, mediates apoptosis and inflammatory response by increasing expression of chemokines such as interluekon-8 (IL-8) and activating small GTPase RhoA (Masamune *et al*., 2001; Takahashi *et al*., 2002; Huang *et al*., 2005).

Nevertheless, little is known about the regulatory mechanisms adopted by *V. vulnificus* to modulate the expression of the phospholipases. No information on the

expression pattern or level of the phospholipases during infection of the pathogen has been reported in previous studies. As a result of this study, the expression of *plp* is growth-phase dependent and reached the maximum level in the late exponential-phase cells (Fig. IV-3). HlyU, a transcriptional regulator of the *V. vulnificus* (Liu *et al*., 2009), also activates *plp* at the transcription level (Figs. IV-3 and IV-4). HlyU is first identified in *Vibrio cholerae* as an activator of *hlyA* (Williams *et al*., 1993) and its homologue of *V. vulnificus* activates *rtxHCA* operon and *vvhA* by direct binding to their promoter regions, respectively (Liu *et al*., 2009; Shao *et al*., 2011). Since RtxA and VvhA play an essential role in the pathogenesis of *V. vulnificus* (Jeong and Satchell, 2012), a mutant with disruption of the *hlyU* gene had attenuated virulence in a mouse model (Liu *et al*., 2007). Consistent with this, Plp is important for the virulence of *V. vulnificus* in mice and tissue culture (Fig. IV-1). Accordingly, HlyU appears to be a master regulator of virulence factors in *V. vulnficus*. Therefore, the coordinate activation of *rtxHCA*, *vvhA*, and *plp* by a common regulator, HlyU, which could be crucial for the overall success of the pathogen during pathogenesis.

In addition to this, CRP and HlyU could have considerable benefits in the regulation of *plp* (Figs. IV-3 and IV-4). First, CRP, which is a central regulator of energy (catabolic) metabolism (Green *et al*., 2014), may recognize host environments by sensing the starvation of specific nutrients imposed by the host cells

and endogenous bacterial flora. In addition, CRP regulation has been observed in the synthesis of the virulence factors of several pathogenic bacteria including *V. vulnificus* (Petersen and Young, 2002; Oh *et al*., 2009; Jang *et al*., 2016). Therefore, CRP could elaborately control the expression of *plp* according to the metabolic changes during infection. Second, previous studies indicated that HlyU is identified as one of genes expressed preferentially *in vivo* condition (Kim *et al*., 2003). Although the exact mechanism to induce the expression of HlyU must be further elucidated, HlyU seems to be induced by sensing host-specific signal such as reactive oxygen species (ROS). Consistent with this hypothesis, the structural position of two cysteine residues of *V. vulnificus* HlyU is similar with that of *V. cholerae* HlyU (Nishi *et al*., 2010; Mukherjee *et al*., 2014), implying that the existence of a redox switch in transcription regulation (Mukherjee *et al*., 2015). Accordingly, HlyU, in conjunction with CRP, might contribute to produce Plp at the right place and time in a tightly regulated fashion.

In summary, *plp* encoding a PLA_2 essential for pathogenesis of *V. vulnificus* was characterized in this study. Secretion of Plp is mediated by T2SS. The *plp* expression was in a growth-phase dependent manner and regulated positively by HlyU and CRP. The regulatory proteins regulate the *plp* expression cooperatively rather than sequentially, and exerted their effects by directly binding to the regulatory region of

P_{plp}. Three distinct HlyU binding sequences centered at -174, -139.5, and -109.5 and a CRP binding sequence centered at -69.5, were identified respectively. It is still difficult to define the implications of the collaboration between HlyU and CRP in terms of pathogenesis of *V. vulnificus*. However, it is likely that the collaboration allows more precise tuning of the *plp* expression by integrating the signals presumably encountered in the host intestine, such as starvation of specific nutrients and thereby enhances the overall success of *V. vulnificus* during pathogenesis.

Chapter V.

Conclusion

Mucin glycoprotein is a major component of mucus layer that is the major site of entry for most pathogens and serves as the initiation surfaces for host-microbe interactions. *Vibrio vulnificus*, a model human enteric pathogen, is a causative agent of fatal septicemia and utilizes the mucin to survive and cause disease in host. Total RNA was isolated from the *V. vulnificus* cells grown with mucin-containing media or exposed to the mucin secreting HT-29 MTX cells and analyzed using RNA-seqeuncing technology. From the analysis, 337 genes whose expression was discriminatively regulated by mucin as a sole carbon source. In addition, 650 genes with altered transcript level in the bacteria exposed to the HT29-MTX cells compared to BME were identified. Interestingly, several virulence related genes encoding metalloprotease, *N*-acetylglucosamine binding protein, cytolysin, and phospholipase were induced by the mucin and mucin-secreting host cells.

By further characterizing the genes up-regulated by mucin, an open reading frame, *gbpA*, of *V. vulnificus* was identified and characterized in this study. Compared to the wild type, the *gbpA* mutant was impaired in binding to mucin-agar and the HT29-MTX cells, and the impaired mucin binding was restored by the purified GbpA provided exogenously. The *gbpA* mutant had attenuated virulence and ability of intestinal colonization in a mouse model, indicating that GbpA is a mucin-binding protein and essential for pathogenesis of *V. vulnificus*. The *gbpA* transcription was

growth-phase dependent, reaching a maximum during the exponential phase. The Fe-S cluster regulator (IscR) and the cyclic AMP receptor protein (CRP) coactivated whereas SmcR, a LuxR homologue, repressed *gbpA*. The cellular levels of IscR, CRP, and SmcR were not significantly affected by one another, indicating that the regulator proteins function cooperatively to regulate *gbpA* rather than sequentially in a regulatory cascade. The regulatory proteins directly bind to the upstream of the *gbpA* promoter P_{gbpA}. The deletion analyses of P_{gbpA} and DNase I protection assays demonstrated that IscR binds to two specific sequences centered at -164.5 and -106, and CRP and SmcR bind specifically to the sequences centered at -68 and -45, respectively. Furthermore, *gbpA* was induced by exposure to H_2O_2, and the induction appeared to be mediated by elevated intracellular levels of IscR.

Identification of regulatory characteristics of *plp* encoding a putative phospholipase was investigated in this study. Construction of the *plp* mutant and evaluation of its phenotypes provided evidences that Plp is a secreted phospholipase A_2 via T2SS and plays a crucial role in the pathogenesis of the organism. The *plp* expression was in a growth-phase dependent manner and regulated positively by transcriptional activator HlyU and CRP. Genetic and biochemical studies demonstrated that the two regulatory proteins regulate *plp* cooperatively rather than sequentially and exerted their effects by directly binding to the *plp* promoter P_{plp}. DNase I protection assays,

together with the deletion analyses of P_{gbpA}, identified the three distinct HlyU binding sequences centered at -174, -139.5, and -109.5 and a CRP binding sequence centered at -69.5, respectively.

References

Almagro-Moreno, S. and Boyd, E. F. 2009. Sialic acid catabolism confers a competitive advantage to pathogenic *Vibrio cholerae* in the mouse intestine. *Infect. Immun.* **77**, 3807-3816

Almargo-Moreno, S., Root, M. Z., and Taylor, R. K. 2015. Role of ToxS in the proteolytic cascade of virulence regulator ToxR in *Vibrio cholerae. Mol. Microbiol.* **98**, 963-976

Autunes, L. C., Ferrerira, R. B., Buckner, M. M., and Finlay, B. B. 2010. Quorum sensing in bacterial virulence. *Microbiology.* **156**, 2271-2282

Awad, M. M., Bryant, A. E., Stevens, D. L., and Rood, J. I. 1995. Virulence studies on chromosomal α-toxin and θ-toxin mutants constructed by allelic exchange provide genetic evidence for the essential role of α-toxin in *Clostridium perfrigens*-mediated gas gangrene. *Mol. Microbiol*. **15**, 191-202

Backert, S. and Meyer, T. F. 2006. Type IV secretion systems and their effectors in bacterial pathogenesis. *Curr. Opin. Microbiol.* **9**, 207-217

Baddal, B., Muzzi, A., Censini, S., Calogero, R. A., Torricelli, G., Guidotti, S., Taddei, A. R., Covacci, A., Pizza, M., Rappuoli, R., Soriani, M., and Pezzicoli, A. 2015. Dual RNA-seq of nontypeable *Haemophilus influenzae* and host cell transcriptomes reveals novel insights into host-pathogen cross talk. *mBio*. **6**, e01765-15

Baek, W. K., Lee, H. S., Oh, M. H., Koh, M. J., Kim, K. S., and Choi, S. H. 2009. Identification of the *Vibrio vulnificus ahpC1* gene and its influence on survival under oxidative stress and virulence. *J. Microbiol.* **47**, 624-632

Bakala N'Goma, J. C., Le Miogne, V., Soismier, N., Laencina, L., Le Chevalier, F., Roux, A. L., Poncin, I., Servaeu-Avesque, C., Rottman, M., Gaillard, J. L., Etinenne, G., Brosch, R., Herrmann, J. L., Canaan, S., and Girard-Misguich, F. 2015. *Mycobacterium abscessus* phospholipase C expression is induced during

colculture within amoebae and enhances *M. abscessus* virulence in mice. *Infect. Immun.* **83**, 780-791

Baumman, P., Baumann, L., and Hall, B. G. 1981. Lactose utilization by *Vibrio vulnificus. Curr. Microbiol.* **6**, 131-135

Bhowmick, R., Ghosal, A., Das, B., Koley, H., Saha, D. R., Ganguly, S., Nandy, R. K., Bhadra, R. K., and Chatterjee, N. S. 2008 Intestinal adherence of *Vibrio cholerae* involves a coordinated interaction between colonization factor GbpA and mucin. *Infect. Immun.* **76**, 4968-4977

Bisharat, N., Bronstein, M., Korner, M., Schnitzer, T., and Koton, Y. 2013. Transcriptome profiling analysis of *Vibrio vulnificus* during human infection. *Microbiology.* **159**, 1878-1887

Boardman, B. K. and Satchell, K. J. 2004. *Vibrio cholerae* strains with mutations in an atypical type I secretion system accumulate RTX toxin intracellularly. *J. Bacteriol.* **186**, 8137-8143

Borezee, E., Pellegrini, E., and Berche, P. 2000. OppA of *Listeria monocytogenes*, an oligopeptide-binding protein requried for bacterial growth at low temperature and invovled in intracellular survival. *Infect. Immun.* **68**, 7069-7077

Bradford, M. M. 1976. A rapid and sensitive method for the quantification of microgram quantities of protein utilizing the principles of protein-dye binding. *Anal. Biochem*. **7**, 248-254

Browning, D. F. and Busby, S. J. 2004. The regulation of bacterial transcription initiation. *Nat. Rev. Microbiol*. **2**, 57-65

Busby, S. and Bbright, R. H. 1997. Transcription activation at class II CAP-dependent promoters. *Mol Microbiol.* **23**, 853-859

Cameron, A, D. and Redfield, R. J. 2007. Non-canonical CRP sites control competence regulons in *Escherichia coli* and many other γ-proteobacteria. *Nuclei Acids Res*. **34**, 6001-6014

Celli, J. P., Turner, B. S., Afdhal, N. H., Keates, S., Ghiran, I., Kelly, C. P., Ewoldt. R. H., McKinley, G. H., So, P., Erramilli, S., and Bansil, R. 2009. *Helicobacter pylori* moves through mucus by reudncing mucin viscoelasticity. *Proc. Natl. Acad. Sci. USA.* **106**, 14321-14326

Chang, J. H., Desvaeaux, D., and Creason, A. L. 2014. The ABCs and 123s of bacterial secretion systems in plant pathogenesis. *Annu. Rev. Phytopathol.* **52**, 317-345

Chatzidaki-Livanis, M., Jones, M. K., and Wright, A. C. 2006. Genetic variation in the *Vibrio vulnificus* group 1 capsular polysaccharide operon. *J. Bacteriol.* **188**, 1987-1998

Chiang, S. and Chuang, Y. 2003. *Vibrio vulnificus* infection: clinical manifestations, pathogenesis, and antimicrobial therapy. *J Microbiol. Immunol. Infect.* **36**, 81-88

Choi, H. K., Park, N. Y., Kim, D., Chung, H. J., Ryu, S., and Choi, S. H. 2002. Promoter analysis and regulatory characteristics of *vvhBA* encoding cytolytic hemolysin of *Vibrio vulnificus*. *J. Biol. Chem.* **277**, 47292-47299

Chung, K. J., Cho, E. J., Kim, M. K., Kim, Y. R., Yang, H. Y., Chung, J. C., Lee, S. E., Rhee, J. H., Choy, H. E., and Lee, T. H. 2010. RtxA1-induced expression of the small GTPase Rac2 plays a key role in the pathogenicity of *Vibrio vulnificus. J. Infect. Dis.* **201**, 97-105

Cianciotto, N. P. 2005. Type II secretion: a protein secretion system for all seasons. *Trends Microbiol*. 13, 581-588

Corfield, A. P., Wagner, S. A., Clamp, J. R., Kriaris, M. S., and Hoskins, L. C. 1992. Mucin degradation in the human colon: production of sialidase, sialate *O*-acetylesterase, *N*-acetylneuraminate lyase, arylesterase, and glycosulfatase activities by strains of fecal bacteria. *Infect. Immun.* **60**, 3971-3978

Costa, T. R., Felisberto-Rodrigues, C., Mir, A., Prevost, M. S., Redzej, A., Trokter, M., and Waksman, G. 2015. Secretion systems in Gram-negative bacteria: structural and mechanistic insights. *Nat. Rev. Microbiol.* **13**, 343-359

Cotter, P. A. and DiRita, V. J. 2000. Bacterial virulence regulation: an evolutionary perspective. *Annu. Rev. Microbiol.* **54**, 519-565

Creecy, J. P. and Conway, T. 2015. Quantitative bacterial transcriptomics with RNA-seq. *Curr. Opin. Microbiol*. **23**, 133-140

Cress, B. F., Englaender, J. A., He, W., Kasper, D., Linardt, R. J., and Koffas, M. A. 2014. Masquerading microbial pathogenesis: capsular polysaccharides mimic host-tissue molecules. *FEMS Microbial. Rev.* **38**, 660-697

Croucher, N. J. and Thomson, N. R. 2010. Studying bacterial transcriptomes using RNA-seq. *Curr. Opin. Microbiol.* **13**, 619-624

Daniels, N. A. 2011. *Vibrio vulnificus* oysters: pearls and perils. *Clin. Infect. Dis.* **52**, 788-792

DePaola, A., Jones, J. L., Woods, J., Burkhardt, W., Calci, K. R., Kranz, J. A., Bowers, J. C., Kasturi, K., Byars, R. H., Jacobs, E., Williams-Hill, D., and Nabe, K. 2010. Bacterial and viral pathogens in live oysters: 2007 United States market survey. *Appl. Environ. Microbiol.* **76**, 2754-2768

Desvaux, M. and Hébraud, M. 2006. The protein secretion systems in *Listeria*: inside out bacterial virulence. *FEMS Microbiol. Rev.* **30**, 774-805

Elmore, S .P. Watts, J. A., Simpson, L. M., and Oliver, J. D. 1992. Reversal of hypotension induced by *Vibrio vulnificus* lipopolysaccharide in the rat by inhibition of nitric oxide synthase *Microb. Pathog.* **13**, 391-397

Etzold, S. and Juge, N. 2014. Structural insights into baterial recognition of intestinal mucins. *Curr. Opin. Struct. Biol.* **28**, 23-31

Fan, J. J., Shao, C. P., Ho, Y. C., Yu, C. K., and Hor, L. I. 2001. Isolation and characterization of a *Vibrio vulnificus* mutant deficient in both extracellular metalloprotease and cytolysin. *Infect. Immun.* **69**, 5943-5948

Fleischhacker, A. S., Stubna, A., Hsueh, K. L., Guo, Y., Teter, S. J., Rose, J. C., Brunold, T. C., Markley, J. L., Münck, E., and Kiley, P. J. 2012. Characterization

of the [2Fe-2S] cluster of *Escherichia coli* transcription factor IscR. *Biochemistry.* **51**, 4453-4462

Flieger, A., Neumeister, B., and Cianciotto, N. P. 2002. Characterization of the gene encoding the major secreted lysophospholipase A of *Legionella pneumophila* and its role in detoxification of lysophosphatidylcholine. *Infect. Immun.* **70**, 6094-6106

Froelich, B. and Oliver, J. D. 2013. Increases in the amount of *Vibrio* spp. in oysters upon addition of exogenous bacteria. *Appl. Environ. Microbiol.* **79**, 5208-5213

Fuangthong, M., Jittawuttipoka, T., Wisitkamol, R., Romasang, A., Duang-nkern, J., Vattanaviboon, P., and Mongkolsuk, S. 2015. IscR plays role in oxidative stress resistance and pathogenicity of a plant pathogen, *Xanthomonas campestris. Microbiol. Res*. **170**, 139-146

Fux, C. A., Costerton, J. W., Stewart, P. S., and Stoodley, P. 2005. Survival strategies of infectious biofilms. *Trends Microbiol*. **13**, 34-40

Ghannoum, M. A. 2000. Potential role of phospholipases in virulence and fungal pathogenesis. *Clin. Microbiol. Rev.* **13**, 122-143

Gavin, H. E. and Satchell, K. J. 2015. MARTX toxins as effector delivery platforms. *FEMS Pathog. Dis.* **73**, ftv092

Giel, J. L., Nesbit, A. D., Mettert, E. L., Fleischhacker, A. S., Wanta, B. T., and Kiley, P. J. 2013. Regulation of iron-sulphur cluster homeostasis through transcriptional control of the Isc pathway by [2Fe-2S]-IscR in *Escherichia coli*. *Mol. Microbiol*. **87**, 478-492

Giel, J. L., Rodionov, D., Liu, M., Blattner, F. R., and Kiley, P. J. 2006. IscR-dependent gene expression links iron-sulphur cluster assembly to the control of O_2-regulated genes in *Escherichia coli*. *Mol. Microbiol.* **60,** 1058-1075

Goo, S. Y., Lee, H. J., Kim, W. H., Han, K. L., Park, D. K., Lee, H. J., Kim, S. M., Kim, K. S., Lee, K. H., and Park, S. J. 2006. Identification of OmpU of *Vibrio*

vulnificus as a fibronectin-binding protein and its role in bacterial pathogenesis. *Infect. Immun.* **74**, 5586-5594

Goss, T. J., Morgan, S. J., French, E. L., and Krukonis, E. S. 2013. ToxR recognizes a direct repeat element in the *toxT*, *ompU*, *ompT*, and *ctxA* promoters of *Vibrio cholerae* to regulate transcription. *Infect. Immun.* **81**, 884-895

Gray, L. D. and Kreger, A. S. 1987. Mouse skin damage caused by cytolysin from *Vibrio vulnificus* and by *V. vulnificus* infection. *J. Infect. Dis.* **155**, 236-241

Green, J., Stapleton, M. R., Smith, L. J., Artymiuk, P. J., Kahramanoglou, C., Hunt, D. M., and Buxton, R. S. 2014. Cyclic-AMP and bacterial cyclic-AMP receptor proteins revisited: adaptation for different ecological niches. *Curr. Opin. Mcirobiol.* **18**, 1-7

Groisman, E. A., Parra-Lopez, C., Salcedo, M., Lipps, C. J., and Heffron, F. 1992. Resistance to host antimicrobial peptides is necessary for *Salmonella* virulence. *Proc. Natl. Acad. Sci. USA.* **89**, 11939-11943

Gururaja, T. L., Levine, J. H., Tran, D. T., Nagangorda, G. A., Ramalingam, K., Ramasubbu, N., and Levine, M. J. 1999. Candidacidal activity prompted by N-terminus histatin-like domain of human salivary mucin (MUC7)1. *Biochim. Biophys. Acata.* **1431**, 107-119

Guttman, J. A. and Finaly, B. B. 2009 Tight junctions as targets of infectious agents. *Biochim. Biophys. Acta*. **1788**, 832-841

Ha, C., Kim, S. K., Lee, M. N., and Lee, J. H. 2014. Quorum-sensing-dependent metalloprotease VvpE is important in the virulence of *Vibrio vulnificus* to invertebrates. *Microb. Pathog.* **72**, 8-14

Hall-Stoodley, L., Costerton, J. W., and Stoodley, P. 2004. Bacterial biofilms: from the natural environment to infectious diseases. *Nat. Rev. Microbiol.* **2**, 95-108

Haas, B. J., Chin, M., Nusbaum, C., Birren, B. W., and Livny, J. 2012. How deep is deep enough for RNA-seq profiling of bacterial transcriptomics? *BMC Genomics.* **13**, 734

Hall-Stoodley, L., Costerton, J. W., and Stoodley, P. 2004. Bacterial biofilms: from the natural environment to infectious diseases. *Nat. Rev. Microbiol.* **2**, 95-108

Høiby, N., Ciofu, O., and Bjarnsholt, T. 2010. *Pseudomonas aeruginosa* biofilms in cystic fibrosis. *Future Microbiol.* **5**, 1663-1674

Homer, K. A., Whiley, R. A., and Beighton, D. 1994. production of specific glycosidase activities by *Streptococcus intermedius* strain UNS35 grwon in the presence of mucin. *J. Med. Microbiol.* **41**, 184-190

Horseman, M. A. and Surani, S. 2011. A comprehensive review of *Vibrio vulnificus*: an important cause of severe sepsis and skin and soft-tissue infection. *Int. J. Infect. Dis.* **15**, e157-166

Hsueh, P., Lin, C., Tang, H., Lee, H., Liu, J., Liu, Y., and Chuang, Y. 2004. *Vibrio vulnificus* in Taiwan. *Emerg. Infect. Dis.* **10**, 1363-1368

Huang, F., Subbaiah, P. V., Holian, O., Zhang, J., Johnson, A., Gertzberg, N., and Lum, H. 2005. Lysophosphatidylcholine increases endothelial permeability: role of PKCα and RhoA cross talk. *Am. J. Physiol. Lung Cell. Mol. Physiol.* **289**, L176-185

Hwang, J., Kim, B. S., Jang, S. Y., Lim, J. G., You, D. J., Jung, H. S., Oh, T. K., Lee, J. O., Choi, S. H., and Kim, M. H. 2013. Structural insights into the regulation of sialic acid catabolism by the *Vibrio vulnificus* transcriptional repressor NanR. *Proc. Natl. Acad. Sci. U.S.A.* **110**, E2829-2837

Imlay, J. A. 2006. Iron-sulphur clusters and the problem with oxygen. *Mol. Microbiol*. **59**, 1073-1082

Istivan, T. S. and Coloe, P. 2006. Phospholipase A in Gram-negative bacteria and its role in pathogenesis. *Microbiology*. **152**, 1263-1274

Jang, K. K., Gil, S. Y., Lim, J. G., and Choi, S. H. 2016. Regulatory characteristics of *Vibrio vulnificus gbpA* encoding mucin-binding protein essential for pathogenesis. *J. Biol. Chem.* **291**, 5774-5787

Jeong, K. C., Jeong, H. S., Rhee, J. H., Lee, S. E., Chung, S. S., Starks, A. M., Escudero, G. M., Gulig, P. A., and Choi, S. H. 2000. Construction and phenotypic evaluation of a *Vibrio vulnificus vvpE* mutant for elastolytic protease. *Infect. Immun.* **68**, 5096-5106

Jeong, H. G., Oh, M. H., Kim, B. S., Lee, M. Y., Han, H. J., and Choi, S. H. 2009. The capability of catabolic utilization of *N*-acetylneuraminic acid, a sialic acid, is essential for *Vibrio vulnificus* pathogenesis. *Infect. Immun.* **77,** 3209-3217

Jeong, H. G. and Satchell, K. J. 2012. Additive function of *Vibrio vulnificus* $MARTX_{Vv}$ and VvhA cytolysins promotes rapid growth and epithelial tissue necrosis during intestinal infection. *PLoS Pathog.* **8**, e1002581

Jeong, H. S., Kim, S. M., Lim, M. S., Kim, K. S., and Choi, S. H. 2010. Direct interaction between quorum-sensing regulator SmcR and DNA polymerase is mediated by integration host factor to activate *vvpE* encoding elastase in *Vibrio vulnificus*. *J. Biol. Chem.* **285**, 9357-9366

Jeong, H. S., Lee, M. H., Lee, K. H., Park, S. J., and Choi, S. H. 2003. SmcR and cyclic AMP receptor protein coactivate *Vibrio vulnificus vvpE* encoding elastase through the RpoS-dependent promoter in a synergistic manner. *J. Biol. Chem.* **278**, 45072-45081

Jensen, P .H., Kolarich, D., and Packer, N. H. 2010. Mucin-type-O-glycosylation – putting them pieces together. *FEBS J.* **277**, 81-94

Johansson, M. E., Ambort, D., Pelaseyed, T., Schùtte, A., Gustafsson, J. K., Ermund, A., Subramani, D. B., Holmėn-Larsson, J. M., Thomsson, K. A., Bergstrőm, J. H., van der Post, S., Rodriguez-Piñeiro, A. M., Sjövall, H., Bäckström, and M., Hansson, G. C. 2011. Composition and functional role of the mucus layer in the intestine. *Cell Mol. Life Sci.* **68**, 3635-3641

Jones, M. K. and Oliver, J. D. 2009. *Vibrio vulnificus*: disease and pathogenesis. *Infect. Immun.* **77**, 1723-1733

Jorth, P., Trivedi, U., Rumbaugh, K., and Whiteley, M. 2013. Probing bacterial metabolism during infection using high-resolution transcriptomics. *J. Bacteriol.* **195**,

4991-4998

Jude, B. A., Martinez, R. M., Skorupski, K., and Taylor, R. K. 2009. Levels of the secreted *Vibrio cholerae* attachment factor GbpA are modulated by quorum-sensing-induced proteolysis. *J. Bacteriol.* **191**, 6911-6917

Juge, N. 2012. Microbial adhesins to gastrointestinal mucus. *Trends Microbiol.* **20**, 30-39

Juge, N., Tailford, L., and Owen, C. D. 2016. Sialidases from gut bacteria: a mini-review. *Biochem. Soc. Transc.* **44**, 166-175

Kang, M. K., Jhee, E. C., Koo, B. S., Yang, J. Y., Park, B. H., Kim, J .S., Rho, H. W., Kim, H. R., and Park, J. W. 2002. Induction of nitric oxide synthase expression b*y Vibrio vulnifius* cytolysin. *Biochem. Biophys. Res. Commun.* **290**, 1090-1095

Kapuscinski, J. 1995. DAPI: a DNA-specific fluorescent probe. *Biotech. Histochem.* **70**, 220-233

Kashimoto, T. S., Ueno, S., Hanakima, M., Hayashi, H., Akeda, Y., Miyoshi, S., Hongo, T., Honda, T., and Susa, N. 2003. *Vibrio vulnificus* induces macrophage apoptosis *in vitro* and *in vivo*. *Infect. Immun.* **71**, 533-535

Katz, J., Sambandam, V., Michalek, S. M., and Balkovetz, D. F. 2000. Characterization of *Porphyromonas gingivalis*-induced degradation of epithelial cell junctional complexes. *Infect. Immun.* **68**, 1441-1449

Kaus, K., Lary, J. W., Cole, J. L., and Olson, R. 2014. Glycan specificity of the *Vibrio vulnificus* hemolysin lectin outlines evolutionary history of membrane targeting by a toxin family. *J. Mol. Biol.* **426**, 2800-2812

Kwak, J. S., Jeong, H. G., and Satchell, K. J. 2011. *Vibio vulnificus rtxA1* gene recombination generates toxin variants with altered potency during intestinal infection. *Proc. Natl. Acad. Sci. USA.* **108**, 1645-1650

Kim, B. S., Hwang, J. W., Kim, M. H., and Choi, S. H. 2011. Cooperative regulation of the *Vibrio vulnificus nan* gene cluster by NanR protein, cAMP receptor protein, and *N*-acetylmannosamine 6-phosphate. *J. Biol. Chem.* **286**, 40889–40899

Kim, B. S. and Kim, J. S. 2002. Cholesterol induce oligomerization of *Vibrio vulnificus* cytolysin specifically. *Exp. Mol. Med.* **34**, 239-242

Kim, H. R., Rho, H W., Park, J. W., Kim J. S., Park, B. H., Kim, U. H., and Park, S. D. 1993. Hemolytic mechanism of cytolysin produced from *V. vulnificus*. *Life Sci.* **53**, 571-577

Kim, S., Bang, Y. J., Kim, D. Y., Lim, J. G., and Choi, S. H. 2014. Distinct characteristics of OxyR2, a new OxyR-type regulator, ensuring expression of Peroxiredoxin 2 detoxifying low levels of hydrogen peroxide in *Vibrio vulnificus*. *Mol. Microbiol.* **93**, 992-1009

Kim, S. H., Lee, B. Y., Lau, G. W., and Cho, Y. H. 2009. IscR modulates catalase A (KatA) activity, peroxide resistance and full virulence of *Pseudomonas aeruginosa* PA14. *J. Microbiol. Biotechnol.* **19**, 1520-1526

Kim, S. M., Lee, D. H., and Choi, S. H. 2012. Evidence that the *Vibrio vulnificus* flagellar regulator FlhF is regulated by a quorum sensing master regulator SmcR. *Microbiology* **158**, 2017-2025

Kim, S. M., Park, J. H., Lee, H. S., Kim, W. B., Ryu, J. M., Han, H. J., and Choi, S. H. 2013. LuxR homologue SmcR is essential for *Vibrio vulnificus* pathogenesis and biofilm detachment, and its expression is induced by host cells. *Infect. Immun.* **81**, 3721-3730

Kim, S. Y., Thanh, X. T., Jeong, K., Kim, S. B., Pan, S. O., Jung, C. H., Hong, S. H., Lee, S. E., and Rhee, J. H. 2014. Contribution of six flagellin genes to the flagellum biogenesis of *Vibrio vulnificus* and *in vivo* invasion. *Infect. Immun.* **82**, 29-42

Kim, Y, R., Lee, S. E., Kim, C. M., Kim, S. Y., Shin, E. K., Shin, D. H., Chung, S. S., Choy, H. E., Progulske-Fox, A., Hillman, J. D., Handfield, M., and Rhee, J. H. 2003. Characterization and pathogenic significance of *Vibrio vulnificus*

antigens preferentially expressed in septicemic patients. *Infect. Immun.* **71**, 5461-5471

Kim, Y. R. Lee, S. E., Kook, H., Yeom, J. A., Na, H. S., Kim, S. Y., Chung, S. S., Choy, H. E., and Rhee, J. H. 2008. *Vibrio vulnificus* RTX toxin kills host cells only after contact of the bacteria with host cells. *Cell Microbiol*. **10**, 848-862

Kim, Y. R. and Rhee, J. H. 2003. Flagellar basal body *flg* operon as a virulence determinant of *Vibrio vulnificus*. *Biochem. Biophys. Res. Commun*. **304**, 405-410

Kirn, T. J., Jude, B. A., and Taylor, R. K. 2005. A colonization factor links *Vibrio cholerae* environmental survival and human infection. *Nature.* **438**, 863-866

Koo, B. S., Lee, J. H., Kim, S. C., Yoon, H. Y., Kim, K. A., Kwon, K. B., Kim, H. R., Park, J. W., and Park, B. H. 2007. Phospholipase A as a potent virulence factor of *Vibrio vulnificus. Int. J. Mol. Med.* **20**, 913-918

Korotkov, K. V., Sandkvist, M., and Hol, W. G. 2012. The type II secretion system: biogenesis, molecular architecture, and mechanism. *Nat. Rev. Microbiol.* **10**, 336-351

Kown, K. B., Yang, J. Y., Ryu, D. H., Rho, H. W., Kim, J. S., Park, J. W., Kim, H. R., and Park, B. H. 2001. *Vibrio vulnificus* cytolysin induces superoxide anion-initiated apoptotic signaling pathway in himan ECV304 cells. *J. Biol. Chem.* **276**, 47518-47523

Kuhle, K. and Flieger, A. 2013. *Current topics in microbiology and immunology.* (Hilbi, H., and Aktories, K., eds) pp. 175-209, 10.1007/978-3-642-40591-4, Springer-Verlag, Berlin, Heidelberg

Lee, B. C., Kim, S. H., Choi, S. H., and Kim, T. S. 2005. Induction of interleukin-8 production via nuclear factor-kappaB activation in human intestinal epithelial cells infected with *Vibrio vulnificus. Immunology.* **115**, 506-515

Lee, B. C., Lee, J. H., Kim, M. W., Kim, B. S., Oh, M. H., Kim, K. S., Kim, T. S., and Choi, S. H. 2008. *Vibrio vulnificus rtxE* is important for virulence, and its expression is induced by exposure to host cells. *Infect. Immun.* **76**, 1509-1517

Lee, D. H., Jeong, H. S., Jeong, H. G., Kim, K. M., Kim, H., and Choi, S. H. 2008. A consensus sequence for binding of SmcR, a *Vibrio vulnificus* LuxR homologue, and genome-wide identification of the SmcR regulon. *J. Biol. Chem.* **283**, 23610-23618

Lee, J. H., Kim, M. W., Kim, B., Kim, S. M., Lee, B. C., Kim, T. S., and Choi, S. H. 2007. Identification and characterization of the *Vibrio vulnificus rtxA* essential for cytotoxicity in vitro and virulence in mice. *J. Microbiol.* **45**, 146-152

Lee, J. H., Rhee, J. E., Park, U. R., Ju, H. M., Lee. B. C., Kim, T. S., Jeong, H. S., and Choi, S.H. 2007. Identification and functional analysis of *Vibrio vulnificus smcR* a novel global regulator. *J. Microbiol. Biotechnol.* **17**, 325-334

Lee, J. H., Rho, J. B., Park, K. J., Kim, C. B., Han, Y. S., Choi, S. H., Lee, K. H., and Park, S. J. 2004. Role of flagellum and motility in pathogenesis of *Vibrio vulnificus*. *Infect. Immun.* **72**, 4905-4910

Lee, K. J., Lee, N. Y., Han, Y. S., Kim, J., Lee, K. H., and Park, S. J. 2010. Functional characterization of the IlpA protein of *Vibrio vulnificus* as an adhesion and its role in bacterial pathogenesis. *Infect. Immun.* **78**, 2408-2417

Lee, N. Y., Lee, H. Y., Lee, K. H., Han, S. H., and Park, S. J. 2011. *Vibrio vulnificus* IlpA induces MAPK-mediated cytokine production via TLR1/2 activation in THP-1 cells, a human monocytic cell line. *Mol. Immunol.* **49**, 143-154

Lee, S. E., Shin, S. H., Kim, S. Y., Kim, Y. R., Shin, D. H., Chung, S. S., Lee, Z. H., Lee, J. Y., Jeong, K. C., Choi, S. H., and Rhee, J. H. 2000. *Vibrio vulnificus* has the transmembrane transcription activator ToxRS stimulating the expression of the hemolysin gene *vvhA*. *J. Bacteriol.* **182**, 3405-3415

Lee, S. J., Jung, Y. H., Ryu, J. M., Jang, K. K., Choi, S. H., and Han, H. J. 2016. VvpE mediates the intestinal colonization of *Vibrio vulnificus* by the disruption of tight junctions. *Int. J. Med. Microbiol.* **306**, 10-19

Lee, S. J., Jung, Y. H., Oh, S. Y., Jang, K. K., Lee, H. S., Choi, S. H., and Han, H. J. 2015a. *Vibrio vulnificus* VvpE inhibits mucin 2 expression by hypermethylation via lipid raft-mediated ROS signaling in intestinal epithelial cells.

Cell Death Dis. **18**, e1787

Lee, S. J., Jung, Y. H., Song, E. J., Jang, K. K., Choi, S. H., and Han, H. J. 2015b. *Vibrio vulnificus* VvpE stimulates IL-1β production by the hypomethylation of the IL-1β promoter and NF-κB activation via lipid raft-dependent ANXA2 recruitment and reactive oxygen species signaling in intestinal epithelial cells. *J. Immunol.* **195**, 2282-2293

Lee, S. J., Jung, Y. H., Oh, S. Y., Song, E. J., Choi, S. H., and Han. H. J. 2015. *Vibrio vulnificus* VvhA induces NF-κB-dependent mitochondrial cell death via lipid raft-mediated ROS production in intestinal epithelial cells. *Cell Death Dis.* **6**, e1655

Lenz, D. H., Mok, K. C., Lilley, B. N., Kulkarni, R. V., Wingreen, N. S., and Bassler, B. L. 2004. The small RNA chaperone Hfq and multiple small RNAs control quorum sensing in *Vibrio harveyi* and *Vibrio cholerae*. *Cell* **118**, 69-82

Lesuffleur, T., Barbat, A., Dussaulx, E., and Zweibaum, A. 1990. Growth adaptation to methotrexate of HT-29 human colon carcinoma cells is associated with their ability to differentiate into columnar absorptive and mucus-secreting cells. *Cancer Res.* **50**, 6334-6343

Li, L., Mou, X., and Nelson, D. R. 2011. HlyU is a positive regulator of hemolysin expression in *Vibrio anguillarum*. *J. Bacteriol.* **193**, 4779-4789

Li, L., Mou, X., and Nelson, D. R. 2013. Characterization of Plp, a phosphatidylcholine-specific phospholipase and hemolysin of *Vibrio anguillarum*. *BMC Microbiol.* **27**, 271

Lim M. S., Kim, J. A., Lim, J. G., Kim, B. S., Jeong, K. C., Lee, K. H., and Choi, S. H. 2011. Identification and characterization of a novel serine protease, VvpS, that contains two functional domains and is essential for autolysis of *Vibrio vulnificus*. *J. Bacteriol.* **193**, 3722-3732

Lim, J. G., Bang, Y. J., and Choi, S. H. 2014. Characterization of the *Vibrio vulnificus* 1-Cys peroxiredoxin Prx3 and regulation of its expression by the Fe-S cluster regulator IscR in response to oxidative stress and iron starvation. *J. Biol. Chem.* **289**, 36263-36274

Lim, J. G. and Choi, S. H. 2014. IscR is a global regulator essential for pathogenesis of *Vibrio vulnificus* and induced by host cells. *Infect. Immun.* **82**, 569-578

Linden, S. K., Sutton, P., Karlsson, N. G., Korolik, V., and MuGuckin, M. A. 2008. Mcins in the mucosal barrier to infection. *Mucosal Immunol.* **1**, 183-197

Liu, M., Alice, A. F., Naka, H., and Crosa, J. H. 2007. The HlyU protein is a positive regulator of *rtxA1*, a gene responsible for cytotoxicity and virulence in the human pathogen *Vibrio vulnificus. Infect. Imuun.* **75**, 3282-3289

Liu, M., Naka, H., and Crosa, J. H. 2009. HlyU acts as an H-NS antirepressor in the regulation of the RTX toxin gene essential for the virulence of the human pathogens *Vibrio vulnificus* CMCP6. *Mol. Microbiol.* **72**, 491-505

Lo, H. R., Lin, J. H., Chen, Y. H., Chen, C. L., Shao, C. P., Lai, Y. C., and Hor, L. I. 2011. RTX toxin enhances the survival of *Vibrio vulnificus* during infection by protecting the organism from phagocyotosis. *J. Infect. Dis.* **203**, 1866-1874

López-Solanilla, E., García-Olmedo, F., and Rodríguez-Palenzuela, P. 1998. Inactivation of the *sapA* to *sapF* locus of *Erwinia chrysanthemi* reveals common features in plant and animal bacterial pathogenesis. *Plant Cell.* **10**, 917-924

Masamune, A., Sakai, Y., Satoh, A., Fujita, M., Yoshida, M., and Shimosegawa, T. 2001. Lysophosphatidylcholine induces apoptosis in AR42 J cells. *Pancreas*. **22**, 75-83

Maston, J. S., Withey, J. H., and DiRita, V. J. 2007. Regulatory networks controlling *Vibrio cholerae* virulence gene expression. *Infect. Immun.* **75**, 5542-5549

McDougald, D., Rice, S. A., and Kjelleberg, S. 2000. The marine pathogen *Vibrio vulnificus* encodes a putative homologue of the *Vibrio harveyi* regulatory gene, *luxR*: a genetic and phylogenetic comparison. Gene. **248**, 213-221

McDougald, D., Rice, S. A., and Kjelleberg, S. 2001. SmcR-depdendent regulation of adaptive phenotypes in *Vibrio vulnificus. J. Bacteriol.* **183**, 758-762

McGuckin, M. A., Lindén, S. K., Sutton, P., and Florin, T. H. 2011. Mucin

dynamics and enteric pathogens. *Nat. Rev. Microbiol*. **9**, 265-278

Mcpherson, V. L., Watts, J. A., Simpson, L. M., and Oliver, J. D. 1991. Physiological effects of the lipopolysaccharide on *Vibrio vulnificus* in mice and rats. *Microbios*. **67**, 141-149

Metzker, M. L. 2010. Sequencing technologies – the next generation. *Nat. Rev. Genet*. **11**, 31-46

Milton, D. L., O'Toole, R., Horstedt, P., and Wolf-Watz, H. 1996. Flagellin A is essential for the virulence of *Vibrio anguillarum*. *J. Bacteriol*. **178**, 1310–1319

Miller, H. K., Kwuan, L., Schwiesow, L., Bernick, D. L., Mettert, E., Ramirez, H. A., Ragle, J. M., Chan, P. P., Kiley, P. J., Lowe, T. M., and Auerbuch, V. 2014. IscR is essential for *Yersinia pseudotuberculosis* type III secretion and virulence. *PLoS Pathog*. **10**, e1004194

Miyoshi, S., Oh, E. G., Hiratai, K., and Shinoda, S. 1993. Exocellular toxic factors produced by *Vibrio vulnificus*. *J. Toxicol. Toxin Rev.* **12**, 253-288

Monturiol-Gross, L., Flores-Díaz, M., Pineda-Padilla, P., Castro-Castro A. C., and Alape-Giron, A. 2014. *Clostridium perfrigens* phospholipase C induces ROS production and cytotoxicity require PKC, MEK1, and NFκB activation. *PLoS One*. **23**, e86475

Mortazavi, A., Williams, B. A., MuCue, K., Schaeffer, L., and Wold, B. 2008. Mapping and quantifying mammalian transcriptomes by RNA-seq. *Nat. Methods*. **5**, 621-628

Mukherjee, D., Datta, A. B., and Chakrabarti, P. 2014. Crystal structure of HlyU, the hemolysin gene transcription activator, from *Vibrio cholerae* N16961 and functional implications. *Biochim. Biophys. Acta*. **1844**, 2346-2354

Mukherjee, D., Pal, A., Chakravarty, D., and Chakrabarti, P. 2015. Identification of the target DNA sequence and characterization of DNA binding features of HlyU, and suggestion of a redox switch for *hlyA* expression in the human pathogen *Vibrio cholerae* from in silico studies. *Nucleic Acids Res*. **43**, 1407-1417

Nesbit, A. D., Giel, J. L., Rose, J. C., and Kiley, P. J. 2009. Sequence-specific binding to a subset of IscR-regulated promoters does not require IscR Fe-S cluster ligation. *J. Mol. Biol.* **387**, 28-41

Neutra, M. R. and Forstner, J. F. 1987. Gastrointestinal mucus synthesis, secretion, and function. In:Johnson LR (ed) Physiology of the gastrointestinal tract. Vol 2. 2nd Ed. Raven, New York. vol 2; pp 975-1009

Ng, W. L. and Bassler, B. L. 2009. Bacterial quorum-sensing network architectures. *Annu. Rev. Genet.* **43**, 197-222

Nishi, K., Lee, H. J., Park, S. Y., Bae, S. J., Lee, S. E., Adams, P. D., Rhee, J. H., and Kim, J. S. 2010 Crystal structure of the transcriptional activator HlyU from *Vibrio vulnificus* CMCP6. *FEBS Lett.* **584**, 1097-1102

Ofek, I., Bayer, E. A., and Abraham S. N. 2013. In *The Prokaryotes* (Rosenberg, E., Delong, E. F., Lory, S., Stackebrandt, E., and Thompson, F., eds) pp. 107–123, 10.1007/978–3-642–30144–5_50, Springer-Verlag, Berlin, Heidelberg

Oh, M. H., Lee, S. M., Lee, D. H., and Choi, S. H. 2009. Regulation of the *Vibrio vulnificus hupA* gene by temperature alteration and cyclic AMP receptor protein and evaluation of its role in virulence. *Infect. Immun.* **77**, 1208-1215

Oliver, J. D. 2005a. *Vibrio vulnificus*. In *Oceans and Health: Pathogens in the Marine Environment.* pp 253-276. Springer

Oliver, J. D. 2005b. Wound infections caused by *Vibrio vulnificus* and other marine bacteria. *Epidemiol. Infect.* **133**, 383-391

Oliver, J. D. 2013. *Vibrio vulnificus*: death on the half shell: a personal fournaly with the pathogen and its ecology. *Microb. Ecol.* **65**, 793-799

Oliver, J. D. 2015. The biology of *Vibrio vulnificus*. *Microbiol. Spectr.* **3**, VE-0001-2014

Outten, F. W., Djaman, O., and Sotrz, G. 2004. A *suf* operon requirement for Fe-S cluster assembly during iron starvation in *Escherichia coli*. *Mol. Microbiol.* **52**,

861-872

Park N. Y., Lee, J. H., Kim, M. W., Jeong, H. G., Lee, B. C., Kim. T. S., and Choi, S. H. 2006. Identification of *Vibrio vulnificus wbpP* gene and evaluation of its role in virulence. *Infect. Immun.* **74**, 721-728

Park, J. H., Cho, Y. J., Chun, J., Seok, Y. J., Lee, J. K., Kim, K. S., Lee, K. H., Park, S. J., and Choi, S. H. 2011. Complete genome sequence of *Vibrio vulnificus* MO6-24/O. *J. Bacteriol*. **193**, 2062-2063

Parkhomchuk, D., Borodina, T., Amstislavskiy, V., Banaru, M., Hallen, L., Krobitsch, S., Lehrach, H., and Soldatov, A. 2009. Transcriptome analysis by strand-specific seqeuncing of complementary DNA. *Nucleic Acids Res.* **37**, e123

Paranjpye, R. N., Johnson, A. B., Baxter, A. E., and Strom, M. S. 2007. Role of type IV pilins in persistence of *Vibrio vulnificus* in *Crassostera virginica* oysters. *Appl. Environ. Microbiol.* **73**, 5041-5044

Paranjpye, R. N., Lara, J. C., Pepe, J. C., Pepe C. M., and Strom, M. S. 1998. The type IV leader peptidase/*N*-methyltrasferase of *Vibrio vulnificus* controls factors required for adherence to HEp-2 cells and virulence in iron-overloaded mice. *Infect. Immun.* **66**, 5659-5668

Parra-Lopez, C., Baer, M. T., and Groisman, E. A. 1993. Molecular genetic analysis of a locus required for resistance to antimicrobial peptides in *Salmonella* typhimurium. *EMBO J.* **12**, 4053-4062

Paranjpye, R. N. and Strom, M. S. 2005. A *Vibrio vulnificus* type IV pilin contributes to biofilm formation, adherence to epithelial cells, and virulence. *Infect. Immun.* **73**, 1411-1422

Petersen, T. N., Brunak, S., von Heijne, G., and Nielsen, H. 2011. SignalP 4.0: discriminating signal peptides from transmembrane regions. *Nat. Method.* **8**, 785-786

Peterson, S. and Young, G. M. 2002. Essential role for cyclic AMP and its receptor protein in *Yersinia enterocolitica* virulence. *Infect. Immun.* **70**, 3665-3672

Pinto, A. C., Melo-Barbosa, H. P., Miyoshi, A., Silva, A., and Azevedo, V. 2011. Application of RNA-seq to reveal the transcript profile in bacteria. *Genet. Mol. Res.* **10**, 1707-1718

Pizzaro-Cerdá, J. and Cossart, P. 2006 Bacterial adhesion and entro into host cells. *Cell*. **124**, 715-727

Rajagopalan, S., Teter, S. J., Zwart, P. H., Brennan, R. G., Phillips, K. J., and Kiley, P. J. 2013. Studies of IscR reveal a unique mechanism for metal-dependent regulation of DNA binding specificity. *Nat. Struct. Mol. Biol.* **20**, 740-747

Ramos, H. C., Rumbo, M., and Sirard, J. C. 2004. Bacterial flagellins: mediators of pathogenicity and host immune responses in mucosa. *Trends Microbiol.* **12**, 509-517

Rutherford, S. T. and Bassler, B. L. 2012. Bacterial quorum sensing: its role in virulence and possibilities for its control. *Cold Spring Harb. Perspect. Med.* **2**, a012427

Saha, R. P., Basu, G., and Chakrabarti, P. 2006. Cloning, expression, purification, and characterization of *Vibrio cholerae* transcriptional activator, HlyU. *Protein Expr. Purif.* **48**, 118-125

Sakaquchi, T., Köhler, H., Gu, X., McCormick, B. A., and Reinecker, H. C. 2002. *Shigella flexineri* regulates tight junction-assoicated proteins in human epithelial cells. *Cell. Microbiol.* **4**, 367-381

Sambrook, J. and Russell, D. W. 2001. *Molecular cloning: a laboratory manual.*, 3rd edn. Cold Spring Harbor, NY: Cold Spring Harbor Laboratory Press.

Satchell, K. J. 2015. Multifunctional-autoprocessing repeat-in-toxin (MARTX) toxins of *Vibrios*. *Microbiol. Spectr.* **3**, VE-0002-2014

Schmiel, D. H. and Miller, V. L. 1999. Bacterial phospholipases and pathogenesis. *Microbes Infect.* **1**, 1103-1112

Schmiel, D. H., Wagar, E., Karamanou, L., Weeks, D., and Miller, V. L. 1998. Phospholipase A of *Yersinia enterocolitica* contributes to pathogenesis in mouse model. *Infect. Immun.* **66**, 3941-3951

Schwartz, C. J., Giel, J. L., Patschkowski, T., Luther, C., Ruzicka, F. J., Beinert, H., and Kiley, P. J. 2001. IscR, an Fe-S cluster-containing transcription factor, represses expression of *Escherichia coli* genes encoding Fe-S cluster assembly proteins. *Proc. Natl. Acad. Sci. U.S.A.* **98**, 14895–14900

Sepp. A., Binns, R. M., and Lechler, R. I. 1996. Improved protocol for colorimetric detection of complement-mediated cytotoxicity based on the measurement of cytoplasmic lactate dehydrogenase activity. *J. Immunol. Methods.* **196**, 175-180

Shao, C. P. and Hor, L. I. 2001. Regulation of metalloprotease gene expression in *Vibrio vulnificus* by a *Vibrio harveyi* LuxR homologue. *J. Bacteriol.* **183**, 1369-1375

Shao, C. P., Lo, H. R., Lin, J. H., and Hor, L. I. 2011. Regulation of cytotoxicity by quorum-sensing signaling in *Vibrio vulnificus* is mediated by SmcR, a repressor of *hlyU*. *J. Bactieriol.* **193**, 2557-2565

Sheffield, P., Garrard, S., and Derewenda, Z. 1999. Overcoming expression and purification problems of RhoGDI using a family of “parallel” expression vectors. *Protein Expr. Pruif.* **15**, 34-39

Sheikh, A., Charles, R. C., Sharmeen, N., Rollins, S. M., Harris, J. B., Bhuiyan, M. S., Arifuzzaman, M., Khanam, F., Bukka, A., Kalsy, A., Porwollik, S., Leung, D. Y., Brooks, W. A., LaRocque, R. C., Hohmann, E. L., Cravioto, A., Loqvinenko, T., Calderwood, S. B., McClelland, M., Graham, J. E., Qadri, F., and Ryan, E. T. 2011. *In vivo* expression of *Salmonella enterica* serotype Typhi genes in the blood of patients with typhoid fever in Bangladash. *PLoS Negl. Trop. Dis.* **5**, e1419.

Silva, A. J., Pham, K., and Benitez, J. A. 2003. Haemagglutinin/protease expression and mucin gel penetration in El Tor biotype *Vibrio cholere*. *Microbiology.* **149**, 1883-1891

Simon, R., Priefer, U., and Pühler, A. 1983. A broad host range mobilization system for *in vivo* genetic engineering: transposon mutagenesis in Gram negative bacteria. *Nat. Biotechnol.* **1**, 784-791

Simpson, L M., White, V. K., Zane, S. F., and Oliver, J. D. 1987. Correlation between virulence and colony morphology in *Vibrio vulnificus*. *Infect. Immun.* **55**, 269-272

Sitkiewicz, I., Stockbauer, K. E., and Musser, J. M. 2006. Secreted bacterial phospholipases A_2 enzymes: better living through phospholiolysis. *Trends Microbiol.* **15**, 63-69

Sorek, R. and Cossart, P. 2010. Prokaryotic transcriptomics: a new view on regulation, physiology, and pathogenicity. *Nat. Rev. Genet.* **11**, 9-16

Stoebel, D. M., Fee, A., and Dorman, C. J. 2008. Anti-silencing: overcoming H-NS mediated repression of transcription in Gram-negative eneteric bacteria. *Microbiology*. **154**, 2533-2545

Strom, M. S. and Paranjpye, R. N. 2000. Epidemiology and pathogenesis of *Vibrio vulnificus*. *Microbes Infect.* **2**, 177-188

Strugnell, R. A. and Wijburg, O. L. 2010. The role of secretory antibodies in infection immunity. *Nat. Rev. Microbiol.* **8**, 656-667

Sudarsan, N., Lee, E. R., Weinberg, Z., Moy, R. H., Kim, J. N., Link, K. H., and Breaker, R. R. 2008. Riboswitches in eubacteria sense the second messenger cyclic di-GMP. *Science* **321**, 411-413

Takahashi, M., Okazaki, H., Ogata, Y., Takeuchi, K., Ikeda, U., and Shimada, K. 2002. Lysophosphatidylcholine induces apoptosis in human endothelial cells through a p38-mitogen-activated protein kinase-dependent mechanism. *Atherosclerosis.* **161**, 387-394

Tatusov, R. L., Fedorova, N. D., Jackson, J. D., Jacobs, A. R., Kiryutin, B., Koonin, E. V., Krylov, D. M., Mazumder, R., Mekhedov, S. L., Nikolskaya, A. N., Rao, B. S., Smirnov, S., Sverdlov, A. V., Vasudevan, S., Wolf, Y. I., Yin, J. J.,

and Natale, D. A. The COG database: an updated version includes eukaryotes. *BMC Bioinformatics.* **11**, 41

Tatusov, R. L., Koonin, E. V., and Lipman, D. J. 1997. A genomic perspective on protein families. *Science.* **278**, 631-637

Testa, J., Daniel, L. W., and Kreger, A. S. 1984. Extracellular phospholipase A_2 and lysophospholipase produced by *Vibrio vulnificus*. *Infect. Immun*. **45**, 458-463

Thornton, D. J. and Sheehan, J. K. 2004. From mucins to mucus: toward a more coherent understanding of this essential barrier. *Proc. Am. Thorac. Soc.* **1**, 54-61

Tseng, T. T., Tyler, B. M., and Setubal, J. 2009. Protein secretion systems in bacterial-host associations, and their description in the gene ontology. *BMC Microbiol*. **9**, S2

Vieira, M. A., Gomes, T. A., Ferreira, A. J., Knöbl, T., Servin, A. L., and Liévin-Le Moal, V. 2010. Two atypical enteropathogenic *Escherichia coli* strains induce the production of secreted and membrane-bound mucins to benefit their own growth at the apical surface of human mucin-secreting intestinal HT29-MTX cells. *Infect. Immun.* **78**, 927-938

Vimr, E. R., Kalivoda, K. A., Deszo, E. L., and Steenbergen, S. M. 2004. Diversity of microbial sialic acid metabolism. *Microbiol. Mol. Biol. Rev.* **68**, 132-153

Walk, S. T., Blim, A. M., Ewing, S. A., Weinstock, J .V., and Young, V. B. 2010. Alteration of the mucin gut microbiota during infection with the parasitic helminth *Heligmosomoides polygyrus*. *Inflamm. Bowel Dis.* **16**, 1841-1849

Weening, E. H., Barker, J. D., Laarakker, M. C., Humphries, A. D., Tsolis, R. M., and Bäumler, A. J. 2005. The *Salmonella enterica* serotype Typhimurium *lpf, bcf, stb, stc, std,* and *sth* fimbrial operons are required for intestinal persistence in mice. *Infect. Immun.***73**, 3358-3366

Westermann, A. J., Förstner, K. U., Amman, F., Barquist, L., Chao, Y., Schulte, L N., Müller, L., Reinhardt, R., Stadler, P. F., and Vogel, J. 2016. Dual RNA-seq unveils noncoding RNA functions in host-pathogen interaction. *Nature.* **529**, 496-

Westermann, A. J., Gorski, S. A., and Vogel, J. 2012. Dual RNA-seq of pathogen and host. *Nat. Rev. Microbiol.* **10**, 618-630

White, S. H., Wimley, W. C., and Selsted, M. E. 1994. Structure, function, and membrane integration of defensins. *Curr. Opin. Struct. Biol.* **5**, 521-527

Wiggins, R., Hicks, S. J., Soothill, P. W., Millar, M. R., and Corfield, A. P. 2001. Mucinases and sialidases: their role in the pathogenesis of sexually transmitted infections. *Sex. Transm. Infect.* **77**, 402-408

Williams, S. G., Attridge, S. R., and Manning P. A. 1993. The transcriptional activator HlyU of *Vibrio cholerae*: nucleotide sequence and role in virulence gene expression. *Mol. Microbiol.* **9**, 751-760

Williams, T. C., Ayrapetyan, M., Ryan, H., and Oliver, J. D. 2014. Serum survival of *Vibrio vulnficus*: Role of genotype, capsule, complement, clinical origin, and *in situ* incubation. *Pathogens.* **3**, 822-832

Wong, E., Vaaje-Kolstad, G., Ghosh, A., Hurtado-Guerrero, R., Konarev, P. V., Ibrahim, A. F., Svergun, D. I., Eijsink, V. G., Chatterjee, N. S., and van Aalten, D.M. 2012. The *Vibrio cholerae* colonization factor GbpA possesses a modular structure that governs binding to different host surfaces. *PLoS Pathog.* **8**, e1002373

Wright, A. C. and Morris, J. G. 1991. The extracellular cytolysin of *Vibrio vulnificus*: inactivation and relationship to virulence in mice. *Infect. Immun.* **59**, 192-197

Wright, A. C., Powell, J. L., Kaper, J. B., and Morris, J. G. 2001. Identification of a group 1-like capsular polysaccharide operon in *Vibrio vulnificus*. *Infect. Immun.* **69**, 6893-6901

Wright, A. C., Powell, J. L., Tnnner, M. K., Ensor, L. A., Karpas, A. B., Morris, J. G., and Sztein, M. B. 1999. Differential expression of *Vibrio vulnificus* capsular polysaccharide. *Infect. Immun.* **67**, 2250-2257

Wu, Y. and Outten, F. W. 2009. IscR controls iron-dependent biofilm formation in *Escherichia coli* by regulating type I fimbria expression. *J. Bacteriol*. **191**, 1248-1257

Yeo, W. S., Lee, J. H., Lee, K. C., and Roe, J. H. 2006. IscR acts as an activator in response to oxidative stress for the *suf* operon encoding Fe-S assembly proteins. *Mol. Microbiol.* **61**, 206-218

Yeung, A. T., Parayno, A., and Hancock, R. E. 2012. Mucin promotes rapid surface motility in *Pseudomonas aeruginosa. mBio* **3**, e00073-12

Yoshida, S., Ogawa, M., and Mizuquchi, Y. 1985. Relation of capsular materials and colony opacity to virulence of *Vibrio vulnificus. Infect. Immun.* **47**, 446-451

Zhao, Y. and Natarajan, V. 2013. Lysophosphatidic acid (LPA) and its receptors: role in airway inflammation and remodeling. *Biochim. Biophys. Acta.* **1831**, 86-92

Zheng, M., Wang, X., Templeton, L. J., Smulski, D. R., LaRossa, R. A., and Storz, G. 2001. DNA microarray-mediated transcriptional profiling of the *Escherichia coli* response to hydrogen peroxide. *J. Bacteriol.* **183**, 4562–4570

국문초록

뮤신은 다양한 종류의 다당류 곁사슬이 폴리펩타이드 골격에 붙어있는 당단백질이며, 장 병원균에 대항할 수 있는 최초의 방어선인 점막의 중요한 성분이다. 병원균이 생존하고 병을 일으키기 위해, 병원균은 숙주의 뮤신과 상호작용하고 그들의 유전체를 변화시킴으로써 숙주 환경에 적응한다. 점막과 세균의 상호작용에 대한 이해를 심화시키고자 본 연구에서는 뮤신과 뮤신을 분비하는 HT29-MTX 숙주세포와의 접촉을 통해 변화하는 패혈증 비브리오균의 유전체를 분석하였다. 0.6% (*wt*/*vol*)의 뮤신이 포함된 M9 배지와 HT29-MTX 숙주세포에 노출되었을때 패혈증 비브리오균의 생장과 생존을 확인하였고, 0.4% (*wt*/*vol*)의 포도당과 0.6% (*wt*/*vol*) 뮤신이 포함된 M9 배지에서 생장하는 패혈증 비브리오균의 전사체의 변화를 관찰하고자 RNA-seq 기술이 사용되었으며 basal medium eagle (BME) 배지와 HT29-MTX 숙주세포에 노출된 패혈증 비브리오균의 유전체 역시 동일한 방법으로 분석되었다. 분석을 통해 패혈증 비브리오균의 유전자 중 377개의 발현이 M9 배지에 영양성분으로서 포함된 뮤신과 포도당에 의해 변화하였으며, 650개의 유전자가 BME와 HT29-MTX 숙주세포 노출에 의해 변화함을 확인하였다. 뿐만 아니라 패혈증 비브리오균의 독성인자인 metalloprotease, *N*-acetylglucosamine 부착 단백질, cytolysin, phospholipase를 생성하는 유전자의 발현이 뮤신과 뮤신을 분비하는 숙주

세포에 의해 유도되었다.

뮤신이 포함된 M9 배지에서 생장할 때 발현이 증가하는 패혈증 비브리오균의 유전자 중 콜레라균의 GbpA의 상동물질인 *N*-acetylglucosamine 부착 단백질을 생성하는 *gbpA* 유전자를 선정해 연구를 진행하였다. 돌연변이주 분석을 통해 GbpA가 뮤신과 HT29-MTX 숙주세포에 부착하는 능력에 기여하였으며, *gbpA* 유전자가 결여된 돌연변이주에서 쥐의 병원성 및 소장 부착 능력이 감소하는 것을 확인하였다. *gbpA*의 발현은 패혈증 비브리오균의 증식기에 의존적이었으며, 지수 생장기에서 발현이 최대가 되었다. 철-황 클러스터 조절자인 IscR, cyclic AMP receptor 단백질인 CRP가 *gbpA*의 발현을 전사 수준에서 증가시켰으며, LuxR 상동물질인 SmcR은 그 발현을 감소시켰다. 세균 내에 존재하는 IscR, CRP 그리고 SmcR은 서로가 상호작용하여 각 단백질 양을 변화시키지 않았기 때문에 각 조절 단백질은 조절 단계에 따라 순차적으로 *gbpA*의 발현을 조절하는 것이 아닌 상호 협력적으로 *gbpA*의 발현을 조절 하였다. Primer extension analysis와 EMSA의 결과를 통해 *gbpA*의 전사가 한 곳에서 발생하였으며, IscR, SmcR 그리고 CRP는 *gbpA*의 프로모터 주변에 직접 결합하는 것을 확인하였다. 프로모터 제거 분석 실험과 DNase I protection 실험을 통해 IscR, SmcR 그리고 CRP가 결합하는 정확한 위치를 규명하였다. 뿐만 아니라 패혈증 비브리오균이 과산화수소에 노출되었을 때 세균 내 증가하

는 IscR양에 의해 *gbpA*의 발현이 유도되었다. 위 결과들은 IscR, CRP 그리고 SmcR이 감염 중 GbpA의 발현 수준을 정교하게 조절하기 위해 협력한다는 것을 의미한다.

뮤신과 뮤신을 분비하는 숙주세포에 노출 되었을 때 특이적으로 발현이 유도되는 패혈증 비브리오균 유전자 중 phospholipase를 생성할 것이라 예상되는 유전자인 *plp*의 특성을 규명하였다. 패혈증 비브리오균의 Plp 단백질은 *Vibrio anguillarum*의 phospholipase와 아미노산 수준에서 67%의 상동성을 보였다. Plp의 기능을 이해하기 위해 *plp* 유전자를 제거한 돌연변이주를 제작하고 병원성을 측정하였다. 정상 균주와 비교했을 때 *plp* 돌연변이주는 HT29-MTX 숙주세포에 대한 세포 독성과 쥐의 병원성이 감소되었다. 유전자 분석 및 분리된 Plp 단백질을 사용한 생화학적 분석을 통해 패혈증 비브리오균의 병원성에 필수적인 Plp가 외부로 분비되는 phospholipase A_2임을 확인하였다. Plp의 발현을 변화시키는 조절단백질들을 알아본 결과, 전사활성자인 HlyU와 CRP가 *plp*의 발현을 증가시켰다. 세균 내에 존재하는 HlyU와 CRP는 서로가 상호작용하여 각 단백질 양을 변화시키지 않았기 때문에 각 조절단백질은 조절 단계에 따라 순차적으로 *plp*의 발현을 조절하는 것이 아닌 상호 협력적으로 *plp*의 발현을 조절하였다. 조절단백질들은 *plp*의 프로모터 영역에 직접 결합하였으며 프로모터 제거 분석 및 DNase I protection 분석 실험을 통해 HlyU는 *plp*의

프로모터 영역의 세 곳에 특이적으로 결합하고, CRP는 한 곳에 특이적으로 결합한다는 사실을 확인하였다. 모든 실험 결과들은 패혈증 비브리오균의 *plp* 유전자는 병원성에 필수적인 phospholipase A_2를 분비하며 그 발현은 HlyU와 CRP에 의해 협력적으로 조절됨을 의미한다.

핵심어: 패혈증 비브리오균, 뮤신, 전사체 분석, 병원성, *N*-aecetyl glucosamine 부착 단백질 (GbpA), Phospholipase A_2 (Plp), 유전자 조절, IscR, CRP, SmcR, HlyU

Student Number: 2011 − 23534